UNIVERSIDADE ESTADUAL DE CAMPINAS

FACULDADE DE ENGENHARIA DE ALIMENTOS

DEPARTAMENTO DE ENGENHARIA DE ALIMENTOS

UNICAMP

Formação, estrutura e propriedades reológicas de sistemas biopoliméricos

Ana Luiza Mattos Braga

Engenheira de Alimentos, 1999 (UNICAMP)

Mestre em Engenharia de Alimentos, 2002 (UNICAMP)

Profa. Dra. Rosiane Lopes da Cunha

Orientadora

Tese apresentada à comissão de pós-graduação da Faculdade de Engenharia de Alimentos da Universidade Estadual de Campinas, para a obtenção do título de Doutor em Engenharia de Alimentos.

Campinas, Março de 2006

BANCA EXAMINADORA

"Agora que sinto amor

 Tenho interesse nos perfumes.

 Nunca antes me interessou que uma flor tivesse cheiro.

 Agora sinto o perfume das flores como se visse uma coisa nova.

 Sei bem que elas cheiravam, como sei que existia.

 São coisas que se sabem por fora.

 Mas agora sei com a respiração da parte de trás da cabeça.

 Hoje as flores sabem-me bem num paladar que se cheira.

 Hoje às vezes acordo e cheiro antes de ver."

<div align="right">(Alberto Caeiro)</div>

*À Rosi e aos professores que durante toda minha
vida escolar subsidiaram-me com os ingredientes
deste produto que hora apresento.*

AGRADECIMENTOS

Ao meu novo primo e grande amigo Zé Marcelo, por ter me mostrado, com sua leveza de viver, a graça de contemplar os detalhes; detalhes de um toque, de um olhar, de um perfume, de um paladar e de um passarinho a cantar.

Às vovós Áurea e Dalva, vovô Zezito e tia Avete, por todo amor, apoio e pensamentos que foram essenciais nesta etapa da vida.

Aos meus pais e irmãos, Gusto e Gui, que sempre me apoiaram em todos os meus passos. Não tenho palavras para expressar a importância de vocês....

À todos que de uma forma ou de outra contribuiram para a elaboração desta tese.

Agradeço a Força, Saúde e Perseverança que me foram dadas durante a vida.

SUMÁRIO

Tese de Doutorado

AUTORA: Ana Luiza Mattos Braga

TÍTULO: **Formação, estrutura e propriedades reológicas de sistemas biopoliméricos.**

ORIENTADORA: Prof. Dra. Rosiane Lopes da Cunha

Depto. Engenharia de Alimentos – FEA – UNICAMP

RESUMO GERAL

A utilização de diversos biopolímeros é uma prática comum nas indústrias de alimentos, especialmente em produtos lácticos, embutidos e a base de soja. O objetivo geral deste trabalho foi estudar as interações entre proteínas e polissacarídeos em sistemas contendo, ou não, co-soluto, em solução aquosa (pH 7,0) ou géis acidificados. Dentre as proteínas e os polissacarídeos utilizados na indústria de alimentos, foram estudados mais profundamente a goma xantana, o caseinato de sódio e o isolado protéico de soja (tanto em solução quanto em géis). Os polissacarídeos jataí (LBG), gelana, Na-alginato e κ-carragena foram estudados apenas em soluções. As interações entre os componentes foram estudadas 1) por microscopias confocal, de força atômica e de contraste de fases e rheo-SALS ("small angle light scattering"); 2) por reologia a baixas e altas deformações, em cisalhamento ou compressão; 3) por análises químicas para determinar o tipo de força das interações. Os estudos sobre as propriedades físicas de soluções puras de biopolímeros mostraram que soluções de proteína seguem um comportamento Newtoniano, enquanto que os polissacarídeos apresentam comportamento Newtoniano a baixa concentração e pseudoplástico com o aumento desta. O tratamento térmico de soluções de xantana bem como a adição de sacarose reduziram a elasticidade da solução, sendo que a adição de sacarose afetou as propriedades reológicas apenas de soluções anisotrópicas ou bifásicas (anisotropia e isotropia simultâneas). Um novo modelo baseado na equação de BST (Blatz, Sharda, Tschoegl, 1974) foi proposto para predizer um maior número de propriedades mecânicas dos géis biopoliméricos tendo sido observado um bom ajuste dos dados. Quanto mais lenta a acidificação promovida por GDL, mais interconectada e forte foi a rede protéica em géis puros de Na-caseinato e SPI. O aumento da tensão e deformação de

ruptura de géis formados com GDL foi obtida pelo aumento da concentração de proteína em géis puros de SPI, pela adição de xantana ou pela redução do conteúdo de proteína em géis contendo xantana. Por outro lado, a adição de xantana enfraqueceu os géis térmicos de SPI, provavelmente devido a ligação deste polissacarídeo com a sub-unidade β-7S. Em soluções aquosas pH 7,0, a κ-carragena foi mais compatível com o Na-caseinato e com SPI do que o Na-alginato. No entanto, os resultados de "rheo-SALS" e CLSM mostraram que misturas de caseinato e alginato apresentaram maior capacidade de formar emulsões do tipo água-água do que sistemas com carragena. Além disto, o sistema com SPI e Na-alginato também formou emulsão, mas com a fase dispersa de proteína gelificada. Misturas com gelana apresentaram-se homogêneas devido a baixa tensão interfacial do sistema.

Palavras-chave: proteína, polissacarídeo, interação, gel, emulsão, biopolímero, solução, reologia, separação de fases, CLSM, "rheo-SALS".

Ph.D. Thesis

AUTHOR: Ana Luiza Mattos Braga

TITLE: Formation, structure and rheological properties of biopolymers systems.

SUPERVISOR: Prof. Dra. Rosiane Lopes da Cunha

Depto. Engenharia de Alimentos – FEA – UNICAMP

ABSTRACT

Biopolymers are widely used in dairy products, canned foods, bakery products, salad dressings, beverages, sauces, soups and other processed foodstuffs to improve textural characteristics, flavour and shelf life. The aim of the present Ph.D. thesis was to study the protein-polysaccharide interactions in aqueous systems (pH 7.0) or acidified gels. It was studied seven different biopolymers used in the food industry, being two proteins and five polysaccharides. Soy protein isolate (SPI), Na-caseinate and xanthan were studied in aqueous solutions and gels systems, while locust bean gum (LBG), gellan, Na-alginate and κ-carrageenan were studied only in aqueous solutions. The protein-polysaccharide interactions were evaluated as following: 1) microstructures – by using confocal (CLSM), atomic force and phase contrast microscopes and rheo-SALS (small angle light scattering); 2) macrostructures, evaluated trough small- and large-strain rheology under shear or compression; 3) chemical analysis - in order to determine the kind of interaction forces that maintained the gels structure. The results on the physical properties of pure biopolymers solutions revealed that the proteins showed Newtonian behaviour, while the polysaccharides showed either Newtonian or non-Newtonian behaviour depending on its type and solution concentration. The annealing temperature of xanthan solutions and the addition of sucrose caused a reduction on the solution elasticity. It was observed that sucrose affected the rheological properties over all frequency range studied for initially anisotropic or biphasic xanthan solutions. It was proposed a new model based on BST (Blatz, Sharda, Tschoegl, 1974) equation to predict a great number of mechanical properties, which revealed a very good fit to the data. The slower the acidification by GDL (glucone-delta-lactone) it was observed a more interconnected and harder network in Na-

caseinate and SPI pure gels. The increase of the breaking stress or strain was obtained by increasing the SPI concentration in pure gels, by adding xanthan or by increasing the protein concentration in gels made with xanthan. In another hand, the addtion of xanthan let to weaker heat-induced SPI gels, which was attributed to the electrostatic interactions between xanthan and the β-7S subunit of SPI. In mixed protein-polysaccharide solutions, the results indicated that κ-carrageenan was more compatible with both soy protein and Na-caseinate than alginate. However, the Na-caseinate – Na-alginate mixture showed a greater capacity to form water-in-water emulsions than Na-caseinate - carrageenan system as observed by rheo-SALS and CLSM. In addition, the system with SPI and Na-alginate also formed emulsions but with a gelified protein dispersed phase. The interfacial tension of systems containing gellan was very low resulting in homogeneous mixtures.

Keywords: proteins, polysaccharides, interaction, gel, emulsion, biopolymer solution, rheology, phase separation, CLSM, rheo-SALS.

CAPÍTULO 1. Introdução geral

1. Introdução

As indústrias de alimentos vêm, cada vez mais, intensificando e diversificando suas linhas de produção. Além disto, tem-se observado que este ramo da indústria tem investido esforços em fabricar produtos com alto valor agregado, podendo-se destacar os produtos lácteos ou a base de soja. Produtos lácteos "light" ou "diet", obtidos a partir da substituição total ou parcial de ingredientes como a gordura, apresentam uma textura diferente da do produto tradicional. Com o intuito de obter-se uma textura similar a este, as novas formulações vêm sendo adicionadas de polissacarídeos e/ou concentrados protéicos. A textura também é vista pelos fabricantes de tofu como fator determinante da aceitabilidade deste produto, ao lado da capacidade de retenção de água que aumenta o peso e consequentemente o valor econômico deste alimento (Abd Karim et al., 1999).

A proteína de soja vem sendo encontrada cada vez mais em uma maior diversidade de produtos, sendo que sua aplicação varia desde substituinte de proteínas em produtos lácteos e em embutidos a diversos tipos de massas e bebidas (Embrapa, 2005). Esta proteína apresenta alto valor nutricional e propriedades funcionais interessantes como gelificante ou espessante, que contribuem para a modificação da textura do alimento (Kinsella, 1979). A soja é capaz de prevenir uma série de doenças como as cardiovasculares, além de auxiliar na prevenção de câncer e osteoporose. Aliada a esta grande aplicabilidade, a soja é importante para a economia nacional, visto que o Brasil é o segundo maior produtor mundial de soja, com 27% do mercado (Embrapa, 2005).

A caseína é a proteína encontrada em maior abundância no leite (80%), tendo quatro frações principais (α_{S1}-, α_{S2}-, β- e κ-caseína) que apresentam-se ligadas na forma de micela no leite (Walstra e Jenness, 1984). O caseinato de sódio (Na-caseinato) é um importante

3

ingrediente lácteo que é obtido a partir da acidificação do leite até o ponto isoelétrico (pH 4,6) da caseína. O precipitado é então lavado e re-suspenso em água com a adição de hidróxido de sódio para obter-se uma solução neutra a qual passa posteriormente por um processo de secagem (Kinsella, 1984). Este ingrediente é usado na indústria de alimentos, principalmente em produtos lácteos como em queijos tipo "cottage" e "cheddar", bebidas e sobremesas. As proteínas do leite apresentam algumas propriedades funcionais importantes como agente espumante, emulsificante e gelificante (Sgarbieri, 1996).

Os polissacarídeos são utilizados nos produtos para aumentar a viscosidade de formulações líquidas, como agentes gelificantes ou ainda para aumentar sua retenção de água (Syrbe et al., 1998, Abd Karim et al., 1999). Os polissacarídeos mais utilizados em alimentos são obtidos a partir de endosperma de plantas, de algas ou por fermentação microbiana. As gomas xantana e gelana são polissacarídeos aniônicos de origem microbiana. Outros dois polissacarídeos aniônicos são os alginatos e as carragenas, ambos obtidos a partir de algas marinhas. Tanto as carragenas quanto a gelana apresentam a capacidade particular de formar géis termo-reversíveis em soluções aquosas (Chaplin, 2005). A xantana, a gelana e a carragena são conhecidas pela mudança da conformação ordenada em forma de hélices à desordenada com a variação da temperatura, concentração e força iônica do sistema (Paradossi e Brant, 1982; Lee e Brant, 2002; Ikeda et al., 2004). A goma jataí, ou locusta é uma galactomanana, representante das gomas neutras extraídas de plantas. As propriedades físico-químicas das galactomananas são fortemente dependentes do conteúdo de galactose no polissacarídeo (Morris, 1990).

As interações que ocorrem entre proteínas e polissacarídeos são interessantes para melhorar algumas características funcionais das proteínas e estes sistemas são comumente encontrados em alimentos. Estudos sobre as interações das proteínas do leite com diferentes

polissacarídeos, utilizando as mais diversas técnicas, têm sido conduzidos por alguns grupos de pesquisa (Zhang e Foegeding, 2003; Braga e Cunha, 2004; Antonov et al., 2004; Moschakis et al., 2005). Não são menos importantes os estudos sobre as interações de proteína de soja com polissacarídeos, embora existam poucos trabalhos sobre este tema na literatura (Carp et al., 1999; Abd Karim et al., 1999; Chang et al., 2003) e um grande aumento na diversidade de produtos a base de soja. Soluções ou géis com mais de um biopolímero exibem comportamentos mais complexos do que misturas de polímeros sintéticos. Isto se deve ao fato de que os biopolímeros possuem um equilíbrio relacionado ao estado de ordem - desordem de conformação, além de apresentar transições e separações de fases em determinadas situações (Cèsaro et al., 1999). Interações entre polímeros resultam em incompatibilidade e formações complexas, sendo exceção a miscibilidade entre os componentes.

As propriedades de um gel protéico, como textura e sinerese, podem ser alteradas não só pela adição de polissacarídeos como também pelas variações na força iônica e pH do sistema (Renkema et al., 2000). A formação de uma rede protéica é o resultado da agregação das moléculas de proteína, a partir da desnaturação prévia destas e/ou da acidificação do sistema. O processo de acidificação pode ser realizado de duas formas, sendo a tradicional através da ação de cultura bacteriana e a outra com o uso de reagentes químicos, como o glucona-delta-lactona (GDL). O uso de GDL apresenta a vantagem de causar um decréscimo lento do pH e evitar algumas dificuldades associadas com o uso de bactérias (Lucey et al., 1998). Utsumi e Kinsella (1985) relataram que as forças moleculares envolvidas na formação de géis térmicos de isolado protéico de soja são pontes de hidrogênio e interações hidrofóbicas, enquanto que o gel é mantido por pontes de hidrogênio e dissulfeto. As forças das interações entre frações protéicas vêm sendo

distinguidas e quantificadas através de solubilidade protéica em diferentes tampões e eletroforese em gel de poliacrilamida (Petruccelli e Añón, 1995). O tampão Tris é usado para romper as interações eletrostáticas, a uréia atua rompendo as pontes de hidrogênio e as interações hidrofóbicas, enquanto as pontes dissulfeto são reduzidas na presença de β-mercaptoetanol (Cheftel et al., 1996).

Misturas aquosas de proteínas e polissacarídeos são geralmente incompatíveis, apresentando separação de fases segregativa em pH 7,0. Em alguns casos, o sistema pode apresentar microseparação de fases com uma morfologia interessante, que pode variar desde estruturas elongadas até a forma de gota. Neste tipo de sistema, cada fase é rica em um dos dois biopolímeros e quando a estrutura formada é do tipo gota, a mistura é considerada uma emulsão água-água (Tolstogusov, 1986). Este tipo de estrutura apresenta características reológicas peculiares e vem sendo utilizada na indústria de alimentos na substituição de gorduras (Capron *et al.*, 2001). Entretanto, algumas peculiaridades das emulsões água-água, como a miscibilidade limitada e os valores extremamente baixos de tensão interfacial, podem adicionar uma complicação extra para a descrição reológica do sistema bem como dos processos de mistura e dispersão dos dois biopolímeros (van Puyvelde *et al.*, 2002).

O estudo reológico de géis e soluções vem ganhando a atenção de vários grupos de pesquisa, visto que pode ser associado com a estrutura, a qual é consequência das interações entre os ingredientes, podendo levar à redução de custos de processos e auxiliando o desenvolvimento de novos materiais e produtos. As propriedades mecânicas obtidas em compressão uniaxial podem ser relacionadas com a textura sensorial e os dados obtidos têm sido ajustados por modelos empíricos ou fundamentais (Foegeding et al.,

2003). Por outro lado, as propriedades reológicas determinadas em cisalhamento, como a viscosidade aparente, são importantes para o dimensionamento de equipamentos. Além destas propriedades reológicas, as obtidas em baixas deformações por compressão ou cisalhamento conferem informações relevantes sobre a estrutura de géis e soluções e sobre a conformação molecular de biopolímeros. O desenvolvimento de técnicas reológicas avançadas, como "rheo-SALS" (reologia em cisalhamento com "Small Angle Light Scattering"), para descrever os parâmetros reológicos de sistemas biopoliméricos são especialmente importantes para o desenvolvimento de produtos gelificados e líquidos. Além disto, diversas técnicas de microscopia têm sido empregadas para dar suporte ao entendimento das propriedades reológicas, cabendo ressaltar as microscopias confocal de varredura laser, de força atômica, de contraste de fases e eletrônica de varredura.

Assim, o entendimento adequado dos comportamentos micro e macroscópicos de sistemas-modelo de alimentos é de grande importância para o desenvolvimento de novos produtos e pode ser obtido a partir do conhecimento da estrutura molecular dos ingredientes, das interações entre os componentes do alimento e das forças intermoleculares que determinam a consistência e a estabilidade física dos produtos (Heertje, 1993).

2. Objetivos

O objetivo geral desta tese de doutorado foi aprofundar o conhecimento sobre as interações entre proteínas e polissacarídeos em sistemas contendo, ou não, co-soluto em pH neutro ou ácido. Dentre as proteínas e os polissacarídeos, foram estudados mais profundamente o caseinato de sódio (Na), o isolado protéico de soja (SPI) e a goma xantana. Adicionalmente, as gomas gelana, jataí (LBG), Na-alginato e κ-carragena foram usadas com o intuito de explicar como as diferentes conformações dos polissacarídeos

afetam o comportamento de soluções contendo uma proteína e um polissacarídeo. O conhecimento das interações entre caseinato de sódio e xantana foi iniciado com a dissertação de mestrado defendida em 2002. Os resultados obtidos levaram ao interesse por estudar sistemas mais simples (contendo somente um biopolímero) e com a adição de outra fonte protéica.

As interações entre os componentes foram estudadas tanto a nível microscópico quanto macroscópico, sendo os objetivos específicos da tese descritos a seguir:

1. Para sistemas gelificados (termicamente e/ou acidificado) foram determinadas as propriedades reológicas a baixas (cisalhamento e compressão uniaxial) e altas deformações (compressão uniaxial), a capacidade de retenção de água dos géis e a microestrutura dos mesmos (microscopia confocal de varredura laser). O tipo de força de interação foi determinado por solubilidade do gel em diferentes tampões e eletroforese em gel de poliacrilamida (Capítulo 4).

2. Para sistemas não-gelificados (mistos e puros) avaliou-se as propriedades reológicas sob cisalhamento, o comportamento das fases, as propriedades térmicas durante a desnaturação das proteínas e a densidade. A microestrutura destes sistemas foi observada em microscópio de contraste de fases, microscópio de força atômica e por "rheo-small angle light scattering" (rheo-SALS) (Capítulos 3 e 5 e Apêndice).

3. Organização da tese em capítulos

Como o objetivo geral da tese foi entender as interações entre proteínas e polissacarídeos em diferentes tipos de sistemas que podem ser encontrados em alimentos, inicialmente foi necessário um estudo sobre as propriedades físicas das soluções puras de biopolímeros (Capítulo 3). O estudo da gelificação (Capítulo 4) foi restringido a três

biopolímeros devido ao elevado número de análises necessárias para entender as interações ocorridas nos sistemas. Para tal, foram escolhidos o Na-caseinato e a xantana, para dar continuidade aos estudos do mestrado, e o SPI, por ser uma fonte de proteína de grande importância para a economia brasileira. O último capítulo da tese (Capítulo 5) descreve o estudo de outros quatro polissacarídeos (gelana, alginato de sódio, jataí e *k*-carragena) além da xantana.

A seguir serão detalhados os conteúdos dos capítulos da tese:

Capítulo 1: Introdução geral (em português).

Capítulo 2: Revisão bibliográfica (em português).

Capítulo 3: Rheological properties of biopolymers aqueous solutions (em inglês).

Parte 1: Physical properties of pure proteins and polysaccharides aqueous solutions

A densidade e as propriedades reológicas em estado estacionário de soluções de sete tipos de biopolímeros utilizados na indústria de alimentos foram determinadas em diferentes concentrações. Os polissacarídeos investigados foram xantana, jataí, gelana, κ-carragena e Na-alginato, enquanto que foram utilizados como fonte de proteína o Na-caseinato e isolado protéico de soja (SPI). Esta parte da tese foi realizada no Laboratory of Food Process Engineering (LMVT) – Eidgenössische Technische Hochschule Zürich (ETHZ) - Suíça pelo programa de estágio de doutorado no exterior financiado pela CAPES.

Parte 2: Rheological behaviour and microstructure of xanthan solutions: annealing temperature and sucrose effects.

Soluções de xantana submetidas a diferentes tratamentos térmicos e adicionadas ou não de sacarose foram avaliadas a partir de ensaios reológicos em cisalhamento a baixas deformações através de varreduras de temperatura e freqüência. Neste estudo, determinou-

se as temperaturas de transição conformacional da molécula e outras transições relacionadas à anisotropia da solução. Além disto, foram realizadas micrografias (microscopia de contraste de fases e microscopia de força atômica) das diferentes amostras a fim de comprovar as transições estudadas. A microscopia de contraste de fases foi realizada no ETHZ-Suíça.

Capítulo 4: Protein-polysaccharide interactions in acidified gels containing Na-caseinate, SPI and/or xanthan (em inglês).

O Na-caseinato e a xantana foram escolhidos para o estudo devido ao conhecimento prévio adquirido no mestrado. As proteínas de soja (SPI) também foram estudadas com o objetivo de adquirir maior informação sobre as interações entre outra proteína globular e a xantana.

Parte 1: The effect of the GDL/caseinate ratio on sodium caseinate gelation.

Diferentes quantidades de glucona-delta-lactona (GDL) foram adicionadas às soluções de caseinato de sódio puro sendo que o processo de gelificação foi acompanhado por medidas reológicas sob cisalhamento e compressão uniaxial. As propriedades reológicas, a capacidade de retenção de água e os tipos de forças de interação protéica do gel em equilíbrio foram determinadas. Este capítulo da tese não apresenta a adição de polissacarídeo por ser continuação dos estudos realizados no mestrado.

Parte 2: Small- and large-strain rheological properties of GDL-induced soy protein isolate gels: effect of gelation temperature and xanthan addition.

Nesta etapa foi: 1) desenvolvido um modelo capaz de predizer todas as propriedades mecânicas de géis formados por biopolímeros baseado na equação proposta por Blatz et al. (1974); 2) estudado o efeito da concentração de SPI, da adição de xantana e da temperatura

de gelificação sobre as propriedades reológicas durante o processo de gelificação (em cisalhamento) e em equilíbrio (compressão) de sistemas com GDL e SPI.

Parte 3: Interactions between soy protein isolate and xanthan in heat-induced gels: the effect of salt addition.

A influência da adição de xantana e/ou KCl nas propriedades de géis térmicos (pH 3,0) de isolado protéico de soja (SPI) foi estudada. Para tal, foram determinadas a solubilidade protéica dos géis e a composição das subunidades do extrato solúvel, bem como as propriedades mecânicas, a capacidade de retenção de água e a microestrutura dos géis mistos.

Capítulo 5: Protein-polysaccharide interactions in aqueous systems pH 7.0. (em inglês)

Parte 1: Rheological and phase-separation behaviours of protein-polysaccharide mixtures pH 7.0

Nesta etapa foi estudado o papel da concentração e do tipo de biopolímero sobre o comportamento de fases de sistemas contendo proteína e polissacarídeo. Para tal foram feitos ensaios de separação de fases, sendo a mistura inicial e as fases ricas em biopolímeros avaliadas por microscopia confocal e reologia. Os polissacarídeos investigados foram gelana, κ-carragena e Na-alginato, enquanto que Na-caseinato e SPI foram as fontes de proteína. Esta etapa foi realizada no Laboratório de Engenharia de Processos (LEP) – Faculdade de Engenharia de Alimentos (FEA) - UNICAMP em conjunto com um aluno de graduação do ETHZ-Suíça como parte da colaboração entre os laboratórios situados no Brasil e na Suíça.

Parte 2: Morphology of protein-polysaccharides mixtures at rest and under shear.

Estudou-se a obtenção de emulsões tipo água-água a partir dos comportamentos morfológicos em repouso por microscopia confocal (CLSM) e sob cisalhamento por "rheo-Small Angle Light Scattering" (rheo-SALS). Os polissacarídeos investigados foram xantana, jataí, gelana, κ-carragena e Na-alginato, enquanto que Na-caseinato e SPI foram as fontes de proteína. A etapa de estudo do "rheo-SALS" foi realizada no LMVT-ETHZ-Suíça e as microscopias foram feitas no DCA-FEA-UNICAMP.

Capítulo 6: Conclusão geral. (em português)

Apêndice: Preliminary studies on the phase separation of biopolymers mixtures. (em inglês)

Neste apêndice são apresentados os resultados preliminares de separação de fases, mostrando como foram escolhidos os sistemas estudados no capítulo 5. Esta etapa foi realizada no LMVT-ETHZ-Suíça.

Anexo: Lista de trabalhos sobre biopolímeros apresentados em congressos ou publicados em revistas no período do doutorado (2002-2006).

4. Referências

ABD KARIM, A.; SULEBELE, G.A.; AZHAR, M.E.; PING, C.Y. Effect of carrageenan on yield and properties of tofu. **Food Chemistry**, v.66, p.159-165, 1999.

ANTONOV, Y.A.; VAN PUYVELDE, P.; MOLDENAERS, P. Interfacial tension of aqueous biopolymer mixtures close to the critical point. **International Journal of Biological Macromolecules**, v.34, p.29-35, 2004.

BLATZ, P.J.; SHARDA, S.C.; TSCHOEGL, N.W. Strain energy function for rubberlike materials based on a generalized measure of strain. **Transactions of the Society of Rheology**, v.18, p.145–161, 1974.

BRAGA, A.L.M.; CUNHA, R.L. The effects of xanthan conformation and sucrose concentration on the rheological properties of acidified sodium caseinate–xanthan gels. **Food Hydrocolloids**, v. 18, p. 977-986, 2004.

CAPRON, I.; COSTEUX, S.; DJABOUROV, M. Water in water emulsions: phase separation and rheology of biopolymer solutions. **Rheologica Acta.** v.40, p.441-456, 2001.

CARP, D.J.; BARTHOLOMAI, G.B.; Pilosof, A.M.R. Electrophoretic studies for determining soy proteins–xanthan gum interactions in foams. **Colloid and Surface B**, v.12, p.309–316, 1999.

CÈSARO, A.; CUPPO, F.; FABRI, D.; SUSSICH, F. Thermodynamic Behavior of mixed biopolymers in solution and in gel phase. **Thermochimica Acta**, v. 388, p. 143-153, 1999.

CHANG, K.L.B.; LIN, Y.S.; CHEN, R.H. The effect of chitosan on the gel properties of tofu (soybean curd). **Journal of Food Engineering**, v.57, p.315–319, 2003.

CHAPLIN, M., available at: http://www.sbu.ac.uk/water/hydrat.html, acessado em 01 de Junho de 2005.

CHEFTEL, J. C.; CUQ, J. L.; LORIENT, D. Amino acids, peptides and proteins. In Food Chemistry, ed. Fenema, O. R.; Acribia: Zaragoza, Spain, 1996; Chapter 3, p. 245-369.

EMBRAPA. Soja: Alimento e Saúde. In: **http://www.cnpso.embrapa.br**, 13/07/2005.

FOEGEDING, E.A.; BROWN, J.; DRAKE, M.A.; DAUBERT, C.R. Sensory and mechanical aspects of cheese texture. **International Dairy Journal**, v.13, p.585-591, 2003.

HEERTJE, I. Structure and Function of Food Products: a review. **Food Structure.** v.12, p.343-364, 1993.

IKEDA, S.; NITTA, Y.; TEMSIRIPONG, T.; PONGSAWATMANIT, R.; NISHINARI, K. Atomic force microscopy studies on cation – induced network formation of gellan. **Food Hydrocolloids**, v.18, p.727 – 735, 2004.

KINSELLA, J. E. Funcional Properties of Soy Proteins. **Journal of American Oil Chemists Society.** v.56, p.242-258, 1979.

KINSELLA, J. E. Milk proteins: physicochemical and functional properties. **CRC Critical Reviews in Food Science and Nutrition.** v.3, p.197-262, 1984.

LEE, H.C.; BRANT, D.A. Rheology of concentrated isotropic and anisotropic xanthan solutions: 3. Temperature dependence. **Biomacromolecules.** v.3, p.742-753, 2002.

LUCEY, J.A.; TAMEHANA, M.; SINGH, H.; MUNRO, P.A. A comparison of the formation, rheological properties and microstructure of acid skim milk gels made with a bacterial culture or glucono-δ-lactone. **Food Research International**. v.31, p.147-155, 1998.

MORRIS, E.R., VUTLER, A.N., ROSS-MURPHY, S.B., REES, D.A., PRICE, J. The fine structures of carob and guar galactomannans. **Carbohydrate Polymers**, 1, 5-21, 1981.

MOSCHAKIS, T.; MURRAY, B.S.; DICKINSON, E. Microstructural evolution of viscoelastic emulsions stabilised by sodium caseinate and xanthan gum. **Journal of Colloid and Interface Science**, v.284, p.714-728, 2005.

PARADOSSI, G.; BRANT, D.A. Light Scattering Study of a Series of Xanthan Fractions in Aqueous Solution. **Macromolecules.** v.15, p.874-879, 1982.

PETRUCCELLI, S., AÑÓN, M.C. Soy protein isolate components and their interactions. **Journal of Agricultural and Food Chemistry**, v.43, p.1762-1767, 1995.

RENKEMA, J.M.S.; LAKEMOND, C.M.M.; DE JONGH, H.H.J.; GRUPPEN, H.; VAN VLIET, T.V. The effect of pH on heat denaturation and gel forming properties of soy proteins. **Journal of Biotechnology.** v.79; p.223-230, 2000.

SGARBIERI, V. C. **Proteínas em alimentos protéicos: propriedades, degradações e modificações**, Livraria Varela Ltda, São Paulo, 1996, p. 216-229.

SYRBE, A.; BAUER, W.J.; KLOSTERMEYER, H. Polymer Science Concepts in Dairy Systems – An Overview of milk protein and food hydrocolloid interaction. **International Dairy Journal**. v.8**,** p.179-193, 1998.

TOLSTOGUSOV, V.B. Functional properties of protein-polysaccharide mixtures. In **Functional properties of food macromolecules.** eds. J.R. Mitchell & D.A. Ledward. London: Elsevier, p. 385-415,1986

URLACHER, B.; NOBLE, O. Xanthan gum. In **Thickening and Gelling Agents for food**, 2^{a}ed., eds. Alan Imenson, Blackie Academic and Professional, Londres, p. 284-311, 1997.

UTSUMI, S.; KINSELLA, J. E. Forces involved in soy protein gelation: effects of various reagents on the formation, hardness and solubility of heat-induced gels made from 7S, 11S and soy isolate. **Journal of Food Science**. v.50, p.1278-1282, 1985.

VAN PUYVELDE, P.; ANTONOV, Y.A.; MOLDENAERS, P. A rheo-optical investigation of shear-induced morphological changes in biopolymeric blends. **Korea-Australia Rheology Journal.** v.14, p.115-119, 2002.

WALSTRA, P.; JENNESS, R. **Dairy Chemistry and Physics**, Wiley, New York, 1984.

ZHANG, G.; FOEGEDING, E.A. Heat-induced phase behavior of β-lactoglobulin/polysaccharide mixtures. **Food Hydrocolloids**, v.17, p.785-792, 2003.

CAPÍTULO 2. Revisão Bibliográfica

1. Proteínas

1.1. Caseínas

O leite tem aproximadamente 3,5% de proteína, sendo 2,9% de caseína e 0,6% de proteínas do soro. A presença de fósforo (P) nas caseínas permite classificá-las como fosfoproteínas. Estas proteínas são ácidas, por serem ricas em ácido glutâmico e aspártico. A composição dos aminoácidos das caseínas lhes confere uma hidrofobicidade ligeiramente superior do que a maioria das proteínas globulares. Esta propriedade permite que as caseínas associem-se facilmente formando complexos de elevado peso molecular, denominados micelas. As caseínas são classificadas em quatro grupos principais de acordo com suas estruturas primárias: α_{s1}, α_{s2}, β e κ (Cheftel *et al.*, 1989).

As α_{s1}-caseínas apresentam uma estrutura pouco ordenada. Além disto, esta fração é a que apresenta a maior carga iônica e, excluindo-se as α_{s2}-caseínas, é a de menor hidrofobicidade. As α_{s2}-caseínas são as mais hidrofílicas devido à maior fosforilação e maior quantidade de resíduos catiônicos, que resulta em elevada afinidade aos íons Ca^{2+}. As β-caseínas são as que apresentam maior hidrofobicidade, sendo que sua molécula possui uma região N terminal muito polar e uma região C terminal hidrofóbica. Além disto, a baixas temperaturas (4 ^{o}C) a β-caseína se dissocia da micela. Já as κ-caseínas possuem a região N terminal hidrofóbica e a região C terminal hidrofílica (Cheftel *et al.*, 1989).

As proteínas do leite apresentam algumas propriedades funcionais importantes como agentes espumantes, emulsificantes e gelificantes, sendo muito utilizadas na formulação de produtos alimentícios (Sgarbieri, 1996). Estas propriedades estão relacionadas à natureza anfótera da micela de caseína. A atividade interfacial das caseínas é

mais notória nas β-caseínas por estas serem mais flexíveis e encontrarem-se desdobradas na interface. Já as κ-caseínas apresentam uma estrutura mais ordenada.

1.2. Isolado protéico de soja (SPI)

A soja é a mais importante fonte protéica de origem vegetal que é utilizada como ingrediente em formulações de alimentos, visto que este grão apresenta 40% de proteínas em sua composição (Sgarbieri, 1996). O isolado protéico de soja é a forma mais purificada das proteínas de soja, possuindo alto valor nutricional e apresentando diversas propriedades funcionais como emulsificante, espumante e espessante, sendo também caracterizado como agente gelificante. Aproximadamente 90% das proteínas de soja são globulinas e as que precipitam em pH 4,5 são tradicionalmente chamadas de glicininas (Kinsella, 1979).

As frações da proteína de soja são caracterizadas de acordo com as suas propriedades de sedimentação ou peso molecular (Wolf *et al*, 1961), apresentando os seguintes coeficientes de Svedberg (S) 2S, 7S, 11S e 15S. Os componentes de baixo peso molecular (2S) são compostos inibidores de tripsina, citocromo e outras globulinas. As duas frações principais possuem pesos moleculares elevados, sendo que 20-35% das proteínas são referenciadas como globulina 7S (β-conglicinina) e 25-35% como globulina 11S (glicinina). Ambas são muito complexas, consistindo de diversas subunidades que facilmente se associam e dissociam sob diferentes condições de pH, força iônica e tratamento térmico (Badley *et al.*, 1975; Kinsella, 1979; Hermansson, 1986).

A glicinina (globulina 11S) consiste de doze cadeias polipeptídicas, sendo 6 ácidas (A) e 6 básicas (B) ligadas (AB) por pontes dissulfeto. Segundo, Badley *et al*. (1975) as sub-unidades AB são associadas dentro de dois anéis com seis sub-unidades (hexâmero), que são mantidos unidos por interações hidrofílicas, como pontes de hidrogênio e

interações eletrostáticas. Embora a estrutura quaternária da globulina 11S seja estável, é possível provocar uma dissociação seqüencial em sub-unidades obtendo-se os seguintes produtos (Sgarbieri, 1996):

$$11S\ (A_6B_6) \longrightarrow\ \sim7S\ (A_3B_3) \longrightarrow\ \sim3S\ (6AB) \longrightarrow\ \sim2S\ (6A+6B)$$

2. Polissacarídeos

Os polissacarídeos são compostos solúveis em água e de elevado peso molecular. Estes ingredientes atuam como estabilizantes e espessantes, devido à sua capacidade de aumentar a viscosidade do sistema podendo, inclusive, formar géis (Syrbe *et al*, 1998). Os polissacarídeos podem ser utilizados como aditivos em produtos com a proposta de redução parcial ou total de gordura. Estes ingredientes atuam suprindo a perda de textura ocasionada pela falta de gordura e evitam a separação de fases em emulsões (Katzbauer, 1998). A seguir serão descritas algumas características dos polissacarídeos utilizados neste trabalho.

2.1. Xantana

A goma xantana é um polissacarídeo microbiano, extracelular, produzido pela bactéria *Xanthomonas campestris*. A estrutura primária da molécula de xantana é composta de uma cadeia principal com unidades de D-glucose ligadas em β (1→4), contendo cadeias ramificadas com duas unidades de manose e uma de ácido glucurônico (Figura 1). O primeiro resíduo de manose é normalmente acetilado no C6 e toda cadeia ramificada possui um grupamento carboxílico no resíduo de ácido glucurônico. O resíduo terminal de manose possui um grau variado de substituição por piruvato (Capron *et al.*, 1997).

A xantana, em solução, passa por uma transição conformacional irreversível de um estado ordenado e rígido para um estado mais desordenado e flexível (desnaturado), com o aumento da temperatura. Essa transição conformacional pode ser medida por algumas

técnicas analíticas como rotação óptica, reologia e calorimetria. A temperatura de transição é, ainda, função de alguns fatores como a concentração da goma e a força iônica do meio, mas geralmente ocorre até 50ºC (Urlacher & Noble, 1997). Além disto, Lee e Brant (2002) observaram uma outra transição que foi relacionada à transição de uma solução anisotrópica para uma isotrópica. Este último fenômeno mostrou-se dependente da temperatura e da concentração.
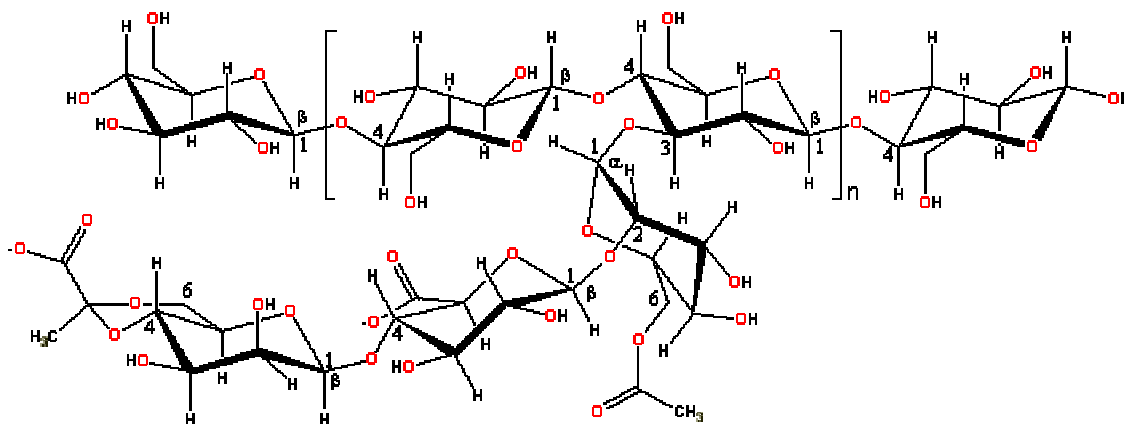
Figura 1. Estrutura molecular da xantana.

2.2. Alginato

Os alginatos são polissacarídeos aniônicos produzidos por algas marrons do gênero *Laminaria*. A sua estrutura primária consiste de uma cadeia principal não ramificada, com unidades de D-ácido manurônico (M) ligados em β-(1→4) e unidades de L-ácido gulurônico (G) ligados em α-(1→4). As unidades M e G são encontradas em blocos e estes ligam-se alternadamente, sendo predominante a sequência de dois ácidos iguais juntos (GGMM) como apresentado na Figura 2 (Capron *et al.*, 2001).
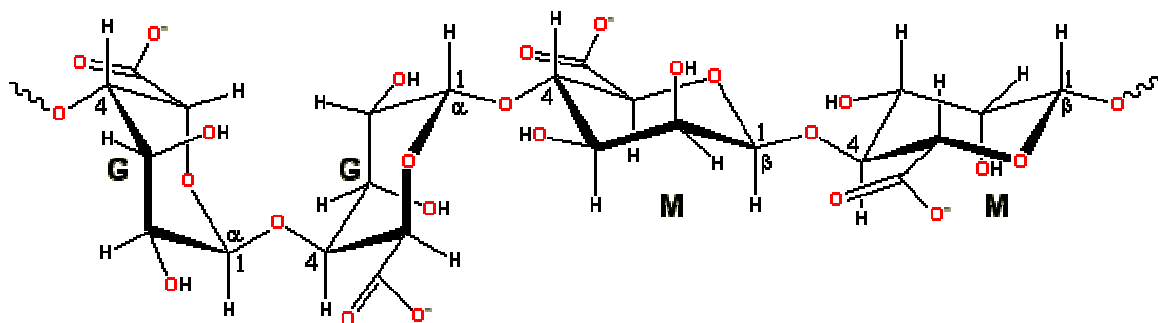
Figura 2. Estrutura molecular do alginato.

2.3. Carragena

Carragena é um termo utilizado para caracterizar um grupo de polissacarídeos extraídos alcalinamente de algas vermelhas, sendo os gêneros *Chondrus*, *Eucheuma*, *Gigartina* e *Iridaea* os mais utilizados para produção. As carragenas são biopolímeros lineares, sulfatados, com derivados de galactose na cadeia primária, sendo classificadas em três principais frações: λ-, ι- e κ-carragena. A κ-carragena é composta de unidades de D-galactose-4-sulfato unidas em α-(1$\rightarrow$3) e 3,6-anidro-D-galactose ligadas em β-(1$\rightarrow$4), que se alternam na cadeia (Figura 3). As carragenas apresentam moléculas muito flexíveis, sendo que a altas concentrações podem formar uma estrutura mais ordenada na forma de duplas hélices, a qual pode levar à formação de géis. A κ-carragena forma géis termorreversíveis a partir do ordenamento molecular com o resfriamento. A presença dos cátions K^+ e Ca^{2+} no sistema contribui tanto para induzir a gelificação a temperaturas mais elevadas, quanto para a formação de géis mais fortes (Chaplin, 2005).
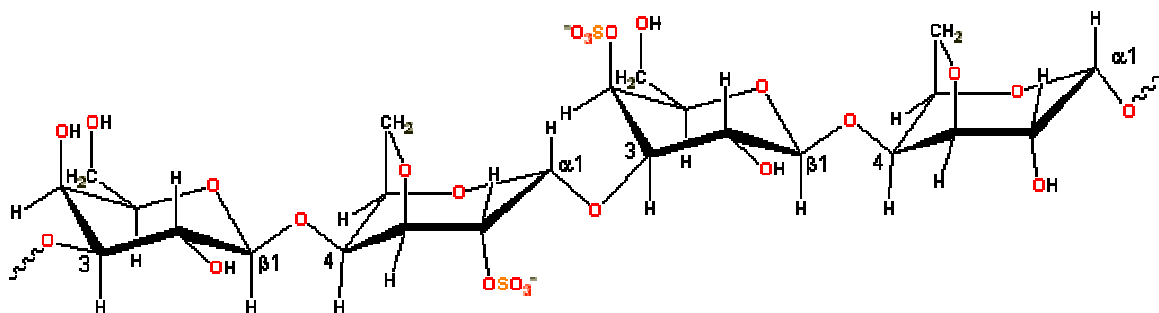
Figura 3. Estrutura molecular da carragena.

2.4. Gelana

A gelana é um polissacarídeo obtido a partir da fermentação bacteriana, com *Sphingomonas elodea*, de forma similar à xantana. Este biopolímero apresenta quatro sacarídeos em sua cadeia principal: L-ramnose ligada em (α−1→3), D-glicose ligada em (β−1→4), e duas unidades de D-ácido glucurônico (Figura 4). Este polímero possui um grupo lateral carboxílico em cada unidade repetida. Soluções de gelana com concentração maior que 1% apresentam transição sol-gel ao redor de 50 °C. Géis termorreversíveis podem ser formados em concentrações muito baixas (0,005% p/p) na presença de cátions (Chaplin, 2005).
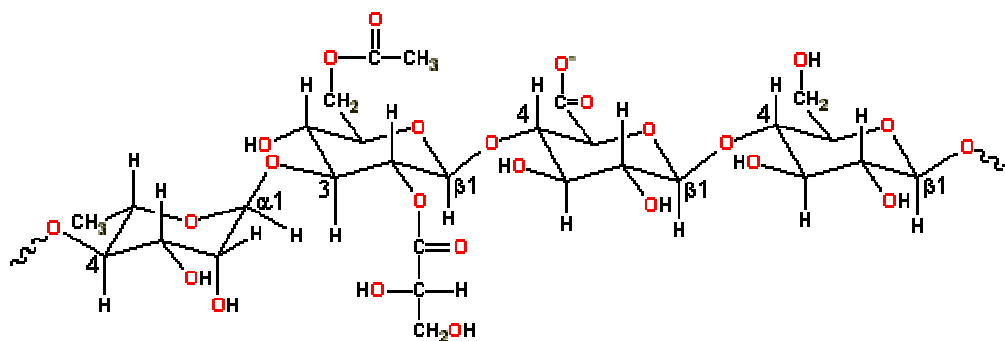
Figura 4. Estrutura molecular da gelana.

2.5. Jataí ou locusta (LBG)

Galactomananas, como a goma jataí (LBG) e goma guar, são biopolímeros hidrofílicos vastamente utilizados na indústria de alimentos como espessantes, estabilizantes e agentes de retenção de água. A goma jataí apresenta um alto peso molecular e é formada por uma cadeia principal de unidades de D-manose unidas por ligações β-(1-4), com diferentes graus de ramificações por grupos de D-galactose ligados em α-(1-6) (Figura 5). Assim, este polissacarídeo é caracterizado por ser neutro e polidisperso, com razão galactose/manose (G/M) igual a ¼ (Fox, 1992).
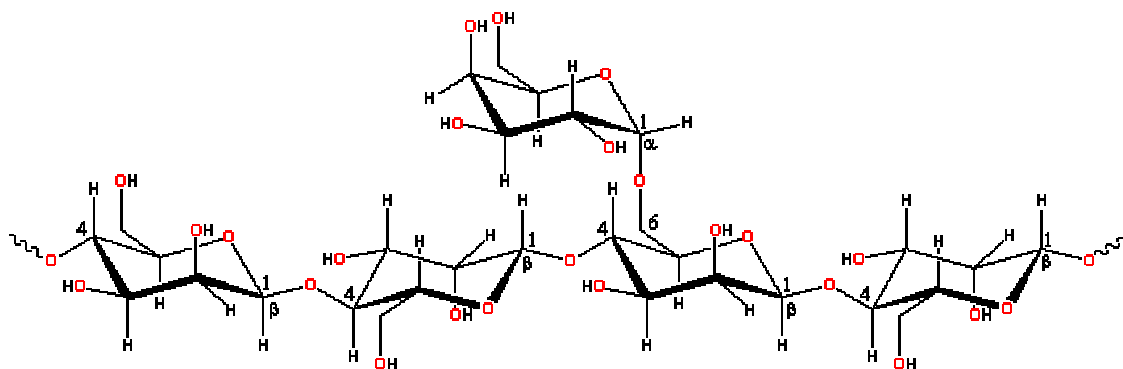
Figura 5. Estrutura molecular da LBG.

Polissacarídeos neutros geralmente apresentam uma baixa solubilidade em água devido à existência de um elevado número de pontes de hidrogênio, que estabilizam as interações intra e intermoleculares. A razão de galactose/manose (G/M) da molécula de jataí tem um papel importante na solubilidade deste polissacarídeo e na dependência da viscosidade da solução com a concentração do polímero. As propriedades físicas em solução são devidas a algumas contribuições das interações das cadeias ramificadas, e principalmente relativas à pouca flexibilidade da cadeia principal de manose (Rinaudo, 2001).

As galactomananas de baixo teor de D-galactose, como a goma jataí, são capazes de gelificar, sendo que as zonas de junção são formadas pela associação de segmentos não substituídos da cadeia principal. As regiões substituídas da molécula permanecem altamente hidratadas, o que impede a precipitação do polissacarídeo. A LBG é relativamente estável a variações de pH, força iônica e temperatura, sendo completamente hidratada entre 75 e 85°C e é capaz de conferir alta viscosidade ainda a baixas concentrações (Lundin e Hermansson, 1995).

3. Géis ácidos

Na indústria de laticínios, a acidificação é resultado da conversão da lactose em ácido lático pelas bactérias lácticas ou pela adição de reagentes químicos. No caso da acidificação direta, o reagente mais utilizado é a glucona-δ-lactona (GDL) que é um éster cíclico neutro produzido através da fermentação da glicose. O GDL é um cristal branco solúvel em água, com um leve sabor doce, e além de não ser tóxico é completamente metabolizado no organismo humano. Quando adicionado ao leite, o GDL se hidrolisa lentamente a ácido glucônico (Figura 6), seguindo uma cinética de primeira ordem (de Kruif, 1997):

$$[GDL]_t = [GDL]_0 \cdot e^{-kt} \tag{1}$$

onde, $[GDL]_0$ é a concentração inicial de GDL no momento da sua adição, $[GDL]_t$ é a concentração de GDL no tempo t e k é a velocidade de reação.

O ácido glucônico encontra-se sempre em equilíbrio com o GDL em solução, sendo que a velocidade desta reação depende da temperatura de processo e do pH da solução aquosa, ou seja, o tempo necessário para a coagulação ou floculação das micelas será maior quanto menor a temperatura de gelificação (de Kruif, 1997). A concentração residual de

GDL atinge 50% em apenas 20min a 60ºC, enquanto que a 20ºC esta atividade decai 10% no mesmo período de tempo.
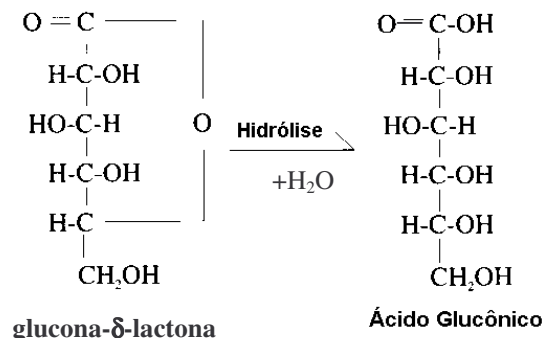
Figura 6. Hidrólise do GDL a ácido glucônico.

4. Interações entre Proteínas-Polissacarídeos

As interações que ocorrem entre proteínas e polissacarídeos são interessantes para melhorar algumas características funcionais das proteínas e estes sistemas são comumente encontrados em alimentos. Sistemas com mais de um biopolímero exibem comportamentos mais complexos do que misturas de polímeros sintéticos. Isto se deve ao fato de que os biopolímeros possuem um equilíbrio relacionado ao estado de ordem - desordem de conformação, além de apresentar transições e separações de fases em determinadas situações (Cèsaro *et al*, 1999). Interações entre polímeros resultam em incompatibilidade e formações complexas, sendo exceção a miscibilidade entre os componentes. O comportamento de uma solução com dois biopolímeros é controlado pelo balanço entre os efeitos entálpicos e a entropia do sistema (Syrbe *et al*, 1998).

Na presença de polissacarídeos, a temperatura de desnaturação de algumas proteínas é alterada ou a capacidade de formação dos géis é modificada. Em solução, as proteínas podem atrair e repelir os polissacarídeos dependendo da sua origem, do pH, da força iônica, da temperatura, da concentração ou do cisalhamento a que são submetidas (Delben e

Stefancich, 1997). Em um sistema ternário pode-se distinguir três possíveis situações de equilíbrio:

1. Incompatibilidade: ocorre a segregação dos biopolímeros. São formadas duas fases aquosas, imiscíveis, e cada espécie de biopolímero fica em uma das duas fases.

2. Coacervação: uma forte atração entre moléculas de dois tipos de biopolímeros geram formações complexas. São formadas duas fases aquosas distintas, sendo que uma das fases contém os dois polímeros e a outra fica sem polímeros.

3. Miscibilidade: ocorre quando a interação entre dois biopolímeros diferentes é similar à interação entre hidrocolóides de uma mesma espécie, ou seja, há uma miscibilidade instantânea (Syrbe *et al*, 1998).

5. Propriedades Reológicas de Alimentos

A reologia é definida como a ciência da deformação e do escoamento, que estuda a forma como os materiais respondem a uma tensão ou deformação aplicada. A reologia é amplamente usada na indústria de alimentos e exemplos de sua aplicação são: projetos de tubulações e equipamentos, determinação da funcionalidade de ingredientes no desenvolvimento de produtos, controle de qualidade, estudos de vida de prateleira e determinação da textura do alimento correlacionando ensaios de análise sensorial com medidas reológicas (Steffe, 1996).

Todo material apresenta uma resposta a uma força externa entre as duas extremidades do comportamento ideal: um sólido elástico e um líquido viscoso. O primeiro é descrito pela lei de Hooke, enquanto que um líquido viscoso ideal obedece à lei de Newton. No entanto, a maior parte dos alimentos comporta-se como um material viscoelástico, ou seja, dependendo da tensão aplicada e da escala de tempo, um corpo

sólido pode apresentar propriedades da fase líquida e um material líquido pode mostrar propriedades de um corpo sólido. O comportamento viscoelástico de alimentos vem sendo largamente estudado em reômetros que cisalham a amostra (força tangencial), enquanto que parâmetros reológicos em tração ou compressão (força normal) vem sendo cada vez mais utilizados na caracterização da textura de produtos alimentícios. Além disto, é possível a caracterização do produto a baixas ou altas deformações independentemente do tipo de força aplicada.

5.1. Ensaios em compressão uniaxial

Em ensaios de compressão uniaxial, uma determinada deformação (ε) é imposta e a resposta tensão normal (σ) é tomada em função do tempo. Esta deformação pode ser suficientemente elevada para levar à ruptura do material. No ponto de ruptura, pode-se determinar as propriedades que fornecem informações sobre as características do material e correlacioná-las com a textura do produto. A tensão (σ_H) e a deformação de Hencky (ε_H), definidas respectivamente pelas Equações 2 e 3, devem ser utilizadas em ensaios de ruptura com altos valores de deformação, porque consideram as modificações que o material passa durante o experimento:

$$\sigma_H = F(t) \cdot \left[H(t)/H_0 \cdot A_0 \right] \tag{2}$$

$$\varepsilon_H = -\ln\left[H(t)/H_0 \right] \tag{3}$$

onde $F(t)$ é a força [N], A_0 [m^2] e H_0 [m] são respectivamente a área e a altura iniciais da amostra e $H(t)$ é a altura no tempo t. As propriedades mecânicas do gel são determinadas através da curva de tensão *versus* deformação de Hencky, sendo o ponto de ruptura o valor máximo desta curva. A parte inicial da curva é linear, sendo o módulo de elasticidade, E, igual ao coeficiente angular.

27

Outro ensaio em compressão interessante é o de relaxação de tensões, no qual o material é submetido repentinamente a uma dada deformação (ε), ao mesmo tempo em que a tensão necessária para mantê-la constante ao longo do tempo é determinada. Como resultado obtém-se a função relaxação (E(t) em fluxo extensional), que é calculada como a razão entre a tensão e a deformação em qualquer instante t, enquanto a deformação permanece constante. Os materiais viscoelásticos relaxam sua estrutura ao longo do tempo chegando a uma tensão de equilíbrio, cujo valor depende da estrutura molecular do material. Alguns sólidos possuem um intervalo de viscoelasticidade linear muito pequeno e/ou apresentam muita sinerese, dificultando a análise do comportamento reológico nesta região. Assim, estes ensaios também podem ser realizados fora do intervalo de viscoelasticidade linear, porém a resolução matemática é bastante complexa ou é realizada através de relações empíricas (Peleg, 1979).

A relação empírica de Peleg (1979) é obtida a partir da normalização da curva de relaxação de tensões (Equação 4).

$$\left(\frac{\sigma_0 \cdot \tau}{\sigma_0 - \sigma(t)} \right) = k_1 + k_2 \cdot \tau \tag{4}$$

em que k_1 e k_2 são constantes, τ é o tempo de relaxação e $\sigma(t)$ é a tensão no tempo t. O parâmetro σ_0 é o valor máximo de tensão medido no início do ensaio.

O tempo de relaxação ($\tau_{0,75}$) para o momento em que $\sigma_\tau = 0,75\sigma_0$ é obtido pela relação abaixo (Equação 5):

$$\tau_{0,75} = \frac{k_1}{4 - k_2} \tag{5}$$

Derivando-se a Equação 1 e resolvendo a equação diferencial para a solução de valor zero tem-se a tensão residual assintótica, S_R, que equivale ao montante de tensão não relaxada ao final do ensaio (Equação 6):

$$S_R = 1 - \frac{1}{k_2}$$
(6)

5.2. Ensaios em cisalhamento

5.2.1. Propriedades reológicas a alta deformação

Grande parte das caracterizações reológicas é realizada em escoamento em estado estacionário, já que convencionalmente, a viscosidade é vista como a propriedade mais importante do material. A viscosidade representa a medida da resistência ao escoamento quando uma tensão de cisalhamento é aplicada. Quando um fluido Newtoniano é submetido a um escoamento, a viscosidade (η) é a constante de proporcionalidade entre a tensão (σ) e a taxa de deformação ($\dot{\gamma}$) (Barnes *et al*., 1989), como apresentado na Equação 7.

$$\sigma = \eta \cdot \dot{\gamma}$$
(7)

No entanto, em alimentos, diversos fluidos não seguem a lei de Newton, sendo então chamados de fluidos não-Newtonianos. A constante de proporcionalidade apresentada na Equação 7 passa a ser conhecida então como viscosidade aparente. No caso de fluidos não-Newtonianos a viscosidade é dependente da taxa de deformação, existindo diversos modelos reológicos para caracterizar tal fluido. Os tipos de curvas de escoamento obtidas pelos modelos mais simples e mais difundidos na literatura são apresentados na Figura 7.
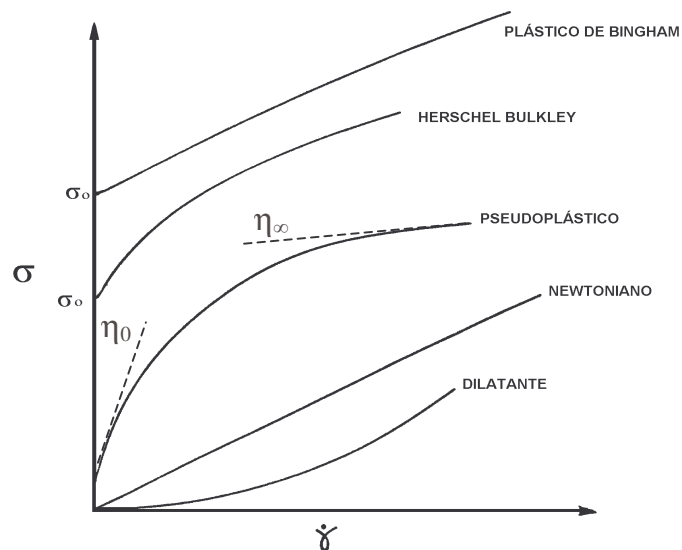
Figura 7. Curvas de escoamento para fluidos Newtonianos e não-Newtonianos.

As soluções de proteínas geralmente apresentam comportamento newtoniano enquanto que grande parte dos polissacarídeos tem comportamento tipo pseudoplástico, especialmente em soluções concentradas. Quando um fluido é pseudoplástico a viscosidade diminui com o aumento da taxa de deformação devido à orientação das moléculas na direção do escoamento o que torna a resistência ao escoamento cada vez menor (Barnes *et al.*, 1989). Fluidos que possuem algum tipo de estrutura, principalmente devido a formação de uma rede macromolecular podem mostrar regiões de viscosidade constante a baixas (η_o) e a altas (η_∞) taxas de deformação (Figura 7). O aparecimento destas regiões está relacionado com as mudanças na estrutura do material em função da taxa de deformação aplicada. Outros fluidos com comportamento não-Newtoniano enquadram-se como dilatantes, plásticos de Bingham e Herschel–Bulkley, sendo que os dois últimos apresentam tensão inicial de escoamento. O comportamento físico de fluidos com tensão inicial de escoamento é usualmente explicado em termos de sua estrutura interna, a qual é capaz de

impedir o movimento para valores de tensão de cisalhamento menores que um valor limite σ_o. Para σ maior que σ_o a estrutura interna colapsa, permitindo que haja escoamento. A estrutura interna pode recuperar-se quando σ passa a ser menor que σ_o (Barnes *et al.*, 1989).

Nos últimos anos, houve um grande desenvolvimento de reômetros a fim de obter-se o comportamento reológico tanto a mais baixas quanto a mais altas tensões de cisalhamento. Com isto, alguns parâmetros de difícil determinação passaram a ser mais estudados, como o η_0 e o η_∞. Roberts et al. (2001) estudaram a expansão de modelos existentes a fim de que todo o espectro da curva de escoamento fosse modelado.

5.2.2 Propriedades reológicas a baixa deformação

A análise de um material viscoelástico é bastante simples quando a razão entre a tensão e a deformação, em qualquer instante ou freqüência, é independente da magnitude de tensão ou deformação aplicada, sendo apenas função do tempo. Nestas condições, o material encontra-se dentro do intervalo de viscoelasticidade linear, pois se trabalha com deformações muito pequenas e a estrutura molecular praticamente não é afetada (Barnes *et al.*, 1989). Na caracterização da viscoelasticidade linear existem vários tipos de experimentos que determinam as relações entre tensão, deformação e tempo. Os mais importantes são os testes de fluência e recuperação (transiente), relaxação de tensões (transiente) e testes oscilatórios (dinâmicos).

Os ensaios oscilatórios em cisalhamento são particularmente úteis para caracterizar a conformação macromolecular e interações intermoleculares em solução. Em um experimento dinâmico ou periódico, uma tensão ou deformação oscilatória senoidal, a uma freqüência ω, é aplicada ao material, sendo medidas a amplitude e a diferença de fase entre

a tensão e a deformação oscilatórias. Nesses ensaios, a deformação (γ) varia com o tempo de acordo com a Equação 8:

$$\gamma = \gamma_0 \operatorname{sen} \omega\, t \tag{8}$$

onde γ_0 é a amplitude máxima de deformação. A tensão correspondente (σ), definida na Equação 9, pode ser representada como a soma dos componentes que estão em fase e 90° fora de fase com a deformação.

$$\sigma = \gamma_0 \left(G'(\omega) \operatorname{sen} \omega t + G''(\omega) \cos \omega t \right) \tag{9}$$

onde $G'(\omega)$ e $G''(\omega)$ são, respectivamente, os módulos de armazenamento e de dissipação de energia. Em um sólido elástico perfeito toda a energia é estocada, ou seja, G'' é zero e a tensão e a deformação estão em fase. Entretanto, para um líquido perfeitamente viscoso, no qual toda energia é dissipada na forma de calor, G' é zero e a tensão e a deformação estão 90° fora de fase. Portanto, G' é uma propriedade relacionada a eventos moleculares de natureza elástica enquanto que G'' refere-se a eventos moleculares de origem viscosa. Considerando o ângulo de fase (δ) entre a deformação e a tensão, a tensão correspondente à Equação 9, pode ser expressa da seguinte forma (Equação 10):

$$\sigma = \sigma_0 \operatorname{sen}\left(\omega t + \delta\right) \tag{10}$$

onde σ_0 é a amplitude máxima de tensão. As Equações 9 e 10 podem ser combinadas para obter-se os parâmetros reológicos G' (Equação 11), G'' (Equação 12) e $\tan\delta$ (Equação 13):

$$G'(\omega) = (\sigma_0/\gamma_0)\cos\delta \tag{11}$$

$$G''(\omega) = (\sigma_0/\gamma_0)\operatorname{sen}\delta \tag{12}$$

$$G''(\omega)/G'(\omega) = \tan\delta \tag{13}$$

Experimentos em reologia dinâmica são adequados para monitorar o processo de gelificação e definir a estrutura de um gel. Este método satisfaz várias condições: 1) não é destrutivo e não interfere na formação do gel; 2) o tempo envolvido nas medidas é relativamente pequeno e 3) os resultados são expressos em propriedades fundamentais.

A descrição do processo de gelificação é entendida experimentalmente a partir de ensaios reológicos a baixas deformações e vem sendo realizada a partir de diferentes aproximações por diversos autores (Tobitani e Ross-Murphy, 1997; Clark *et al*., 2001). Uma controvérsia freqüentemente encontrada é com relação à definição de um critério reológico para a determinação do ponto de gel. Um dos critérios mais utilizados é o da igualdade dos módulos de armazenamento (G') e de dissipação de energia (G"), porém outros critérios que vêm sendo adotados são: o momento em que o módulo de armazenamento começa a crescer rapidamente (Ikeda e Nishinari, 2001) ou em que a taxa de aumento deste módulo apresenta o primeiro decréscimo (Gosal e Ross-Murphy, 2000). Entretanto, um critério mais rigoroso formulado por Winter e Chambon (1986), no qual a razão G"/G' independe da freqüência no ponto de gel, ainda é pouco aplicado em alimentos (Braga, 2002) por ser de difícil execução experimental (Tobitani e Ross-Murphy, 1997). Segundo este critério, o comportamento da relaxação de tensões de um sistema polimérico segue a lei da potência (Equação 14) no ponto de gel:

$$G(t) = St^{-n} \tag{14}$$

onde $S = G_0\lambda_0^{n}$ é a força do gel, que depende da flexibilidade das cadeias moleculares e das ligações (o módulo G_0 e o menor tempo de relaxação λ_0 são parâmetros característicos do material) e *n* é o expoente de relaxação, que possui valores entre 0 e 1. Os módulos

33

dinâmicos G' e G'' também podem ser deduzidos a partir da Equação 14 e correlacionados com o expoente de relaxação n (Equação 15):

$$G'(\omega) = \frac{G''(\omega)}{\tan\delta} = S\,\omega^n\,\Gamma(1-n)\cos(\frac{n\pi}{2}), \qquad 1/\lambda_0 > \omega > 0 \qquad (15)$$

na qual ω é a freqüência angular, Γ é a função gama de Euler, G' e G'' são, respectivamente, os módulos de armazenamento e de dissipação e δ é o ângulo de fase.

Assim, a gelificação coincide com o momento no qual a dependência das propriedades viscoelásticas com a freqüência segue uma relação do tipo lei da potência com o mesmo expoente n e $\tan\delta$ possui o mesmo valor, independente da freqüência analisada (Equação 16).

$$\tan\delta = \tan(\frac{n\pi}{2}) \qquad (16)$$

A igualdade das curvas de $\tan\delta$ pode ser obtida através de ensaios reológicos em função do tempo a diferentes freqüências ou de um ensaio de reologia de múltiplas freqüências (multi-wave), no qual uma tensão senoidal composta (Equação 17) é aplicada à amostra:

$$\sigma = \sum_{i=0}^{m} \sigma_i \,\mathrm{sen}(\omega_i t) \qquad (17)$$

onde $\omega_1 = \omega_f$; $\omega_2 = n_2\omega_f$; $\omega_3 = n_3\omega_f$, sendo que o índice f refere-se à freqüência fundamental e i ao número de termos da somatória.

A tensão aplicada é a soma da série de Fourier das tensões individuais, sendo que esta soma deve ser menor do que a amplitude crítica, σ_c, dada pelo intervalo de viscoelasticidade linear. A deformação a cada freqüência, e, portanto G' e G'', são obtidos pela técnica conhecida como Espectroscopia Mecânica com Transformada de Fourier.

6. Difração de luz

6.1. Ensaios reo-ópticos (Small angle light scattering– SALS)

Há décadas sabe-se que durante o escoamento de um material as microestruturas dispersas neste são de alguma forma alteradas pelo cisalhamento. Como é grande a dificuldade de trabalhar-se com sistemas multifásicos, originalmente Taylor (1932) estudou a deformação de uma única gota em cisalhamento. Esse estudo mostrou que uma gota sob ação do cisalhamento foi extendida ao formato de um filamento até que esse quebrou-se em uma série de gotas de tamanhos iguais quando o cisalhamento foi interrompido. Um estudo teórico deste fenômeno foi realizado por Tomotika (1935), que demonstrou que um filamento líquido em uma matriz viscosa desintrega devido a ação da instabilidade de Rayleigh na interface. Tomotika (1935) também mostrou que a taxa de crescimento e o comprimento de onda da instabilidade são função apenas da razão de viscosidades entre as fases dispersa e contínua, da tensão interfacial e do raio inicial do filamento. Atualmente, os estudos conduzidos por Taylor (1932) e Tomotika (1935) vêm sendo utilizados para descrever as alterações morfológicas ocorridas na fase dispersa de sistemas biopoliméricos, bem como para quantificar sua tensão interfacial (van Puyvelde et al., 2002; Guido et al., 2002).

Grande parte dos estudos em soluções aquosas biopoliméricas são conduzidos através do cisalhamento de uma gota (Guido et al., 2002). Sistemas biopoliméricos multifásicos (por exemplo, emulsão água-água) têm sido investigados a partir do uso da técnica de "Small angle light scattering" (SALS) (van Puyvelde et al., 2002), a qual fornece informações sobre estruturas da ordem micrométrica. Desde a década de 90, esta técnica tem sido utilizada para o estudo de materiais poliméricos. Recentemente, alguns grupos de

pesquisa desenvolveram instrumentos a partir da combinação da técnica de SALS com um reômetro (Reo-SALS), tendo ainda em alguns casos um microscópio acoplado. Assim com um Reo-SALS é possível investigar, ao mesmo tempo, desde as propriedades reológicas do sistema, a tensão interfacial, o grau de anisotropia da estrutura deformada, o diâmetro médio da gota, os comportamentos de quebra e coalescência de gotas até a formação de estruturas complexas como micelas. O esquema de um Reo-SALS é mostrado na Figura 8.
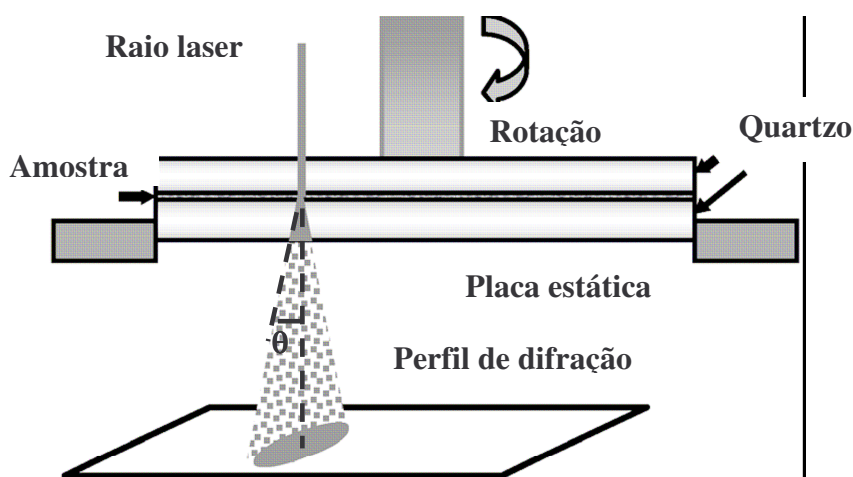
Figura 8. Desenho esquemático da técnica Reo-SALS.

O instrumento Reo-SALS consiste de um reômetro modificado para passagem de um raio laser pela amostra. A geometria do reômetro é de quartzo e geralmente são utilizadas placas paralelas ou cilíndros concêntricos, sendo que a última aumenta em muito a complexidade do sistema pela necessidade do uso de lentes focalizadoras após a luz passar pela amostra. A luz é propagada pela amostra sendo, então, difratada e interceptada por uma tela feita de plástico semi-transparente com um papel preto no centro para absorver a luz transmitida no eixo principal (ângulo igual a 0). A imagem resultante é gravada por

uma câmera CCD localizada abaixo da tela de plástico e conectada a um computador. Assim, a intensidade de luz espalhada pode ser analisada em função do ângulo θ (entre a luz espalhada e o eixo principal). Em instrumentos com placas paralelas, a luz é propagada na direção da variação de velocidade (direção do "gap"), sendo que a estrutura é obtida no plano do escoamento (direção do cisalhamento) e neutro (direção do raio da geometria). Quando cilindros concêntricos são utilizados, a luz é propagada na direção neutra e a estrutura é observada no plano do escoamento e da variação de velocidade.

A luz espalhada é analisada na faixa do ângulo θ entre 2° e 12°, o que significa uma faixa de valor absoluto do vetor q de espalhamento (vetor entre o ponto central e a borda da figura obtida, calculado em qualquer direção do plano e com sentido indicando para a borda da figura) entre 0,3 – 2 μm^{-1}. O valor absoluto do vetor de espalhamento é definido na Equação 18:

$$q = \left(\frac{4\pi}{\lambda}\right) \cdot \mathrm{sen}\left(\frac{\theta}{2}\right) \tag{18}$$

onde λ é o comprimento de onda do laser e θ é o ângulo de espalhamento de luz.

A Figura 9 mostra alguns exemplos de estrutura obtidos por SALS (Figura 9A) e o respectivo esquema microscópico (Figura 9B). Podem ser definidos cinco regimes de comportamento da fase dispersa com a aplicação de cisalhamento. O regime I (não apresentado) refere-se ao momento inicial da amostra em repouso e é similar ao regime II. No regime II, o perfil de espalhamento é circular, o que é típico de estruturas isotrópicas e neste regime o nível de cisalhamento é muito pequeno (valor dependente da amostra). No regime III, a luz espalhada assume uma forma similar a uma elipse com os tamanhos dos eixos sendo dependentes do cisalhamento empregado. A elipse apresenta-se com o eixo maior na direção perpendicular ao escoamento (Figura 9A), o que corresponde a uma fase

dispersa elongada na direção do escoamento (Figura 9B). No regime IV, o perfil de luz obtido apresenta-se como filamentos perpendiculares à direção do escoamento, sugerindo que a fase dispersa elongada (regime III) transformou-se em uma estrutura percolada orientada na direção do escoamento. Além disto, o tamanho lateral da fase elongada e o contraste entre as duas fases diminui com o aumento da taxa de deformação (Figura 9B, d). O regime V é caracterizado pela formação de uma fase / homogeneização do sistema induzida pelo alto cisalhamento. Neste caso, o perfil de SALS não apresenta nenhuma luz espalhada (Kume et al., 1995).
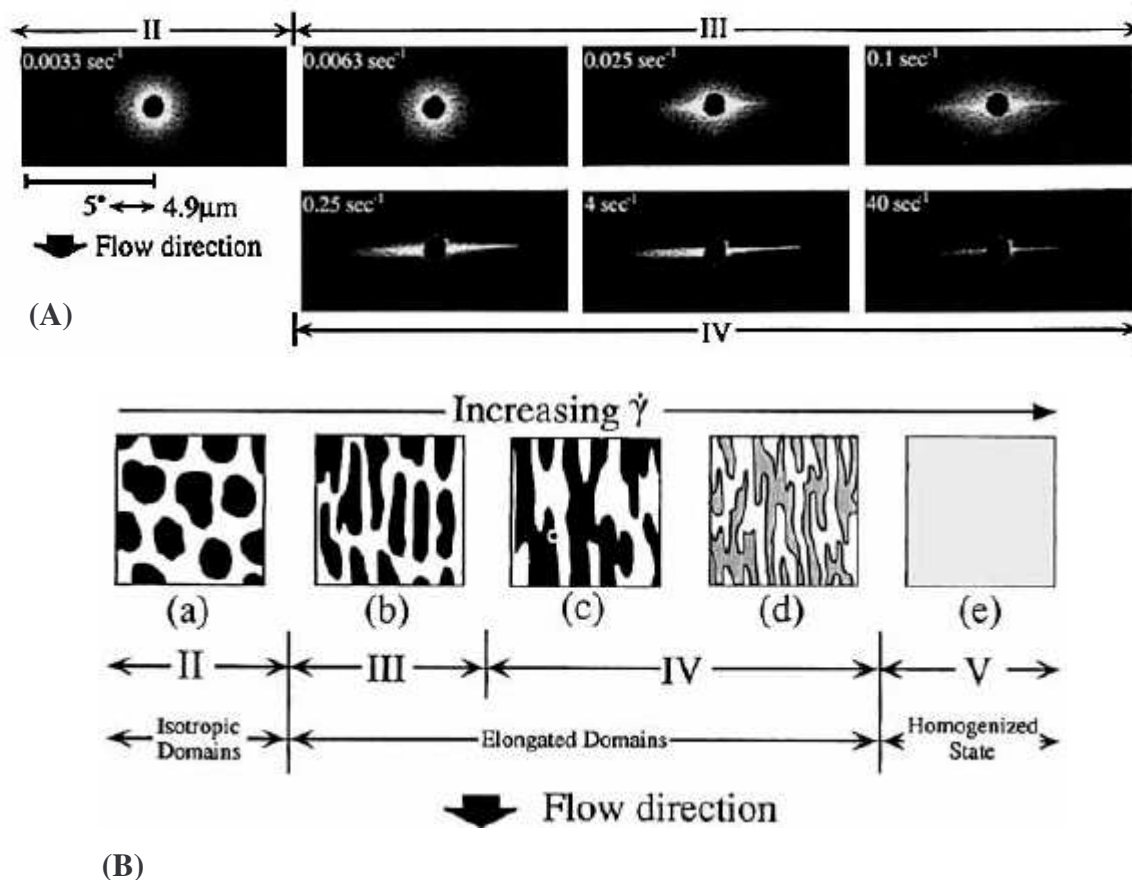
Figura 9. (A) Perfil de SALS e (B) esquema da microestrutura de sistemas poliméricos bifásicos sob cisalhamento. Os regimes II, III e IV são obtidos para taxa de deformação menor do que a crítica para mistura (Kume et al., 1995).

7. Referências

BADLEY, R. A.; ATKINSON, D.; HAUSER, H.; OLDANI, D.; GREEN, J. P. & STUBBS, J. M. The Structure, physical and chemical properties of the soy protein glycinin. **Biochimica and Biophysica Acta**. v.412, p.214-228, 1975.

BARNES, H.A.; HUTTON, J.F.; WALTERS, K. **An introduction to rheology.** Amsterdam: Elsevier Science Publishers, 199 p, 1989.

BRAGA, A. L. M. **Caracterização das interações macromoleculares em géis ácidos de caseína-xantana-sacarose: análises reológicas e térmica**. Campinas, 2002. Dissertação (Mestrado em Engenharia de Alimentos) - Universidade Estadual de Campinas.

CAPRON, I.; BRIGANDT, G.; MULLER, G. About the native and renatured conformation of xanthan exopolysaccharide. **Polymer**, v. 38, p. 5289-5295, 1997.

CAPRON, I.; COSTEUX, S.; DJABOUROV, M. Water in water emulsions: phase separation and rheology of biopolymer solutions. **Rheologica Acta**. v.40, p.441-456, 2001.

CÈSARO, A.; CUPPO, F.; FABRI, D.; SUSSICH, F. Thermodynamic Behavior of mixed biopolymers in solution and in gel phase. **Thermochimica Acta,** v. 388, p. 143-153, 1999.

CHAPLIN, M., **Polysaccharide Hydration**. http://www.sbu.ac.uk/water/hydrat.html. 01/07/2005.

CHEFTEL, J. C.; CUQ, J. L.; LORIENT, D. **Proteinas Alimentarias: Bioquímica, Propriedades funcionales, Valor nutritivo, Modificaciones químicas**. Editorial Acribia, Zaragoza, p.179-220, 1989.

CLARK, A. H.; KAVANAGH, G. M.; ROSS-MURPHY, S. B. Globular protein gelation – theory and experiment. **Food Hydrocolloid**, v. 15, p. 383-400, 2001.

DE KRUIF, C.G. Skim milk acidification. **Journal of Colloid and Interface Science.** v. 185, p. 19-25, 1997.

DELBEN, F.; STEFANCICH, S. Interaction of Food Proteins with Polysaccharides I: properties upon Mixing. **Journal of Food Engineering.** v. 31, p. 325-346, 1997.

FOX, J. E. Seed Gums In: **Thickening and gelling agents for food**. Ed. A. Imenson., Chapman and Hall, Londres, Inglaterra, p.153-170, 1992.

GOSAL, W. S.; ROSS-MURPHY, S. B. Globular Protein Gelation. **Current Opinion in Colloid & Interface Science.** v.5, p. 188-194, 2000.

GUIDO, S.; SIMEONE, M.; ALFANI, A. Interfacial tension of aqueous mixtures of Na-caseinate and Na-alginate by drop deformation in shear flow. **Carbohydrate Polymers.** v.48, p.143–152, 2002.

HERMANSSON, Soy Protein Gelation. **Journal of American Oil Chemists Society**. v. 63, p.658-666, 1986.

IKEDA, S.; NISHINARI, K. On solid-like rheological behaviors of globular proteins solution. **Food Hydrocolloids.** v. 15, p. 401-406, 2001.

KATZBAUER, B. Properties and applications of Xanthan gum. **Polymer Degradation and Stability.** v. 59, p. 81-84, 1998.

KINSELLA, J. E. Funcional Properties of Soy Proteins. **Journal of American Oil Chemists Society.** v. 56, p. 242-258, 1979.

KUME, T.; ASAKAWA, K.; MOSES, E.; MATSUZAKA, K.; HASHIMOTO, T. A new apparatus for simultaneous observation of optical microscopy and small-angle light scattering measurements of polymers under shear flow. **Acta Polymer**. v.46, p.79-85, 1995.

LEE, H.C.; BRANT, D.A. Rheology of concentrated isotropic and anisotropic xanthan solutions: 3. Temperature dependence. **Biomacromolecules**, v. 3, p. 742-753, 2002.

LUNDIN, L.; HERMANSSON, A. Supermolecular aspects of xanthan-locust bean gum gels based on rheology and electron microscopy. **Carbohydrate Polymers.** v. 26, p. 129-140, 1995.

PELEG, M. Characterization of the stress relaxation curves of solid foods. **Journal of Food Science.** v. 44, p. 277-281, 1979.

RINAUDO, M. Relation between the molecular structure of some polysaccharides and original properties in sol and gel states. **Food Hydrocolloids.** v. 15, p. 433-440, 2001.

ROBERTS, G.P.; BARNES, H.A.; CAREW, P. Modelling the flow behaviour of very shear-thinning liquids. **Chemical Engineering Science**. v. 56, p. 5617-5623, 2001.

SGARBIERI, V. C. **Proteínas em alimentos protéicos: propriedades, degradações e modificações**. Livraria Varela Ltda, São Paulo, p.139-157, 1996.

STEFFE, J.F. **Rheological Methods in Food process Engineering.** Freeman Press, East Lansing, p. 1-93, 1996.

SYRBE, A.; BAUER, W.J.; KLOSTERMEYER, H. Polymer Science Concepts in Dairy Systems – An Overview of milk protein and food hydrocolloid interaction. **International Dairy Journal.** v. 8, p. 179-193, 1998.

TAYLOR, G.I. The viscosity of a fluid containing small drops of another fluid. **Proceedings of the Royal Society of London.** v. A138, p. 41-48, 1932.

TOBITANI, A.; ROSS-MURPHY, S. B. Heat-induced gelation of globular proteins. 1. Model for the effects of time and temperature on the gelation time of BSA gels. **Macromolecules**, v. 30, p. 4845-4854, 1997.

TOMOTIKA, S. On the instability of a cylindrical thread of a viscous liquid surrounded by another viscous fluid. **Proceedings of Royal Society of London.** v.A150, p.322-337, 1935.

URLACHER, B.; NOBLE, O. Xanthan gum. In **Thickening and Gelling Agents for food,** 2 ed., Ed. A. Imenson, Blackie Academic and Professional, Londres, p. 284-311, 1997.

VAN PUYVELDE, P.; ANTONOV, Y.A.; MOLDENAERS, P. Rheo-optical measurement of the interfacial tension of aqueous biopolymer mixtures. **Food Hydrocolloids**, v.16, p.395-402, 2002.

WINTER, H.H.; CHAMBON, F. Analysis of linear viscoelasticity of a crosslinking polymer at the gel point. **Journal of Rheology**, v. 30, p. 367-382, 1986.

WOLF, W. J.; BABCOCK, G. E. & SMITH, A. K. Ultracentrifugal differences in soybean protein composition. **Nature**, v. 191, p. 1395-1396, 1961.

CHAPTER 3. Rheological properties of biopolymers aqueous solutions.

1ˢᵗ PART: Physical properties of pure proteins and polysaccharides aqueous solutions.

(in collaboration with LMVT-ETHZ-Switzerland)

Abstract

The aim of this work was to examine the physical properties of seven biopolymers (proteins and polysaccharides) aqueous solutions widely used in the food industry. The polysaccharides investigated were xanthan, LBG, gellan, κ-carrageenan and Na-alginate, while sodium caseinate and soy protein isolate (SPI) were the proteins source. The proteins solutions showed Newtonian behaviour for all concentrations studied, while the polysaccharides exhibited either Newtonian or non-Newtonian behaviour depending on its type and solution concentration. The biopolymers solutions showed different trends for density and apparent viscosity values depending on the biopolymer type (protein and polysaccharide) and of the biopolymer source. For a given concentration and shear rate, the increase of apparent viscosity and the reduction of density of the biopolymer solution followed the order: 1) proteins, 2) microbial polysaccharides (xanthan and gellan), 3) plant seeds polysaccharide (LBG) and 4) seaweeds polysaccharides (Na-alginate and κ-carrageenan). The determined critical overlap concentration (C*) value was not observed for microbial polysaccharides, but increased in the following order for the others biopolymers studied: LBG<Na-alginate<κ-carrageenan<Na-caseinate<SPI.

Key-words: proteins, polysaccharides, physical properties.

1. Introduction

Water-soluble high molecular weight polysaccharides or proteins are biopolymers that serve a variety of functions in food systems, such as enhancing viscosity, creating gel-structures, formation of a film, control of crystallization, inhibition of syneresis, improving texture, encapsulation of flavors and lengthening the physical stability, etc. (Dickinson, 2003). These functional ingredients are widely used in dairy products, canned foods, bakery

products, salad dressings, beverages, sauces, soups and other processed foodstuffs to improve textural characteristics, flavour and shelf life.

A variety of proteins used in food industry as ingredients can be obtained from animals or legume seeds. Soy proteins are the most important representative of legume proteins due to their high protein level and well-balanced amino-acid composition (Van Vliet et al., 2002). The soy protein fractions can be classified by their sedimentation constants, showing approximate Svedberg coefficients of 2S, 7S, 11S and 15S. The two major globulins in soybeans are β-conglycinin and glycinin, also called 7S and 11S, respectively. Milk is a colloidal emulsion of protein particles, with casein being the main protein (~80%). Four main types of casein, α_{S1}-,α_{S2}, β- and κ-casein, can be distinguished in milk and are present in a mass ratio of about 4:1:4:1.3. All casein in milk occurs in micelles, which are fairly large particles of colloidal size (Walstra and Jenness, 1984). However, the micellar structure of casein is destroyed during the manufacture of sodium caseinate (Kinsella, 1984). Na-caseinate is an ingredient widely used in a range of food formulations because of its nutritional value and functional properties.

Many gums are extracted from plants, others from seaweeds or microbial fermentation. Locust bean gum (LBG) is a galactomannan extracted by grinding the endosperm portions of the seeds of the legume plant *Ceretonia siliqua* L. Galactomannans are neutral polysaccharides composed of linear main chains. Physico-chemical properties of galactomannans are strongly influenced by the galactose content (Morris, 1990) and the distribution of the galactose units along the main chain (Launay et al., 1986). LBG solutions are almost completely unaffected by pH or heat processing due to its neutral character (Glicksman, 1969).

The two most used seaweeds polysaccharides in the food industry are carrageenans and alginates. Carrageenans are a family of polymeric sulphated galactans extracted from various species of red seaweed and they are extensively used for their ability to form thermoreversible gels in water or aqueous salt solutions (Chaplin, 2005). Alginates are linear polysaccharides produced as a structural component in marine brown algae. The sequence of the alginate chain in terms of the sugar monomers β-D-mannuronate (M) and a-L-guluronate (G) influences the viscosity and also determines the ability of the molecule to form gels with divalent cations (Moe et al., 1995).

Gellan gum is an anionic extracellular polysaccharide produced by fermentation of *Sphingomonas elodea*. It has been a subject of interest since its discovery in the 1980s (Kang et al., 1982). Gellan is well-known due to its gelling capacity at high concentrations or in the presence of cations. Different gel characteristics can be obtained by varying the degree of acylation, as well as the type and concentration of cations. Xanthan is also an anionic polysaccharide produced by the bacterium *Xanthomonas campestris*. In the majority of food applications, its primary function is as viscosity enhancer (Speers and Tung, 1986). The changes in composition, mainly the extent of acetylation and pyruvylation, affect properties of xanthan solutions (Sutherland, 1994). A wide range of different behaviours may be obtained for each biopolymer due to the variation of composition with the source or processing conditions.

The rheological properties of fluid food should be carefully taken into account for designing and modeling purposes. Calculations in the processes involving fluid flows such as pump sizing, extraction or filtration requires the knowledge of large strain-rheological data (Marcotte et al., 2001). Polysaccharide solutions are generally non-Newtonian shear-

thinning fluids as the apparent viscosity decreases with increasing shear rate. Several models have been used to characterize the flow behavior of gum solutions and among them power law model has been frequently used for the determination of rheological properties of the fluid food. The knowledge of the viscous properties of biopolymer solutions in the low shear rate Newtonian domain is of practical value for predicting their efficiency as thickeners in liquid foods or as stabilizers in dispersed systems. Such characteristics could be obtained from the relation between the Newtonian viscosity data and the biopolymer concentration in order to predict a diluted (C*) and semi-diluted (C**) critical concentration regions (Launay et al., 1997).

The concentration of the biopolymer, and consequently the existence of entanglements is of particular importance on the rheological behaviour and other physical properties of the systems, as density. The aim of this work was to determine the rheological properties and density of seven biopolymers aqueous solutions of great application in the food industry. The polysaccharides investigated were xanthan, LBG, gellan, κ-carrageenan and Na-alginate, while sodium caseinate and soy protein isolate (SPI) were the proteins source.

2. Material and methods

2.1. Material

The proteins used to prepare the model systems were casein (Sigma Chemical Co., USA) and soy protein isolate (SPI) obtained from defatted soy flour (Bunge Alimentos S.A., Brazil). The polysaccharides used were sodium (Na)-alginate, κ-carrageenan, and gellan obtained from CP Kelco (USA) and xanthan and LBG purchased from Sigma Chemical Co. (USA). The moisture contents (% w/w) of casein, SPI, xanthan, LBG, Na-

alginate, κ-carrageenan, gellan were, respectively, 6.51 ± 0.10, 6.44 ± 0.07, 8.36 ± 0.23, 5.44 ± 0.01, 5.75 ± 0.21, 7.84 ± 0.07 and 6.42 ± 0.12.

The soy proteins isolation procedure followed the method described by Petruccelli and Añón (1995). Defatted soy flour was dispersed in distilled water (1:10 w/w) and the pH was adjusted to 8.0 with 2N NaOH. The dispersion was gently stirred for 2h at room temperature and then centrifuged at 10,000 x g for 30 min at 4ºC in a Sorvall RC5 Plus centrifuge (GSA-rotor, Dupont, UK). The supernatant was adjusted to pH 4.5 with 2N HCl and centrifuged at 5,000 x g (Sorvall GSA-rotor) for 15 min at 4ºC. The precipitate was then suspended in water and the pH adjusted to 8.0 with 2N NaOH, followed by freeze-drying of the suspension. The protein (N x 6.25) and ash contents of the powder were, respectively, 91.25 ± 0.45 and 3.45 ± 0.04.

2.2. Preparation of biopolymers stock solutions

The Na-caseinate solution was prepared by dispersing casein powder in milli-Q water using magnetic stirring for 2 h at a maximum temperature of 50°C. The pH was constantly adjusted to 7.0 with 10M NaOH. The soy protein isolate (SPI) solution (milli-Q water) was prepared at room temperature by magnetic stirring until the complete powder hydration and the pH was adjusted to 7.0 with 1M HCl. The polysaccharide solutions were prepared by dispersing the powders in milli-Q water at room temperature by magnetic stirring, then heating in a water bath with a fixed temperature and time (Table 1). The prepared solutions were immediately cooled down to room temperature in an ice bath, and none of them gelified after this process. The insoluble particles of proteins and polysaccharides solutions were separated by centrifugation in a Sigma centrifuge 3K30 (rotor no 33310 – Sigma Laborzentrifugen GmbH, Germany) at 60,000 x g for 60 minutes

_____

at 25°C (Antonov et al., 2004), except for κ-carrageenan and gellan solutions that were already purified (without any insoluble particles). The pH of all solutions were adjusted to 7.0. The concentration of proteins solutions varied in the range of 1-10% (w/w), while the range of polysaccharides concentrations was 0.1-4% (w/w).

Table 1. Temperature and time used to prepare the polysaccharide solutions.

Polysaccharide	Temperature (°C)	Time (min)
Xanthan (Braga and Cunha, 2004)	25	60
Na-Alginate (Capron et al., 2001)	70	30
LBG (Schorsch et al., 1999)	80	30
Gellan (Ikeda et al., 2004)	90	60
κ-carrageenan (Hemar et al., 2002)	90	60

2.3. Physical properties

The density and the steady state rheological properties were obtained for each biopolymer solution at different concentrations at 25°C. Density data were obtained in triplicate in an oscillating tube densimeter DM38 (Anton Paar, Austria).

The apparent viscosity (η) as a function of shear stress was determined in triplicate using a stress-controlled rheometer (MCR 300, Paar Physica, Austria). A double wall concentric cylinder was used and the external diameter of the rotating bob was 13.3 mm, while the internal diameter was 12.8 mm. The stationary cylinder had an internal diameter of 12.3 mm and an external diameter of 13.8 mm. The measurements were done at 25°C in duplicate. Flow curves were obtained by an up-down-up steps program using different shear stress range to each sample. This range was determined from a shear rate-control experiment, in which the maximum shear rate was 300 s^{-1}. The last step (steady state flow)

was taken for further data analysis. Flow properties were described by the power-law fitting to rheological data (Equation 1).

$$\sigma = k\dot{\gamma}^{n}$$ (1)

where $\dot{\gamma}$ is the shear rate (s^{-1}); s is the shear stress (Pa); k is the consistency index ($Pa.s^{n}$) and n is the flow behavior index. The latter allows to distinguish whether the solution behaves as a Newtonian (n = 1) or non-Newtonian liquid (n<1).

The critical overlap concentration (C*) was determined by plotting specific viscosity (η_{sp}) as a function of concentration on logarithmic axes as described by Morris et al. (1981). The inflection point of the curve was taken as an indicative of C*. The specific viscosity was determined by the ratio of the Newtonian viscosities of the solution and solvent as described by Equation 2.

$$\eta_{sp} = \left(\frac{\eta}{\eta_{solv}}\right) - 1$$ (2)

where η_{solv} is the solvent viscosity, which is 0.001 Pa.s for water at 25 ^{o}C.

3. Results and discussion

3.1. Density

The knowledge of the physical properties is important in order to characterize the biopolymer solution and to predict and gain information of the mixed solution behaviour. Antonov et al. (2004) and Scholten et al. (2002) have shown that the density difference between two coexisting phases of a protein-polysaccharide mixture give information about the interfacial tension of the mixture. The density of pure biopolymer solutions as a function of concentration is shown in Equations 3 (R^2=0.999), 4 (R^2=0.986) and 5

(R²=0.996). It was found three behaviours for the different kind of biopolymers, such that the density of all proteins could be represented by Equation 3 and the density of microbial polysaccharide followed the relation described in Equation 4, while the density of plant and seaweeds polysaccharides are described by Equation 5. The different slopes observed by comparing Equations 3-5 could be attributed to two possible factors working either separately or concomitantly: (i) the differences in the molecular weight; (ii) a different reduction of the solution volume with the increase of the concentration, as a result of the molecular structures at low concentration and molecular assemblies/network formed in concentrated solutions. Regarding the polysaccharides, the second factor seemed to influence more the concentration dependence of density, since carrageenan (Equation 5) and xanthan (Equation 4) have the two greater molecular weights and they showed different behaviour. From the slope of Equations 4 and 5 it can be supposed that microbial polysaccharides entrap less solvent than plant and seaweeds biopolymers at the studied concentrations. This is in agreement with the non-gelling ability of xanthan and also of gellan at concentrations less than 10 g/L, instead they show assemblies formation (Miyoshi et al., 1996).

$$\rho_{PR} = 3 \cdot C_{PR} + 996 \quad , 10 < C_{PR} < 100 \ g/L \tag{3}$$

$$\rho_{X,G} = 4 \cdot C_{X,G} + 996 \ , \ 1 < C_X < 20 \ g/L \ \text{and} \ 2 < C_G < 8 \ g/L \tag{4}$$

$$\rho_{C,A,LBG} = 5 \cdot C_{C,A,LBG} + 996 , 1 < C_C < 40 \ g/L , 1 < C_A < 30 \ g/L \ \text{and} \ 1 < C_{LBG} < 20 \ g/L \tag{5}$$

where ρ is the density, C is the concentration (g/L) and the subscripts PR, X, LBG, A, C and G correspond to, respectively, protein, xanthan, locust bean gum, alginate, κ-carrageenan and gellan.

3.2. Rheological properties

The flow curves, at 25°C, of the seven studied biopolymers are shown in Figure 1. The two proteins (Figure 1a) showed Newtonian behaviour for all concentrations studied (1-10%). At low concentration, the viscosities of both proteins solutions were similar, but for a 10% protein solution the Na-caseinate sample showed a 10 fold greater viscosity as compared to SPI sample. The polysaccharides showed either Newtonian or non-Newtonian behaviour depending on its type and solution concentration. Figures 1B-1C show that at low concentration, κ-carrageenan, Na-alginate and LBG behaved as Newtonian fluids. The transition to the non-Newtonian behaviour for κ-carrageenan (Figure 1b), Na-alginate (Figure 1c) and LBG (Figure 1d) occurred, respectively, at 2.5%, 1.5% and 0.5%. In contrast, gellan (Figure 1e) and xanthan (Figure 1f) showed non-Newtonian behaviour even for the lowest concentration studied, 0.2% and 0.1%, respectively. The apparent viscosities (η) of microbial polysaccharides (xanthan and gellan) were higher than those obtained for plant or seaweeds biopolymers at a given concentration and shear rate. The η values for κ-carrageenan and Na-alginate, both seaweed biopolymers, were very similar for the same shear rates and concentration. LBG seemed to have an intermediate behaviour between seaweeds and microbial polysaccharides. For all samples the η values increased with increasing biopolymers concentration as expected.

In non-Newtonian solutions the apparent viscosity decreased with increasing shear rate, which is typical of a shear thinning behavior. For those samples it was observed a Newtonian region in the low shear rate range before the shear thinning behavior. The power law model (Equation 1) was used to describe the rheological properties of those solutions. To evaluate the zero shear viscosity, η_0, the initial slope of the shear stress–shear rate curve

was determined. The critical shear rate obtained from the intersection of the power-law and

the constant viscosity region, η_0, moved to lower values with the increase of concentration

for each polysaccharide. Moreover, regarding the polysaccharide type the increase of the

critical shear rate followed the order: microbial < plant < seaweeds. The different values of

this critical point are associated with the formation and disruption of entanglements. For

higher shear rates, disruption predominates over formation of new entanglements;

molecules align in the direction of flow and the apparent viscosity decreases with

increasing shear rate (Sittikijyothin et al., 2005).
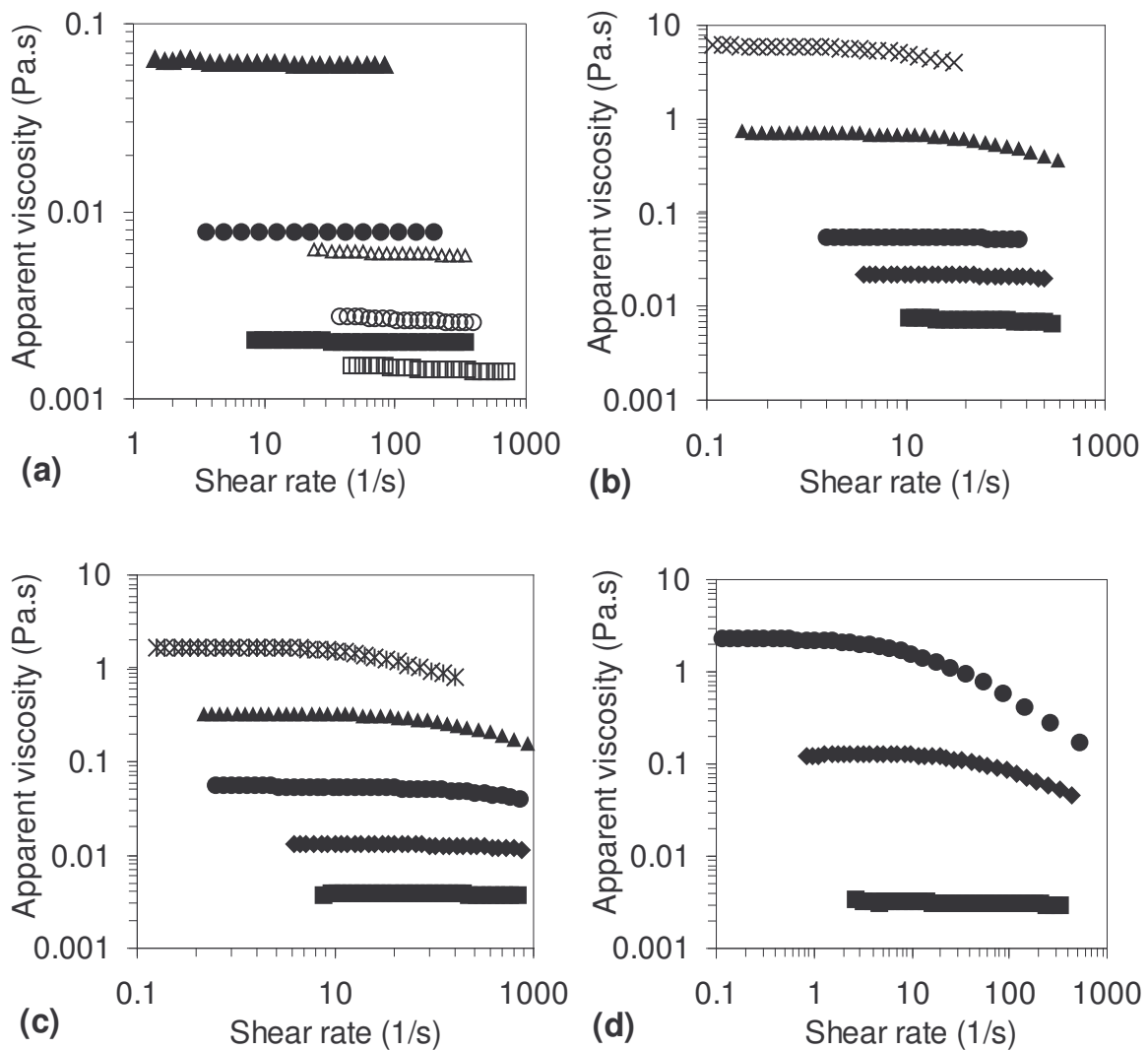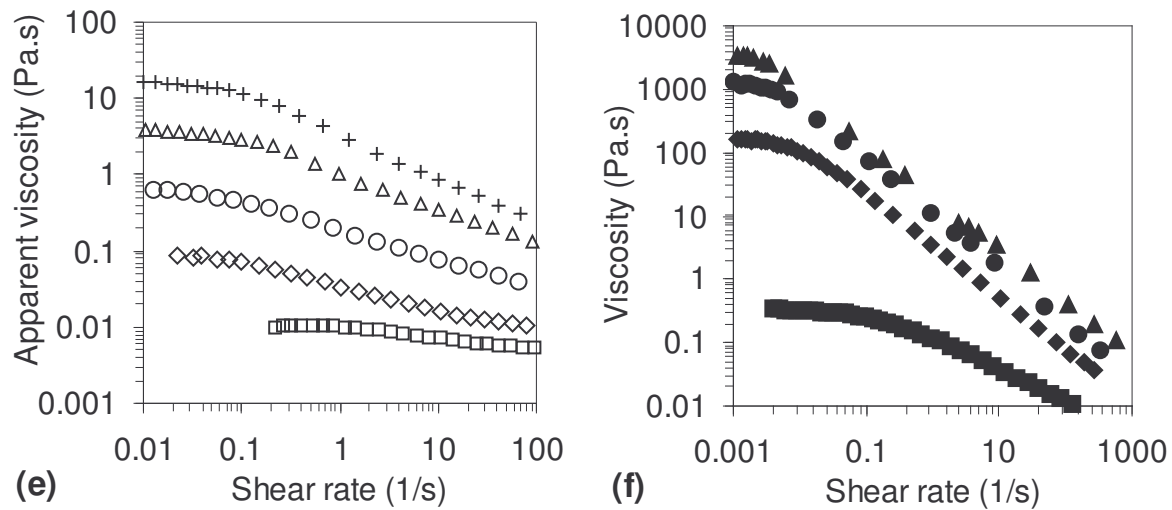
Figure 1. Flow curves of proteins (Na-caseinate and SPI) and polysaccharides at different concentrations (wt%), at 25 ^{o}C. a) Na-caseinate (closed symbols) and SPI (open symbols): 1% (■), 5% (●), 10% (▲); b) κ-carrageenan: 0.1% (■), 0.5% (◆), 1% (●), 2.5%(▲), 4% (×); c) Na-alginate: 0.1% (■), 0.5% (◆), 1% (●), 2%(▲), 3% (✳); d) LBG: 0.1% (■), 0.5% (◆), 1% (●); e) gellan: 0.2% (□), 0.4% (◇), 0.6% (○), 0.8% (△), 1% (+); f) xanthan: 0.1% (■), 0.5% (◆), 1% (●), 2%(▲).

Figure 2 shows that the concentration dependence of the flow behaviour index n followed an exponential decay for the different polysaccharides, except for κ-carrageenan that could not be evaluated due to few data in the shear-thinning region. Xanthan showed the lowest n values followed by gellan and LBG, which were very similar. Some authors (López et al. 2004, Martínez-Padilla et al. 2004) had previously reported similar n values for xanthan solutions. Xanthan and Na-alginate showed an initial steeper decrease of n followed by a plateau region with the increase of concentration. This indicate that the capacity of molecular organization under shear did not increased after a given polysaccharide concentration. It could be suggested that xanthan and Na-alginate formed an anisotropic ordered aggregates at higher concentrations.

55
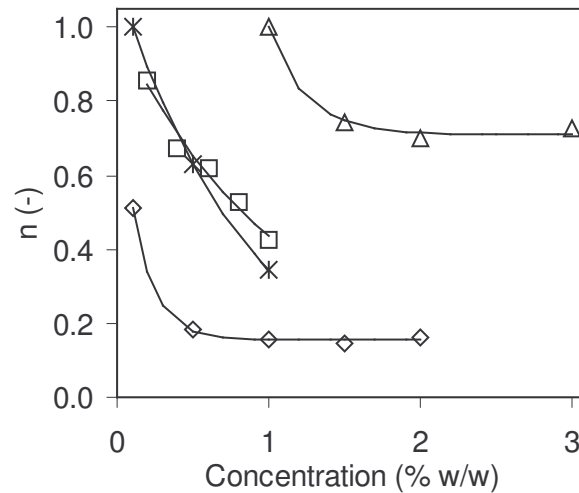
Figure 2. Variation of the flow behavior index, n, as a function of polysaccharide concentration. Na-alginate (Δ), gellan (□), LBG (✳), xanthan (◊).

Different solution regimes can be distinguished by plotting the specific viscosity (Equation 2) versus concentration on a log-log scale (Morris et al., 1981), as shown in Figure 3 for the different biopolymers studied here. Launay et al. (1997) have suggested that some polysaccharides show two critical concentrations: C*, the point at which reduced viscosity first departs from linearity, and C**, where a second departure occurs. These two points delimit three regions: dilute (C<C*), semi-dilute (C*<C<C**) and concentrated (C>C*) as follows:

• In the dilute regime (C<C*): polymer coils have "infinite dilution" dimensions;

• In the semi-dilute regime (C*<C<C**): polymer coils are in contact and progressively shrink as concentration increases;

• In the concentrated regime (C>C**): polymer coils have reached their limiting size (unperturbed or q-dimensions). In this regime, polymer chains entangles more.

Among the polysaccharides studied, the lower C* value was found for LBG, C*=0.25% (see below), followed by Na-alginate (Figure 3a), C*=0.7%, and κ-carrageenan

(Figure 3b), C*=0.9%. In the case of κ-carrageenan it was observed a second deviation of the curve from the linearity, in which C** was equal 1.8%. It was not possible to determine C* for gellan (Figure 3b) and xanthan (Figure 3c). However, Martínez-Padilla et al. (2004) reported a specific viscosity equal to 2 for 0.1% gellan, which indicates that gellan had one critical point between 0.1 and 0.2%. Launay et al. (1997) reported a C** value equal to 0.1% for xanthan aqueous solutions, while Milas et al. (1990) observed other two regions, C*=0.0126 and C**=0.078%, for xanthan in water. Probably because of the helical chains of xanthan and gellan, there is a tendency to entangle at a very low concentration (Wang et al., 2001). This would not happen with the used κ-carrageenan, since it had low salt concentration showing helix formation at temperatures below 25 $^\circ$C.

Below C*, Na-alginate and κ-carrageenan showed the same concentration dependence of η_{sp} ($C^{0.9}$), which resembled that expected for random coil polymers, $C^{1.3}$ (Morris et al., 1981). For LBG (Figure 3b), it was observed a discontinuity between 0.1% and 0.5%, but there was not sufficient data to quantify exactly the correct concentration. Thus, for low concentrations, it was plotted a power law dependence of viscosity on concentration with the exponent equal to 1.16 as found by Richardson et al. (1998) for LBG. The C* for LBG was then determined and a value equal to 0.25% was obtained, which was very close to that reported by Richardson et al. (1998) work.

The concentrated regime (C>C**) was characterized by a power law dependence of viscosity on concentration. For typical polymers, the exponent is usually found to be in the range 3.3–5 (Launay et at., 1986). In the present case, the slopes found for Na-alginate (3.1), xanthan (3.7), LBG (4.2), gellan (4.2) and κ-carrageenan (4.9) were well within the

usual range. It has been claimed that slopes higher than 3.3 could be explained by the creation of "hyperentanglements" (Morris et al., 1981).

Figure 3c shows that after 1% xanthan the specific viscosity of the solution deviates from the expected trend. Harding (1997) reported that for some polyanionic polysaccharides in a salt-free aqueous solution the conventional reduced viscosity versus concentration plot can depart from its positive slope. Moreover, the reduced viscosity can show a maximum value and then decrease with the increase in biopolymer concentration.

For the proteins the concentrations regimes were different from those found for the polysaccharides. Only C^* was observed, independent on the protein type. Na-caseinate showed a lower C^*, equal 3%, as compared to the value obtained for SPI, 6.5%. This shows that SPI is more hydrophobic than caseinate as reported previously by Grinberg and Tolstoguzov (1997) and that it is more compacted and entangles less, although soy proteins have a higher molecular weight than that of the caseins. The slope of the power relations before and after C^* were similar for both proteins.

58
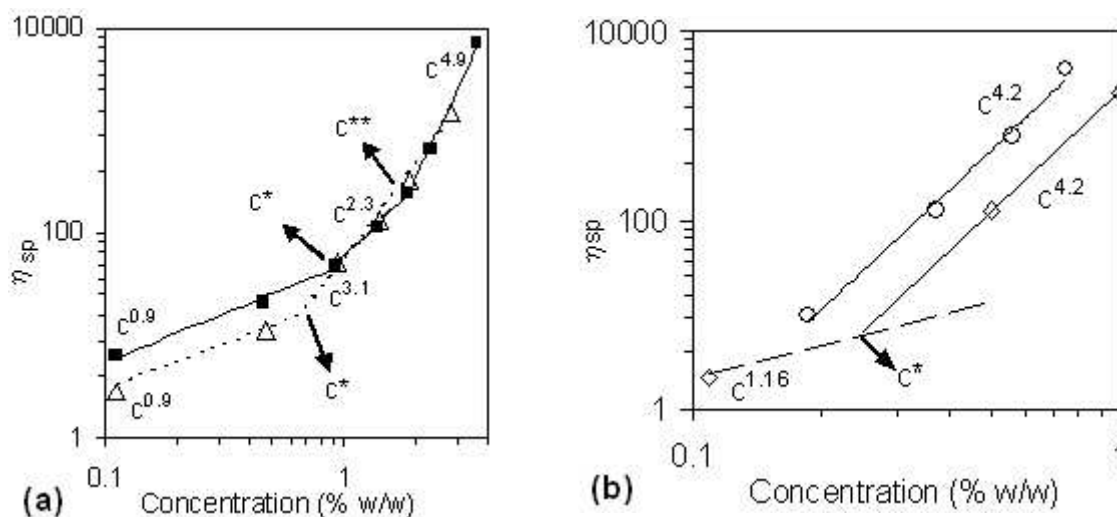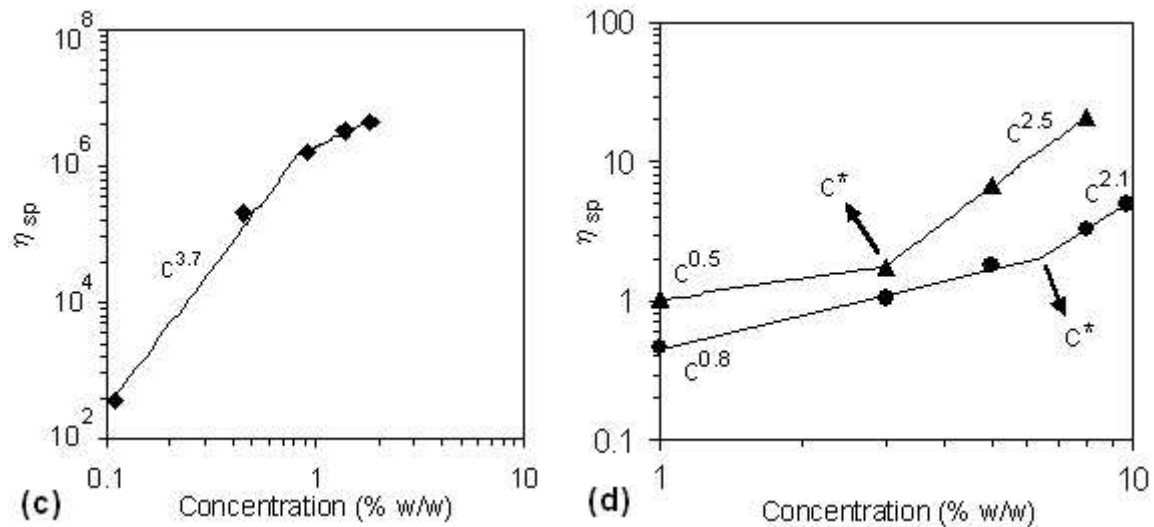
Figure 3. Concentration dependence of specific viscosity η_{sp} for polysaccharides and proteins. a)Na-alginate ($\triangle$), κ-carrageenan ($\blacksquare$); b LBG ($\diamondsuit$),gellan ($\bigcirc$); c) xanthan ($\blacklozenge$); d) SPI ($\bullet$), Na-caseinate ($\blacktriangle$). The long dashed line (b) represents the power law found by Richardson et al. (1981) for LBG.

4. Conclusion

The biopolymers solutions showed different trends for density, apparent viscosity and critical overlap concentration depending on the biopolymer type (protein and polysaccharide) and of the biopolymer source. The concentration dependences of density were the same for the two proteins studied. In addition, Na-caseinate showed a lower overlap concentration (C*) than SPI, which was attributed to the more hydrophobic character of SPI that tend to be more compacted. The proteins showed Newtonian behaviour for all concentrations studied, while the polysaccharides showed either Newtonian or non-Newtonian behaviour depending on its type and solution concentration. For a given concentration and shear rate, the increase of apparent viscosity and the reduction of density of the polysaccharide solution followed the order: 1) microbial polysaccharides (xanthan and gellan), 2) plant seeds polysaccharide (LBG) and 3) seaweeds

polysaccharides (Na-alginate and κ-carrageenan). The density trend was attributed to a lower capacity of microbial polysaccharides to entrap solvent than plant and seaweeds biopolymers. It was not possible to observe a C* for xanthan and gellan, while the increase of C* for the others polysaccharides followed the above order.

5. Acknowledgements

6. References

Antonov, Y.A., Van Puyvelde, P., Moldenaers, P. (2004). Interfacial tension of aqueous biopolymer mixtures close to the critical point. International Journal of Biological Macromolecules, 34, 29-35.

Braga, A.L.M., Cunha, R.L. (2004). The effects of xanthan conformation and sucrose concentration on the rheological properties of acidified sodium caseinate–xanthan gels. Food Hydrocolloids, 18, 977-986.

Capron, I., Costeux, S., Djabourov, M. (2001). Water in water emulsions: phase separation and rheology of biopolymer solutions. Rheologica Acta, 40, 441-456.

Chaplin, M., available at: http://www.sbu.ac.uk/water/hydrat.html accessed 2005 June 01.

Dickinson, E. (2003). Hydrocolloids at interfaces and the influence on the properties of dispersed systems. Food Hydrocolloids, 17, 25–39.

Glicksman, M. (1969). Gum technology in the food industry. New York: Academic Press.

Grinberg, V.Y., Tolstoguzov, V.B. (1997). Thermodynamic incompatibility of proteins and polysaccharides in solutions. Food Hydrocolloids, 11, 145-158.

Harding, S.E. (1997). The intrinsic viscosity of biological macromolecules. Progress in measurement, interpretation and application to structure in dilute solution. Progress in Biophysics and Molecular Biology, 68, 207-262.

Hemar, Y., Hall, C.E., Munro, P.A., Singh, H. (2002). Small and large deformation rheology and microstructure of k-carrageenan gels containing commercial milk protein products. International Dairy Journal, 12, 371-381.

Ikeda, S., Nitta, Y., Temsiripong, T., Pongsawatmanit, R., Nishinari, K. (2004). Atomic force microscopy studies on cation-induced network formation of gellan. Food Hydrocolloids, 18, 727-735.

Kang, K.S., Colegrove, G.T., Veeder, G.T. (1982). Deacetylated polysaccharide S-60. US Patent 4,326,052.

Kinsella, J.E. (1984). Milk proteins: physicochemical and functional properties. CRC Critical Reviews in Food Science and Nutrition, 3, 197-262.

Launay, B. Doublier, J.L., Cuvelier, G. (1986). Flow properties of aqueous solutions and dispersions of polysaccharides. In Functional properties of food macromolecules, J.R. Mitchell & D.A. Ledward (Eds.), London: Elsevier Applied Science, pp. 1-78

Launay, B., Cuvelier, G., Martinez-Reyes, S. (1997). Viscosity of locust bean, guar and xanthan gum solutions in the Newtonian domain: a critical examination of the $\log(\eta_{sp})_0$-$\log C[\eta]_0$ master curves. Carbohydrate Polymers, 34, 385-395.

López, M.J., Vargas-García, M.C., Suarez-Estrella, F., Moreno, J. (2004). Properties of xanthan obtained from agricultural wastes acid hydrolysates. Journal of Food Engineering, 63, 111–115.

Marcotte, M., Hoshahili, A.R.T., Ramaswamy, H.S. (2001). Rheological properties of selected hydrocolloids as a function of concentration and temperature. Food Research International, 34, 695–703.

Martínez-Padilla, L.P., López-Araiza, F., Tecante, A. (2004). Steady and oscillatory shear behavior of fluid gels formed by binary mixtures of xanthan and gellan. Food Hydrocolloids, 18, 471–481.

Milas, M., Rinaudo, M., Knipper, M., Schuppiser, J.L. (1990). Flow and viscoelastic properties of xanthan gum solutions. Macromolecules, 23, 2506–2511.

Miyoshi, E.; Takaya, T.; Nishinari, K. (1996). Rheological and thermal studies of gel- sol transition in gellan gum aqueous solutions. Carbohydrate Polymers, 30, 109-119.

Moe, S., Draget, K. I., Skjåk-Bræk, G., & Smidsrød, O. (1995). Alginates. In Food polysaccharides and their applications, A. M. Stephen (Ed.). New York: Marcel Dekker.

Morris, E.R. (1990). Mixed polymer gels. In Food gels, P. Harris, London: Elsevier Applied Science, pp. 291-360.

Morris, E.R., Vutler, A.N., Ross-Murphy, S.B., Rees, D.A., Price, J. (1981). The fine structures of carob and guar galactomannans. Carbohydrate Polymers, 1, 5-21.

Petruccelli, S., Añón, M.C. (1995). Thermal aggregation of soy protein isolates. Journal of Agricultural and Food Chemistry, 43, 3035-3041.

Richardson, P.H., Willmer, J., Foster, T. (1998). Dilute solution properties of guar and locust bean gum in sucrose solutions. Food Hydrocolloids, 12, 339-348.

Scholten, E., Tuinier, R., Tromp, R.H., Lekkerkerker, H.N.W. (2002). Interfacial tension of a decomposed biopolymer mixture. Langmuir, 18, 2234-2238.

Schorsch, C., Jones, M.G., Norton, I.T. (1999). Thermodynamic incompatibility and microstructure of milk protein/locust bean gum/sucrose systems. Food Hydrocolloids, 13, 89-99.

Sittikijyothin, W., Torres, D., Gonçalves, M.P. (2005). Modelling the rheological behaviour of galactomannan aqueous solutions. Carbohydrate Polymers, 59, 339–350.

Speers, R.A., Tung, M.A. (1986). Concentration and temperature dependence of flow behavior of xanthan gum dispersions. Journal of Food Science, 51, 96–98 and page 103.

Sutherland, I.W. (1994). Structure–function relationships in microbial exopolysaccharides. Biotechnology Advances, 12, 393–448.

Van Vliet, T., Martin, A. H., Bos, M. A. (2002). Gelation and interfacial behaviour of vegetable proteins. Current Opinion in Colloid and Interface Science, 7, 462-468.

Walstra, P., Jenness, R. (1984). Dairy Chemistry and Physics, Wiley: New York.

Wang, F., Sun, Z., Wang, Y.J. (2001). Study of xanthan gum/waxy corn starch interaction in solution by viscometry. Food Hydrocolloids, 15, 575-581.

CHAPTER 3. Rheological properties of biopolymers aqueous solutions.

2ⁿᵈ PART: Rheological behaviour and microstructure of xanthan solutions: annealing temperature and sucrose effects

Abstract

The rheology of annealed xanthan solutions (between 10 - 90ºC during 1h) added by sucrose was studied in oscillatory shear experiments. Xanthan solutions showed three different transitions passing through anisotropic, biphasic and isotropic regions. It was observed many birefringence aggregates by light microscope in the anisotropic and biphasic regions. The temperature of annealing affected the elasticity of the solution for all xanthan concentrations studied, but the duration of the annealing (heat-cooling scan or 1h at a fixed temperature) was important only for the highly anisotropic solution. The addition of sucrose affected the rheological properties over all frequency range studied but only for initially anisotropic or biphasic xanthan solutions. Sucrose probably played a role of promoting biopolymer intra-molecular aggregation for less concentrated solutions and by reducing the intermolecular junction zones in more concentrated solutions.

Keywords: xanthan, sucrose, annealing temperature, isotropy / anisotropy

1. Introduction

Xanthan is a high-molecular-weight anionic polysaccharide produced from the fermentation broths of the bacterium *Xanthomonas campestris*. This polysaccharide is used in wide variety of applications and it is a good stabilizer for food products (Capron et al., 1998). The structure of this polymer consists of a linear (1-4)-β-D glucose backbone with a charged trisaccharide side chain on every second glucose residue (Jansson et al., 1975). The secondary conformation of xanthan molecule is known to undergo a conformational transition (T_m) from helix to coil as the temperature is raised, which is also a function of ionic strength of the solution, the nature of the electrolyte and the pH (Paradossi et al., 1982). In addition, Lee and Brant (2002) observed a second transition that was attributed to

an anisotropic-isotropic transition, which was dependent on solution temperature and polysaccharide concentration.

Although xanthan is considered as a non-gelling hydrocolloid, some authors (Yoshida et al., 1998, Iseki et al., 2001) obtained hydrogels in solutions that were annealed at high temperature and subsequently cooled. It was suggested that the gelation phenomena takes place after the formation of stable junction zones during heat treatment. Extensive work has already been done to elucidate the temperature-induced transition of xanthan molecules. Studies on the native and renatured structure have been mainly conducted by using atomic force microscopy (AFM). The AFM sample preparation requires a dilute solution and a drying step that proved to be good to elucidate the coil-helix transition (melting transition). However, few works were done with systems in the concentrated regime (Lee and Brant, 2002, Capron et al., 1998, Lim et al., 1984).

The effect of the addition of some co-solutes, such as NaCl, on xanthan solutions is known to strength the elastic characteristic of this polysaccharide (Lee and Brant, 2002). However, few works have studied the influence of low molecular weight sugars upon the properties of hydrocolloids solutions (Richardson et al., 1998), although sucrose is widely used in the food industry. Basaran et al. (1999) studied the diffusion of sucrose (10-40 wt %) in xanthan solutions showing that xanthan did not affect this property. However, the rheological properties at high frequencies of a mixture of xanthan and a high sugar content (74-78 wt %) solutions showed that the polysaccharide acted retarding the mobility of sucrose molecules causing them to behave as in glassy state (Saggin and Coupland, 2004). However, for our knowledge there is no work that focuses on the effect of sucrose molecules on the rheological behaviour of concentrated xanthan solutions.

The aim of this work was to understand the effect of annealing temperature and sucrose addition on the rheological properties of concentrated xanthan solutions. In addition, the morphologies of such solutions were observed under light and atomic force microscopes in order to relate them to the temperature induced rheological transitions.

2. Materials and Methods

2.1. Material

Sucrose (Synth, Brazil) and xanthan gum, (Sigma-Aldrich Co., USA) were used to prepare the mixed systems. The xanthan powder showed moisture content of $8.36 \pm 0.23\%$ (wt% wet basis), an average molecular weight (gel permeation chromatography) of 1795.4 kDa and the following cations content (atomic absorption spectroscopy): 2.6% Na^+, 0.4% Ca^{2+} and 4.0% K^+.

2.2. Preparation of Solutions

Xanthan solutions at different concentrations (Table 1) were prepared under mechanical stirring during 1 hour at different temperatures (10, 20, 50, 75, 80 and 90 ºC) and subsequently cooled to 10 ºC. An appropriate amount of sucrose (0, 7.5, 15% w/v) was gently mixed to xanthan solutions at 10 ºC.

Table 1. Nomenclature used for xanthan solutions at different concentrations.

Xanthan concentration (%)	0.05	0.1	0.5	1	3.5
Sample nomenclature	X005	X01	X05	X1	X35

2.3. Rheological Measurements

Oscillatory shear measurements were done using a stress-controlled rheometer (Carri-Med CSL^{2}500, TA Instruments, England). Stainless steel cone and plate geometry of

60 mm diameter was used and two types of experiments were performed. 1) Temperature sweeps were done at frequency of 0.1 Hz for solutions without sucrose and annealed at 10ºC. The temperature was raised to 82 ºC at 1ºC/min and then lowered to 10ºC at the same rate. For the 0.05 and 0.1% xanthan concentrations, a frequency of 0.3 Hz and a rate of 3 ºC/min were used to improve the measurement sensibility. 2) Frequency sweeps were carried out for all xanthan solutions and xanthan-sucrose mixtures, from 0.01 to 10 Hz at 0.15 Pa and 10 ºC. The Lissajous figures at each temperature or frequency were plotted to ensure that G' (storage modulus) and G" (loss modulus) were always measured within the linear viscoelastic regime. To prevent evaporation, samples were covered with a Newtonian oil.

Three different regions were observed in the complex viscosity (η^*) – temperature curve, being the transitions of the regions determined as following:

1) First transition (T_a): occurred at the end of the initial constant value of η^*, identified as anisotropic-biphasic temperature-induced transition;

2) Second transition (T_i): at the sharp deflection of the slope of complex viscosity – temperature curve. This temperature characterizes the transition between the biphasic to fully isotropic region.

3) Third transition (T_m): it was associated to the helix-coil (melting) transition. It was adopted a criterium in which the temperature was determined from the interception of the maximum slope of the curve with the second region with finite constant η^* level (see Figure 1a).

2.4. Differential interference contrast (DIC) microscopy

A Zeiss Axioplan microscope (Zeiss Ltd., D-Oberkochen) under DIC and polarized light modes was used to photograph the xanthan solutions at 100x. A drop of xanthan solution (0.1, 1 and 3.5%) was placed onto a clean glass slide, covered with glass cover-slip and sealed with nail polish to prevent evaporation.

2.5. Atomic force microscopy (AFM)

A piece of freshly cleaved mica was placed into a 0.05% xanthan solution (X005) and the polysaccharide was allowed to adsorb onto the mica. After 1min, the mica was removed and air dried at room temperature in small covered Petri dishes. Specimens were examined using an Autoprobe CPAFM from Thermomicroscopes (USA) operating in non-contact mode.

3. Results and Discussion

3.1. Xanthan behaviour in water

It is known that xanthan molecule undergoes a temperature transition from double helical form to a disordered form that is a function of ionic strength. The characteristic temperature T_m is near room temperature for salt-free aqueous xanthan at low polymer concentrations and increases to values well above 100°C in the presence of salt (Paradossi et al., 1982, Paoletti et al., 1983, Capron et al., 1997). Figures 1a, 2a and 3a show the rheological behaviour of xanthan solutions in a temperature range of 10-80 °C for different solution concentrations, such that T_m could be determined for a great range of polymer concentration. The rheological behaviour was related to solutions micrographs shown in Figures 1b, 2b, 3b and 3c. The X005 sample showed a linear dependence of $\eta^*(\omega)$ on temperature over all range measured (Figure 1a), indicating that any temperature-induced transition took place at concentrations lower than 0.05%. Figures 1c, 1d and 1e show the

AFM micrographs of xanthan molecules present in X005 sample. It was observed flexible molecules at 25 °C (Figures 1c and 1d) as well as molecular aggregates (Figure 1e). Similar loop-like and flexible structures were previously observed by Capron et al., 1998 for native xanthan solutions. It was difficult to observe isolated xanthan molecules, being more common the visualization of aggregates, which were formed during the drying process. Thus, it was not possible to do a more accurate statistical quantitative analysis revealing the dimensions of the molecules.
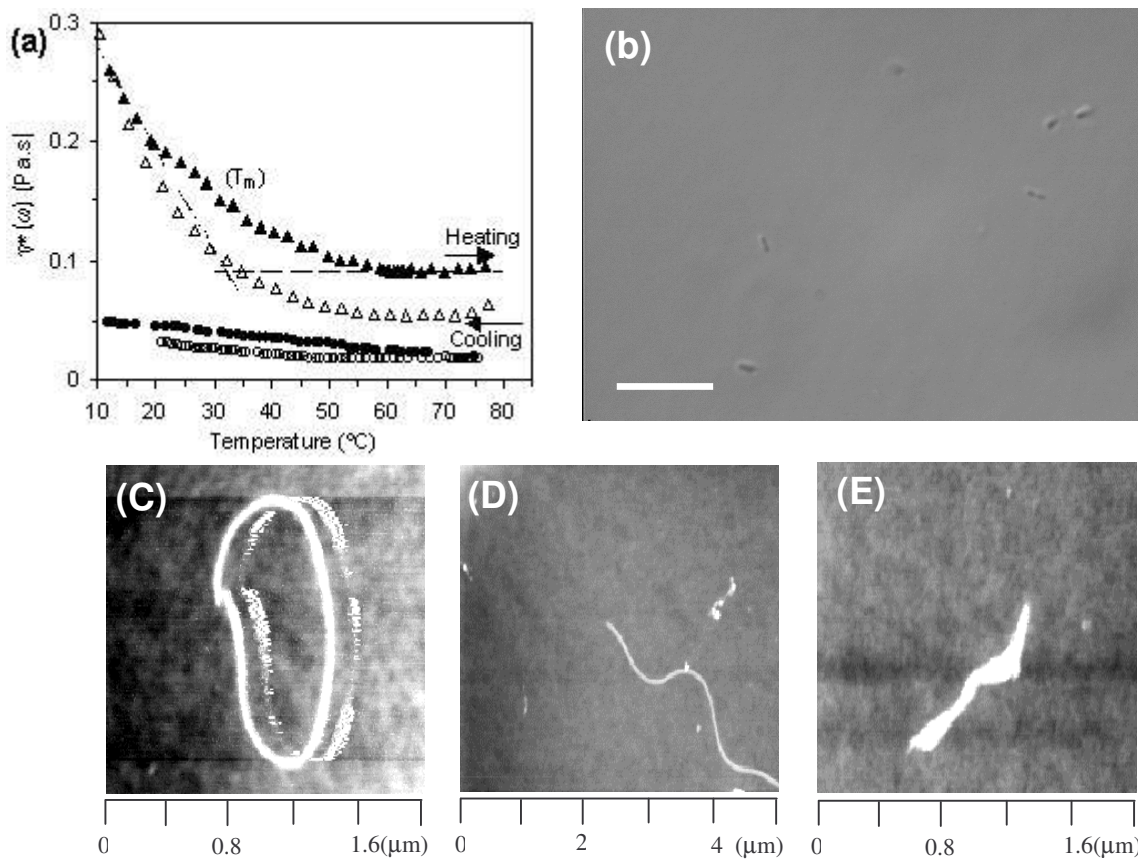
Figure 1. a) Temperature dependence of $\eta^*(\omega)$ for X005 (●) and X01 (▲) on heating (closed symbols) and cooling (open symbols). Dashed line represents the method used to determine T_m. b) DIC micrograph of the X01 sample at 25°C. Scale bar = 50 μm. c, d and e) AFM micrographs at 25 °C of native xanthan molecule diluted in water.

For X01 the $\eta^*(\omega)$ value drops as the temperature increased approaching asymptotically a finite constant level. This solution did not emit any light when observed through polarized light (PL) microscopy indicating that it was fully isotropic. So, the only transition that could take place at such concentration is the helix-coil one (T_m). Helix xanthan solutions have a higher relative viscosity than the more flexible disordered form (Lee and Brant, 2002). For X01 the complex viscosity decreases from 10°C to 60°C showing that the helix-coil transition is a wide process over a range of 50°C (Figure 1a). The increase of temperature cause a continuously change of the ordered form of the molecule to a disordered form resulting in an intermediate conformation that consist of disordered regions held together by a segment of ordered chains (Bordi et al., 1996, Capron et al., 1997). From that behaviour the melting point was considered as a midpoint transition and determined to be 32 °C. This value is in very good agreement with the value of 33 °C found by Jones et al. (1987) and 35 °C reported by Bordi et al. (1996) for a 0.1% xanthan solution. Figure 1b shows the DIC micrograph of X01 solution at 25 °C prior to the heating step. It could be observed few small aggregates (<12.5 μm) probably formed by the double helix molecules, being the solution quite homogeneous.

Figure 2a shows the variation of $\eta^*(\omega)$ with temperature for X05 and X1 samples, which were not anisotropic at 25°C as observed by a completely dark PL micrographs. For those samples it was possible to observe three temperature-induced transitions. Lee and Brant (2002) also reported three transitions for more concentrated samples, being the transition occurring at high temperature related to the well-known helix-coil transition. The first transition was referred as an anisotropic to biphasic transition (T_a), in which the solution had initially a lyotropic characteristic and became a dispersion of anisotropic phase

71

within an isotropic phase. The second was associated to the transition between the biphasic region and the fully isotropic region (T_i). All transition temperatures (T_a, T_i and T_m) increased with xanthan concentration, being the melting temperature calculated to be 52ºC and 68ºC for X05 and X1, respectively. The anisotropic transition (T_a) was associated with the end of the first flat part of the curve, as will be discussed later, being the values for X05 and X1, respectively, 17ºC and 19ºC. The isotropic transition temperatures (T_i) were 33°C and 46°C, respectively, for X05 and X1. Figure 2b shows the DIC micrograph for X1 solution at 25°C, being observed a higher amount of aggregates then those revealed in Figure 1b. However, most of the aggregates had the same size and some of them could reach up to 21 μm length.
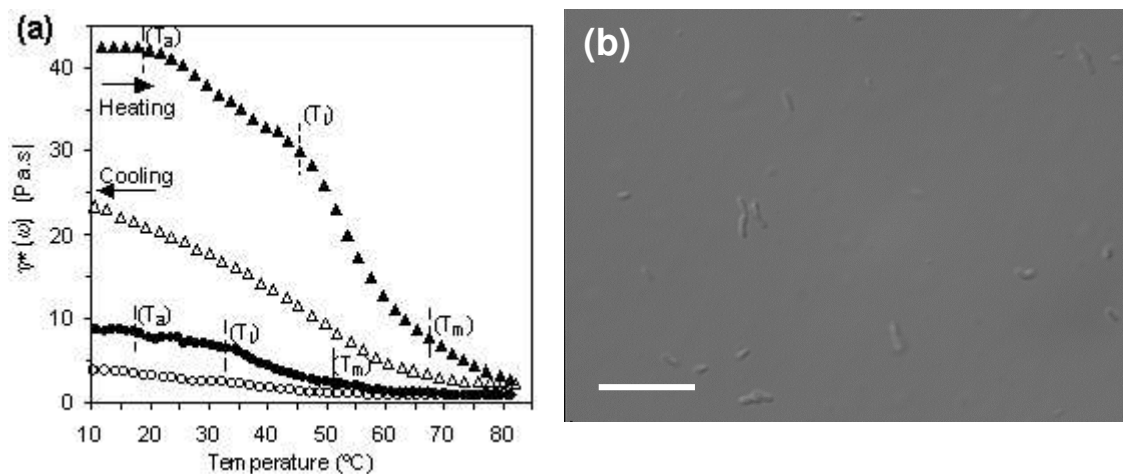
Figure 2. a) Temperature dependence of $\eta^*(\omega)$ for X05 (●) and X1 (▲) on heating (closed symbols) and cooling (open symbols). b) DIC micrograph of the X1 sample at 25ºC. Scale bar = 50 μm.

Figure 3 shows the variation of complex viscosity with the temperature for X35 as well as the corresponding DIC and PL micrographs at 25 ºC. The X35 sample was anisotropic at 25°C even without the application of shear (Figure 3c). The PL micrograph showed birefringence as the light was transmitted through two crossed polarizer disks. This

behaviour was checked by rotating one of the polar by 45°, but maintaining them crossed. It was observed a micrograph similar to that of Figure 3c but the black areas became white, while the white areas of Figure 3c became black. From that behaviour it could be established that the initial flat part of η^* curve (Figure 3a) is referred to the anisotropic domain, being T_a for X35 equal 48°C. For that sample the isotropic transition (T_i) was determined to be 73°C. Lim et al. (1984) observed permanent birefringence in concentrated xanthan solutions (1 and 3%) under shear. However, in the present work the X1 sample did not show birefringence probably because of the different xanthan sources.
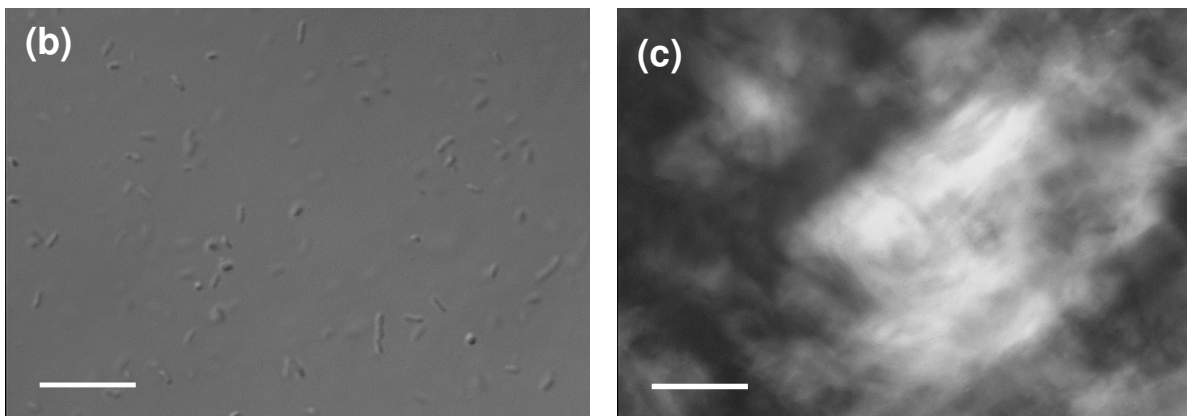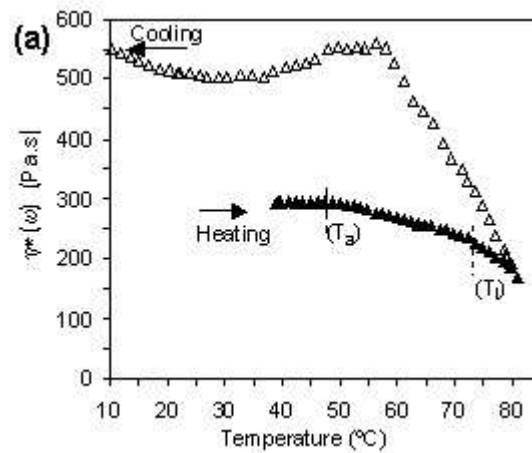
Figure 3. a) Temperature dependence of $\eta^*(\omega)$ for X35. b) DIC micrograph of the X35 sample at 25°C. c) Polarized (PL) micrographs of the X35 sample at 25°C. Scale bars = 50 μm.

Figure 3b shows the DIC micrograph for X35 sample, being observed that the aggregates had the same size of those verified in Figure 2b, although the concentration of aggregates increased. Comparing the three DIC micrographs (Figures 1b, 2b and 3b) it is possible to observe that the amount of aggregates is only a function of the polymer concentration. The optical birefringence was probably governed by the amount of those aggregates, resulting in an anisotropic solution (Figure 3c). In addition, it was observed that at a fixed polymer concentration the aggregate size reduced as the temperature increased and they recovered their original size after cooling back to room temperature (result not shown). Thus, it could be suggested that the solution domain was a function of the amount and size of the aggregates.

The cooling curve showed a small thermal hysteresis for X01 and X005, which were initially fully isotropic. At 10°C, the complex viscosity had the same value of the initial solution (native). Thus, it could be supposed that the renatured form was the same of the native one or that the solution concentration was not high enough to promote a network formation after the heating step. For X05 and X1 the complex viscosity values were smaller at the cooling cycle than on heating cycle. Thus, the isotropic transition caused some irreversible rearrangements on xanthan molecules that produced a less elastic solution at 10°C than the initial anisotropic sample. On cooling below T_m the reassembly of chains generates an architecture which differs from the original one and depends on whether the heat treatment was performed on dilute or concentrated solution (Smith et al, 1981). For X35, the transition to isotropic domain occurred near the final temperature (82°C), being the only sample where the final temperature of the sweep was lower than T_m. Thus, the molecular rearrangements occurred mainly in the biphasic domain and the new entanglements were probably formed with double helix molecules. This kind of

rearrangements (between helix molecules) revealed to be stronger than those that occurred from coil molecules. Capron et al. (1998) observed the same behaviour for a 2% xanthan solution. These authors verified from AFM micrographs that at high polymer concentration the double strands can form permanent associations with neighbouring molecules. However, dilute solutions showed mainly intramolecular associations instead of intermolecular organization.

Braga and Cunha (2004) showed that xanthan solutions (0.1 to 1%) that were annealed at 20, 50 or 80°C and then cooled to 10°C presented different rheological behaviour. In the present work the same behaviour was also observed for X35 (Figure 4d), such that the G* curve was shifted to lower values as the annealing temperature increased. Bordi et al. (1996) did not observed any effect of the annealing performed at 50°C during 1h of xanthan solutions (semi-diluted and concentrated regimes) on its conductomeric behaviour. Such differences between the results could be attributed to the different techniques used. Comparing the rheological results of Braga and Cunha (2004) for 0.5 and 1% annealed xanthan solution with those of Figure 2a it can be seen a similar reduction of complex viscosity value at 10 ^{o}C between heating and cooling cycles. From such results it is possible to affirm that the less concentrated solutions have a renatured conformation different to the native one just by increasing the temperature and cooling back, such that the annealing during 1h did not affect the rheological properties. However, for X35 the η* of non-annealed solution increased almost 2-fold after the cooling cycle (Figure 3a), while the annealed solution (Figure 4d) had a η* value half of that found for native solution at 10°C. Thus, the annealing up to 80°C during 1h hour modifies the renatured conformation for the highly anisotropic xanthan solution (Figures 3c and 4d).

3.2. Xanthan behaviour in sucrose solutions

Figure 4 shows the effect of sucrose on the rheological properties (at 10°C) of xanthan solutions annealed at different temperatures during 1h. For samples with low polymer concentration (X01) the addition of sucrose did not affect the rheological properties of the aqueous solution independent on the annealing temperature (Figure 4a). Similar behaviour was observed for X05 when the solutions were annealed at 50ºC or 80ºC/1h (Figure 4b). However, as sucrose concentration increased up to 15% the elastic character of solutions annealed at 20ºC decreased by 15-20%. It is interesting to note that at 20ºC xanthan solution was in the anisotropic region, at 50ºC the isotropic transition had already occurred and at 80ºC the molecule had a coil conformation (Figure 2a).
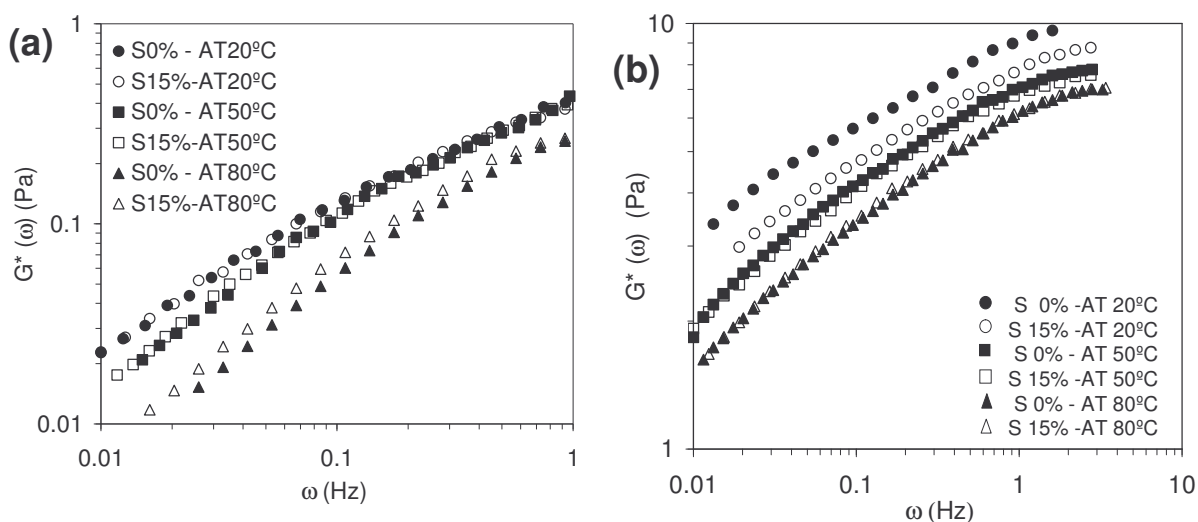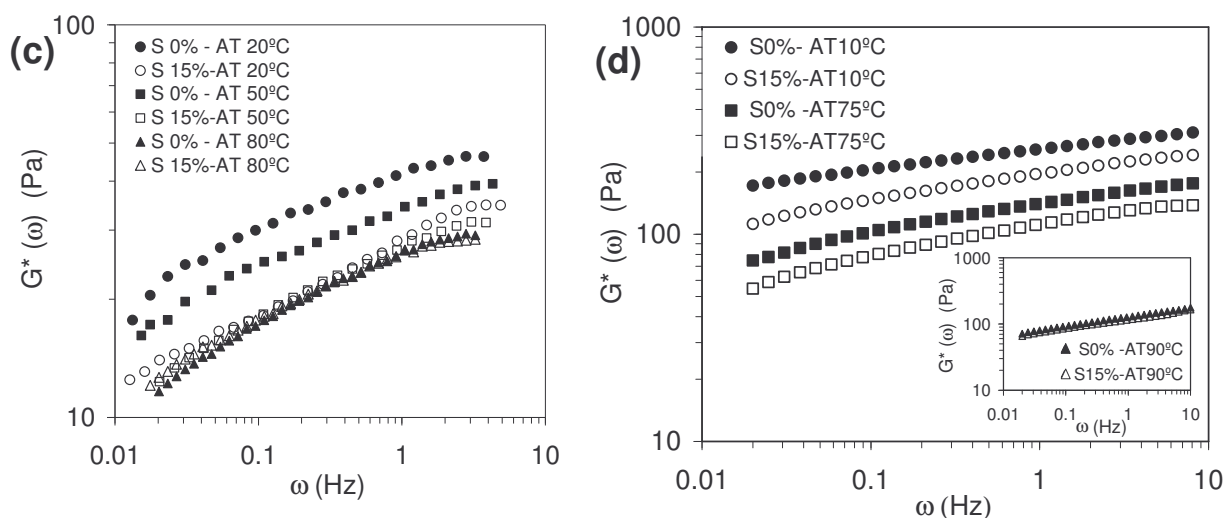
Figure 4. Temperature dependence of G*(ω) for different concentrations of the xanthan solutions at 10°C. The solutions were prepared at different annealing temperatures (AT) and added by 15% of sucrose (S). a) X01, b) X05, c) X1, d) X35.

Figure 4c shows that for the X1 solution annealed at 20°C and 50°C the addition of sucrose led to a negative effect on complex modulus. Nevertheless, sucrose did not influence the rheological properties when solutions were annealed at 80°C, which corresponded to a coil conformation in a fully isotropic domain (Figure 2a). The 1% xanthan solutions annealed at 20°C and 50°C were so affected by sucrose that their rheological properties became similar of those of a solution annealed at 80°C. Figure 4d shows that for X35 the addition of sucrose decreased the rheological properties of solutions annealed in a very broad range of temperature (10-75°C) and then cooled to 10°C. However, at a higher annealing temperature (90°C), in which the solution was in isotropic domain, sucrose did not influenced G* at 10°C. From the above results it is possible to suggest that sucrose only affected the rheological properties of solutions that were annealed at temperatures in which the solution was in the anisotropic or biphasic domain.

Table 2 shows the magnitude (%) of the negative effect of sucrose on G* at two different frequencies, 0.02 Hz and 1 Hz. The sucrose effect could be divided in four groups

77

(Table 2), namely, 1) no sucrose effect as observed for X01 solutions and for xanthan solutions well within the isotropic domain; 2) a small sucrose effect (14-19%) was seen for X05 solution annealed at 20 ^{o}C; 3) an intermediate sucrose effect (21-27%) was observed for more concentrated xanthan solutions (X1 and X35) annealed at the biphasic/isotropic transition domain; 4) a high sucrose effect (24-35%) was checked for more concentrated xanthan solutions (X1 and X35) that were annealed in the anisotropic or biphasic domain. In general it was observed a higher sucrose effect on G* values obtained at lower frequencies, as the molecular structures has sufficient time to rearrange. Thus, the sucrose seems to affect the dissociation/formation of xanthan assemblies. Launay et al. (1997) and Garcia et al. (2000) observed that the Huggins coefficient found for xanthan in 10% sucrose aqueous solution were higher (>1) than those obtained in water. This means that 10% aqueous sucrose solution is a bad solvent for xanthan and the molecule can be in a more compacted form for the less concentrated systems, resulting in lower G* values.

Table 2. Percentage of reduction on G* at 10 ^{o}C after 15% sucrose addition at 0.02 Hz and 1 Hz for different annealed xanthan samples.

Sample	Solution domain at the annealing temperature	Percentage of reduction on G* after 15% sucrose addition	
		at 0.02 Hz	at 1 Hz
X05-AT20	Anisotropic/biphasic transition	19	14
X1-AT50	Biphasic/isotropic transition	27	22
X35-AT75	Biphasic/isotropic transition	27	21
X1-AT20	Anisotropic/biphasic transition	32	32
X35-AT10	Anisotropic	35	24

The mechanism that could be associated with the lowering of the elasticity for the more concentrated xanthan-sucrose solutions (X1 and X35) is the kosmotropic effect of

sucrose in aqueous systems. In more concentrated polysaccharide solutions the amount of free water is reduced due to the well-known water binding capacity of xanthan. Thus, a fixed amount of added sucrose (eg. 15%) seems to act effectively as a more concentrated sucrose solution. In the presence of excess sucrose, the amount of free water necessary to form junction zones is reduced (Nishinari et al., 1990). The junction zones formed by the dissociation of the assemblies during the annealing could break more easily, resulting in a lower elasticity of the xanthan-sucrose solution as compared with the one without sucrose.

4. Conclusion

Xanthan solutions showed three different transitions from anisotropic-biphasic domain, biphasic-isotropic region and helix-coil conformation that were dependent on temperature and solution concentration. The latter was reversible only for concentrations lower than 0.1%. It was observed many birefringence aggregates by light microscope in the anisotropic and biphasic regions. The size and amount of those aggregates reduced with the temperature increase and the concentration decrease, respectively. The temperature of annealing affected the elasticity of the solution for all xanthan concentrations, but the duration of the annealing (heat-cooling scan or 1h at a fixed temperature) was important only for the highly anisotropic solution. The addition of sucrose affected the rheological properties over all frequency range studied but only for initially anisotropic or biphasic xanthan solutions. Sucrose probably played a role of promoting biopolymer intra-molecular aggregation for less concentrated solutions and by reducing the intermolecular junction zones in more concentrated solutions.

5. Acknowledgment

6. References

Basaran, T.K., Coupland, J.N., McClements, D.J. (1999). Monitoring molecular diffusion of sucrose in xanthan solutions using ultrasonic velocity measurements. Journal of Food Science, 64, 125-128.

Bordi, F., Cametti, C., Paradossi, G. (1996). Conformational changes of xanthan in salt-free aqueous solutions: a low-frequency electrical conductivity study. Journal of Physical Chemistry, 100, 7148-7154.

Braga, A.L.M., Cunha, R.L. (2004). The effects of xanthan conformation and sucrose concentration on the rheological properties of acidified sodium caseinate-xanthan gels. Food Hydrocolloids, 18, 977-986.

Camesano, T.A., Wilkinson, K.J. (2001). Single molecule study of xanthan conformation using atomic force microscopy. Biomacromolecules, 2, 1184-1191.

Capron, I., Alexandre, S., Muller, G. (1998). An atomic force microscopy study of the molecular organization of xanthan. Polymer, 39,5725-5730.

Capron, I., Brigand, G., Muller, G. (1997). About the native and renatured conformation of xanthan exopolysaccharide. Polymer, 38, 5289-5295.

Chaplin, M. Available from: http://www.sbu.ac.uk/water/hydrat.html, acessed 2005 October 30.

Garcia, M.H.F., Freitas, I.C., Cunha, R.L., Menegalli, F.C. Intrinsic viscosity of xanthan gum in water with different solutes. In: Proceedings of the Eighth International Congress on Engineering and Food. Lancaster, Pennsylvania: Technomic Publishing Co, v.1, p.504-508, 2000.

Iseki, T., Takahashi, M., Hattori, H., Hatakeyama, T., Hatakeyama, H. (2001). Viscoelastic properties of xanthan gum hydrogels annealed in the sol state. Food Hydrocolloids, 15, 503-506.

Jansson, P.E., Kenne, L., Lindberg, B. (1975). Structure of extracellular polysaccharide from Xanthomonas campestris. Carbohydrate Research, 45, 275-282.

Jones, S.A., Goodall, D.M., Cutler, A.N., Norton, I.T. (1987). Application of Conductivity Studies and Polyelectrolyte Theory to the Conformation and Order-Disorder Transition of Xanthan Polysaccharide. *European Biophysics Journal with Biophysics Letters*, 15, 185-191.

Launay, B., Cuvelier, G., Martinez-Reyes, S. (1997). Viscosity of locust bean, guar and xanthan gum solutions in the Newtonian domain: a critical examination of the log $(\eta_{sp})_0$ – log $C[\eta]_0$ master curves. Carbohydrate Polymers, 34, 385-395.

Lee, H.C., Brant, D.A. (2002). Rheology of concentrated isotropic and anisotropic xanthan solutions: 3. Temperature dependence. Biomacromolecules, 3, 4, 742-753.

Lim T., Uhl, J.T., Prud'Homme, R.K. (1984). Rheology of self-associating concentrated xanthan solutions. Journal of Rheology, 28, 367-379.

Nishinari, K., Watase, M., Williams, P.A., Phillips, G.O. (1990). kappa.-Carrageenan gels: effect of sucrose, glucose, urea, and guanidine hydrochloride on the rheological and thermal properties. Journal of Agricultural and Food Chemistry, 38, 1188-1193.

Paoletti, S., Cesàro, A., Delben, F. (1983). Thermally induced conformational transition of xanthan polyelectrolyte. Carbohydrate Research, 123, 173-178.

Paradossi, G., Brant, D.A. (1982). Light Scattering Study of a Series of Xanthan Fractions in Aqueous Solution. Macromolecules, 15, 874-879.

Richardson, P.H., Willmer, J., Foster, T.J. (1998). Dilute solution properties of guar and locust bean gum in sucrose solutions. Food Hydrocolloids, 12, 339-348.

Saggin, R., Coupland, J.N. (2004). Rheology of xanthan/sucrose mixtures at ultrasonic frequencies. Journal of Food Engineering, 65, 49-53.

Smith, I.H., Symes, K.C., Lawson, C.L., Morris, E.R. (1981). Influence of the pyruvate content of xanthan on macromolecular association in solution. International Journal of Biological Macromolecules, 3, 129-134.

Yoshida, T., Takahashi, M., Hatakeyama, T., Hatakeyama, H. (1998). Annealing induced gelation of xanthan/water systems. Polymer, 39, 5, 1119-1122.

CHAPTER 4. Protein-polysaccharide interactions in acidified gels containing Na-caseinate, SPI and/or xanthan

1st PART: The effect of the GDL/caseinate ratio on sodium caseinate gelation

(in collaboration with CBMEG-IB-UNICAMP)

Abstract

The influence of the acidification rate and of final pH on the properties of sodium caseinate gels (2-6% w/v) prepared by acidification with glucono-δ-lactone (GDL) at 10ºC was investigated. The rheological properties of the systems were analysed under shear at incipient gelation and under uniaxial compression throughout the entire gelation process. The water holding capacity (WHC) of these gels and their amount of soluble protein in different media were also evaluated. Up to ~50% of the total κ-casein content was soluble in gels with higher amount of GDL, and this contributed to the high WHC observed under this condition. The acidification rate did not affect the rheological properties measured under shear, but the GDL/caseinate ratio used had a significant effect on the steady state properties. Fast acidification resulted in lower Young modulus and stress at fracture values, but higher residual stress values and relaxation times. In contrast, slow acidification produced a more interconnected network, probably because of the extensive reorganization or rearrangement within the segments near the isoelectric point.
Keywords: acidification rate, gel, glucono-δ-lactone, sodium caseinate.

1. Introduction

Milk is a colloidal emulsion of protein particles, with casein being the main protein (~80%). Four main types of casein, α_{S1}-,α_{S2}-, β- and κ-casein, can be distinguished in milk and are present in a mass ratio of about 4:1:4:1.3. All casein in milk occurs in micelles, which are fairly large particles of colloidal size (Walstra & Jenness, 1984). However, the micellar structure of casein is destroyed during the manufacture of sodium caseinate

(Kinsella, 1984). Na-caseinate is an ingredient widely used in a range of food formulations because of its nutritional value and functional properties, such as its gelling capacity.

A gel structure is formed during milk/caseinate acidification as a result of the dissociation and aggregation of casein fractions. The two acidification processes used in the dairy industry result in a slow reduction of pH that can require more than 15 h (Lucey, Tamehana, Singh & Munro, 1998). In the traditional process, milk is acidified by bacteria, which ferment lactose to lactic acid. A second process that has gained the attention of food industry is direct acidification by the addition of lactone, such as glucono-δ-lactone (GDL). GDL is an internal ester that spontaneously hydrolyzes to form gluconic acid and has first-order reaction hydrolysis kinetics (de Kruif, 1997). The use of GDL avoids some of the difficulties associated with starter bacteria, such as variable activity and variation with the type of culture used. In addition, during gelation with GDL, the final pH of the system is a function of the amount of lactone added, whereas starter bacteria produce acid until they are inhibited by the low pH (Lucey et al., 1998).

Rheology is a powerful tool for analyzing the different steps involved in milk clotting and in gel formation, and for assessing the texture of the final product. Mechanical properties may be related to sensory texture and have been determined by empirical or fundamental methods. The benefit of using fundamental rheological methods to evaluate the mechanical elements of texture is that they can be linked to theories that explain molecular mechanisms. These theories could describe the food and predict the influence of various elements of the food or process conditions on the final product. However, models to predict complex systems, such as dairy foods, need to be modified continuously in order to fit the food texture more closely. The use of simplified model systems is very important for

providing a scientific framework (Foegeding, Brown, Drake & Daubert, 2003). The most important factors controlling the rheological properties of acid-induced caseinate gels are the protein content, the pH, the ionic strength and the presence of other components (de Kruif, 1997; Chen, Dickinson & Edwards, 1999).

The purpose of this work was to evaluate the effect of the acidification rate and of the final pH on sodium caseinate gelation and the gel properties at steady state. Different amounts of glucono-δ-lactone was added to Na-caseinate solutions and the rheological properties were measured under shear and compression during gelation. In addition, the effect of the amount of GDL on the steady state gel network properties was assessed by the water holding capacity (WHC), uniaxial compression, protein solubility and gel electrophoresis.

2. Material and methods

2.1. Material

The ingredients used to prepare the model systems were casein and glucono-δ-lactone (Sigma Chemical Co., St Louis, MO). The casein powder was characterized by atomic absorption (AA) spectroscopy in the Institute of Chemistry at UNICAMP, and the following composition of ions was obtained: Na=0.16%, Ca=0.14% e K=0.08%. The protein (N x 6.38), ash and moisture content of the casein powder were 88.2 ± 0.9%, 0.84 ± 0.08% and 6.5 ± 0.1% (wet basis), respectively.

2.2. Preparation of solutions and gels

Sodium caseinate solutions were prepared by dissolving the casein powder in deionised water at a maximum temperature of $50^{o}C$, with magnetic stirring for 2 h. Sodium

hydroxide (10 M) was added to keep the pH at 6.7. Different amounts of GDL were added to the sodium caseinate solutions at 10ºC and the mixture then poured into the rheometer or into cylindrical plastic tubes (30 mm in diameter and 30 mm height) for gel formation. The rheological properties during gelation at 10ºC were obtained by oscillatory shear measurements up to the gel point, and by compression tests up to steady state (~3 days). In addition, the WHC, protein solubility, electrophoresis and compression tests were done 4 days after the addition of GDL. The pH of the gels was monitored during the entire process.

The caseinate concentrations used to prepare the gels ranged from 2 to 6%. The concentration of GDL used in each formulation depended on GDL/caseinate ratio, which was 0.14, 0.16 or 0.18. For rheological oscillatory measurements, a ratio of 0.36 was also used to obtain faster acidification.

2.3. Gel properties measurements

2.3.1. Rheological oscillatory measurements

The oscillatory shear measurements were done using a stress-controlled rheometer (Carri-Med CSL^{2}500, TA Instruments, England). Time sweep measurements were done during the gelation process at 10ºC, 0.1 Hz and 0.1 Pa. A double wall concentric cylinder was used and the external diameter of the rotating bob was 21.96 mm, while the internal diameter was 20.38 mm. The stationary cylinder had an internal diameter of 20 mm and an external diameter of 22.38 mm. The Lissajous figures at various times were plotted to ensure that the measurements of G' (storage modulus) and G'' (loss modulus) were always obtained within the linear viscoelastic region.

2.3.2. Mechanical properties and pH

The decay in pH caused by GDL hydrolysis was measured using a Sentron 2001 pH meter (Sentron Inc., USA) equipped with an electrode calibrated at the reaction temperature over the pH range from 7.0 to 4.0. Uniaxial compression experiments were done using a TA-XT2*i* texture analyser (Stable Microsystems Ltd., England) equipped with an acrylic cylindrical plate (35 mm diameter). All measurements were done in triplicate at 10ºC and the fracture test was done throughout all the gelation process up to the steady state. The stress relaxation test was done only at steady state (4 days after the addition of GDL).

For rupture tests, gels were compressed to 80% of their original height using a crosshead speed of 1 mm/s. The force and height values were transformed into Hencky stress (σ_H) – Hencky strain (ε_H) curves (Steffe, 1996). The rupture properties (stress and strain) were obtained from the maximum point of the stress-strain curve, while the Young modulus was the slope of the initial linear region of this curve. The stress relaxation measurements were done within the non-linear viscoelastic region because the gels showed some syneresis during the test. These measurements were done during 7 min with an initial crosshead speed of 7 mm/s. The Peleg empirical correlation (Peleg, 1979) was used to fit the experimental data, with the relaxation time and the residual stress being obtained as responses.

2.3.3. Water holding capacity of gels

A disc of gel (1.5-2.0 g), equilibrated at room temperature, was cut into two pieces. Each piece was placed on a disc of Whatmann # 1 filter paper (Maidstone, U.K.) and positioned in the middle position of a 50 mL centrifuge tube. Water loss was determined in triplicate by weighing the gel before and after centrifugation at 173 g for 10 min (Ikeda &

Foegeding, 1999) in a T62.1 centrifuge (VEB MLW Medizintechnik Leipzig, Germany). The WHC values were calculated using Equation 1:

$$\text{WHC}(\%) = 100 \cdot \left[1 - \left(\frac{\text{Water}_{\text{loss}}(g)}{\text{Water}_{\text{gel}}(g)} \right) \right] \qquad (1)$$

where Water$_{gel}$ is the amount of water in the gel before centrifugation.

2.3.4. Protein solubility of gels

Samples were dispersed either in distilled water (pH 8.0) or in a pH 8.0 buffer (0.086 M Tris, 0.09 M glycine and 4 mM Na$_2$EDTA) (Lupano, Dumay & Cheftel 1992; Shimada & Cheftel, 1988). Samples (8.5 mg protein/mL) were homogenized at room temperature with an Ultra Turrax model T18 basic homogenizer (IKA, Germany) for 2 min and then centrifuged (F0850-rotor, Allegra^{TM} 64R Beckman, USA) at 20,000 x g for 15 min at 25°C. Protein solubility was determined in triplicate from supernatants and expressed as 100 x protein content in the supernatant / total protein content. Three independent extractions were done with each solvent. Protein concentrations were determined at 280 nm in a Beckmann Du-70 spectrophotometer (Beckmann, USA) using an apparent extinction coefficient ($E_{1cm}^{1mg/mL}$) of 0.947 for proteins dispersed in water and 0.942 for Tris buffer. The extinction coefficients were obtained by measuring the absorbance at 280 nm of a 1 mg/mL soy protein solution, the concentration of which was determined by the Kjeldhal method.

2.3.5. Electrophoresis of proteins

Urea polyacrylamide gel electrophoresis (PAGE) was done using the method of Andrews (1983) with minor modifications. Solutions with soluble proteins from gels (extracted in water and Tris buffer) were diluted with an equal volume of a pH 6.0 buffer [3

mL of stacking buffer (pH 6.7; 0.062 M Tris-HCl + 7 M urea); 2 mL of 87% glycerol; and

0.1 mL of β-mercaptoethanol]. Samples (10 μL of a solution at 1.5 mg/mL) were loaded

onto the gel. The gels were run at 200 V in a Mini Cell Protean electrophoresis unit (Biorad

Laboratories, USA) and then stained with 0.25% (v/v) Comassie Brilliant Blue, in

ethanol:acetic acid:water (45:10:45, v/v) followed by distaining with acetic

acid:ethanol:water (5:10:85, v/v).

2.4. Statistical analysis

The results were evaluated by analysis of variance (ANOVA) using the software

Statistica (5.0 version, USA), with the sources of variation being the caseinate

concentration and the GDL/caseinate ratio.

2.4.1. Mechanical properties and pH during gelation

A full factorial design was used to evaluate the influence of caseinate and GDL on

gelation. Table 1 shows the range of concentrations used in the 2^2 factorial design, as well

as the abbreviations that will be used in the Results and Discussion sections. The most

important effects associated with the response variables (pH, Young modulus and stress

and strain at fracture) were evaluated. The mathematical models that predicted the gel

properties as a function of the variables studied were considered valid if $F_{calc}/F_{tab}>1$.

Table 1. Coded levels and real values (in parentheses) for the factorial design, as well as the abbreviations of the formulations used. C is the caseinate concentration, G is the GDL/caseinate ratio, p is the positive level (+1), n is the negative level (-1) and c is the intermediate level (0).

Abbreviation of formulations	C (wt/v)	G (wt/wt)
CnGn	-1 (2)	-1 (0.14)
CnGp	-1 (2)	+1 (0.18)
CpGn	+1 (6)	-1 (0.14)
CpGp	+1 (6)	+1 (0.18)
CcGc	0 (4)	0 (0.16)

A first-order kinetics equation (Equation 2) was used to fit the mechanical properties and pH data as a function of time, with the reaction constant (k) values also being a response variable of the factorial design. The other response variable was the final pH (pH$_f$).

$$X = X_{ss} + C \cdot \exp(-kt) \tag{2}$$

where X is the measured property, X$_{ss}$ is its steady state value, k is the reaction constant, t is the time after GDL addition and C is a fitting parameter.

2.4.2. Protein solubility and steady state properties

The differences between the means of several treatments were assessed using the Tukey procedure (software Statistica, 5.0 version, USA), with p<0.05 for protein solubility and p<0.15 for the water holding capacity, stress relaxation properties and mechanical properties of the gels.

3. Results

3.1. Gelation process

The G'-G" crossover times (t_g) of acidified Na-caseinate systems (Table 2) were considered here as the gel time since most studies of milk/caseinate gelation have adopted this criterion (Curcio, Gabriele, Giordano, Calabrò, de Cindio & Iorio, 2001) or similar ones (Lucey, van Vliet, Grolle, Geurts & Walstra, 1997; Horne, 2003). The gelation time varied from ~100 to ~710 min, depending on the system (Table 2). The variation coefficient of the gel time was about 15% for gels with GDL/caseinate ratio of 0.18 and 0.36 and lower than 10%, when the ratio was 0.14 or 0.16. The pH at this point (pH_g) was about 5.0–5.1 for all systems. A similar pH was reported by Lucey et al. (1997) for acidified Na-caseinate gels (pH ~5.1) and by Roefs and van Vliet (1990) for the gelation of milk (pH ~5.0). The gel time (t_g) decreased by about 80-85% as the GDL/protein ratio increased from 0.14 to 0.36, for a given amount of caseinate. This marked variation can be attributed mainly to the first order degradation kinetics of GDL, in which gluconic acid (weak acid) is constantly produced and the back-reaction is negligible (de Kruif, 1997). Because the same amount of H^+ is needed to attain the caseinate clotting in all samples (similar pH_g), an increase in the GDL concentration reduced the gel time. A similar trend towards a reduction in gel time was observed as the protein concentration increased from 2% to 6% and the acidogen/protein ratio was maintained constant. However, in this case, the decrease in gelation time was 20-35%, indicating that the gel time was also governed by the association/dissociation of casein particles, which depends on the change in the ionic and solubility characteristics of the casein molecules (de Kruif, 1997).

Table 2. The G'-G" crossover times (min) for formulations with different amounts of caseinate and different GDL/caseinate ratios.

GDL/caseinate ratio (wt/wt)	Caseinate (w/v)		
	2%	4%	6%
0.14	711	671	573
0.16	564	437	370
0.18	424	363	339
0.36	130	105	99

The development of the gel network structure in Na-caseinate solutions acidified at different rates is shown in Figure 1. The gelation profile in Figure 1A was plotted against the reduced time, t/t_g, shifting the data along the horizontal axis in order to eliminate the effect of the kinetics of GDL hydrolysis. At the gel point, the values of G* were similar (around 0.1 Pa) and thereafter all curves showed a monotonic increase in G* with time (Figure 1A). Reducing the caseinate concentration resulted in a slower initial rate of G* growth, such that at a given reduced time (t/t_g = 1.075) G* was ~10 Pa, ~30 Pa and ~70 Pa for 2%, 4% and 6% caseinate gels, respectively. For each caseinate concentration, the plots fell on a single master curve. Figure 1B shows the changes in tan δ as a function of the reduced time for sodium caseinate solutions acidified with GDL. Two systems for each Na-caseinate concentration (GDL/caseinate ratios of 0.14 and 0.18) were chosen to illustrate the tan δ profile since the other formulations showed the same pattern. The profile shows an initial fast reduction in the tan δ values (up to t/t_g = 1.01), followed by a steady decrease to about 0.25 at the end of the oscillatory tests.
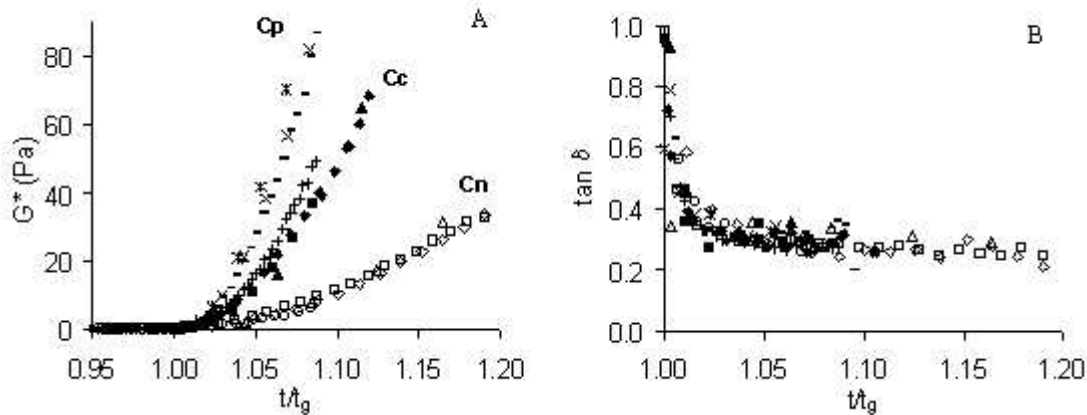
Figure 1. Rheological properties of acidified sodium-caseinate solutions as a function of the reduced time, t/t_g. A) Complex modulus (G*) B) Loss tangent (tan δ). The oscillatory tests were done at 10ºC and 0.1 Hz for solutions with different GDL/caseinate ratios for each sodium-caseinate content (Cp = 6%, Cc = 4%, Cn = 2%).

A 2^2 factorial experimental design was used to evaluate the effect of the caseinate concentration and of the amount of GDL (GDL/caseinate ratio) on the final pH and the rate of variation of the gel properties. Figure 2 shows the changes in pH as a function of time for sodium caseinate solutions acidified with GDL. GDL was rapidly hydrolysed to gluconic acid and resulted in a fast reduction of the pH during the first 1,000 min, after which the pH decreased steadily.
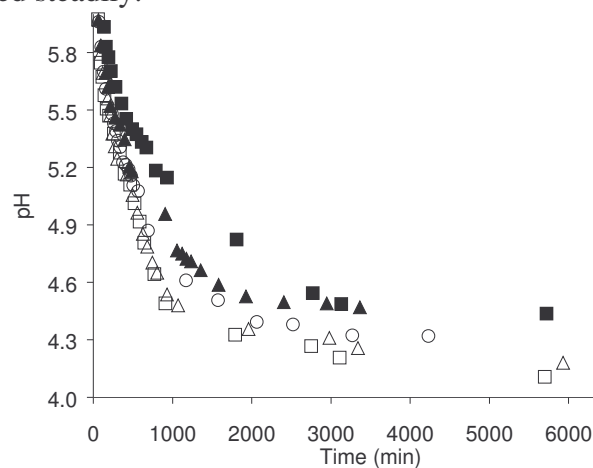
Figure 2. Changes in the pH of sodium-caseinate solutions during acidification with different concentrations of GDL. Formulations: (■) CnGn, (□) CnGp, (○) CcGc, (▲) CpGn, (△) CpGp.

The mechanical properties under uniaxial compression during gel formation (Figure 3) were analysed after the G'-G" crossover for each sample (Table 2 and Figure 3). At this time, all gels were self-supporting. The Young modulus values increased as a function of time (Figure 3A), in a manner similar to the profile for stress at fracture (results not shown), whereas the strain at fracture (Figure 3B) decreased with time. For each property, the profiles could be divided into three groups of formulations (Cn, Cc, Cp) that were dependent on the caseinate concentration. A positive correlation was observed between the caseinate content and gel properties at all times, thus indicating that these samples were more elastic, hard and firm. In addition, the higher the caseinate content the greater the changes in the Young modulus (Figure 3A) and stress at fracture values (data not shown) as a function of time. Such behaviour was not observed for strain at fracture (Figure 3B). The values of samples with a low GDL content (CnGn and CpGn) became greater than those with a high GDL/caseinate ratio during gelation, which indicated the formation of a harder and firmer structure. The properties of all gels still changed after periods >30 h (1,800 min). In addition, the Young modulus and stress at fracture reached the steady state faster as the GDL/caseinate ratio increased.

(A)

96

(B)
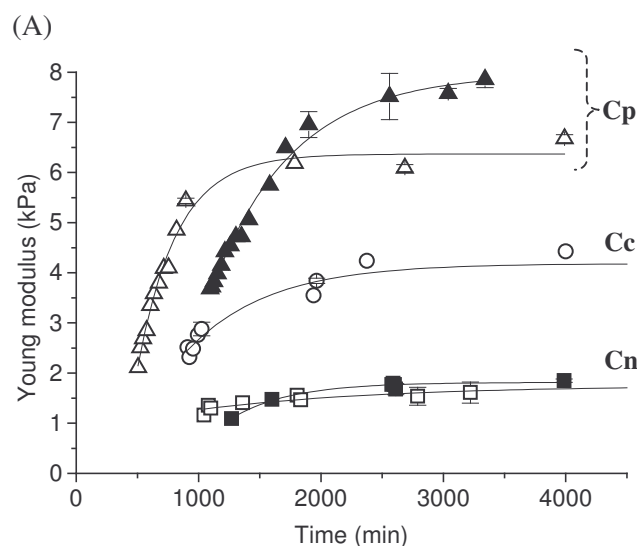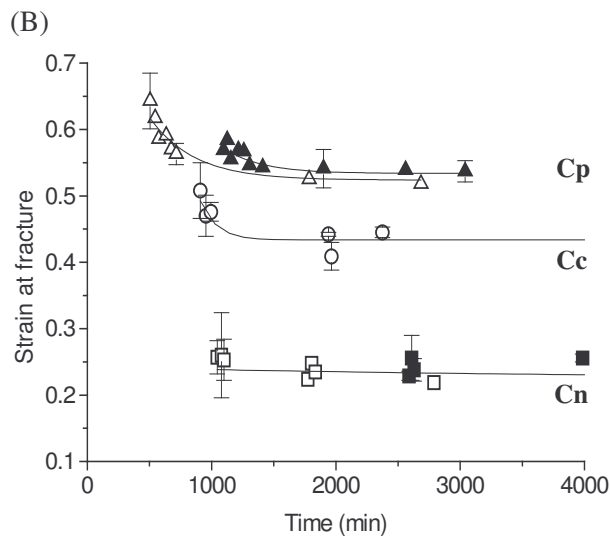
Figure 3. Mechanical properties of caseinate gels as a function of the acidification time. A) Young modulus, B) Strain at fracture. Gels were prepared with different amounts of protein and GDL. Formulations: (■) CnGn, (□) CnGp, (○) CcGc, (▲) CpGn, (△) CpGp.

Only the caseinate concentration affected the rate of variation of the Young modulus, while both the caseinate concentration and the GDL/caseinate ratio had a positive effect on the rate by which the stress at fracture increases with ageing time (Figure 4). However, the rate of the variation of the strain at fracture with time was not significantly ($p<0.1$) affected by either variable. The rate of decrease in pH (k-pH) was dependent on the caseinate concentration and the GDL/caseinate ratio. Both variables had a positive influence on the rate of acidification, although the effect of GDL was more pronounced in systems with a low caseinate concentration (Figure 2). The codified mathematical model described in Equation 3 was obtained to predict the pH_f as a function of the GDL/caseinate ratio.

$$pH_f = 4.42 - 0.135(GDL/caseinate)$$

(3)

This model could be used from levels –1 to +1 of the factorial design. The correlation coefficient (0.955) and the F-test (F_{calc}/F_{tab}=1.93) showed that the model was

97

reliable ($F_{calc}/F_{tab} > 1$). The final pH was affected only by the GDL/caseinate ratio, and values between 4.1 and 4.5 were obtained for all of the GDL/caseinate ratios used.
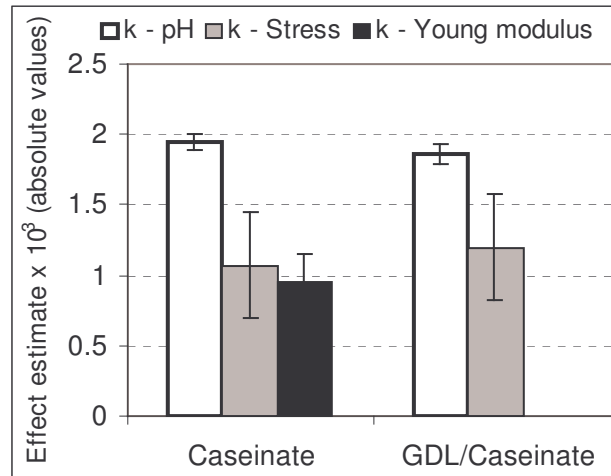
Figure 4. Effect of caseinate concentration and GDL/caseinate ratio on the reaction constant (k) obtained by varying the pH, stress at fracture and Young modulus with time.

3.2. Gel properties at steady state

The steady state properties of acid gels as a function of the GDL/caseinate ratio used are shown in Figure 5. No stress relaxation behaviour was observed for 2% Na-caseinate gels because of the spontaneous syneresis within the measurement cell after the initial fast uniaxial compression required for this test. Consequently, the gel lost its mechanical contact with the cell wall and the measured force dropped to zero (Merino, Lau & Dickinson, 2004). The residual stress (Figure 5A) was positively influenced by the GDL concentration in high protein gels. These values ranged between 0.08-0.12, but were about 0.04 for 4% protein gels, thus showing that the caseinate concentration affected this response. The GDL concentration had a positive effect on the relaxation time (Figure 5B) of 4% protein gels, with values ranging from 6 s to 10 s.

The mechanical properties of the gels (Figure 5C, 5D and 5E) were significantly influenced by the caseinate concentration. The stress at fracture (Figure 5C), Young modulus (Figure 5D) and the strain at fracture (Figure 5E) showed values of 500-5,000 Pa, 1,500-6,500 Pa and 0.2-0.5, respectively; the strain at fracture was the property least affected by the caseinate concentration. However, the effect of the GDL/caseinate ratio used was dependent on the response and on the amount of protein. The strain at fracture (Figure 5E) was not influenced by the GDL concentration at all protein concentrations. An increase in the GDL concentration tended to reduce the Young modulus and the stress at fracture of caseinate gels. However, the mechanical property obtained at small deformation (Figure 5D) showed large deviations for high protein gels and resulted in statistically similar values for 2% and 6% caseinate concentrations. The WHC increased from 10% to 50% as the caseinate concentration increased from 2% to 6%. An increase in the amount of GDL/g of protein also increased the capacity of 4% and 6% caseinate gels to retain water within the network. However, the effect of the amount of GDL was not as strong as that obtained with variations in the protein content since of the WHC values increased from 25% to 30% for 4% protein gels and from ~40 to 50% for 6% protein gels (Figure 5F).
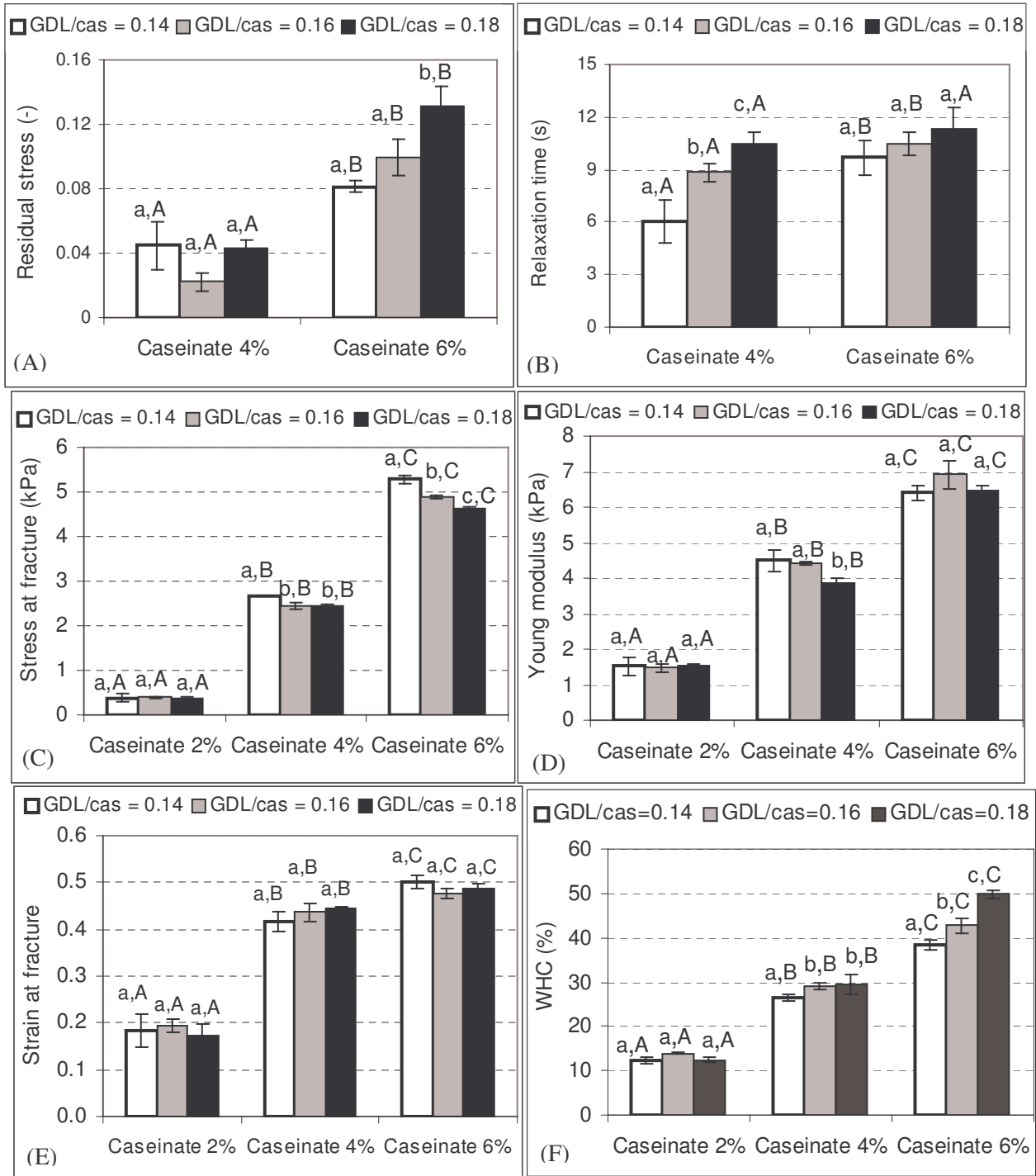
Figure 5. Steady state properties of sodium-caseinate gels acidified with different amounts of GDL. A) Residual stress, B) Relaxation time, C) Stress at fracture, D) Young modulus, E) Strain at fracture, F) Water holding capacity (WHC). Different letters indicate significant differences at $p<0.15$ (small letters: variation of the property with the GDL/caseinate ratio at a fixed caseinate concentration; capital letters: variation of the property with caseinate concentration at a fixed GDL/caseinate ratio).

The amount of soluble protein in different solutions and the electrophoretic profile can provide useful information on the network structure and on the composition and types of bonds involved. These measurements were done only for 4% and 6% Na-caseinate gels since these gels differed significantly differences in their steady state properties as a function of their content of GDL. Figure 6A shows the solubility of 4% and 6% Na-caseinate gels in two extraction media (deionised water and Tris buffer, pH 8.0) and the effect of different GDL/caseinate ratios used in the solution acidification. The solubility of proteins in Tris buffer was about 100% and did not vary significantly with the caseinate concentration or GDL/protein ratio. In contrast, the solubility of proteins in water was low (2-6%) and depended significantly ($p<0.05$) on the amount of acidulant added at all caseinate concentrations.
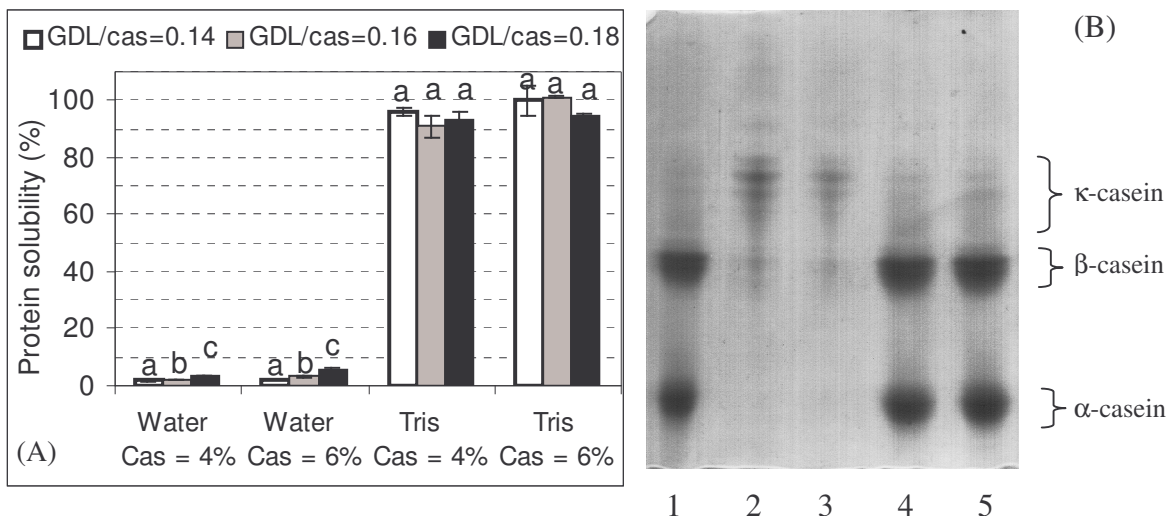
Figure 6. Protein solubility of 4% and 6% sodium-caseinate gels acidified with different amounts of GDL in water and Tris buffer. A) Total protein content (different letters indicate significant differences at $p<0.05$), B) Electrophoretic profiles of casein: Lane 1) Sodium-caseinate solution pH 6.7, Lanes 2 and 4) 4% caseinate and GDL/caseinate = 0.18, Lanes 3 and 5) 6% caseinate and GDL/caseinate = 0.18. Extraction solutions: Lanes 2 and 3) deionised water, Lanes 4 and 5) Tris buffer, pH 8.0.

The composition of the water-soluble and Tris-soluble protein fractions from different Na-caseinate gels was determined by urea-PAGE (Figure 6B). Electrophoresis

101

with urea was better than SDS-PAGE for separating the casein fractions because the distance between the bands was greater. Lane 1 (control) shows the typical electrophoretic profile of a sodium-caseinate solution (pH 6.7) with three major casein bands (κ, β and α-casein). The low intensity κ-casein band was difficult to observe, while α and β-casein showed diffuse bands. This variation in intensity reflected the different proportion of each fraction present in the sodium-caseinate solution, and it was necessary to load concentrated samples in order to observe the κ-casein band. The electrophoretic profile of the water-soluble protein (lanes 2 and 3) differed from that of the Tris-soluble protein (lanes 4 and 5) in that only the κ-casein band was seen, whereas lanes 4 and 5 showed all of the bands seen with the sodium caseinate solution (pH 6.7). These findings agreed with the absorbance results that indicated 100% protein solubility in Tris buffer. The distribution of the κ-casein band seen in lanes 2 and 3 was very broad. Pepper and Farrell (1982) and Farrell et al. (1996) reported that κ-casein in whole casein exists as disulfide-bonded polymers with a wide size distribution. The pattern of κ-casein band observed here probably resulted from the dissociation of this casein fraction into lower molecular weight aggregates because of the β-mercaptoethanol used in the electrophoresis buffer.

4. Discussion

In this study, different GDL/caseinate ratios were used in order to obtain fast and low rates of acidification and also different gel pH values at steady state. Figures 1 and 3 indicate that the gelation profile was more sensitive to the caseinate concentration than to the GDL/caseinate ratio used. Two distinct stages were involved in the gelation process promoted by GDL (Chen & Dickinson, 2000): the initial setting up of the gel network

(Figure 1), and subsequent development through bond strengthening and/or local rearrangements (Figure 3).

At the start of gelation ($\sim t_g$), the increase in G* probably reflected the increased contact between the caseins mediated by particle fusion and interparticle rearrangements that can occur even before gelation (Mellema, Walstra, van Opheusden & van Vliet, 2002b). The structural characteristics of the gels were very similar for the different GDL/caseinate ratios used at each caseinate concentration since all of the G* *versus* t/t_g plots fell on a single master curve (Figure 1A). However, the presence of different amounts of protein affected the rate of gelation (as indicated by the slope of the G* curves) and the gel elasticity (as indicated by the values of G* at a given reduced time). During the initial stage of the acidification process, a substantial repulsive force remains between particles so that particles may collide many times before sticking (Martin & Adolf, 1991). Thus, the protein effect was observed probably because the contact between particles was favoured due to a great number of molecules. All gels had similar values of loss tangent as a function of reduced time (Figure 1B). This means that the ratio of the amount of energy dissipated by relaxation of the protein-protein bonds relative to the amount of elastic energy stored in small distortions of the protein-protein bonds was independent of the protein content and the GDL/caseinate ratio. The different effects of the amount of protein on the G* and tan δ values indicated that the dynamics of the casein strands were similar (similar tan δ), but that there was a greater number of strands (network connections) in more concentrated protein gels, such that the network elasticity was dependent on the amount of protein present.

The rate of acidification of caseinate solutions may affect the dissociation of caseins, the rate of aggregation, and the time available for rearrangement of the aggregating

protein particles (Lucey et al., 1998), thereby resulting in different gel steady state properties. A high GDL/protein ratio reduces the gelation time, but also causes "over-acidification" (pH<pI) (Chen et al., 1999; Dickinson & Merino, 2002). In the present work the final pH ranged from 4.1 to 4.5 for GDL/caseinate ratio of 0.18 to 0.14, respectively. Figure 6A shows that a small amount of proteins was not bound in the caseinate network, and corresponded to κ-casein (Figure 6B). Because of its higher isoelectric point (pI 5.3-5.8), κ-casein would be more soluble at pH ~4.1-4.5 than α- or β- casein (pI 4.2 and 4.7 respectively; Hudson, 1984). This soluble fraction was present in a small amount because of its low concentration (12.7%) in the original sodium-caseinate (Walstra & Jenness, 1984). However, a dissociation of 46.7% of the total κ-casein was obtained in 6% caseinate gels acidified with the highest amount of GDL. This amount was determined by the absorbance analysis, considering that all soluble protein in water extract was κ-casein (lanes 2-3 of Figure 6B). Thus, this "over-acidification" and consequently different degrees of κ-casein dissociation and final gel pH is another point to be affecting the gel steady state properties.

By analysing more than one property, it was easier to understand the overall structural characteristics of the gel. The significant (p<0.15) differences associated with the amount of GDL used were not observed for all caseinate concentrations partly because of variations in the accuracy of the different techniques employed (Figure 5). The mechanical properties were explored by investigating the change in stress as a function of the strain under uniaxial compression. A gradual increase in strain resulted in a proportional increase in sample stress (linear viscoelastic range) during the initial stages. In general, particulated gels have a much shorter linear region than cross-linked polymer gels, and this complicates

the measurement of Young modulus. Because of the high deviations associated with this analysis, a negative effect of GDL concentration on this property was observed only for 4% caseinate gels, while the stress at fracture showed the same tendency for 4% and 6% protein gel. The shorter ageing time near the isoelectric point of casein, when a high amount of GDL was used, could partly explain the lower mechanical properties of the gels (Figures 5C and 5D). The longer ageing time seen near the isoelectric point when using low amounts of GDL may contribute to the continued fusion and rearrangement of casein particles and result in a highly interconnected network (Lucey et al., 1997). The weaker network could also be attributed to the lower pH (Figure 3), since beyond the isoelectric point (pI) the repulsive electrostatic forces overcome the net attractive forces and some κ-casein was dissociated of the network. However, those properties might have been more affected by the rate of acidification.

The relaxation properties of the gels as a function of the amount of GDL showed a response that was opposite to that of the Young modulus and stress at fracture. Both the residual stress and relaxation time showed a general tendency to increase with increasing amounts of GDL, thus indicating that this network was more elastic. One possible explanation for this contradictory effect of the amount of GDL on the network properties could be because of the time scale of the applied deformation taking also into consideration the geometry of the network (straight or a curved strand) (Bremer, Bijsterbosch, Schrijvers, van Vliet & Walstra, 1990; Mellema, van Opheusden & van Vliet, 2002a). Gels with curved strands may have a higher residual stress than those with less curved strands because they can support greater deformations for long time or store a higher amount of

elastic energy. However, when applying a continuous deformation until the fracture some fragile points of the curved strands can be responsible for the low stress at fracture.

The increase in the WHC of the gels with increasing amount of GDL was apparently more related to the amount of dissociated κ-casein than to the network dynamics. Slow gelation produced gels with a lower capacity to retain water. Although, faster acidification is often considered to lead to the formation of coarser networks (Lucey et al., 1998). The increased dissociation of κ-casein as the pH was lower than pI could also be contributing to the high WHC. The dissociated fraction increased by about 2-fold (from 14.1% to 29.5%) for gels with 4% protein and by about 3-fold (from 15.7% to 46.7%) for 6% caseinate gels as the GDL/caseinate ratio increased from 0.14 to 0.18. Thus, the positive effect of the amount of GDL on the WHC could also be explained by an increase in protein-water affinity.

5. Conclusions

The results of this study show that an adequate interpretation of the dynamics of the caseinate network requires the use of different techniques. In general, all of the properties associated with gelation were affected by the caseinate concentration, whereas the effect of the GDL/caseinate ratio depended on the time scale analysed. At the start of gelation, the GDL/caseinate ratio did not influence the rheological properties obtained under shear, but affected the rate of change in pH and in stress at fracture after the gel point. The steady state mechanical and relaxation properties seemed to be governed by the rate of acidification. The gel obtained with fast acidification was weaker at rupture but had a higher capacity to store elastic energy. In contrast, slow acidification yielded a hard, firm

network, probably because of extensive reorganization or rearrangement within the segments. The addition of high GDL/caseinate ratio produced gels with a greater capacity to retain water that was mainly attributed to the high degree of κ-casein dissociation at the lower pH.

6. Acknowledgements

7. References

Andrews, A.T. (1983). Proteinases in normal bovine milk and their action on caseins. *Journal of Dairy Research*, *50*, 45-55.

Bremer, L.G.B., Bijsterbosch, B.H., Schrijvers, R., van Vliet, T., & Walstra, P. (1990). On the fractal nature of the structure of acid casein gels. *Colloids and Surfaces*, *51*, 159-170.

Chen, J.S., & Dickinson, E. (2000). On the temperature reversibility of the viscoelasticity of acid-induced sodium caseinate emulsion gels. *International Dairy Journal*, *10*, 541-549.

Chen, J.S., Dickinson, E., & Edwards, M. (1999) Rheology of acid-induced sodium caseinate stabilized emulsion gels. *Journal of Texture Studies*, *30*, 377-396.

Curcio, S., Gabriele, D., Giordano, V., Calabrò, V., de Cindio, B., & Iorio, G. (2001). A rheological approach to the study of concentrated milk clotting. *Rheologica Acta*, *40*, 154-161.

de Kruif, C.G. (1997). Skim milk acidification. *Journal of Colloid and Interface Science*, *185*, 19-25.

Dickinson, E., & Merino, L.M. (2002). Effect of sugars on the rheological properties of acid caseinate-stabilized emulsion gels. *Food Hydrocolloids, 16*, 321-331.

Farrell, H.M.J., Cooke, P.H., King, G., Hoagland, P.D., Groves, M.L., Kumosinski, T.F., & Chu, B. (1996). Particle sizes of casein submicelles and purified k-casein. In N. Parris, A. Kato, L.K. Creamer, J. Pearce, *Macromolecular Interactions in Food Technology (*pp. 61-79). American Chemical Society: Washington.

Foegeding, E.A., Brown, J., Drake, M.A., & Daubert, C.R. (2003). Sensory and mechanical aspects of cheese texture. *International Dairy Journal*, *13*, 585-591.

Horne, D.S. (2003). Casein micelles as hard spheres: limitations of the model in acidified gel formation. *Colloids and Surfaces A: Physicochemical Engineering Aspects*, *213*, 255-263.

Hudson, B.J.F. (1984). *Developments in Food Proteins v. 3* (pp. 1-60). Elsevier Applied Science: London.

Ikeda, S., & Foegeding, E. A. (1999). Effects of lecithin on thermally induced whey protein isolate gels. *Food Hydrocolloids*, *13*, 239-244.

Kinsella, J.E. (1984). Milk proteins: physicochemical and functional properties. *CRC Critical Reviews in Food Science and Nutrition*, *3*, 197-262.

Lucey, J.A., Tamehana, M., Singh, H., & Munro, P.A. (1998) A comparison of the formation, rheological properties and microstructure of acid skim milk gels made with a bacterial culture or glucono-delta-lactone. *Food Research International, 31*, 147-155.

Lucey, J.A., van Vliet, T., Grolle, K., Geurts, T., & Walstra, P. (1997). Properties of acid casein gels made by acidification with glucono-delta-lactone. 1. Rheological properties. *International Dairy Journal*, *7*, 381-388.

Lupano, C.E., Dumay, E., & Cheftel, J.C. (1992). Gelling properties of whey protein isolate: influence of calcium removal by dialysis or diafiltration at acid or neutral pH. *International Journal of Food Science and Technology*, *27*, 615-628.

Martin, J.E., & Adolf, D. (1991). The sol-gel transition in chemical gels. *Annual Review of Physical Chemistry, 42*, 311-339.

Mellema, M., van Opheusden, J.H.J., & van Vliet, T. (2002a). Categorization of rheological scaling models for particle gels applied to casein gels. *Journal of Rheology*, *46*, 11-19.

Mellema, M., Walstra, P., van Opheusden, J.H.J., & van Vliet, T. (2002b). Effects of structural rearrangements on the rheology of rennet-induced casein particle gels. *Advances in Colloid and Interface Science*, *98*, 25-50

Merino, L.M., Lau, K., & Dickinson, E. (2004). Effects of low-methoxyl amidated pectin and ionic calcium on rheology and microstructure of acid-induced sodium caseinate gels. *Food Hydrocolloids*, *18*, 271-281.

Peleg, M. (1979). Characterization of the stress relaxation curves of solid foods. *Journal of Food Science*, *44*, 277-281.

Pepper, L., & Farrell, H.M.J. (1982). Interactions leading to the formation of casein submicelles. *Journal of Dairy Science*, *65*, 2259-2266.

Roefs, S.P.F.M., & van Vliet, T. (1990). Structure of acid casein gels. 2. Dynamic measurements and type of interaction forces. *Colloids and Surfaces*, *50*, 161-175.

Shimada, K., & Cheftel, J.C. (1988). Texture characteristics, protein solubility, and sulphydryl group/disulfide bond contents of heat-induced gels of whey protein isolate. *Journal of Agricultural and Food Chemistry*, *36*, 1018-1025.

Steffe, J.F. (1996). *Rheological Methods in Food Process Engineering*. East Lansing: Freeman Press.

Walstra, P., & Jenness, R. (1984). *Dairy Chemistry and Physics*, Wiley: New York.

CHAPTER 4. Protein-polysaccharide interactions in acidified gels containing Na-caseinate, SPI and/or xanthan

2nd PART: Small- and large-strain rheological properties of GDL-induced soy protein isolate gels: effect of gelation temperature and xanthan addition.

Abstract

The linear, non-linear and fracture properties of GDL (glucono-δ-lactone)-induced tofu model systems were studied as a function of protein content, xanthan addition and acidification temperature. The decrease of the breaking stress or strain could be obtained by decreasing the SPI concentration in pure gels or by increasing the protein concentration in gels made with xanthan. Another option for the latter gels would be the increase of acidification temperature. It was proposed a new equation based on BST-equation (Blatz et al., Trans. Soc. Rheol. 18, (1974) 145) to obtain a greater number of mechanical properties of gels. Two more parameters could be predicted as compared to BST equation namely, 1) stress at fracture, 2) strain at fracture. In addition, the Young modulus (E) and the elasticity parameter (n) were also predicted. The behaviour of SPI gels under compression was well described by the proposed equation and the predicted mechanical properties did not showed significantly ($p<0.05$) differences from the experimental true stress and Hencky strain at fracture. In addition, the correlation between n and fracture parameters was very interesting, since it enables the manipulation of the breaking stress and strain of the gel.

1. Introduction

Typical food proteins of interest for the industry include those derived from milk, soy, fish and egg, which are used in a number of food products. Soy proteins are the most important representative of legume proteins due to their high protein level and well-balanced amino-acid composition (Van Vliet et al., 2002). The most recognized soy food product in the world is tofu and the manufacturers are concerned with the yield, which is of economic importance, and texture that determines its acceptability (Abd Karim et al.,

113

1999). Tofu is traditionally made by the addition of calcium sulphate or glucono-δ-lactone (GDL), which are used as coagulants (Abd Karim et al., 1999).

The functional properties of soy protein isolates (SPI) reflect the composition and structure of their globulins, which correspond to 50 – 90% of the total proteins (Utsumi, et al., 1984). The soy protein fractions can be classified by their sedimentation constants, showing approximate Svedberg coefficients of 2S, 7S, 11S and 15S. The two major globulins in soybeans are β-conglycinin and glycinin, also called 7S and 11S, respectively. The glycinin subunits consist of two polypeptide components linked via disulfide bonds (AB), one with acidic (A) and the other with basic (B) isoelectric points (Staswick et al., 1984). β-conglycinin is a trimeric glycoprotein consisting of at least six combinations of three subunits: α, α' and β (Thanh & Shibasaki, 1977).

In spite of the increasing demand for food products containing soy protein, very little is known about the interactions of soy proteins with other ingredients in foods. Some studies have been conducted on the addition of polysaccharides to tofu in order to enhance the gel properties. The addition of both, carrageenan (Abd Karim et al., 1999) and chitosan (Chang et al., 2003) increased the water holding capacity, although they had different effects on the mechanical properties of tofu made with GDL. However, the studies about the interactions between soy protein and xanthan were done only for heat-induced gels (Hua et al., 2003, Braga et al., 2006a) or foams (Carp et al., 1999). The application of heat-induced gelation on globular proteins has limitations or is not always desired (Barbut and Foegeding, 1993). In contrast, cold gelation is easier to control, more efficient and an advantage might be that heat-labile or volatile compounds can be added (in the gelation step) without any losses or off-flavor occurring. However, this process is more complex

114

than the heat-induced gelation one and also results in new attractive textures (Weijers et al., 2006).

When a gel-type food is consumed, the perception of texture can be in part explained by its mechanical properties (Li et al., 1999). The mechanical properties have been determined by empirical or fundamental methods and the use of simplified model systems is very important for providing a scientific framework (Foegeding et al., 2003). Uniaxial compression measurements up to rupture can provide information about the mechanical properties at small and large deformations. The former gives the elasticity modulus (Young modulus) that is obtained from the slope of the initial linear region of the stress-strain curve. The latter is associated to the fracture properties, being the fracture stress and strain that reflect, respectively, hardness and deformability of gels.

However, the non-linear region, between the linear region and fracture, is still relatively ill understood. Phenomenological models have been applied to large-strain behavior in attempts to quantify the extent of non-linearity, or deviation from ideal elastic behavior (Blatz et al., 1974; Peleg, 1984). The BST equation (Blatz et al., 1974) has been most recently applied to biopolymer gels to describe and quantify non-linear behavior, but the interpretation of the parameters estimated from this model have varied (Bot et al., 1996; Groot et al., 1996). Recently, Barrangou et al. (2006) suggested a new polynomial equation to describe the non-linear region of gels and reported a better data fit for agarose gels than the one obtained by using BST equation. However, both models describe the linear and non-linear behaviours only up to the fracture point, but the mechanical properties at fracture can not be predicted.

The objectives of this work were (1) to develop a model that could predict a greater number of mechanical properties, including the linear, non-linear and fracture properties.

115

For that purpose, it was used the BST equation that describes two parameters (Young modulus and non-linear elasticity); (2) to evaluate the effects of xanthan addition and acidification temperature (reaction rate) on the mechanical properties of GDL-SPI gels.

2. Material and methods

2.1. Materials

The ingredients used to prepare the model systems were xanthan and glucono-δ-lactone (GDL) obtained from Sigma Chemical Co. (USA) and soy protein isolate (SPI) produced from defatted soy flour (Bunge Alimentos S.A., Brazil). The protein, ash and moisture content of the SPI and xanthan powder are shown in Table 1.

Table 1. Characterization of the biopolymers used to prepare the model systems.

Biopolymer	Moisture [%] (wet basis)	Protein [N% x 6.25] (wet basis)	Ash [%] (wet basis)
SPI	6.44 ± 0.07	91.25 ± 0.45	3.45 ± 0.04
Xanthan	8.36 ± 0.23	4.13 ± 0.08	11.93± 0.29

2.2. Preparation of soy protein isolate

Defatted soy flour was dispersed in distilled water (1:10 w/w) and the pH adjusted to pH 8.0 with 2N NaOH. The dispersion was gently stirred for 2h at room temperature and then centrifuged at 10,000 x g for 30 min at 4ºC in a Sorvall RC5 Plus centrifuge (GSA-rotor, Dupont, UK). The supernatant was adjusted to pH 4.5 with 2N HCl and centrifuged at 5,000 x g (Sorvall GSA-rotor) for 15 min at 4ºC. The precipitate was then suspended in water and the pH adjusted to 8.0 with 2N NaOH, followed by freeze-drying of the suspension (Petruccelli and Añón, 1995).

2.3. Preparation of biopolymer solutions and gels

Soy protein isolate and xanthan stock solutions were prepared at ambient temperature by magnetic stirring and the pH was adjusted to 7.0. These stock solutions were mixed at different concentrations and temperatures (10 and 25 ^{o}C) as shown in Table 2 before the addition of glucono-delta-lactone. The concentration of GDL used in each formulation depended on GDL/SPI ratio, which was defined experimentally (Results and Discussion section) in order to obtain a steady state final pH (pH$_f$) equal to 4.5 (SPI isoelectric point). The levels of GDL/SPI ratio used in the screening to obtain the adequate GDL concentration to achieve the isoelectric point at steady state varied from 0.13-0.3 and it was according to previous works in the literature (Dybowska and Fujio, 1998, Roesch et al., 2004, Tay et al., 2005).

Table 2. Concentrations of SPI and xanthan used to prepare the model systems.

SPI (%)	Xanthan (%)	Acidification temperature (^{o}C)
4	0.0	25
6	0.0	25
8	0.0	25
4	0.2	25
6	0.2	25
8	0.2	25
4	0.2	10
6	0.2	10
8	0.2	10

After GDL addition, the mixture was poured into the rheometer or into cylindrical plastic tubes (20 mm diameter and 20 mm height) for gel formation. The small deformation rheological properties during gelation at 25 ºC were obtained by oscillatory shear

measurements. In addition, the samples were kept at 25 ºC for 24 h or 10 ºC for 3 days after GDL addition before performing the uniaxial compression measurements.

2.4. Gel properties measurements

2.4.1. pH

The pH of the gels was monitored during the entire gelation process. The decay in pH caused by GDL hydrolysis was measured using a Sentron 2001 pH meter (Sentron Inc., USA) equipped with an electrode calibrated at the reaction temperature over the pH range from 7.0 to 4.0.

2.4.2. Rheological oscillatory measurements

The oscillatory shear measurements were done using a stress-controlled rheometer (Carri-Med CSL^2500, TA Instruments, England). Time sweep measurements were done during the gelation process at 25 ºC, 0.1 Hz and 0.1 Pa. A double wall concentric cylinder was used for systems without polysaccharide. The external diameter of the rotating bob was 21.96 mm, while the internal diameter was 20.38 mm. The stationary cylinder had an internal diameter of 20 mm and an external diameter of 22.38 mm. Cone and plate geometry (angle 2°, diameter 60 mm) was used for samples containing xanthan. The Lissajous figures at various times were plotted to ensure that the measurements of G' (storage modulus) and G" (loss modulus) were always obtained within the linear viscoelastic region.

2.4.3. Compression measurements

Compression measurements were done using a TA-XT2*i* texture analyser (Stable Microsystems Ltd., England) equipped with an acrylic cylindrical plate (30 mm diameter). All measurements were done in triplicate at 25 ºC when the gels attained the steady state

properties. The gels were compressed to 80% of their original height using a crosshead speed of 1 mm/s.

The force (F) and height (H) values were transformed into true stress (σ) and Hencky strain (ε_H), Equations 1 and 2 respectively, in order to account the increase in surface area during compression (Steffe, 1996). The rupture properties (stress and strain at fracture) were obtained from the maximum point of the stress-strain curve, while the Young modulus (E_{linear}) was the slope of the initial linear region of this curve.

$$\sigma = F(t)\left(\frac{H(t)}{H_0 \cdot A_0}\right) \tag{1}$$

$$\varepsilon_H = -\ln\left(\frac{H(t)}{H_0}\right) \tag{2}$$

where A_0, H_0 are the initial cross sectional area and initial height of the sample, respectively and t is the time during the compression test.

The compression behaviour of each gel was modeled using Equation 3, which is a modification of BST equation (Blatz et al., 1974).

$$\sigma = \sigma_0 + \frac{2E}{n}\left(\lambda^{-n} - \lambda^{-2n}\right), \lambda \geq 1 \tag{3}$$

and,

$$\lambda = \frac{R(t)}{R_0} \tag{4}$$

where λ is the stretch ratio, R_0 is the initial gel radius, $R(t)$ is the gel radius at each compression time, σ_0 is the initial stress of the sample, E is the Young modulus that characterizes the linear elastic behaviour at small deformations, and n is regarded as an empirical measure of the non-linear elastic behaviour at large deformations. Non-linear least squares regression was used to fit the Equation 3 to stress (Equation 1) and stretch

(Equation 4) data, where E and n were fitting parameters. Equation 3 was used to fit the data up to just after the fracture point.

The stress (Equation 5), stretch (Equation 6) and strain (Equation 7) at fracture can be obtained by the zero response of the derivative of Equation 3 ($d\sigma/d\lambda$). The strain at fracture was calculated from the stretch at fracture value considering an incompressible gel (constant volume).

$$\sigma_f = \sigma_0 + \frac{E}{2n} \tag{5}$$

$$\lambda_f = \sqrt[n]{2} \tag{6}$$

$$\varepsilon_f = -\ln\left(\frac{1}{\lambda^2}\right) \tag{7}$$

where the subscript f is referred to the fracture point.

2.5. Statistical analysis

Values reported for compression properties represent the mean of three replicates, and the error is reported as standard deviation. The results were evaluated by analysis of variance (ANOVA) using the software Statistica (5.0 version, USA), with the sources of variation being the SPI concentration and the gel type (xanthan addition and gelation temperature). The differences between the means of several treatments were assessed using the Tukey procedure with $p < 0.05$.

3. Results and discussions

3.1. Determination of GDL/SPI ratio

In previous works, the range of GDL/SPI ratio used to induce the gelation of SPI, tofu or SPI fractions varied from 0.1 (Tay et al., 2005) up to 0.3 (Dybowska and Fujio, 1998). Thus, a screening of GDL/SPI ratio was carried out to determine a suitable

concentration of GDL required to attain the SPI isoelectric point (pH 4.5) at steady state. Figure 1 shows the steady state pH achieved in SPI (2-8%) solutions after the addition of different amount of GDL. During gelation with GDL, the final pH of the system was a function of the amount of lactone added (Lucey et al., 1998). GDL was rapidly hydrolysed to gluconic acid and resulted in a fast reduction of the pH during the first 200 min, after which the pH decreased steadily (results not shown). The optimum GDL/SPI ratio to reach the isoelectric point at steady state depended on the SPI concentration, being 0.17% for 2 and 4% SPI solutions and 0.14% for samples containing 6 and 8% of SPI. It means that the suitable GDL concentration for 2, 4, 6 and 8% SPI solutions would be, respectively, 0.34, 0.68, 0.84 and 1.12% (w/w). The increment in the GDL concentration as a function of SPI content took into account the buffering capacity of the soy proteins and keeps the acidification rates comparable to one another (Roesch et al., 2004).
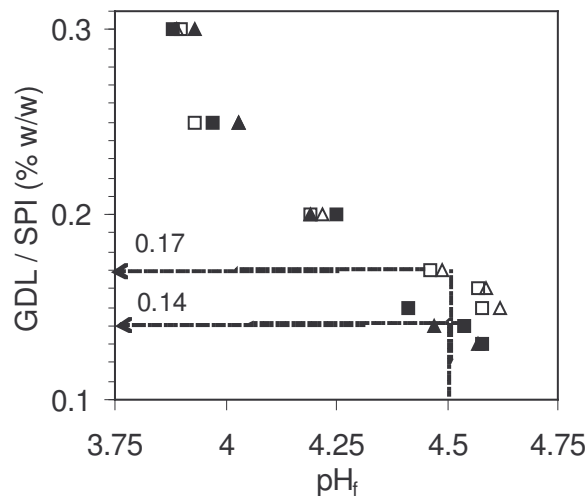
Figure 1. Steady state final pH (pH_f) of GDL-SPI gels at 25°C using different values of GDL/SPI ratio. SPI concentrations: 2% (△), 4% (□), 6% (▲), 8% (■).

3.2. Small-strain oscillatory rheological properties

The development of the gel network structure at 25°C for GDL acidified SPI and SPI-xanthan solutions is shown in Figure 2. The G'-G" crossover times (t_g) of systems was

the criterion considered to determine the gel time. The gelation profile in Figure 2 was plotted against the reduced time, t/t_g, shifting the data along the horizontal axis in order to eliminate the effect of the kinetics of GDL hydrolysis. At the gel point, the values of G* were very low (up to 1.5 Pa) and thereafter all curves showed a monotonic increase in G* with time. The reduction in SPI concentration or the addition of xanthan resulted in a slower initial rate of G* growth, such that at a given reduced time (t/t_g = 1.6) G* was ~30 Pa, ~120 Pa and ~220 Pa for 8% SPI-xanthan, 4% SPI and 8% SPI gels, respectively.

The gelation time for all concentrations studied of pure SPI systems was ~80 min and the pH at this point (pH_g) was near 5.6 at 25°C (Figure 2). Similar pH was reported by Roesch et al. (2004) for acidified SPI/milk gels (pH ~5.8). However, these authors observed a decrease of the gel time with the increase of the percentage of SPI content in skim milk-SPI mixtures. Braga et al. (2006b) showed that the gel time of GDL-induced Na-caseinate systems was dependent on the protein concentration. Thus, the variation of gel time found by Roesch et al. (2004) could be attributed to the presence of milk proteins.
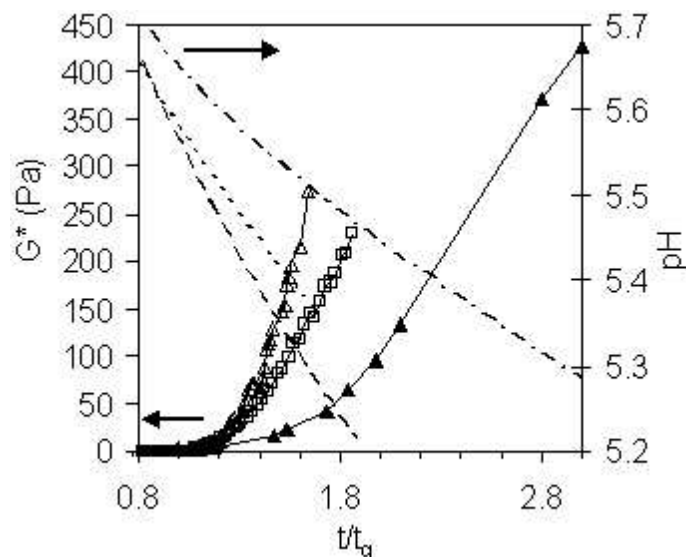
Figure 2. Complex modulus (G*) and pH evolution during the acidification of SPI solutions as a function of the reduced time (t/t_g). Systems: 4% SPI- G* (□), pH (dashed line); 8% SPI- G* (Δ), pH (dotted line); 8% SPI + 0.2% xanthan- G* (▲), pH (dot/dashed line).

Figure 2 also shows that the addition of 0.2% xanthan in 8% SPI sample reduced the G'-G" crossover time to ~50 min, while the pH_g was almost the same, 5.7. In the presence of milk proteins or xanthan the gel time and network strength of SPI systems changed, although the pH_g was kept almost the same. SPI is highly unstable in the pH range from 5-6, since most of the fractions isoelectric points occur within this range of pH, 4.8-5.4 for A-11S, 4.9 for α-7S, 5.2 for α'-7S and 5.7-6.0 for β-7S (Hermansson, 1986). Thus, the decrease of the gel time with the addition of xanthan could be explained by an increase of SPI instabilities caused by the screening of the excluded volume effect when another biopolymer is also present. On the other hand, the decrease of the network strength at the beginning of gelation could be related to SPI-xanthan specific interactions. Figure 2 shows that from the pH 5.7 (gel point and isoelectric point of β-7S) to 5.4 (isoelectric point of A-11S) the network strength is higher for 8%SPI gel than for 8%SPI-xanthan gel. Mohamad Ramlan et al., (2004) observed that the α-7S and β-7S subunits contribute to the increase of gel hardness relative to the complete 7S protein. In addition, Braga et al. (2006a) reported that xanthan preferentially interacts with the β-7S fraction of SPI in acid heat-induced gels. These indicate that the lower strength observed for SPI-xanthan gel could be attributed to a linkage between the β-7S with xanthan such that this fraction was not corroborating to the network strength.

3.3. Compression rheological properties

The difference between the model described in Equation 3 and BST equation is the addition of an initial stress parameter (σ_0) and a change on the first power exponent from n to –n. The insert of the initial stress parameter was necessary because the data aquired did not started from zero, as previously observed for agarose gels (Barrangou et al., 2006). The

change in the exponent signal modified the behaviour of the stress-stretch curve enabling

the prediction of two more parameters as compared to BST equation, namely, 1) stress at

fracture and 2) strain at fracture. These two parameters could be obtained by making the

first derivative of stress in relation to stretch equal to zero. In addition, the present equation

also predicts the two parameters previously obtained from BST equation, namely, 1) Young

modulus, E and 2) elasticity parameter in the non-linear region, n. The schematic

representation of Equation 3 is shown in Figure 3 in order to discuss the meaning of the

parameter E and the exponent n.
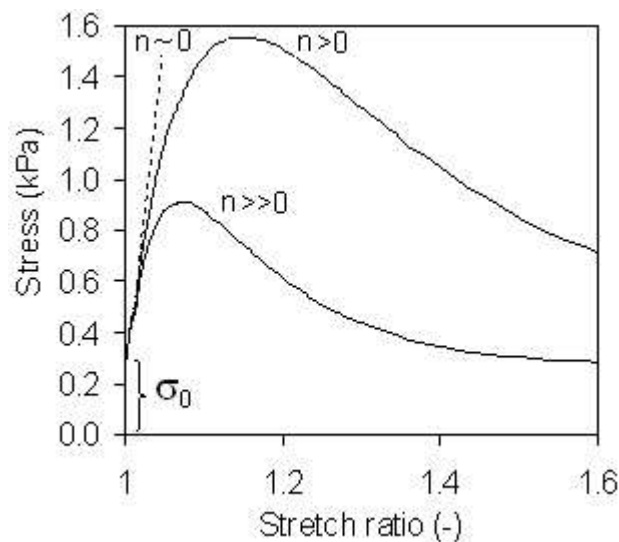
Figure 3. Schematic representation of Equation 3 for different values of n, n>0. The dashed line represents the ideal elastic behaviour obtained for very low n values (n~0). The solid lines represent the behaviour for higher n values (n>0, n>>0).

The BST equation was originally proposed to provide a good fit to data for

elastomers obtained in various deformation fields up to the point of rupture (Blatz et al.,

1974). The estimated parameter E (or 3G in shear) is usually interpreted as the elasticity

modulus in the linear region and it is obtained from the initial slope of the stress/strain

curve. The same meaning can be used for the model proposed here. As mentioned above,

the negative signal in the first exponent of Equation 3 resulted in the observation of a

maximum in the stress-stretch curve, which can be physically related to the fracture point of the gel under uniaxial compression. Figure 3 shows an inverse correlation between positive n values and the fracture stress and strain values. The value of n is also associated with the variation of the slope of the curve before the fracture point. This rate of slope change (n) can be regarded as a measure of deviation from ideal Hookean behaviour. When the material is deformed a strain-weakening phenomenon can arise resulting in an increase of the stress with the deformation slower than in the ideal case. Figure 3 shows that the strain-weakening effect become more pronounced as n values increase from n~0 to n>>0. This means that a more fragile gel will also present a shorter linear interval and a high n value

An example of data modelling for SPI systems at 25°C is shown in Figure 4 and Equation 3 provided a good fit to the raw data. Equation 3 could describe well the data from the beginning up to just after the maximum of the stress-stretch curve, beyond that the model deviates from the experimental data. The gel with lowest SPI concentration had the poorest fit, which was a result of the difficulties associated with the experimental compression of a very fragile gel resulting in a high dispersion of the data. The model also showed a good fit to experimental data of SPI-xanthan gels made at 10 ^{o}C, with exception for the sample containing 4% SPI. However, the latter system and those of SPI-xanthan made at 25 ^{o}C could be fitted up to the fracture point, as the previous models described in the literature (Blatz et al., 1974, Barrangou et al., 2006).
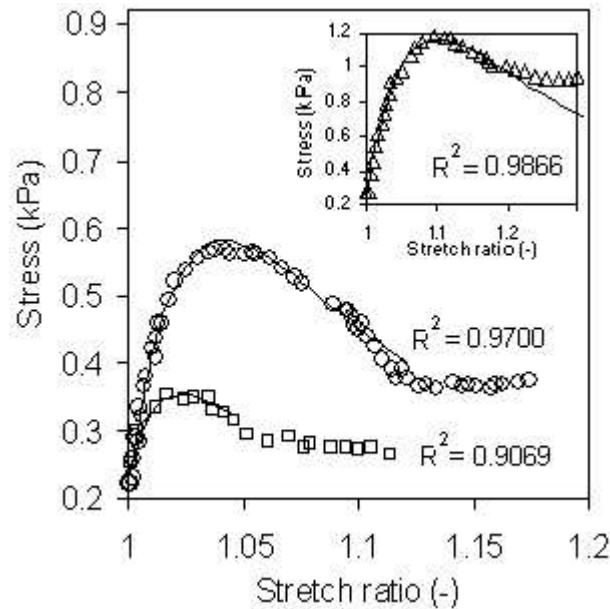
Figure 4. Stress-stretch profile of GDL-SPI gels at 25 °C. Systems: 4% SPI (□), 6% SPI (○), 8% SPI (Δ). The lines represent fits according to the model of Equation 3.

Figure 5 shows the effect of SPI concentration on the non-linear elastic parameter n. A gradual decrease of n with the increase of protein content was observed for the GDL-SPI gels. In contrast, an increase of this parameter was found for systems containing xanthan, independent of the gelation temperature. On gelation at lower temperature, the curve of the dependence of n on SPI concentration shifts to a lower n level. The original work of Blatz et al. (1974) suggested that the parameter n is a material constant and is therefore independent of concentration. However, it was found here that n changed with the protein concentration for SPI and SPI-xanthan gels that. Bot et al. (1996) and Barrangou et al. (2006) also reported a dependence of n on gel concentration when studying, respectively, gelatin and agarose gels.

The specific effects of xanthan addition and acidification temperature on the dependence of SPI concentration (C) on n were evaluated. The knowledge of the way that a large-deformation parameter depends on protein concentration is of particular importance for new products development. The dependence of n on SPI concentration was estimated by

fitting a first order exponential equation to data using non-linear least squares regression. The following exponential equations were obtained for the SPI gels (Equation 7), SPI-xanthan gels at 25°C (Equation 8) and SPI-xanthan gels at 10°C (Equation 9):

$$n = -16.2 + 88.4 \cdot e^{-0.16C} \tag{7}$$

$$n = 14.4 - 45 \cdot e^{-0.31C} \tag{8}$$

$$n = 6.4 + 128.7 \cdot e^{-0.76C} \tag{9}$$

Figure 5. Variation of n as a function of SPI concentration for GDL-induced gels: SPI at 25 ^{o}C (■), SPI + 0.2% xanthan at 25 ^{o}C (▲), SPI + 0.2% xanthan at 10 ^{o}C (○). The solid lines represent the exponential fit to n values.

The velocity of variation of n with the SPI concentration was greater for gels with xanthan as compared with those without the polysaccharide. As mentioned before, the former gels showed exponential growth n dependence, while the latter systems showed exponential decrease. This approach revealed that the mechanism for strain-weakening is not the same for SPI and SPI-xanthan gels. The former group of gels will probably show strain-hardening at very high protein content. However, the protein-polysaccharide interactions in SPI-xanthan gels could not lead to the observation of strain-hardening phenomenon. Regarding the gelation temperature, the faster n variation was found for the

lowest gelation temperature. This indicates that for the latter systems the n value attained faster the steady state, such that beyond ~12% SPI the gels would show similar large-deformation behaviour. The change of the gelation temperature did not affect very much the strain-weakening mechanism found out for gels containing xanthan.

In order to check if the model from Equation 3 gives reliable parameters, the Young modulus obtained from Equation 3 (E_{model}) was compared to those obtained from the linear regression (E_{linear}) of the initial part of the stress-strain curve (Figure 6). There was no significant difference at $p < 0.05$ between E_{model} and E_{linear} except for the gels containing 4% SPI (Figure 6A) and 4% SPI-xanthan 0.2% acidified at 10 ^{o}C. Previous works on gelatine and agarose gels (Barrangou et al., 2006) showed, respectively, a higher and lower value of the estimated modulus as compared to the modulus obtained from the linear fit.

Figure 6. Variation of Young modulus (E) as a function of SPI concentration for GDL-induced gels: SPI at 25 °C (a), SPI + 0.2% xanthan at 25 °C (b), SPI + 0.2% xanthan at 10 °C (c). Different letters indicate significant differences at $p < 0.05$ (small letters: variation of E_{model} with SPI concentration for each type of GDL-gel; capital letters: comparisson between E_{model} and E_{linear} for each concentration and GDL-gel type).

The model also showed a good prediction for stress at fracture as compared with the values from the true stress-Hencky strain curve (Figure 7). All samples were not statistically significantly different $p < 0.05$, except the gel with 4% SPI and xanthan at 10°C.

As the value of E_{model} was in good agreement with E_{linear}, the poor prediction of stress at fracture was attributed to the n value (Equation 5).
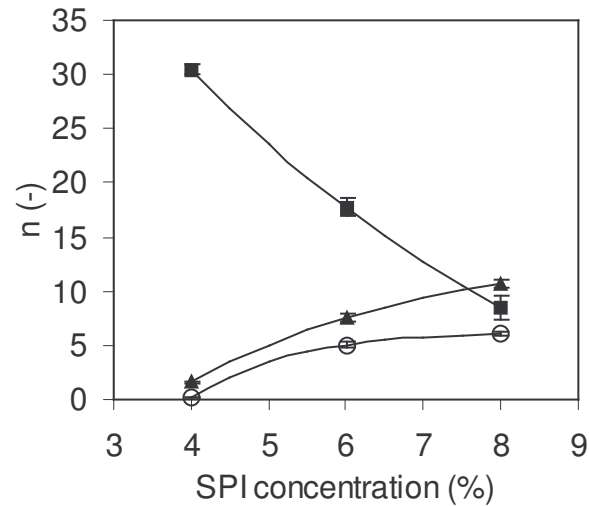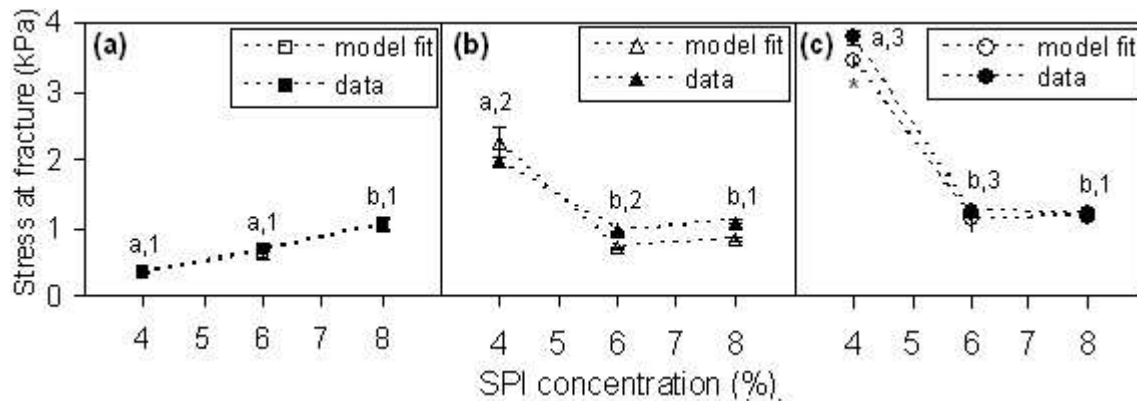

Figure 7. Variation of stress at fracture as a function of SPI concentration for GDL-induced gels: SPI at 25°C (a), SPI + 0.2% xanthan at 25°C (b), SPI + 0.2% xanthan at 10°C (c). Different letters and numbers indicate significant differences at $p<0.05$ (letters: variation of the property with SPI concentration for each type of GDL-gel; numbers: variation of the property with type of GDL-gel for each SPI concentration). * Value divided by 6.

The prediction of the strain at fracture values (Figure 8) was very good for systems that the data was fitted beyond the fracture point. However, a poor correlation between the model prediction and experimental strain at fracture was observed when the data was fitted up to the fracture point (4% SPI of Figure 8c). It is interesting to note that the tendency shown by the strain at fracture predicted from the model for gels with xanthan was the same for both gelation temperatures (Figures 8b and 8c). However, it was not observed a clear fracture point for SPI-xanthan gels acidified at 25 °C, such that only the predicted values were shown in Figure 8b. Those gels showed a sponge-like visual appearance and at large deformation and it was observed a stress flat part followed by a continuous non-linear increase of the stress. All the above comparisons showed that the present model could be used as a good predictor for all compression parameters.

129

Figure 3 and Equations 5 and 6 show that the non-linear elastic parameter affects not only the curve appearance, but also the stress and strain at fracture values. This correlation between n and fracture parameters is very interesting, since it enables the manipulation of the breaking stress and strain of the gel: for example by enhancing the elasticity parameter n it would be possible to decrease the breaking stress or strain of a gel in a very elegant way. This could be obtained by decreasing the SPI concentration in pure gels or by increasing the protein concentration in gels made with xanthan. Another option for the latter gels would be the increase of gelation temperature.
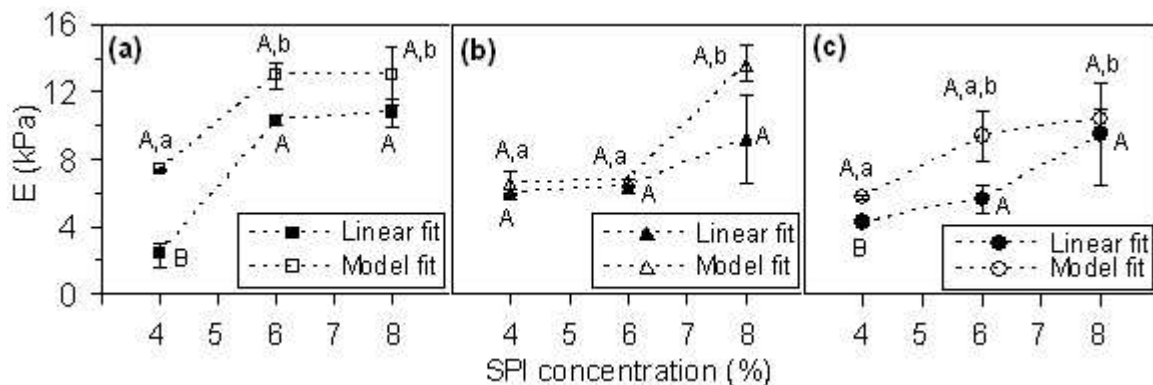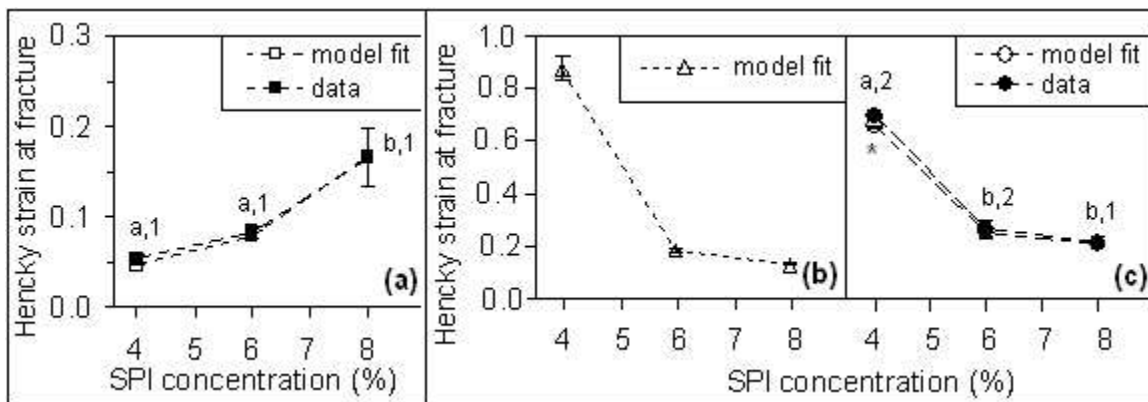

Figure 8. Variation of Hencky strain at fracture as a function of SPI concentration for GDL-induced gels: SPI at 25°C (a), SPI + 0.2% xanthan at 25°C (b), SPI + 0.2% xanthan at 10°C (c). Different letters and numbers indicate significant differences at p<0.05 (letters: variation of the property with SPI concentration for each type of GDL-gel; numbers: variation of the property with type of GDL-gel for each SPI concentration). * Value divided by 15.

3.4. Interactions between SPI and xanthan

The effects of SPI concentration, xanthan addition and gelation temperature on gel properties are shown in Figure 6 for Young modulus, Figure 7 for stress at fracture and Figure 8 for strain at fracture. The addition of 0.2% xanthan reduced the visual syneresis of SPI gels and increased significantly the stress at fracture (p<0.05), which was more pronounced for systems containing low amount of SPI (Figure 7). However, SPI and SPI-

130

xanthan gels with 8% of protein showed statistically similar properties. Carrageenan at relatively low concentration (0.2%) has shown to enhance the water holding capacity of a 10% soybean protein gel without affecting its hardness (Abd Karim et al., 1999). These two anionic polysaccharides seem to have similar effects on the gel hardness of high protein content gels. The addition of xanthan resulted in more deformable gels as compared to pure SPI samples (Figure 8), but the Young modulus was only affected (decreased) for the 6% SPI gel (Figure 6). The lower acidification temperature increased significantly the stress at fracture of SPI-xanthan gels (Figures 7b and 7c), but did not affected the Young modulus (p<0.05). As 6 and 8% SPI-xanthan gels at 25°C showed a sponge-like visual appearance the strain at fracture behaviour could not be compared to those of the gels prepared at 10°C.

The increase of the protein content in SPI pure gels resulted in harder, firmer and more deformable gels. SPI-xanthan gels showed a trend of decreasing the stress and strain at fracture with the increase of SPI concentration (Figures 7 and 8), but the Young modulus increased with the protein content. Thus, xanthan seems to interact with soy proteins in different ways, depending on the amount of protein present in the gel. As mentioned before, the gels with more than 6% protein showed a sponge-like appearance. The presence of holes could explain the lower stress at fracture found as compared to 4% SPI-xanthan gels. In general, xanthan seems to assist the protein aggregation and network formation. At high protein concentration and acidification temperature, the aggregation happened faster (Figure 2) and in a random way, such that the sponge-like appearance was formed. In addition, the strands formed in that process were more elastic than those for the systems with lower protein content.

4. Conclusions

The model proposed enabled the prediction of two more parameters, the stress and strain at fracture, as compared to the BST equation. In addition, the Young modulus and non-elastic parameter (n) could also be predicted as was previous possible with BST equation. It was observed a good fit of the model equation to the raw data from the linear region up to and beyond the fracture point. The estimated Young modulus, stress and strain at fracture showed a good correlation with the linear Young modulus, true stress and Hencky strain at fracture, validating the model. An exponential fit was used to determine the dependence of n on SPI concentrations, which may be useful in predicting the rheological properties of tofu model systems (SPI and SPI-xanthan gels). This has future commercial advantages as the mechanical properties are related to sensory texture and consequently product acceptability. The addition of xanthan reduced the gel time, but resulted in a less elastic network in the beginning of the gelation process. However, at steady state, xanthan reduced the visual syneresis of SPI gels and increased both the stress and strain at fracture, although the Young modulus was statistically similar to SPI gels. The lower gelation temperature increased significantly the stress at fracture of SPI-xanthan gels.

5. Acknowledgements

6. References

Abd Karim, A., Sulebele, G.A., Azhar, M.E., Ping, C.Y. (1999). Effect of carrageenan on yield and properties of tofu. *Food Chemistry*, 66, 159-165.

Barbut, S., Foegeding, E. A. (1993). Ca^{2+}-induced gelation of preheated whey protein isolate. *Journal of Food Science*, 58, 867–871.

Barrangou, L.M., Daubert, C.R., Foegeding, E.A. (2006). Textural properties of agarose gels. I. Rheological and fracture properties. *Food Hydrocolloids*, 20, 184–195.

Blatz, P. J., Sharda, S. C., Tschoegl, N. W. (1974). Strain energy function for rubberlike materials based on a generalized measure of strain. *Transactions of the Society of Rheology*, 18, 145–161.

Bot, A., van Amerongen, I. A., Groot, R. D., Hoekstra, N. L., Agterof, W. G. M. (1996). Large deformation rheology of gelatin gels. *Polymer Gels and Networks*, 4, 189–227.

Braga, A.L.M., Azevedo, A., Marques, M.J., Menossi, M., Cunha, R.L. (2006a). Interactions between soy protein isolate and xanthan in heat-induced gels: the effect of salt addition. *Food Hydrocolloids,* accepted.

Braga, A.L.M., Menossi, M., Cunha, R.L. (2006b). The effect of the glucono-δ-lactone/caseinate ratio on sodium caseinate gelation. *International Dairy Journal,* 16, 389-398.

Carp, D. J., Bartholomai, G. B., Pilosof, A. M. R. (1999). Electrophoretic studies for determining soy proteins–xanthan gum interactions in foams. *Colloid and Surface B,* 12, 309–316.

Chang, K.L.B., Lin, Y.S., Chen, R.H. (2003). The effect of chitosan on the gel properties of tofu (soybean curd). *Journal of Food Engineering*, 57, 315–319.

Dybowska, B.E., Fujio, Y. (1998) Optical properties of the pre-gel and gel state of soy proteins gelled by GDL under different physical conditions. *Journal of Food Engineering*, 36, 123-133.

Foegeding, E.A., Brown, J., Drake, M.A., Daubert, C.R. (2003). Sensory and mechanical aspects of cheese texture. *International Dairy Journal*, 13, 585-591.

Groot, R.D., Bot, A., Agterof, W.G.M. (1996). Molecular theory of strain hardening of a polymer gel: Application to gelatin. *Journal of Chemical Physics*, 104, 9202–9219.

Hermansson, A. M. (1986). Soy protein gelation. *Journal of American Oil Chemists Society*, 63, 658-666.

Hua, Y., Cui, S. W., Wang, O. (2003). Gelling property of soy protein–gum mixtures. *Food Hydrocolloids*, 17, 889-894.

Li, H., Errington, A. D., Foegeding, E. A. (1999). Isostrength comparison of large-strain (fracture) rheological properties of egg white and whey protein gels. *Journal of Food Science*, 64, 893–898.

Lucey, J.A., Tamehana, M., Singh, H., Munro, P.A. (1998) A comparison of the formation, rheological properties and microstructure of acid skim milk gels made with a bacterial culture or glucono-delta-lactone. *Food Research International, 31*, 147-155.

Mohamad Ramlan, B. M. S., Maruyama, N., Takahashi, K., Yagasaki, K., Higasa, T., Matsumura, Y., et al. (2004). Gelling properties of soybean β-conglycinin having different subunit compositions. *Bioscience Biotechnology and Biochemistry*, 68, 1091–1096.

Peleg, M. (1984). Application of nonlinear phenomenological rheological models to solid food materials, *Journal of Texture Studies*, 15, 1–22.

Petruccelli, S., Añón, M.C. (1995). Thermal aggregation of soy protein isolates. *Journal of Agricultural and Food Chemistry*, 43, 3035-3041.

Roesch, R., Juneja, M., Monagle, C., Corredig, M. (2004). Aggregation of soy/milk mixes during acidification. *Food Research International*, 37, 209–215

Staswick, P. E., Hermodson, M. A., Nielsen, N. C. (1984). Identification of the cystine which links the acidic and basic components of the glycinin subunits. *Journal of Biological Chemistry*, 259, 13431-13435.

Steffe, J.F. (1996). *Rheological Methods in Food Process Engineering*. East Lansing: Freeman Press.

Tay, S.L., Xu, G.Q., Perera, C.O. (2005). Aggregation profile of 11S, 7S and 2S coagulated with GDL. *Food Chemistry*, 91, 457–462.

Thanh, V. H., Shibasaki, K. (1977). Beta-conglycinin from soybean proteins. Isolation and immunological and physicochemical properties of the monomeric forms. *Biochimica and Biophysica Acta*, 490, 370-384.

Utsumi, S., Damodaran, S., Kinsella, J. E. (1984). Heat-induced interactions between soybean proteins: preferential association of 11S basic subunits and β subunits of 7S. *Journal of Agricultural and Food Chemistry*, 32, 1406-1412.

Van Vliet, T., Martin, A. H., Bos, M. A. (2002). Gelation and interfacial behaviour of vegetable proteins. *Current Opinion in Colloid and Interface Science*, 7, 462-468.

Weijers, M., van de Velde, F., Stijnman, A., van de Pijpekamp, A., Visschers, R.W. (2006). Structure and rheological properties of acid-induced egg white protein gels. *Food Hydrocolloids*, 20, 146–159.

CHAPTER 4. Protein-polysaccharide interactions in acidified gels containing Na-caseinate, SPI and/or xanthan

3ʳᵈ PART: Interactions between soy protein isolate and xanthan in heat-induced gels: the effect of salt addition.

(in collaboration with CBMEG and DA-IB- UNICAMP)

Abstract

The influence of xanthan and/or KCl addition on the properties of heat-induced soy protein isolate (SPI) gels at pH 3.0 was studied. Changes in protein solubility and subunit composition as well as in the mechanical properties, microstructure and water holding capacity of the gels were determined. The effect of KCl addition on each biopolymer solution was also investigated. The results indicated that SPI-xanthan gels prepared without KCl were mainly stabilized by non-covalent (H-bonding and hydrophobic) and SS bond interactions, whereas in gels containing KCl, electrostatic interactions were also involved in maintaining the gel structure. The β-7S subunit was probably the fraction electrostatically linked to the xanthan. The different values found for the mechanical properties after the addition of xanthan and/or KCl, were associated with the coarseness of the gel. Xanthan and KCl probably showed a synergistic effect on the Young modulus because KCl induced a conformation transition of the xanthan molecules.

Keywords: heat-induced gel, interactions, salt, soy protein isolate, xanthan.

1. Introduction

Soy proteins are the most important representative of legume proteins due to their high protein level and well-balanced amino-acid composition, showing great potential in the substitution of meat and dairy proteins (Van Vliet, Martin & Bos, 2002). They are applied in a wide range of food products especially because of their ability to form gels with good water holding capacity on heating. The functional properties of soy protein isolates reflect the composition and structure of their globulins, which correspond to 50 – 90% of the total proteins (Utsumi, Damodaran & Kinsella, 1984). The soy protein fractions can be classified by their sedimentation constants, showing approximate Svedberg

coefficients of 2S, 7S, 11S and 15S. The two major globulins in soybeans are β-conglycinin and glycinin, also called 7S and 11S, respectively. The glycinin subunits consist of two polypeptide components linked via disulfide bonds (AB), one with acidic (A) and the other with basic (B) isoelectric points (Staswick, Hermodson & Nielsen, 1984). At ambient temperature and pH 7.6, glycinin forms hexameric complexes (11S) with two rings each containing three hydrophobically associated subunits. At pH 3.8 this protein is mainly present in the form of trimeric complexes (7S-form), while at pH 3.0 glycinin may be dissociated into the 3S form (1AB) (Wolf, Rackis, Smith, Sasame & Babcock, 1958). β-conglycinin is a trimeric glycoprotein consisting of at least six combinations of three subunits: α, α' and β (Thanh & Shibasaki, 1977).

The formation of protein networks is considered to be a result of the balance between protein-protein and protein-water interactions and of the attraction and repulsion forces occurring between adjacent polypeptide chains (Cheftel, Cuq & Lorient, 1996). The molecular forces involved in the formation of heat-induced soy protein gels are probably hydrogen bonds and hydrophobic interactions, whereas in gel maintenance the forces involved are disulfide and hydrogen bonds (Utsumi & Kinsella, 1985). The gel formation process and network structure could be affected by the addition of salts (increasing ionic strength) and changes in pH (Lakemond, de Jongh, Hessing, Gruppen & Voragen, 2000). Generally the pH of food products ranges from pH 3 to 7 and the ionic strength varies from 0.02 to 0.2 M.

Sodium chloride (NaCl) is widely employed in food products, but the ingestion of great amounts of this salt can increase the risk of hypertension (Abernethy, 1979) and urinary calcium loss (Bell, Eldrid & Watson, 1992). To avoid this, the NaCl could be

partially substituted by KCl, although this change could have an effect on protein stability and, consequently, on the product texture and water holding capacity. The effect of partial or complete replacement of NaCl with KCl on protein and gel properties has been investigated for dairy systems (Katsiari, Voutsinas, Alichanidis & Roussis, 1997) and for different proteins from seed flour (Ogungbenle, Oshodi & Oladimeji, 2002; Arogundade, Akinfenwa & Salawu, 2004).

Protein functionality can also be modified by interactions with other ingredients such as polysaccharides, present in many food systems (Tolstogusov, 1993). Xanthan is a high molecular weight anionic polysaccharide commonly used as a stabilizer and thickener in food products. This polymer consists of a linear (1-4)-β-D glucose backbone with a charged trisaccharide side chain on each second glucose residue (Jansson, Kenne & Lindberg, 1975). Hua, Cui and Wang (2003) observed in a soy protein–xanthan mixed gel, that the protein component was the supporting phase even at a xanthan concentration as high as 1%. Carp, Bartholomai and Pilosof (1999) studied the foaming and solubility properties of soy proteins as affected by xanthan gum. However, to our knowledge, there are no publications on the effect of KCl addition on the properties of soy protein-xanthan systems.

The purpose of this work was to investigate soy protein/xanthan interactions as a function of KCl concentration in heat-induced gels, by evaluating water holding capacity and uniaxial compression measurements. The synergistic/antagonistic effect between proteins and polysaccharides was also studied from the structural characteristics of gels, as assessed by confocal laser microscopy and the electrophoretic pattern of the soluble proteins. Furthermore, the soy protein-KCl and xanthan-KCl binary systems were studied

according to their thermal and rheological properties, respectively, in order to clarify the molecular conformation of the biopolymers that participated in the network formation.

2. Material and methods

2.1. Material

Soy protein isolate (SPI) was obtained from defatted soy flour (Bunge Alimentos S.A., Brazil). Xanthan gum was obtained from Sigma-Aldrich Co. (USA) and KCl from Merck KGaA. (Germany).

2.2. Preparation of soy protein isolate

Defatted soy flour was dispersed in distilled water (1:10 w/w) and the pH adjusted to pH 8.0 with 2N NaOH. The dispersion was gently stirred for 2h at room temperature and then centrifuged at 10,000 x g for 30 min at 4ºC in a Sorvall RC5 Plus centrifuge (GSA-rotor, Dupont, UK). The supernatant was adjusted to pH 4.5 with 2N HCl and centrifuged at 5,000 x g (Sorvall GSA-rotor) for 15 min at 4ºC. The precipitate was then suspended in water and the pH adjusted to 8.0 with 2N NaOH, followed by freeze-drying of the suspension (Petruccelli & Añón, 1995a). The protein (N x 6.25), moisture and ash contents of the SPI powder were, respectively, 89.3 ± 0.3%, 6.7 ± 1.6% and 3.29 ± 0.02% (wet basis).

2.3. Preparation of biopolymer solutions and gels

A soy protein isolate solution was prepared at ambient temperature by magnetic stirring with or without KCl. The xanthan powder was dispersed in water (3% w/w) at pH 3.0 with mechanical stirring for 1 h at 80ºC. This solution was subsequently cooled to 10ºC and diluted according to the concentrations of the two factorial designs (Table 1). The rheological properties of a 0.3% xanthan solution were also compared with those of a

solution with the same xanthan concentration, but prepared by a 10-fold dilution of a 3% solution.

Table 1. Coded levels and real values for the SPI, xanthan and KCl concentrations used in at least one of the three factorial designs.

Level	SPI (% w/w)	Xanthan (% w/w)	KCl (M)
-1	10	0.05	0.01
0	12	0.175	0.14
+1	14	0.3	0.27

The xanthan and SPI (or SPI-KCl) solutions were mixed at different concentrations according to the factorial designs and the pH adjusted to 3.0. The mixed solutions were placed into glass tubes (30 mm diameter and 30 mm height) and closed tightly with stoppers. Gelation was carried out by heating the glass tubes in a water bath at 90ºC for 30 min (Damodaran, 1988), followed by immediate cooling in an ice bath. The samples were kept at 10ºC for 20 h before analyzing the gel properties.

2.4. Factorial designs

The different model systems were chosen according to two factorial designs with 2^2 trials (SPI-KCl and SPI-xanthan gels) and another factorial design with 2^3 trials (SPI-xanthan-KCl gels). Table 1 shows the ranges of the SPI, xanthan and KCl concentrations used in the factorial designs.

2.5. Differential scanning calorimetry (DSC)

DSC studies were performed in a DSC 2920 Modulated DSC differential scanning calorimeter (TA Instruments, USA). Indium and water were used to calibrate the temperature scale and enthalpic response of the equipment. The measurements were done

with four different samples containing 20% (w/w) protein dispersed in water or in salt solution at pH 3.0 and 7.0. The amount of KCl used (0.54 M) was calculated based on the KCl/SPI ratio of 0.27, which was obtained considering the 2^2 experimental design (SPI-KCl) sample with maximum salt and minimum protein contents. A DSC hermetic pan containing about 10-15 mg of sample was tightly sealed and placed in the DSC cell. An empty capsule was used as the reference. The samples were analyzed at 10 ℃/min from 10 to 110℃ in triplicate. The temperature at which denaturation started, known as the onset denaturation temperature T_{onset}, was calculated by taking the intercept of the baseline and the extrapolated maximum slope of the peak. The peak denaturation temperature T_{peak} was considered to be the temperature at maximum heat flow. The enthalpy of thermal denaturation was calculated from the area of the endothermic peak.

2.6. Intrinsic Viscosity

The viscosities of the xanthan solutions were measured using a size 100 Cannon-Fenske semi-micro capillary viscometer (Cannon Instrument Co., USA). The viscometer was immersed in a water bath maintained at 10.0 ± 0.5℃. Solvent runs (water and 0.4 M KCl solution) were performed frequently to calibrate the instrument. The relative viscosity of a given solution η_{rel} (defined as the ratio between the solution and solvent viscosities) was determined by measuring the relative efflux times in the capillary. Viscosity values were based on at least 3-4 efflux time readings taken for various concentrations of xanthan solution. All measurements were made in the concentration range from about 0.05 to 0.004% (w/v).

2.7. Rheological oscillatory measurements

A stress-controlled rheometer (Carri-Med CSL^{2}500, TA Instruments, England) with an acrylic cone and plate geometry (diameter 60 mm) was used to make the oscillatory rheological measurements. Stock solutions were prepared at 0.3% (w/w) or at 3% (w/w) and diluted to 0.3% (w/w). Xanthan solutions (0.3% w/w) with or without KCl were poured directly onto the plate of the instrument at 10ºC. Frequency sweeps were done from 0.01 to 10 Hz at 0.35 Pa and 10ºC. The Lissajous figures at each frequency were plotted to ensure that the measurements of G' (storage modulus) and G" (loss modulus) were always obtained within the linear viscoelastic region.

2.8. Mechanical properties of the gels

Uniaxial compression experiments in triplicate were done using a TA-XT2*i* texture analyzer (Stable Microsystems Ltd., England) with an acrylic cylindrical plate (35 mm diameter). Gels were compressed to 80% of their original height using a crosshead speed of 1 mm/s. All measurements were done at 10ºC after 20 h of gel formation. The force and height values obtained were transformed into true stress (σ_H) – true strain (ε_H) curves (Steffe, 1996). The rupture properties were associated with the maximum point of the stress-strain curve and the Young modulus (E) was the slope of the first linear interval of the stress-strain curve.

2.9. Water holding capacity (WHC) of the gels

A cylindrical gel (~1.0 g) was placed on a disc of Whatman # 1 filter paper (Whatman, U.K.) and positioned in the middle of a 50 mL centrifuge tube. The water loss was determined by weighing the gel before and after centrifugation at 4,000 g for 10 min at 15ºC (Kocher & Foegeding, 1993) in a Sorvall RC5 Plus centrifuge using a SS-34 rotor

(Dupont, UK). The WHC values were expressed as the percent of the ratio of the amount of water remaining to the initial amount of water present in the gel.

2.10. Protein solubility of the gels

Samples were dispersed either in distilled water at pH 8.0 (DW), in a pH 8.0 buffer (0.086 M Tris, 0.09 M glycine and 4 mM Na$_2$EDTA) (B), or in the same buffer containing other reagents, namely 1) 6 M urea (BU), 2) 1% β-mercaptoethanol (BM) and 3) 6 M urea plus 1% β-mercaptoethanol (BUM) (Shimada & Cheftel, 1988). Tris buffer disrupts the electrostatic interactions, urea acts by disrupting the H-bonding and hydrophobic interactions, while the SS bond is reduced when the solvent contains β-mercaptoethanol (Cheftel et al., 1996). Samples (8.5 mg protein/mL) were homogenized at room temperature with an Ultra Turrax model T18 basic homogenizer (IKA, Germany) for 2 min and then centrifuged at 20,000 x *g* for 15 min at 25°C in an Allegra^{TM} 64R Beckman centrifuge with a F0850 rotor (Beckman, USA). The protein solubility was determined from the supernatants and expressed as 100 x protein content in the supernatant / total protein content. Three independent extractions were done with each solvent. The protein concentrations were determined at 280 nm in a Beckman Du-70 spectrophotometer (Beckman, USA) using an apparent extinction coefficient ($E_{1cm}^{1mg/mL}$) of 1.141 for proteins dispersed in water and of 1.193 for the pH 8.0 buffer. The extinction coefficients were obtained by measuring the absorbance at 280 nm of a 1 mg/mL soy protein solution, the concentration being determined by the Kjeldhal method.

2.11. Electrophoresis

SDS-polyacrylamide gel electrophoresis (PAGE) was carried out following the method of Laemmli (1970). The samples containing soluble proteins from the gel, extracted

in different media, were diluted with an equal volume of a pH 6.8 buffer (62.5 mM Tris-HCl, 20% glycerol, 2% SDS, 0.05% bromophenol blue) containing (reducing condition) or not containing (non-reducing condition) 5% β-mercaptoethanol. Commercial molecular weight markers covering the 6,000 to 181,500 Da molecular weight range were used (Sigma-Aldrich Co., USA). The gels were run at 120 V through the stacking (4% polyacrilamide) and separating (12% polyacrilamide) gels, in a Mini Cell Protean electrophoresis unit (Biorad Laboratories, USA). The gels were stained with 0.25% (v/v) Coomassie Brilliant Blue, in ethanol:acetic acid:water (45:10:45, v/v), followed by destaining with acetic acid:ethanol:water (5:10:85, v/v). The densitometric analyses of the bands were done using the Eagle Eye II system and the software Stratagene Eagle Sight (Stratagene, USA).

2.12. Confocal scanning laser microscopy (CSLM)

Protein dispersions were prepared using the fluorescent dye Rhodamine B (50 μL of a 0.4% rhodamine solution/100 mL protein solution), which stains the protein. Mixed gels with intermediate concentrations of each ingredient (12% SPI + 0.153% xanthan or 12% SPI + 0.153% xanthan + 0.14 M KCl) were observed. Samples of the mixed solution were placed on microscope slides, covered with a glass cover slip and sealed with nail polish to prevent evaporation. In order to obtain the mixed gels, the slides were transferred to a plastic box, covered with a thin layer of soy oil to enhance heat transfer and heated in a water bath at 90ºC for 30min. A dual-channel laser confocal system (MRC 1024 UV, Biorad, USA) mounted on an Axiovert 100 Zeiss inverted microscope and equipped with Ar-Kr lasers was used to observe the gels. A wavelength of 568 nm was used to excite the rhodamine-labeled proteins. The settings for contrast, brightness and iris diameter were

adjusted and kept constant throughout the observations. Images were taken using a water immersion objective at 40x.

3. Results and discussion

3.1. Rheology of the xanthan-KCl solutions

Information on molecule characteristics, such as conformation, hydration and flexibility, can be obtained from the measurement of the intrinsic viscosity of a polymer (Harding, 1997). Figure 1 shows the concentration dependence of the reduced viscosity of xanthan at 10ºC in water and in a 0.4 M KCl solution (both at pH 3.0). The Huggins equation (Equation 1), which expresses the reduced viscosity (η_{SP}/C) of a polymer as a function of concentration (C), was found to be suitable for both xanthan solutions in the dilute region.

$$\eta_{SP}/C = [\eta] + k_H [\eta]^2 C \tag{1}$$

where [η] is the intrinsic viscosity, C is the xanthan concentration, η_{SP}/C is the reduced viscosity and k_H is the Huggins parameter.
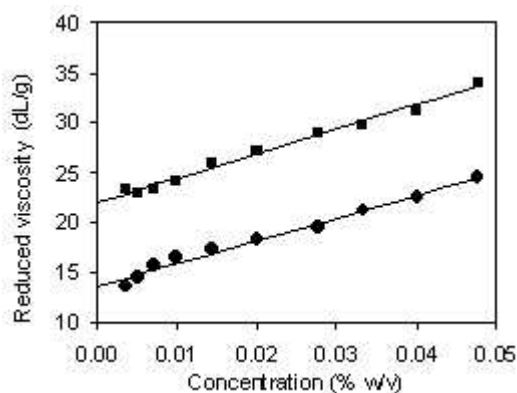
Figure 1. Reduced viscosity of xanthan solutions at 10ºC. Solvents: (■) deionized water, (●) 0.4 M KCl solution.

146

_____

The intrinsic viscosities, $[\eta_{sp}/C]_{c\cong 0}$, of xanthan dispersed in water and in a salt solution at pH 3.0, were 22 and 13.5 dL/g, respectively. The addition of salt decreased the intrinsic viscosity by approximately 35%, which indicates a reduction in the hydrodynamic size of the molecule (Rochefort & Middleman, 1987) since the charge screening reduces the influence of coulombic interactions on the polymer conformation. The value for intrinsic viscosity obtained in water was lower than that reported by Yevlampieva, Pavlov and Rjumtsev (1999), 41 dL/g, and Wang, Sun and Wang (2001), 44.9 dL/g at 25ºC. These differences can be attributed to the lower pH (3.0) and temperature (10ºC) of the present system, as well as to different xanthan sources.

The Huggins parameter k_H gives information about the solvent quality and a low Huggins constant (k_H=0.478) was observed for the xanthan dispersion in water at pH 3.0 and a value of 1.2 for the salt solution. Values between 0.3-0.7 have been suggested for perfect solutions, whereas values of $k_H \geq 1$ would encourage aggregate formation (Millard, Dintzis, Willett & Klavons, 1997). This indicates that water at pH 3.0 is a good solvent, while the salt solution promoted self-association of the macromolecule.

The rheological behavior of xanthan solutions can give information on the molecular conformation/aggregation of the polysaccharide. Figure 2 shows the frequency dependence of the elastic (G') and viscous (G'') moduli of two xanthan solutions (0.3% w/w) prepared in different ways, to gain information about the effect of dilution on the molecular aggregates. A 3% solution was prepared at 80ºC and subsequently diluted to 0.3% (referred to as X-1). The other solution analyzed was prepared directly at 0.3% and 80ºC (referred to as X-2). The X-2 solution exhibited a typical dilute solution behavior with the crossover of the two moduli at the highest frequency tested. The X-1 solution showed a

very different pattern although both solutions had the same concentration. The G'-G"

crossover was shifted to a lower frequency (~0.02 Hz) and the elastic modulus was larger

than that of the X-2 solution for the whole frequency range. This difference could be

explained by the formation of hydrogels during the preparation of the 3% xanthan sample at

80 ^{o}C (Iseki et al., 2001). It could be suggested that the dilution of the 3% xanthan hydrogel

resulted in a solution with insoluble aggregates. The X-1 solution was used to prepare the

mixed gels.
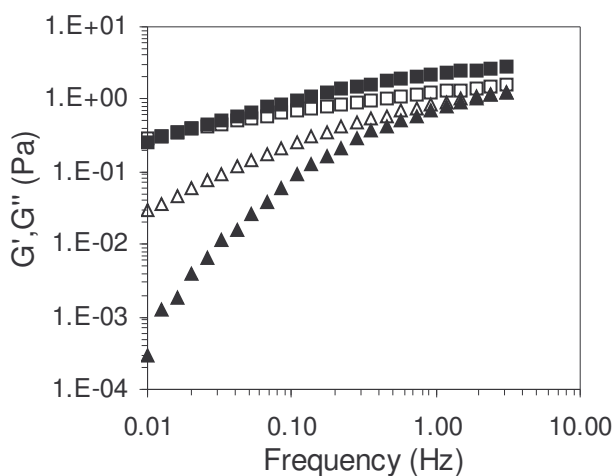
Figure 2. Frequency dependence of G' (solid symbols) and G" (open symbols) at 10ºC for xanthan solutions prepared at 80ºC with different ways of preparation: 3% with subsequent dilution to 0.3% or X-1 (squares); and 0.3% or X-2 (triangles).

The rheological properties of the X-1 solution after the addition of 0.4 M KCl were

also investigated (Figure 3). The addition of salt resulted in a more structured solution with

G'>G" throughout the entire frequency range analysed and with higher moduli values as

compared to the water system. This positive effect of KCl on the xanthan solution

properties was previously observed with NaCl (Rochefort & Middleman, 1987). Such

behavior with salt solutions was explained by the salt-induced disorder-order transition and

the tendency to strengthen the intermolecular associations between the xanthan molecules.

148

The addition of salt promotes screening of the electrostatic repulsion of the trisaccharide sidechains, allowing for the adoption of a helical backbone conformation (Rochefort & Middleman, 1987). Increases in the KCl concentration from 0.05 (data not shown) to 0.4 M did not influence the rheological behavior of the solution, showing that above 0.05 M KCl, the conformation and interactions of the xanthan molecule should be the same.
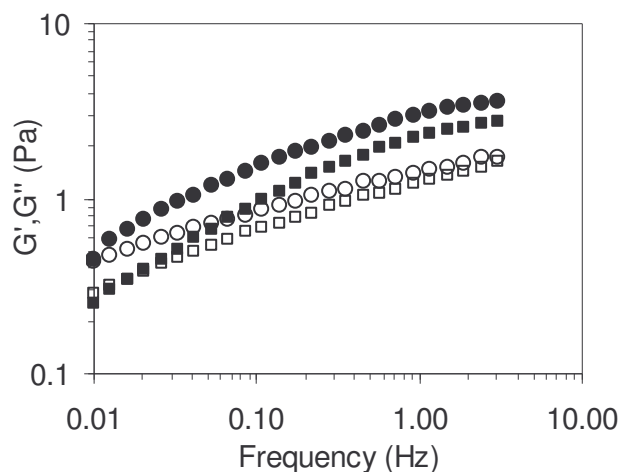
Figure 3. Frequency dependence of G' (solid symbols) and G" (open symbols) at 10ºC for 0.3% xanthan solutions obtained from a 3% solution. Solvents: (squares) deionized water, (circles) 0.4 M KCl solution.

3.2. Thermal behavior

DSC experiments were performed to determine the characteristics of SPI dispersions prior to mixture with xanthan and subsequent heat-induced gelation. Figure 4 shows typical examples of DSC thermograms of soy protein isolate, the denaturation enthalpy and temperature for each sample treatment being obtained (Table 2). The DSC results revealed varying effects of pH and salt addition on the stability of soy protein isolate. SPI dispersions at pH 7.0 showed two endothermic transitions for both samples, which can be attributed to thermal denaturation of the 7S protein at the lower temperature and of the 11S proteins at the higher temperature (Hermansson, 1986). The high

temperature for the denaturation of glycinin (11S) could be attributed to the high stability of its structure and conformation due to hydrogen or disulfide bonds (Kim, Kim, Yang & Kwon, 2004). The addition of KCl increased the denaturation temperatures (T_{onset} and T_{peak}) due to the stabilizing effects of salts. Table 2 shows an increase in denaturation temperature of about 8 ºC for β-conglycinin (7S) and 13 ºC for glycinin (11S). This effect could be attributed to two possible factors working either separately or concomitantly: (i) neutralization of charged side chains of the amino acid residues thus reducing inter and/or intra chain repulsion, and (ii) salt stabilized water structure (Damodaran, 1988). Table 2 shows similar total enthalpies for SPI dispersions at pH 7.0 and the value of ΔH_T found for SPI dispersion without salt addition agreed with that observed by Puppo et al. (2004).
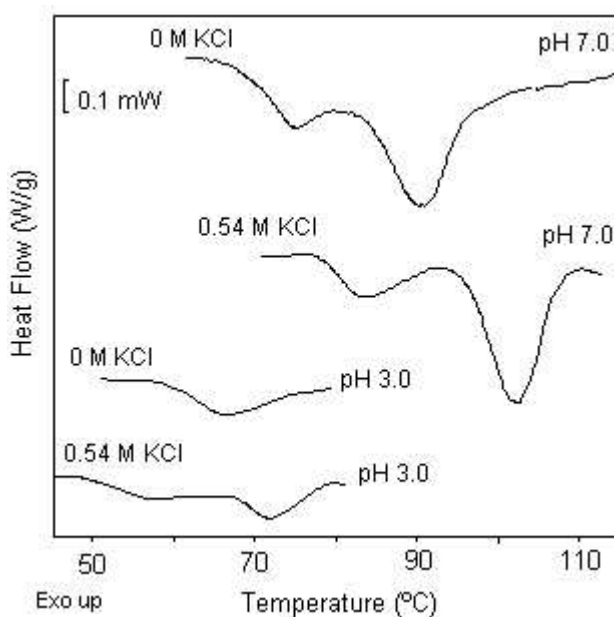
Figure 4. DSC thermograms of 20% (w/w) soy protein isolate dispersions with 0 M and 0.54 M KCl at pH 7.0 and 3.0. The scanning rate was 10ºC/min.

Table 2. Effect of pH and KCl addition on total denaturation enthalpy (ΔH_T) and on the denaturation temperatures, onset (T_{onset}) and peak (T_{peak}), of soy protein isolate.

Treatment	ΔH_T	T_{onset} (ºC)		T_{peak} (ºC)	
	(J/g protein)	1st peak	2nd peak	1st peak	2nd peak
0 M KCl - pH 7.0	10.80 ± 1.25	69.7 ± 0.2	83.5 ± 0.1	74.8 ± 0.0	90.3 ± 0.1
0.54 M KCl – pH 7.0	9.99 ± 0.14	78.3 ± 0.6	97.1 ± 0.0	82.8 ± 0.1	102.4 ± 0.1
0 M KCl - pH 3.0	1.80 ± 0.26	59.8 ± 0.1	------	66.0 ± 0.5	------
0.54 M KCl – pH 3.0	3.21 ± 0.33	51.1 ± 0.7	67.1 ± 0.5	56.7 ± 0.2	71.8± 0.2

The thermograms of SPI at pH 3.0 presented a unique endotherm peak for the sample without KCl and two endothermic transitions for the dispersion with salt (Figure 4). However, all peaks were localized in a low temperature region (~50-70ºC) as compared to the peaks observed for SPI at pH 7.0 (Table 2). At pH 3.0 the endothermic transition related to 11S denaturation was not observed, due to the acidic denaturation of glycinin, which starts at pH 3.75 and reaches a maximum at pH 2 (Koshiyama, 1972). At this low pH, the charge distribution differs from that at pH 7.0, and apparently leads to differences in the quaternary structure and protein stability (Renkema, Lakemond, de Jongh, Gruppen & van Vliet, 2000). At pH 3.0 and low ionic strength most of the glycinin is in a 3S (1AB) form and part of the glycinin in a 7S form (Wolf et al., 1958). The low T_{onset} value (59.81 ± 0.12 ºC) observed for SPI at pH 3.0 was similar to that obtained by Puppo et al. (2004) for β-conglycinin (63.00 ± 0.31 ºC) and glycinin (59 ± 0.23 ºC) at pH 3.0, and also by Renkema, Gruppen and van Vliet (2002) for β-conglycinin (55ºC) at pH 3.0. A comparison of these

values suggests that the single peak observed could indicate a superimposed transition of the dissociated 11S fraction and the β-conglycinin. The 3S form of glycinin does not give a cooperative transition (Danilenko et al., 1987), which implies that heat stability of the 7S glycinin is not very high and that it unfolds before β-conglycinin. All the transitions observed were irreversible since during the second heating scan, no transitions could be observed under any of the conditions studied.

3.3. Properties of heat-induced soy protein-xanthan gels

3.3.1. Protein solubility of gels and SDS-PAGE of gel extracts

Figure 5 shows the solubility of SPI gels and SPI gels with xanthan and/or KCl in several extraction media. Intermediate concentrations of the ingredients in the 2^3- factorial design, were used to prepare the gels, and a gel with only SPI was used as the control. Regarding the gels containing xanthan, the amount of soluble protein in B (buffer pH 8.0) was slightly greater then in the gels without polysaccharide. This trend could be attributed to disruption of the electrostatic interactions between the negative sites of xanthan and the positive regions of SPI at pH 3.0. For the others buffers (BU and BM) it was not observed any effect on the solubility with the addition of xanthan in SPI or SPI-KCl gels. Thus, the analyses of soluble proteins in DW (deionized water) and in BUM (buffer + urea + β-mercaptoethanol) were only carried out for the SPI and SPI-KCl gels, since xanthan could only interact via electrostatic forces.
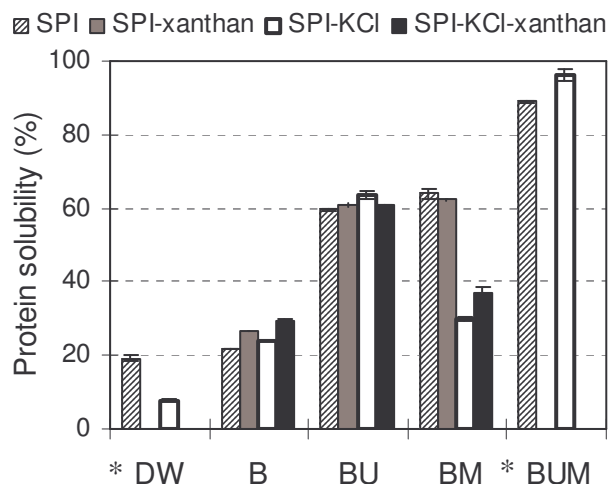
Figure 5. Solubility of the protein constituents of different heat-induced gels at pH 3.0: SPI (12%), SPI (12%) – KCl (0.14 M), SPI (12%) – xanthan (0.135 %), SPI (12%) – xanthan (0.135 %) – KCl (0.14 M). Extraction solutions: (DW) deionised water; (B) buffer (pH 8.0); (BU) buffer (pH 8.0) plus urea; (BM) buffer (pH 8.0) plus β-mercaptoethanol; (BUM) buffer (pH 8.0) plus urea and β-mercaptoethanol. *SPI-xanthan and SPI-xanthan-KCl gels were not evaluated due to the absence of samples.

The amount of soluble protein in the gels prepared with KCl (SPI-KCl and SPI-KCl-xanthan) in DW and BM media was different from that obtained for the gels without salt. The protein solubility in DW decreased from 19 to 8% when the gel was prepared with KCl, which could be attributed to the salting out effect (Hermansson, 1978). Protein constituents of the SPI-KCl gel were more soluble in B (~25%) than in DW, but for the gel without KCl the solubility of the proteins in B (~22%) was similar to that obtained in DW (~19%). The above results could suggest that the addition of salt favors indirectly the hydrophobic interactions, due to electrostatic interactions between counterions of the salt and protein macroions.

Figure 5 also shows that the amount of soluble protein constituents in gels without KCl was similar (~60%) in BU and BM. However, in gels with KCl the amount of soluble

protein decreased to ~30% in BM and remained the same in BU. It is interesting to note that the sum of the effect of each reagent on protein solubility was equal to 100% for gels without KCl, but when salt was present this sum was lower than 70%. Thus, two hypothesis can be suggested: 1) the salt could hinder the formation of SS bonds, in agreement with other studies with SPI gels under acidic conditions, in which little or no formation of SS bonds was found (Puppo, Lupano & Añón, 1995); 2) there could be equal amounts of SS bonds in gels with and without KCl, but the reducing agent was unable to reach all the SS bonds in the gels with salt. However, the solubility in BUM was almost 100% in all gels, indicating the presence of more disulfide bonds in gels with KCl than was revealed by extraction in BM, confirming hypothesis 2. The addition of urea unfolds the protein molecules, leading to greater exposure of SS bonds, which favors the reduction reaction by β-mercaptoethanol (Petruccelli & Añón, 1995b). The lower amount of soluble proteins observed in BM could result from the presence of large random aggregates formed by non-covalent interactions (H-bonding and hydrophobic) and SS bonds that were somehow localized inside the core. In addition, these aggregates would be large (>0.2 μm according to Lakemond, de Jongh, Paques, van Vliet, Gruppen and Voragen (2003)) such that they precipitated when the system was centrifuged at 20,000 x g for 15 min at 25°C. The results indicated that SPI-xanthan gels prepared without KCl were mainly stabilized by non-covalent (H-bonding and hydrophobic) and SS bond interactions, whereas in gels with KCl, electrostatic interactions were also involved in maintaining the gel structure.

The effects of xanthan and KCl on the subunit composition of soluble proteins as well as on the formation of high molecular weight aggregates were evaluated from the electrophoretic patterns of the soluble proteins in the different buffers. Figure 6 shows the

electrophoretic patterns using non-reducing conditions for the DW and BU extracts. The results for the B extract were similar to those of the BU (not shown) one. The different components present in the SPI powder were identified by comparison with molecular weight markers and with the literature results (Petruccelli & Añón, 1995c). The bands found in the SPI powder under non-reducing conditions (with β-mercaptoethanol) were: α and α' subunits of β-conglycinin (α– and α'-7S); β subunit of β-conglycinin (β–7S); acidic polypeptides of glycinin (A-11S) and basic polypeptides of glycinin (B-11S) and the AB subunit of glycinin (AB-11S). Low molecular weight fractions (**) and four bands of large soluble aggregates (*) with molecular weights above 115.5 kDa were also observed (Figure 6). Petruccelli and Añón (1995c) previously suggested that the α and α' subunits of the β-conglycinin probably formed the aggregates present in the two first bands (greater intensity). The other two bands would contain the latter subunits plus the A polypeptide of 11S.

The DW extract (lane 3) showed two bands with high intensity corresponding to the AB subunit of glycinin and to the β-subunit of β-conglycinin. There were also small amounts of low molecular weight peptides (25.9-37.1 kDa) and traces of free α–7S, α'-7S, A-11S and B-11S subunits. The presence of soluble AB-11S revealed that the disulfide bridge between the A and B polypeptides was not broken, which was attributed to the low reactivity of the SS-SH interchange at this low pH *(Shimada & Cheftel, 1988)*. The material dissolved in BU consisted of three major proteins that entered the gel and were associated with the A and B polypeptides of glycinin and the β subunit of β-conglycinin. In addition, a high molecular weight aggregate ([1]) was observed, that migrated into the stacking but not into the separating gel, and a second aggregate ([2]), that did not migrate into the stacking

gel. The aggregate-2 was probably 1) a new aggregate formed during the gelation process; 2) the hexameric form of glycinin (300-380 kDa), since the A-11S and B-11S bands showed lower intensities, compared to those under reducing conditions (results not shown).
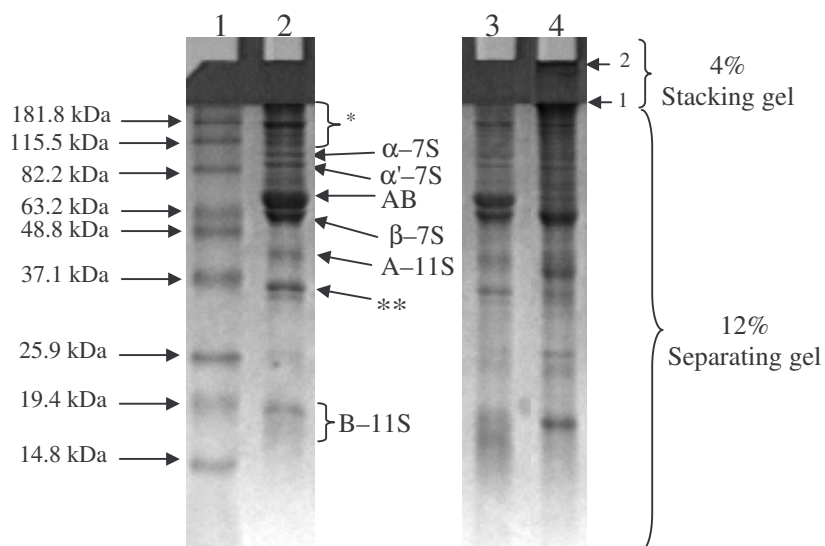
Figure 6. SDS-PAGE under non-reducing conditions: Lane 1 = molecular weight markers; Lane 2 = SPI powder; Lane 3 = soluble proteins of SPI gels extracted with deionized water; and Lane 4 = soluble proteins of SPI gels extracted with buffer (pH 8.0) plus urea. *aggregates with MW higher than 115.5 kDa; **low MW fractions.

The effects of xanthan or KCl on the linkages between protein fractions were obtained by analysing the optical density of the bands of the gels run under reducing conditions. Figure 7 shows the statistical comparison among different types of mixed biopolymer gels, of the amounts of soluble fractions dissolved in B or BM. In this Figure, the protein composition of the SPI gels (with or without KCl) extracted by BUM, was referred to as the standard composition, giving 12.2% α-7S, 12% α'-7S, 16.4% β-7S, 32.8% A-11S, 26.6% B-11S. The soluble proteins of the gels in BU showed a similar composition (p<0.1). However, the subunit composition of the proteins soluble in B and BM were different from the standard (Figure 7). Figure 7A shows that the addition of KCl

to gels increased the proportion of α and α'-7S, while the B-11S soluble in buffer (pH 8.0) was reduced. Regarding the BM extracts (Figure 7B), an increase in the proportion of A-11S and a decrease in B-11S polypeptides was observed, whilst the others did not change. This means that the addition of KCl resulted in a higher proportion of A-11S linked by SS bonds. One possible interpretation of these results is that the random aggregation of proteins promoted the self-association of A-11S or its linkage with the α and α'-7S polypeptide *(*Petruccelli & Añón, 1995c*)*. The B-11S fraction could be self-associated due to its more hydrophobic character, showing a lower proportion of SS bond linkages. Figure 7A also shows a decrease in the A-11S polypeptide and an increase in the β-7S subunit when xanthan was added to the SPI gels. This result suggests that electrostatic interactions between xanthan and soy conglycinin were mainly with the β-7S.

A ▨ Standard ▨ SPI ▤ SPI-xanthan ☐ SPI-KCl ▪ SPI-KCl-xanthan

157
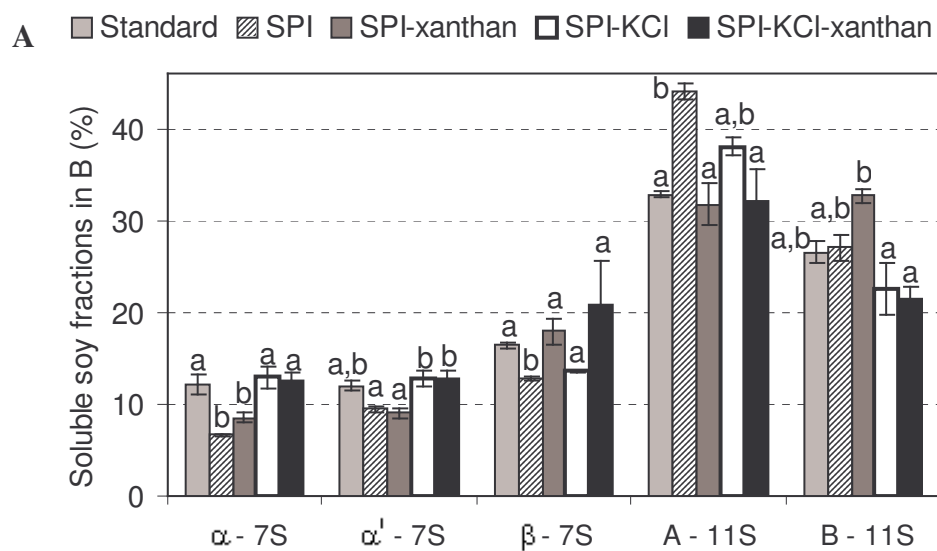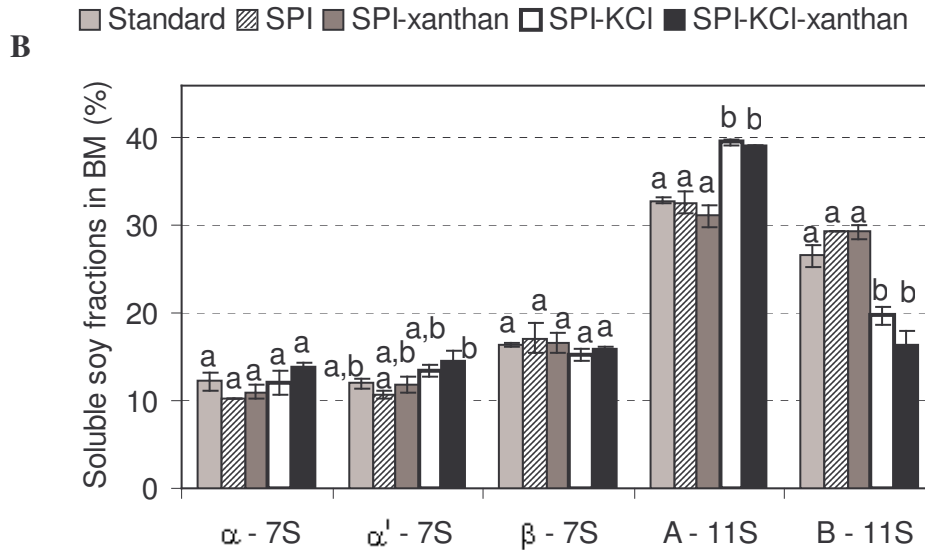
Figure 7. Effects of the addition of xanthan or KCl on the composition of the soluble protein subunits of SPI gels extracted in (A) buffer (pH 8.0) and (B) buffer (pH 8.0) plus β-mercaptoethanol. Different letters indicate significant differences at $p<0.10$ (the variation was analyzed for each fraction).

3.3.2. CSLM and macroscopic properties of gels

An indication of the type of gel network formed is given by the appearance of the gels. The initial mixed solution was translucent and became opaque on acidification. Near the pI (pH ~4.0-5.0) the solution was highly opaque with granular aggregates of different sizes. Beyond this point, these particles were re-dissolved, but the solution remained slightly opaque. At pH 3.0 the gels made with KCl were opaque and those prepared without the salt showed an appearance between a yellowish transparent and a slightly opaque gel. Opaque gels are formed when fluctuations in polymer density approach macroscopic size and effectively scatter light. On the other hand, transparent gels have an almost homogeneous network (Oakenfull, Pearce & Burley, 1997). The former are usually the result of random aggregation (coarse network), and the latter to the association of

molecules into strands in a more ordered way (fine-stranded) (Hermansson, 1986). However, depending on the ionic strength and pH, linear polymers and random aggregates could be mixed together in the same gel to form translucent or opaque gels (Doi, 1993).

Structural observations of SPI-xanthan gels revealed a clear difference in network structure on addition of KCl (Figure 8). White and gray areas in the pictures represent protein, while black areas represent the pores of the network containing the continuous phase without protein. In the gel without salt, the fluorescent signal was uniform throughout the sample, indicating that the SPI particles were homogeneously distributed (Figure 8A). This gel could be categorized as fine-stranded (Foegeding, Bowland & Harding, 1995).

The effect of increasing ionic strength on the microstructure of the gel matrix was observed when 0.14 M KCl was added (Figure 8B). Monovalent chloride ions induce the formation of a fine stranded matrix at ionic strength values below 0.1 M (Totosaus, Montejano, Salazar & Guerrero, 2002). Figure 8B shows a mixed structure predominantly formed by random bright aggregates with different sizes and shapes, but also showing regions resembling the fine structure of Figure 8A (below the line). Renkema (2004) reported a soy protein gel (pH 3.8) with coarse microstructure at a slightly higher ionic strength, but with smaller aggregates as compared to those obtained in SPI-xanthan-KCl gels (Figure 8B). At pH 3.0, the most likely interaction involving the two biopolymers was that between the positively charged regions on the proteins and the negatively charged carboxyl groups of the xanthan. The addition of salt (Figure 8B) resulted in screening of the exclusion volume effect and a coupled network with both biopolymers was probably formed. The SPI-xanthan gel also showed some regions nearly devoid of protein, which could be due to the presence of xanthan.

159
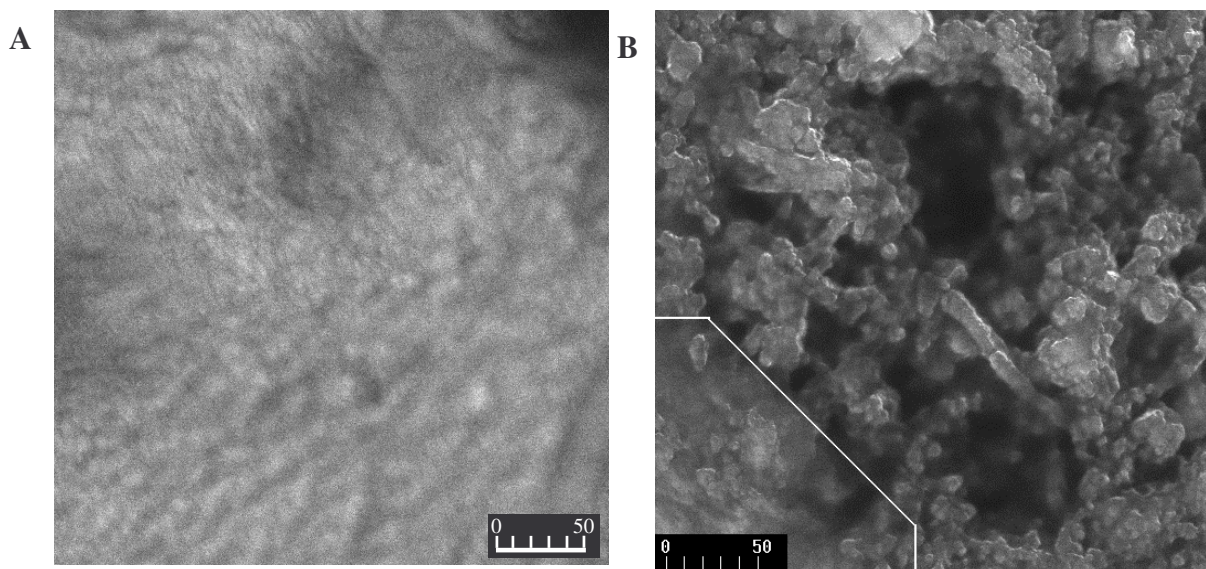
Figure 8. CSLM photos of heat-induced SPI-xanthan gels at pH 3.0 with intermediate concentrations (factorial design) of ingredients. A) 12% (w/w) SPI and 0.153% (w/w) xanthan, B) 12% (w/w) SPI, 0.153% (w/w) xanthan and 0.14 M KCl. Scale bars in μm.

Gel properties, which depend on the pH and ionic strength of the system, are closely related to the type of protein structure (Foegeding, Bowland & Harding, 1995). Figure 9 shows the water holding capacity (WHC), strain at fracture, Young modulus and stress at fracture of SPI-xanthan gels as a function of KCl content. The composition of the gels without KCl was chosen according to the 2^2-factorial design (SPI-xanthan). Gels with the same composition and containing the lowest (0.01 M) and highest (0.27 M) KCl concentrations were also investigated, corresponding to the negative (-1) and positive (+1) salt levels of the 2^3-factorial design (Table 1). The effects of these variables on the gel properties were statistically analyzed, these results being used to better understand the tendencies shown in Figure 9. Figure 9A shows that the xanthan and KCl concentrations were the main factors responsible for the changes in the WHC values. In the systems without salt, an increase in xanthan content changed the WHC from ~50% to ~70%, while at the highest KCl concentration, all the values were lower and closer, about 30-40%. The

strain at fracture values (Figure 9B) were also greatly affected by the KCl concentration, with values >0.5 for systems with low KCl and small strain values (<0.5) at the highest salt content. Figure 9C shows that the xanthan concentration had a negative effect on the Young modulus values in gels without KCl, but at the highest salt concentration, the polysaccharide had a positive effect. The KCl concentration had a great effect on the Young modulus, especially at high xanthan concentrations. The values increased from ~4-5 kPa to ~15-18 kPa with the addition of 0.27 M KCl.

Figures 9A and 9B show that the WHC and strain at fracture first increased with the addition of 0.01 M KCl and then decreased when more KCl (0.27 M) was added to systems with low xanthan concentrations. However, at the higher xanthan concentrations, the WHC and strain values did not show such an initial increase, decreasing with the addition of any KCl concentration. This fact could be explained by an intensification of the solute effect, since there was less water available in the system due to the high capacity of xanthan to bind water. The behavior described above was probably due to salting-in and salting-out effects. For systems without KCl, it was observed a positive effect of xanthan on WHC, since polysaccharides are good water binders. This corroborates to the above hypothesis of intensification of the solute effect at high xanthan content.
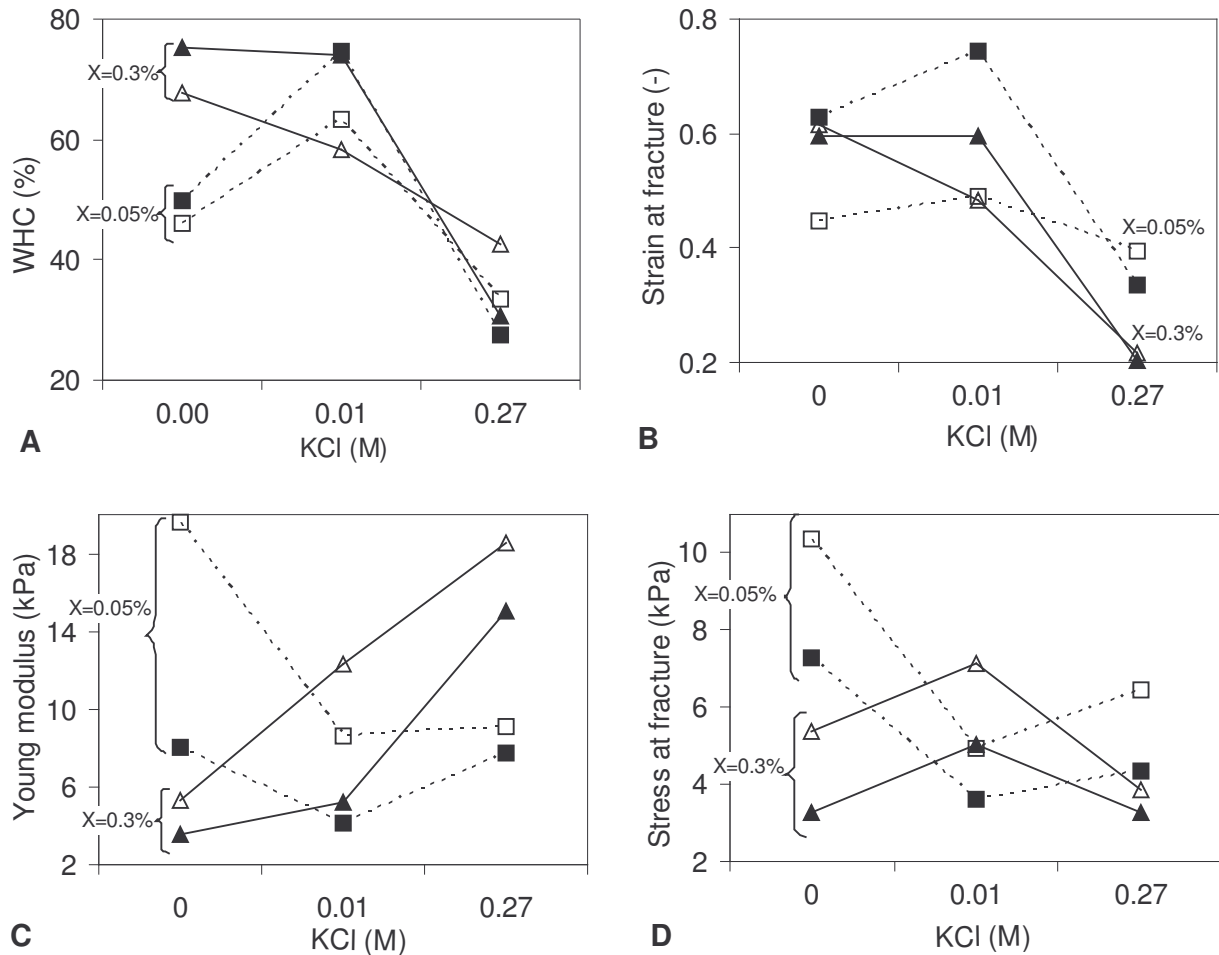
Figure 9. Variation in the water holding capacity (A), strain at fracture (B), Young modulus (C) and stress at fracture (D) at three KCl concentrations. X is the xanthan concentration: 0.05 wt% (■, □), 0.3 wt% (▲, △). SPI: 10 wt% (■, ▲), 14 wt% (□, △).

At low salt concentration or ionic strength values below 0.1 M (Hermansson, 1978), ions of neutral salts may increase the solubility of soy proteins (salting-in) by reacting with the charged sites, resulting in an increase in the water holding capacity of the gels. However, at higher salt concentrations, protein solubility decreases (salting-out) as a result of competition between the protein and the salt ions for the water molecules (Cheftel et al., 1996). The latter effect results in random protein aggregation and a gel with low WHC, since gels with large pores inhibit the capacity to immobilize solvent via capillary forces (Ziegler & Foegeding, 1990). Such an event was better observed for systems with high

162

protein and polysaccharide concentrations. The strain at fracture showed exactly the same tendencies as the WHC as a function of KCl concentration, for all systems (Figure 9B). It is known that a more aggregated structure (salting out effect) leads to a less elastic network (Foegeding, Bowland & Harding, 1995).

The Young modulus values rose with increasing salt content for systems with high xanthan contents, while showing a minimum value at 0.01 M KCl for gels with a low polysaccharide concentration (Figure 9C). This tendency was the opposite of that observed for strain at fracture. The great increase in the Young modulus values at high xanthan and KCl concentrations could be due to the more elastic character of xanthan solutions at low deformations (Figure 3), with the addition of salt. The stress at fracture values (Figure 9D) showed almost the same tendency observed for the Young modulus. The different behaviors at high salt content could be attributed to the deformation scale from which the properties were obtained. The Young modulus is a small deformation property and gives more information about the linkage of biopolymers. Stress at fracture is obtained at large deformations such that not only the strength of the strands is important but also the size of the holes. Figure 8B shows that even for 0.14 M KCl there are holes of about 90 x 40 μm. Above a certain size, the holes probably made the network more fragile, as observed by the drop in stress at fracture.

For systems without salt, the stress at fracture decreased with the increase of xanthan concentration (Figure 9D). It was discussed above (Figure 7) that xanthan probably preferentially interacted with β-7S. In addition, the confocal microstructure of SPI-xanthan gel showed some regions nearly devoid of protein. Thus, it can be suggested that at least

163

part of xanthan and β-7S were not in the main protein network, which would induce the reduction of the gel hardness.

4. Conclusions

The increase in KCl content led to more elastic xanthan solutions, and such behavior can be attributed to the ordered conformation of this polysaccharide. At pH 3.0, all 7S and 11S subunits seemed to participate in the network, although they were associated in different ways depending on the composition of the gels (with or without KCl or xanthan). The β-7S subunit was probably the fraction electrostatically linked to the xanthan. It was suggested that at least part of xanthan and β-7S were not in the main protein network, which would induce the reduction of the gel hardness for gels without KCl. The addition of KCl to SPI gels affected the mechanical properties of the gels and their water holding capacity, which was explained by the salting in and salting out effects. Gels with low amounts of ingredients were more deformable and showed greater WHC, salting-in effects being observed. When the content of one of the ingredients (KCl or xanthan) was increased, the salting-out effect occurred.

5. Acknowledgements

6. References

Abernethy, J. D. (1979). Sodium and potassium in high blood pressure. *Food Technology,* 33, 57-59.

Arogundade, L. A., Akinfenwa, M. O., Salawu, A. A. (2004). Effect of NaCl and its partial or complete replacement with KCl on some functional properties of defatted Colocynthis citrullus seed flour. *Food Chemistry,* 84, 187–193.

Bell, R. R., Eldrid, M. M., Watson, F. R. (1992). The influence of NaCl and KCl on urinary calcium excretion in healthy-young women. *Nutrition Research,* 12, 17-26.

Carp, D. J., Bartholomai, G. B., Pilosof, A. M. R. (1999). Electrophoretic studies for determining soy proteins–xanthan gum interactions in foams. *Colloid and Surface B,* 12, 309–316.

Cheftel, J. C., Cuq, J. L., Lorient, D. (1996). Amino acids, peptides and proteins. In O.R., Fenema, *Food Chemistry* (pp. 245-369), Zaragoza: Acribia.

Damodaran, S. (1988). Refolding of thermally unfolded soy proteins during the cooling regime of the gelation process: effect on gelation. *Journal of Agriculture and Food Chemistry* 36, 262–269.

Danilenko, A. N., Bikbov, T. M., Grinberg, V. Y., Leontyeva, A. L., Burova, T. V., Surikov, V. V., Borisov, Y. A., Tolstoguzov, V. B. (1987). Effect of pH on the thermal stability of 11S-globulin of Glycinine Max seeds as indicated by differential scanning microcalorimetry. *Biofizika,* 32, 402-406.

Doi, E. Gels and gelling of globular proteins. (1993). *Trends Food Science and Technology*, 4, 1-5.

Foegeding, E. A., Bowland, E. L., Harding, C. (1995). Factors that determine the fracture properties and microstructure of globular protein gels. *Food Hydrocolloids* 9, 237-249.

Harding, S. E. (1997). The intrinsic viscosity of biological macromolecules. Progress in measurement, interpretation and application to structure in dilute solution. *Progress in Biophysics and Molecular Biology,* 68, 207-262.

Hermansson, A. M. (1978). Physico-chemical aspects of soy proteins structure formation. *Journal of Texture Studies*, 9, 33-58.

Hermansson, A. M. (1986). Soy protein gelation. *Journal of the American Oil Chemists Society,* 63, 658-666.

Hua, Y., Cui, S. W., Wang, O. (2003). Gelling property of soy protein–gum mixtures *Food Hydrocolloids*, 17, 889-894.

Iseki, T., Takahashi, M., Hattori, H., Hatakeyama, T., Hatakeyama, H. (2001). Viscoelastic properties of xanthan gum hydrogels annealed in the sol state. *Food Hydrocolloids*, 15, 503-506.

Jansson, P. E., Kenne, L., Lindberg, B. (1975). Structure of extracellular polysaccharide from Xanthomonas campestris. *Carbohydrate Research,* 45, 275-282.

Katsiari, M. C., Voutsinas, L. P., Alichanidis, E., Roussis, I. G. (1997). Reduction of sodium content in feta cheese by partial substitution of NaCl by KCl. *International Dairy Journal*, 7, 465-472.

Kim, K. S., Kim, S., Yang, H. J., Kwon, D.Y. (2004). Changes of glycinin conformation due to pH, heat and salt determined by differential scanning calorimetry and circular dichroism. *International Journal of Food Science and Technology* 39, 385–393.

Kocher, P. N., Foegeding, E. A. (1993). Microcentrifuge-based method for measuring water-holding of protein gels *Journal of Food Science*, 58, 1040-1046.

Koshiyama, I. (1972). Acid induced conformation changes between 7S and 11S globulins in soybean seeds. *Journal of Science Food Agricultural*, 23, 853–859.

Laemmli, U. K. (1970). Cleavage of structural proteins during the assembly of the head of bacteriophage T4. *Nature*, 227, 685-689.

Lakemond, C. M. M., de Jongh, H. H. J., Hessing, M., Gruppen, H., Voragen, A. G. J. (2000). Soy Glycinin: Influence of pH and ionic strength on Solubility and molecular structure at ambient temperatures. *Journal of Agricultural and Food Chemistry*, 48, 1985-1990.

Lakemond, C. M. M., de Jongh, H. H. J., Paques, M., van Vliet, T., Gruppen, H., Voragen, A. G. J. (2003). Gelation of soy glycinin, influence of pH and ionic strength on network structure in relation to protein conformation. *Food Hydrocolloids*, 17, 365-377.

Millard, M. M., Dintzis, F. R., Willett, J. L., Klavons, J. A. (1997). Light-scattering molecular weights and intrinsic viscosities of processed waxy maize starches in 90% dimethyl sulfoxide and H_2O. *Carbohydrates*, 74, 687-691.

Oakenfull, D., Pearce, J., Burley, R. W. (1997). Protein gelation. In S., Damodaran, A., Paraf, *Food Proteins and their applications (*pp 111-142). New York: Marcel Dekker.

Ogungbenle, H. N., Oshodi, A. A., Oladimeji, M. O. (2002). Effect of salts on the functional properties of benniseed (Sesamum radiatum) seed flour. *International Journal of Food Science and Nutrition*, 53, 5-14.

Petruccelli, S., Añón, M. C. (1995a). Thermal aggregation of soy protein isolates. *Journal of Agricultural and Food Chemistry*, 43, 3035-3041.

Petruccelli, S., Añón, M. C. (1995b). Partial reduction of soy protein isolate disulfide bonds. *Journal of Agricultural and Food Chemistry*, 43, 2001-2006.

Petruccelli, S., Añón, M. C. (1995c). Soy protein isolate components and their interactions. *Journal of Agricultural and Food Chemistry*, 43, 1762-1767.

Puppo, M. C., Lupano, C. E., Añón, M. C. (1995). Gelation of soybean protein isolates in acidic conditions. Effect of pH and protein concentration. *Journal of Agricultural and Food Chemistry*, 43, 2356–2361.

Puppo, M. C., Chapleau, N., Speroni, F., Anton, M. L., Michel, F., Añón, M. C., Anton, M. (2004). Physicochemical modifications of high-pressure-treated soybean protein isolates. *Journal of Agricultural and Food Chemistry*, 52, 1564–1571.

Renkema, J. M. S. (2004). Relations between rheological properties and network structure of soy protein gels. *Food Hydrocolloids*, 18, 39-47.

Renkema, J. M. S., Lakemond, C. M. M., de Jongh, H. H. J., Gruppen, H., van Vliet, T. (2000). The effect of pH on heat denaturation and gel forming properties of soy proteins. *Journal of Biotechnology*, 79, 223-230.

Renkema, J. M. S., Gruppen, H., van Vliet, T. (2002). Influence of pH and ionic strength on heat-induced formation and rheological properties of soy protein gels in relation to denaturation and their protein compositions. *Journal of Agricultural and Food Chemistry*, 50, 6064–6071.

Rochefort, W. E., Middleman, S. (1987). Rheology of xanthan gum: salt, temperature, and strain effects in oscillatory and steady shear experiments. *Journal of Rheology*, 31, 337-369.

Shimada, K., Cheftel, J. C. (1988). Texture characteristics, protein solubility and sulfhydryl group/disulfide bond contents of heat-induced gels of whey protein isolate. *Journal of Agricultural and Food Chemistry*, 36, 1018-1025.

Staswick, P. E., Hermodson, M. A., Nielsen, N. C. (1984). Identification of the cystine which links the acidic and basic components of the glycinin subunits. *Journal of Biological Chemistry*, 259, 13431-13435.

Steffe, J.F. (1996) *Rheological Methods in Food Process Engineering*. East Lansing: Freeman Press.

Thanh, V. H., Shibasaki, K. (1977). Beta-conglycinin from soybean proteins. Isolation and immunological and physicochemical properties of the monomeric forms. *Biochimica and Biophysica Acta*, 490, 370-384.

Tolstogusov, V. B. (1993). Functional Properties of food proteins. Role of interactions in protein systems. In K.D., Schwenke, R., Mothes, *Food proteins. Structure and functionality* (pp 203-209). Weinheim: VHC.

Totosaus, A., Montejano, J. G., Salazar, J. A., Guerrero, I. (2002). A review of physical and chemical protein-gel induction. *International Journal of Food Science and Technology*, 37, 589–601.

Utsumi, S., Kinsella, J. E. (1985). Forces involved in soy protein gelation: effects of various reagents on the formation, hardness and solubility of heat-induced gels made from 7S, 11S and soy isolate. *Journal of Food Science*, 50, 1278-1282.

Utsumi, S., Damodaran, S., Kinsella, J. E. (1984). Heat-induced interactions between soybean proteins: preferential association of 11S basic subunits and β subunits of 7S. *Journal of Agricultural and Food Chemistry*, 32, 1406-1412.

Van Vliet, T., Martin, A. H., Bos, M. A. (2002). Gelation and interfacial behaviour of vegetable proteins. *Current Opinion in Colloid and Interface Science*, 7, 462-468.

Wang, F., Sun, Z., Wang, Y. J. (2001). Study of xanthan gum/waxy corn starch interaction in solution by viscometry. *Food Hydrocolloids*, 15, 575-581.

Wolf, W. J., Rackis, J. J., Smith, A. K., Sasame, H. A., Babcock, G. E. (1958). Behavior of the 11S protein of soybeans in acid solutions I. Effects of pH, ionic strength and time on ultracentrifugal and optical rotary properties. *Journal of the American Chemical Society*, 80, 5730-5735.

Yevlampieva, N. P., Pavlov, G. M., Rjumtsev, E. I. (1999). Flow birefringence of xanthan and other polysaccharide solutions. *International Journal of Biological Macromolecules*, 26, 295-301.

Ziegler, G. R., Foegeding, E. A. (1990). The gelation of proteins. In J.E., Kinsella, *Advances in Food Nutrition Research* (pp 203-298), San Diego, CA: Academic Press.

CHAPTER 5. Protein-polysaccharide interactions in aqueous systems at pH 7.0.

1ˢᵗ PART: Rheological and phase-separation behaviours of protein-

polysaccharide mixtures at pH 7.0

(in collaboration with LMVT-ETHZ-Switzerland)

Abstract

Phase separation, rheological and confocal laser scanning microscopy (CLSM) experiments were performed to characterize different mixtures of proteins and polysaccharides. The results showed that SPI was more hydrophobic than the Na-caseinate, which induced the gelation of the protein rich phase after centrifugation of SPI – Na-alginate and SPI – κ-carrageenan systems. However, gellan did not induce the gel formation, indicating that this polysaccharide could be used as thickening in soy products. The results indicated that κ-carrageenan was more compatible with both soy protein and Na-caseinate than alginate. The confocal micrographs revealed different degree of separation for a fixed centrifugation condition (60000 x g during 1 h). This suggests that the centrifugation conditions should be carefully chose for each protein-polysaccharide mixture. The rheological behaviour of the systems varied from a diluted solution to a gel passing through the formation of water-in-water emulsions. In addition, it was suggested that the storage modulus value of the protein rich-phase can be used as an indicator of the degree of phase separation.
Keywords: proteins, polysaccharides, CLSM, rheology, phase separation.

1. Introduction

From the last two decades, the food industries are putting great effort on developing new products with attractive textures. Different types of polysaccharides and proteins have been added to milk products in order to partially replace the fat or sugar. Soy proteins have been applied in a wide range of food products especially because of their ability to form gels with good water holding capacity on heating, showing great potential in the substitution of meat and dairy proteins (Van Vliet et al., 2002). Carrageenans are the most

171

used polysaccharides in dairy products, altough the mechanism of compatibility of this seaweed, anionic and linear polysaccharide with milk proteins remains in discussion (Spagnuolo et al., 2005). Other seaweed, anionic and linear polysaccharides that have been receiving great attention from the industry are the alginates that show a good water-in-water emulsion capacity (Capron et al., 2001, Antonov et al., 2004). Among the microbial polysaccharides, gellan is widely utilized in the industries due to its ability to form clear and heat- and acid-resistant thermoreversible gels with aqueous media. In addition, from a scientific point of view, it is often regarded as a model system for investigating gelation mechanisms of helix-forming polysaccharides such as agarose and carrageenans (Ikeda et al., 2004).

Proteins and polysaccharides are usually incompatible showing segregative phase separation at pH 7.0. The conditions necessary for phase separation vary according to the biopolymers and the presence of co-solutes. They are dependent on specific structure and compositional features, as well as on the molecular weight and conformation of the biopolymers (Zeman and Patterson, 1972). The phase behaviour of proteins and polysaccharides has received attention in the last decade and the works have been especially done by Tolstogusov and others (Polyakov et al., 1980; Grinberg and Tolstoguzov, 1997; Tolstoguzov, 2003). The most studied mixtures in the last years has used gelatin or skim milk as protein source, but few works were done using soy proteins.

The rheological behaviour of aqueous biopolymer mixtures is quite different from that of a pure biopolymer solution due to the hydrodynamic influence of the dispersed phase (Palierne, 1990, Simeone et al., 2002). The morphology of the system can add information to the rheological description of the biopolymers mixtures. The confocal microscopy is especially important to give information about the dispersed phase shape,

distribution and volume fraction. In addition, it can give support to the choices of the centrifugation parameters.

The aim of this work was to understand the role of different biopolymers and its concentration on the phase behaviour of a protein-polysaccharide system. The polysaccharides investigated were gellan, κ-carrageenan and Na-alginate, while sodium caseinate and soy protein isolate were the proteins source. In addition, the rheological properties of the initial mixture and the separated phases were measured and the microstructures of those systems were observed under confocal laser scanning microscope.

2. Material and methods

2.1. Material

The proteins used to prepare the model systems were casein (Sigma Chemical Co., USA) and soy protein isolate (SPI) obtained from defatted soy flour (Bunge Alimentos S.A., Brazil). The polysaccharides used were sodium (Na)-alginate, κ-carrageenan, and gellan, all of them obtained from CP Kelco (USA). Table 1 shows the chemical characterization of each biopolymer. The moisture and ash contents were determined using the gravimetric method, in which the initial and final samples were weighed. The ash was obtained by heating the powder at 550°C until it becomes a carbon-free sample (AOAC, 1996). For moisture analysis the powder was dried in a vacuum-oven at 60 ^{o}C until the sample weight reached a constant value. The protein content was carried out using the Kjeldahl method (AOAC, 1996).

The soy proteins isolation procedure followed the method described by Petruccelli and Añón (1995). Defatted soy flour was dispersed in distilled water (1:10 w/w) and the pH

was adjusted to 8.0 with 2N NaOH. The dispersion was gently stirred for 2h at room temperature and then centrifuged at 10,000 x g for 30 min at 4ºC in a Sorvall RC5 Plus centrifuge (GSA-rotor, Dupont, UK). The supernatant was adjusted to pH 4.5 with 2N HCl and centrifuged at 5,000 x g (Sorvall GSA-rotor) for 15 min at 4ºC. The precipitate was then suspended in water and the pH adjusted to 8.0 with 2N NaOH, followed by freeze-drying of the suspension.

Table 1. Characterization of the biopolymers used to prepare the model systems.

Biopolymer	Moisture [%] (wet basis)	Protein [N% x 6.25] (wet basis)	Ash [%] (wet basis)
Casein	6.51 ± 0.10	89.64 ± 1.55	0.84 ± 0.08
SPI	6.44 ± 0.07	91.25 ± 0.45	3.45 ± 0.04
Na-alginate	5.75 ± 0.21	0.44 ± 0.01	21.52 ± 0.23
κ-carrageenan	7.84 ± 0.07	0.44 ± 0.03	15.29 ± 0.16
Gellan	6.42 ± 0.12	0.47 ± 0.02	9.85 ± 0.02

2.2. Preparation of biopolymers stock solutions

The Na-caseinate solution was prepared by dispersing casein powder in milli-Q water using magnetic stirring for 2 h at a maximum temperature of 50 ^{o}C. The pH was constantly adjusted to 7.0 with 10M NaOH. The soy protein isolate (SPI) solution (milli-Q water) was prepared at room temperature by magnetic stirring until the complete powder hydration and the pH was adjusted to 7.0 with 1M HCl. The polysaccharide solutions were prepared by first dispersing the powders in milli-Q water at room temperature by magnetic stirring and after heating in a water bath with a fixed temperature and time (Table 2). The prepared solutions were immediately cooled down to room temperature in an ice bath, and none of them gelified after this process. The insoluble particles of proteins and polysaccharides solutions were separated by centrifugation in an ultracentrifuge L8-80 M

(Beckman, USA) at 60,000 x *g* for 60 minutes at 25 °C (Antonov et al., 2004), except for κ-carrageenan and gellan solutions that were already purified (without any insoluble particles). The pH of all solutions was adjusted to 7.0. The concentrations of proteins, seadweeds polysaccharides and gellan solutions were 8%, 4% and 1% (w/w), respectively.

Table 2. Temperature and time used to prepare the polysaccharide solutions

Polysaccharide	Temperature (°C)	Time (min)
Gellan (Ikeda et al., 2004)	90	60
κ-carrageenan (Hemar et al., 2002)	90	60
Na-Alginate (Capron et al., 2001)	70	30

2.3. Preparation of biopolymers mixtures and phase separation

Biopolymer mixed solutions (MS) were obtained by mixing the purified solutions of protein and polysaccharide during 1 h at room temperature by magnetic stirring. These solutions were poured into polycarbonate tubes of 25 mL that were centrifuged in an ultracentrifuge L8-80M (Beckman, USA) at 60,000 x g during 60 minutes (Antonov et al., 2004). Two meniscus were marked on the outside of the centrifuge tubes in order to determine the amount (volume) of the protein and polysaccharide rich phases The phases were then carefully withdrawn and stored in separate beakers for further analyses (rheology, CLSM and chemical analysis).

Preliminary studies (Apendice) on different protein-polysaccharides MS were conducted in order to determine the concentration of biopolymers that would lead to incompatible mixtures that form two equilibrium phases after centrifugation. The selected systems are shown in Table 3. Almost all of the selected systems had similar zero shear viscosities of MS (estimated from the data obtained in Chapter 3-1ˢᵗ part). In addition, it

was studied two different compositions for SA and SC systems in order to understand the role of the viscosity on the phase separation behaviour.

Table 3. Composition of the initial mixture at pH 7.

Mixture	Nomenclature	Nominal protein amount* [%]	Nominal polysaccharide amount* [%]
Na-caseinate / Na-Alginate	CA	3.0	2.3
Na-caseinate / Carrageenan	CC	3.0	2.3
Na-caseinate / Gellan	CG	5.0	0.4
SPI / Na-Alginate	SA1	3.0	1.5
SPI / Na-Alginate	SA2	3.0	2.3
SPI / Carrageenan	SC1	3.0	1.4
SPI / Carrageenan	SC2	3.0	2.3
SPI / Gellan	SG	5.0	0.4

* The values of protein and polysaccharide concentration are based on the amount of powder added considering the moisture content.

2.4. Chemical analyses

The protein concentration was determined in triplicate by Kjeldahl method (AOAC, 1996). The polysaccharide concentration was also determined in triplicate using the phenol-sulphuric acid reaction followed by the measurement of the solution light absorption in the visible wavelength region (Dubois et al., 1956) using a Beckmann spectrophotometer DU/70 (Beckman, USA). The light absorption was made at three different wavelengths corresponding to the points P_1, P_2 and P_3 of Figure 1, which depended on the polysaccharide type. These values were determined from a previous wavelength scan in the visible region. The calibration curves of the polysaccharides were obtained for concentrations in the range of 10-100 μg/mL.
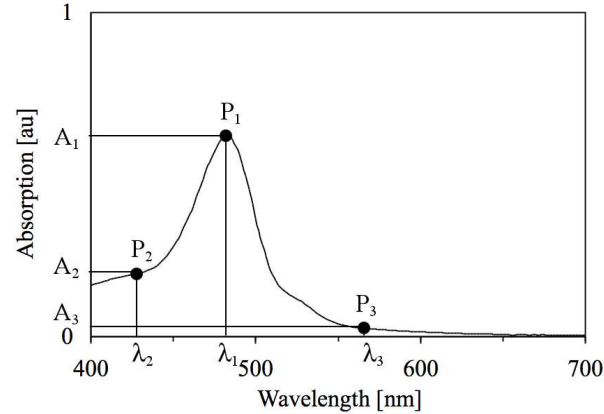
Figure 1. Typical light absorption curve of a polysaccharide solution with the description of the wavelengths used for the polysaccharide quantification.

The mass balances errors between the initial (MS) and final (PR$_{rp}$ plus PS$_{rp}$) protein or polysaccharide content were calculated according to Equations 1 and 2.

$$Error(\%) = \left|100 - MB_B\right| \tag{1}$$

$$MB_B = 100 \cdot \frac{C_{B,PSrp} \cdot VR_{exp} + C_{B,PRrp}}{C_{B,MS} \cdot \left(VR_{exp} + 1\right)} \tag{2}$$

where MB is the mass balance (%), C is the concentration (%) and VR$_{exp}$ is the experimental volume ratio (see Equation 3 below). The subscripts B, MS, PSrp and PRrp are, respectively, biopolymer (protein or polysaccharide), mixed solution, polysaccharide rich-phase and protein rich-phase.

2.5. Volume ratio analysis

The volume ratio method was developed to obtain the binodal line for a liquid-liquid phase separation (Polyakov et al., 1980). However, some protein-polysaccharide mixtures resulted in a liquid-gel phase separation, such that the precision of the above method was checked (Results and Discussion section). The volume of each phase was

quantified by filling the centrifuge tube with water up to the meniscus marks and weighing the amount of water added. The Equation 3 was used for further analysis:

$$VR_{exp} = \frac{V_{PSrp}}{V_{tot}}$$ (3)

where VR_{exp} is the volume ratio determined experimentally from the meniscus marks, V_{PSrp} is the volume of the polysaccharide rich phase and V_{tot} is the total volume of the mixture SM1.

The lever-arm rule (Antonov et al., 2004) was used to check the experimental volume data above (Equations 4, 5 and 6). The density of each phase was considered to be 1 g/cm^3 for the calculations since the density of the most concentrated phase was 1.06 g/cm^3 (Chapter 3-1st part).

$$VR_{calc} = \frac{V_{PSrp}}{V_{tot}} = \frac{A}{B}$$ (4)

$$A = X_{PRrp} - X_{SM1}$$ (5)

$$B = X_{PRrp} - X_{PSrp}$$ (6)

where VR_{calc} is the volume ratio calculated from chemical analysis and X is the protein concentration.

2.6. Rheological tests

A stress-controlled rheometer (Carri-Med CSL^{2}500, TA Instruments, England) was used to accomplish the steady and oscillatory rheological measurements. The initial mixture (MS) and the protein and polysaccharide rich-phases were placed on the rheometer and the measurements were made in triplicate at 25 °C. Cone-plate, rough plate-plate or double concentric cylinder geometry (Table 4) were used depending on the sample. The double concentric cylinders were used for samples with zero shear viscosity (η_0) lower than 0.8

Pa.s. The cone-plate geometry was chosen for the samples with η_0 values in the range of 0.8-10 Pa.s. The rough plate-plate was used for high viscous samples ($\eta_0 > 10$ Pa.s) and for those systems that showed slippage due to syneresis.

Table 4. Applied geometries for rheological measurements

Geometry	Diameter [mm]	Gap [μm]	Material
Cone-plate	60	67	Stainless steel
Rough plate-plate	40	53	Stainless steel
Double concentric cylinders	External rotating: 43.92 Internal rotating: 40.76 External stationary: 44.76 Internal stationary: 40.00		Acrylic

2.6.1. Steady shear flow curves

Flow curves were obtained by applying an up-down-up steps program using different shear stress range to each sample. This range was determined from a shear rate-control experiment, in which the maximum shear rate was 300 [s^{-1}]. At each programmed step 150 points were measured. The last step (steady flow) was taken to plot the apparent viscosity (η) versus shear rate.

2.6.2. Dynamic oscillatory measurements

A stress sweep test was carried out at 25 ºC and constant frequency of 0.1 Hz, for every sample, in order to find out the limit of the linear viscoelastic zone. Frequency sweeps were done from 0.02 to 10 Hz at 25 ºC at a fixed stress within the linear viscoelastic range. The storage (G'(ω)) and loss (G''(ω)) moduli were plotted as a function of frequency.

2.7. Confocal laser scanning microscope (CLSM)

The initial protein-polysaccharide mixture (MS) and the protein and polysaccharide rich-phases were observed under confocal laser scanning microscope (CSLM). Rhodamine B was added and mixed carefully with about 1 mL of sample. Such a fluorescent dye was used in order to stain the protein. The samples were placed in indentations of microscope slides, covered with a glass cover slip and sealed with nail polish to prevent evaporation. A dual-channel laser confocal system (MRC 1024 UV, Biorad, USA) mounted on an Axiovert 100 Zeiss inverted microscope and equipped with Ar-Kr lasers was used for the trials. The Ar-Kr lasers emitted polarized light with a wavelength of 568 nm exciting the Rhodamine-labeled proteins. Images were taken using a 40x water immersion objective and a 100x oil immersion objective. To obtain a representative structure 15 micrographs of each sample were taken. The sizes of the inclusions (highest length or area) were quantified using the software Image J. for Macintosh.

3. Results and discussion

3.1. Visual appearance and volume ratio of biopolymers mixed solution after centrifugation.

The visual appearance of the mixtures (MS) after centrifugation in test tubes at 60000 x *g* during 60 minutes at 25 °C can be observed in Figure 2. All mixed solutions (MS), excluding the CG mixture formed a transparent and liquid polysaccharide rich phase (PS_{rp}) after centrifugation at the top of the tube. The $CG-PS_{rp}$ was a translucent gel (1.6% of polysaccharide) that easily broke releasing water. This could be explained by the gellan ability to form brittle gels at concentrations higher than 1%. The mixtures containing κ-

carrageenan (CC, SC) and the SA mixture formed opaque and gelified protein rich-phases (PR_{rp}) at the bottom of the tubes. Such gels were apparently harder for the SPI systems, while the CC-PR_{rp} gel was a more deformable one. The mixed systems containing gellan (CG and SG) formed a liquid PR_{rp}. The CA mixture formed a highly viscous and opaque PR_{rp}.

a) CA	b) CC	c) CG	d) SA₂	e) SC₂	f) SG
PS_{rp}: liquid	PS_{rp}: liquid	PS_{rp}: gel	PS_{rp}: liquid	PS_{rp}: liquid	PS_{rp}: liquid
PR_{rp}: liquid	PR_{rp}: gel	PR_{rp}: liquid	PR_{rp}: gel	PR_{rp}: gel	PR_{rp}: liquid
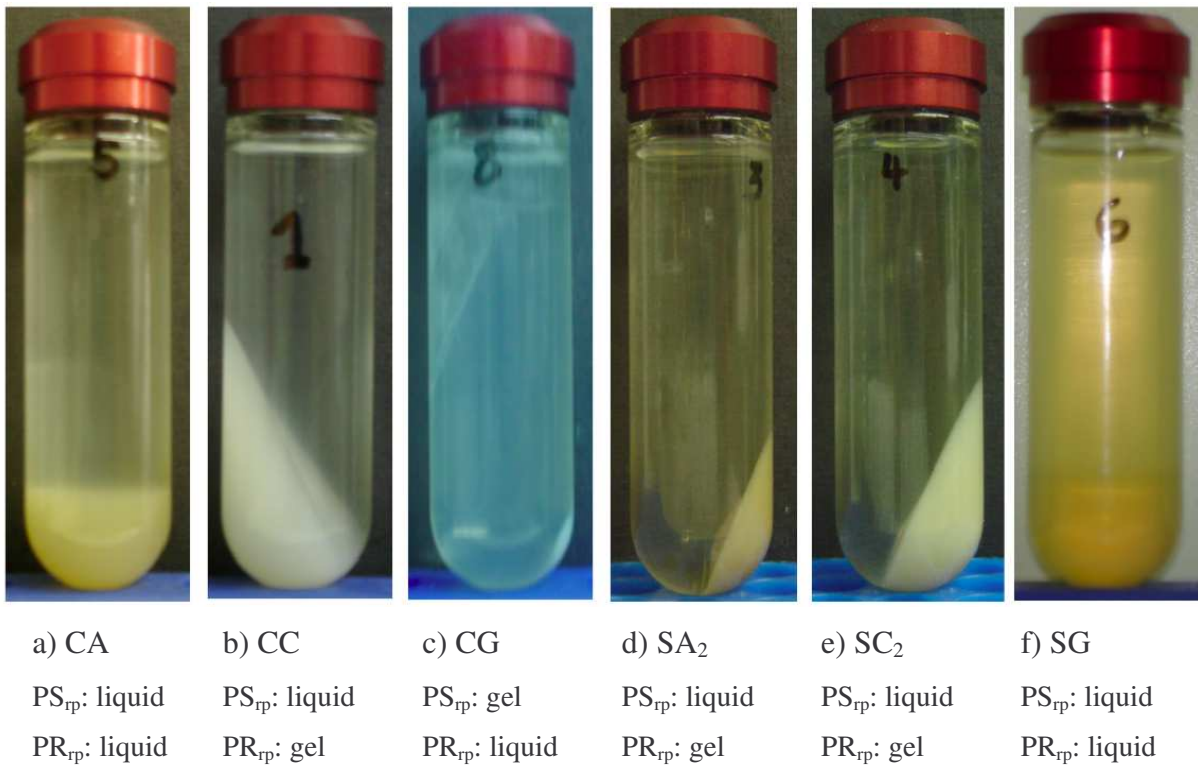
Figure 2. Visual appearance of the mixtures after centrifugation at 60000g during 60 min.

The analysis of the volume ratio adds information for the determination of the tie-lines of a phase diagram. The volume ratio method was developed for a liquid-liquid phase separation (Polyakov et al., 1980). However, some protein-polysaccharide mixtures resulted in a liquid-gel phase separation (Figure 2), being necessary to check the precision of the mentioned method. The experimental phase volume ratio (VR_{exp}) was determined using the measured volumes of the phases (Table 5). The volume ratio was also calculated (VR_{calc}) based on the protein concentration of MS, PS_{rp} and PR_{rp}. A specific procedure to

withdraw the phases was done for each mixture, as the separated phases showed different

properties (Figure 2). The top and bottom phases separated from CA and CC mixtures were

withdrawn by means of a pipette. For SA and SC mixtures the top phase was taken out by

means of a pipette and the gelified bottom phase was removed with a spatula. The gelified

CG-PS$_{rp}$ was taken out before the liquid protein rich-phase. The SG mixture probably had

very low interfacial tension as it was easily remixed. Thus, it was first withdrawn half of

the PS$_{rp}$, then the whole PR$_{rp}$ and finally the rest of the PS$_{rp}$ using pipettes.

Table 5. Volume ratio obtained by measuring the phase volume (VR$_{exp}$) and calculated
from protein concentration in each phase (VR$_{calc}$).

	CA	CC	CG	SA2	SC2	SG
VR$_{exp}$ [%]	81.70±1.20	70.64±0.41	17.42±3.53	91.98±0.32	86.93±1.05	76.90±0.51
VR$_{calc}$ [%]	79.93	68.17	5.37	91.59	86.10	84.93

The systems of CA, CC, SA$_2$ and SC$_2$ exhibited differences between VR$_{calc}$ and

VR$_{exp}$ lower than 2.5%. The differences between VR$_{calc}$ and VR$_{exp}$ for the systems

containing gellan were 8% (SG) and 12% (CG). Such differences would be related to the

difficult to withdraw the phases, which affected the determination of biopolymers

concentration. In addition, the volume measurement of the CG system was not easy

because the phase boundary showed some flat parts and others with an inclination (Figure

2c). However, in spite of the experimental difficulties, it can be considered that the results

showed a reasonable agreement. In this way, it can be concluded that the visual method for

volume determination was very good and that in some cases it could be extended to gelified

systems. It is also interesting to note that the range of VR as between 70-90%, except for

CG mixture. This revealed that the volumes of the polysaccharide phase were usually much

higher than the volume of PR$_{rp}$ due to the higher hydrophilic character of the

polysaccharides as compared with proteins. In the CG system this did not happen because of the gelling ability of gellan at high concentration, such that polymer-polymer interactions would prevail over the polymer-water one.

3.2. Chemical analysis, rheology and microscopy of MS systems and their rich-phases

In the following sections it will be discussed the rheological and phase behaviour of MS systems. The degree of separation achieved by centrifugation was evaluated by examining samples of the top and bottom phase under a confocal microscope and by chemical characterization of protein and polysaccharide content.

3.2.1. SPI - Na-alginate mixtures

Figure 3 shows the tie-line of the SA_2 system obtained by chemical analyses of MS, PR_{rp} and PS_{rp} and the corresponding micrographs made with CSLM. The protein and polysaccharide concentrations were respectively 3.0% and 2.5% for MS, 1.2% and 2.6% for PS_{rp} and 22.5% and 1.0% for PR_{rp}, with a mass balance relative error smaller than 4%. The micrographs show white areas that contain fluorescent protein stained by Rhodamine B, while the dark areas indicate the absence of protein. The micrograph of MS sample showed a polysaccharide continuous phase containing several irregular shaped protein aggregates with sizes lower than 10 μm. Fluorescence was regularly distributed for PR_{rp} sample indicating that the protein was homogenously distributed in the sample. Black regions devoid of protein can be pointing out to the presence of concentrated polysaccharide (the maximum region size of 6 μm). The PS_{rp} contained spherical protein aggregates with diameters up to 4 μm (Figure 3). The equilibrium between the phases is achieved when both phases are free of inclusions even when observed at high

184

magnification, such as 100x (Simeone et al., 2004). Thus, the previous structural observations of PR_{rp} and PS_{rp} indicated that complete separation was not reached with the centrifugation conditions used here.
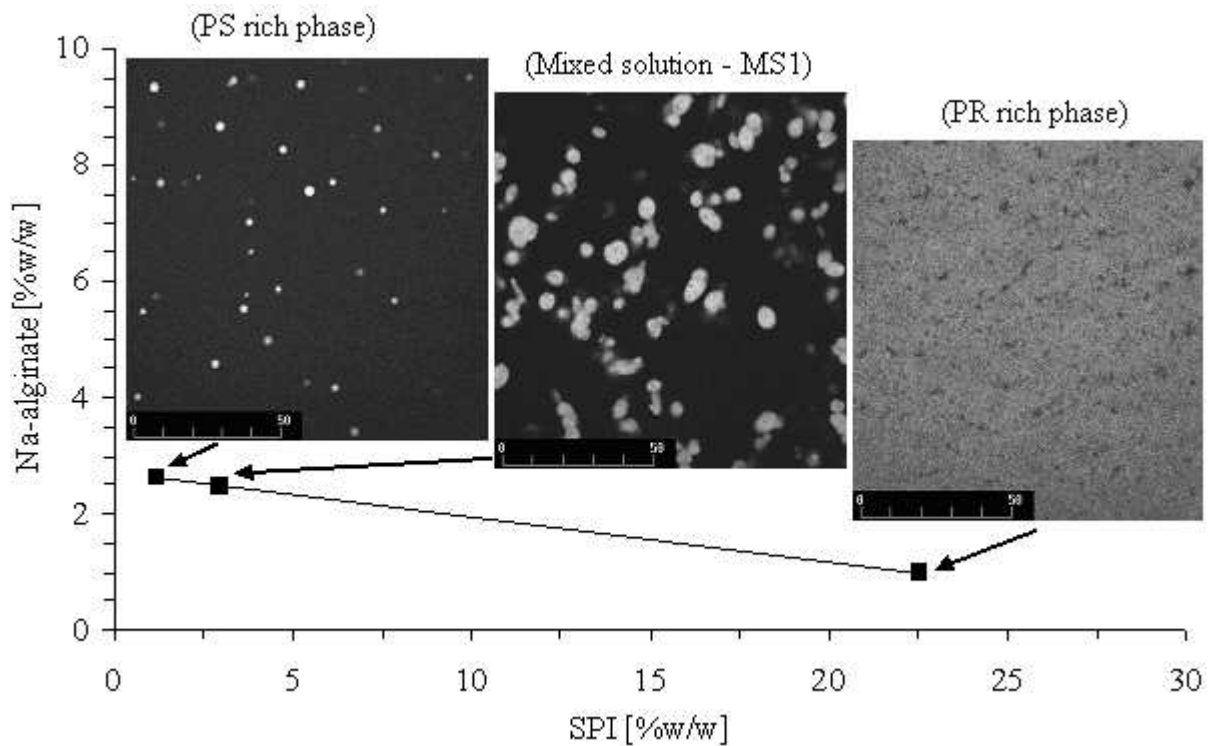

Figure 3. Confocal micrographs at 25 °C of the mixed solution, protein and polysaccharide rich phases of SA_2 (SPI - Na-alginate) system. Squares are experimentally determined biopolymer concentrations of MS, PR_{rp} and PS_{rp}. The light regions in the micrographs indicate protein area, scale bar = 50μm.

Dynamic (Figure 4a) and steady state (Figure 4b) rheological measurements were performed for the SA_2 system. The mixed solution and the PS_{rp} exhibited similar rheological properties at both small and high deformation measurements. The mechanical spectrum of these samples showed diluted solution behaviour with loss modulus (G'') higher than storage modulus (G') over the entire frequency range, but approaching each other at higher frequencies without moduli crossover (Steffe, 1996). Flow curves for these samples (Figure 4b) exhibited Newtonian behaviour up to 10 s⁻¹, with a constant apparent

185

viscosity (η) value of 0.8 Pa.s. In addition, a slightly shear-thinning behaviour was developed at higher shear rate values. The protein rich phase behaved as gel-like materials (Figure 4a) with the G' values higher than G'' values, although at low frequencies G' was only two times greater than G''. This protein phase was shear-thinning and it was not possible to observe the zero shear viscosity value in the studied shear rate range (Figure 4b). In addition, it was observed thixotropy in such systems (results not shown) probably due to the rupture or rearrangements of the gel network after shear.
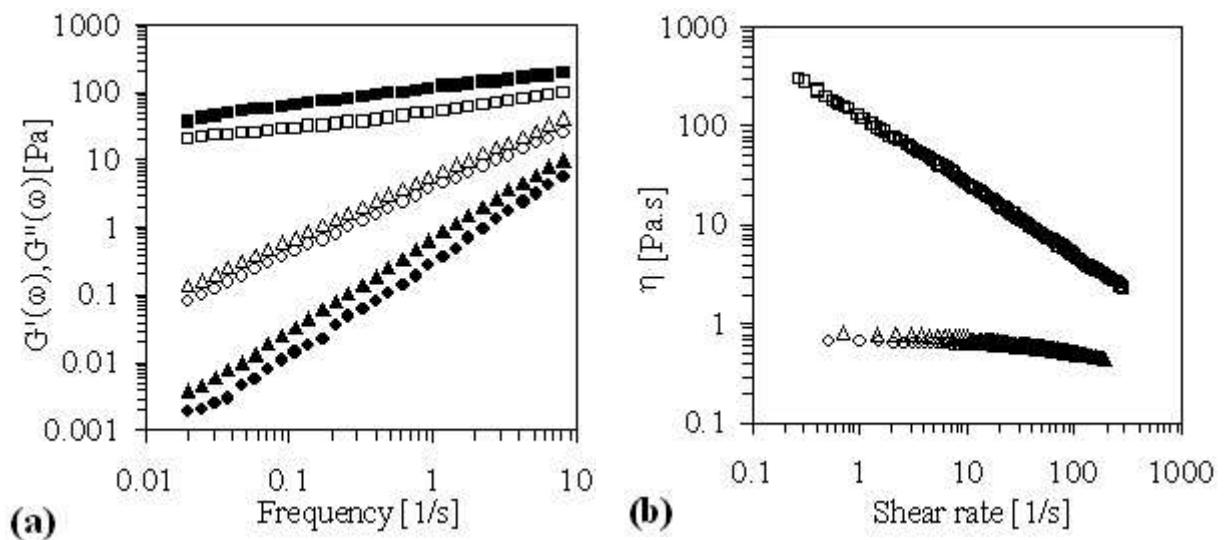

Figure 4. Frequency sweep (a) and flow curve (b) for SA_2 system (SPI 3% – Na-alginate 2.5%) mixed solution (▲) and the rich protein (■) and polysaccharide (●) phases after centrifugation at 60000g for 1h. Closed symbols correspond to G'(ω) and open symbols correspond to G''(ω) or η.

A second SA mixture (SA_1) containing lower amount of polysaccharide (1.5%) was examined through CLSM to check the effect of polysaccharide/protein ratio on the degree of phase separation. In addition, the rheological behaviour of this system before and after centrifugation was examined at small and high deformations. The structure of PR_{rp} from SA_1 (Figure 5) resembled to the micrograph observed for PR_{rp} from SA_2 (Figure 3).

However, less dark regions could be detected in the protein rich phase of SA$_1$, indicating a better phase separation. The reduction of the polysaccharide content in MS did not have a strong effect on the dynamic rheological behaviour (Figure 6a). The G' and G'' curves for protein and the polysaccharide rich phases were shifted to lower values.
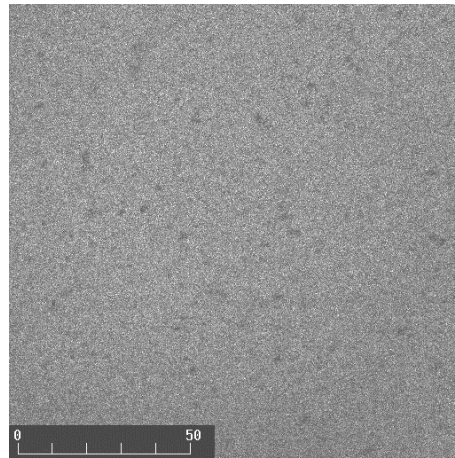

Figure 5. CLSM micrograph of PR$_{rp}$ obtained from SA$_1$ mixture
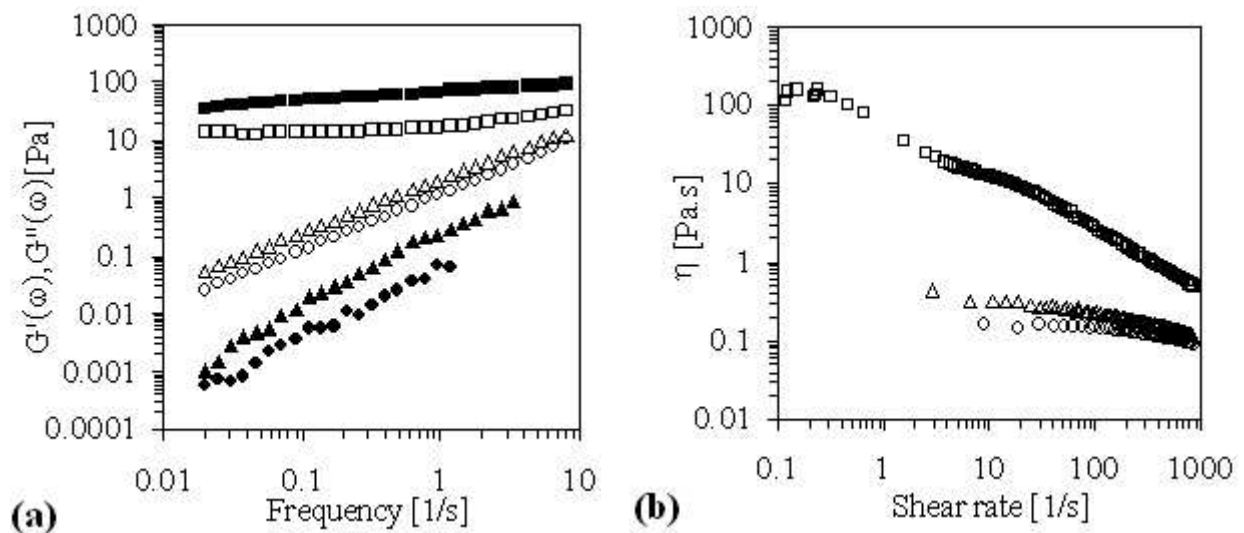

Figure 6. Frequency sweep (a) and flow curves (b) for SA$_1$ system (SPI 3% – Na-alginate 1.5%), mixed solution (▲), protein (■) and polysaccharide (●) rich-phases after centrifugation at 60000g for 1h. Closed symbols correspond to G'(ω) and open symbols correspond to G''(ω) or η.

The zero shear viscosity values decreased by a factor of 2 for MS and ~4 for PS_{rp} (Figure 6b). The lower viscosity of the MS probably assisted a higher degree of phase separation during centrifugation as noticed in Figure 5. The PR_{rp}–SA_1 showed a different behaviour, being observed two plateau regions. The first one at low shear rate corresponded to the zero shear viscosity, whereas the second one could be attributed to slippery effects (Pal, 2000) due to syneresis observed visually. In addition, the viscosity of PR_{rp} of SA_1 was greater than that of SA_2 independent of the shear rate. This could be attributed to a more interconnected protein network, with less polysaccharide inclusions and is another indication of the greater degree of phase separation achieved in SA_1 as compared to SA_2.

3.2.2. SPI - carrageenan mixtures

The biopolymer concentrations of all SC_1 and SC_2 systems were measured and plotted (Figure 7). The content of protein (C_{pr}) and polysaccharide (C_{ps}) of the SC_2 system was respectively 3.1% and 2.2% in the mixed solution, 16.2% and 1.7% in the protein rich phase and 1.0% and 2.4% in the polysaccharide rich phase, with the mass balances error lower than 6%. The C_{pr} and C_{ps} of the SC_1-system were, respectively, 3.0% and 1.4% in MS, 14.3% and 1.0% in the protein rich phase and 1.3% and 1.4% in the polysaccharide rich phase, with the mass balances error lower than 4.5%.The position of the tie-lines indicated that the phase separation of the SC_2-system was not complete, since the PR_{rp} of SC_2 and SC_1 could never be onto the same binodal. Tolstoguzov (1995) described that the tie-lines for a ternary protein-polysaccharide-water system could be asymmetric. In addition, the tie-lines could converge into a single point for gelling systems.
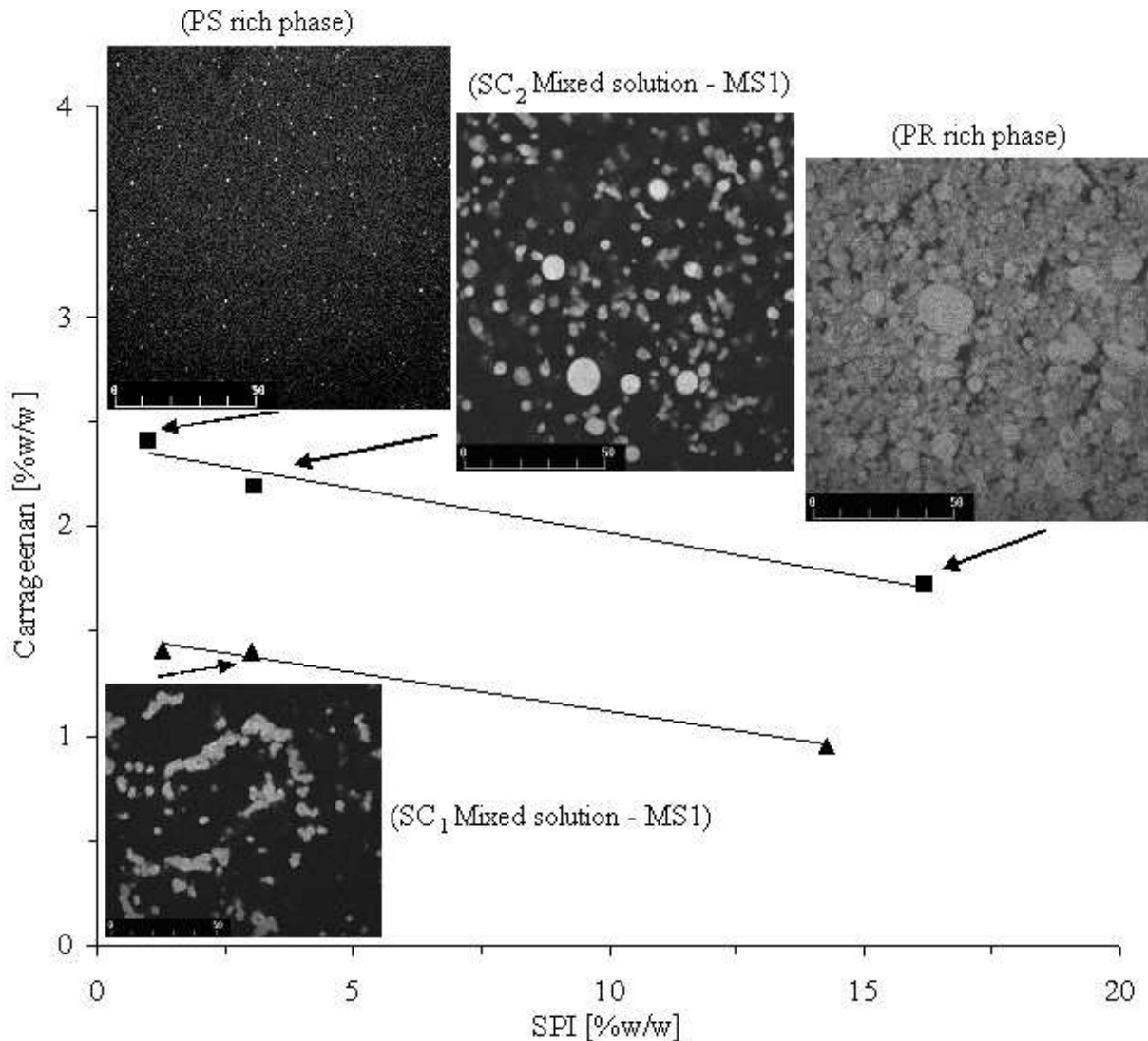
Figure 7. Confocal micrographs at 25 ^{o}C of the mixed solution, protein- and polysaccharide-rich phases of SC$_1$ and SC$_2$ (SPI – Carrageenan) systems. Closed symbols are experimentally determined biopolymer concentrations of MS, PR$_{rp}$ and PS$_{rp}$. The light regions in the micrographs indicate protein area, scale bar = 50µm.

The mixed solution of SC$_2$ showed both irregular shaped (< 10 µm) and spherical (diameter < 15 µm) aggregates of protein. In contrast, mixed solution of SC$_1$ did not contain spherical aggregates but only irregular shaped ones, which formed bigger and elongated secondary structures with up to 30 µm length. The lower viscosity of SC$_1$ associated with the lower amount of polysaccharide in the mixed solution (see Figures 8

189

and 9 below) probably let to the formation of protein assemblies. In addition, Simeone et al. (2004) showed that the interfacial tension between the coexisting phases has a direct linear dependence with the length of the tie-line, which could explain the formation of spherical protein inclusion in the initial mixture of SC_2. The micrograph of PS_{rp} of SC_2 showed inclusions of protein with a size up to 2 μm, whereas the micrograph of PS_{rp} of SC_1 was black and devoid of protein. That was another evidence for the lower level of phase separation for SC_2. A gelified particulated structure could be observed for PR_{rp} (Figures 2 and 7) in contrast with the fine stranded gel observed for the PR_{rp} of SA_2 (Figures 2 and 3).

In Figure 8a the elastic and loss moduli of the SC_1 system are shown as a function of frequency. The mechanical spectrum of the protein rich phase showed a gel-like structure with $G'(\omega)$ greater than $G''(\omega)$ and slightly dependent on frequency. The mixed solution and the polysaccharide rich phase exhibited diluted solution behaviour with an estimated cross-over point (at 1000 s^{-1}) far away from the highest examined frequency. The flow behaviour of the SC_1 system shown in Figure 8b was similar to the one of the SA_1 system (Figure 6). The protein rich phase showed shear-thinning behaviour (Figure 8b) and exhibited slippage at low shear rates. The mixed solution and the polysaccharide rich phase showed both zero shear viscosity of 0.2 Pa.s.
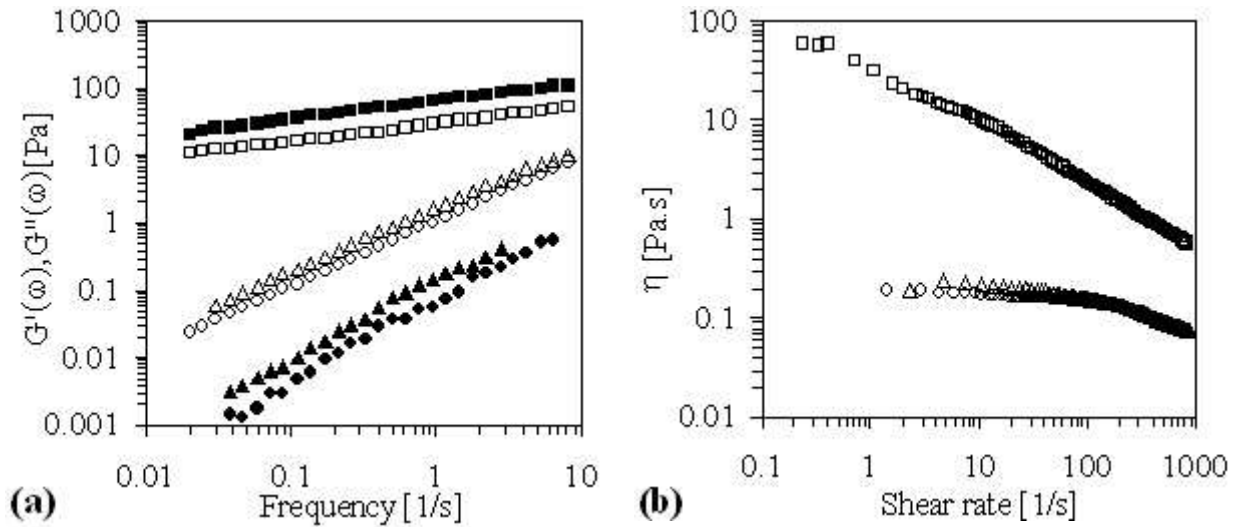
Figure 8. Frequency sweeps (a) and flow curves (b) for SC_1-system (SPI 3% – carrageenan 1.4%) mixture (▲), protein (■) and polysaccharide (●) rich-phases after centrifugation at 60000g for 1h. Closed symbols correspond to G'(ω) and open symbols correspond to G"(ω) or η.

The oscillatory and steady state rheological behaviour of the SC_2 system are shown in Figure 9. The protein rich phase of SC_2 was highly shear-thinning (Figure 9b). In contrast to SC_1, the zero shear viscosity of the mixed solution was greater than the one of PS_{rp}, both exhibiting a first Newtonian plateau up to around 10 s⁻¹. In addition, the SC_2 initial mixture showed a Newtonian viscosity 10-fold greater than that found for SC_1 mixture. It is interesting to note that the flow characteristics of PR_{rp} of SPI-polysaccharide systems containing the same amount of biopolymers (SA_1 and SC_1 / SA_2 and SC_2) were very similar.
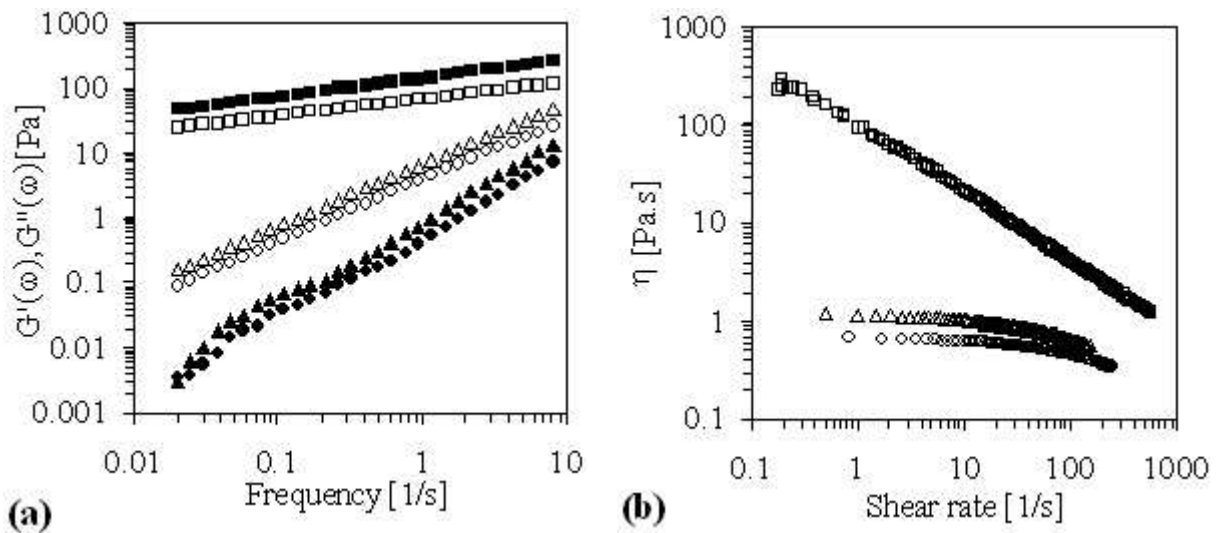
Figure 9. Frequency sweeps (a) and flow curves (b) for SC$_2$-system (SPI 3.1% – carrageenan 2.2%) mixture (▲), protein (■) and polysaccharide (●) rich-phases after centrifuging at 60000g for 1h. Closed symbols correspond to G'(ω) and open symbols correspond to G''(ω) or η.

The protein rich phase exhibited weak gel-like properties. The mixed solution and the polysaccharide rich phase exhibited similar mechanical spectrum. A "shoulder" in the G'(ω) curves was observed indicating an increase in the elasticity at low frequencies. Capron et al. (2001) and Simeone et al. (2002) also observed a "shoulder" in the G'(ω) curve, which was associated to a terminal relaxation time of the blend of viscoelastic liquids and attributed to the relaxation of shape of the droplets. The increase of the elasticity at lower frequencies was more pronounced for MS than for PS$_{rp}$. In addition, this phenomenon was not observed in SC$_1$ system. For the latter system, there were not any spherical protein aggregates for MS (Figure 10) and any protein inclusions could be observed in PS$_{rp}$ micrograph. The above results indicated that the "shoulder" phenomenon was related to the morphological characteristics and to the degree of interfacial tension of the system, while its intensity was also influenced by the volume fraction.

3.2.3. SPI - gellan mixture

The biopolymer concentrations of the SG system were measured, plotted and put together with the corresponding micrographs (Figure 10). The protein and the polysaccharide concentrations of the SG system were respectively 4.8% and 0.39% for the mixed solution, 7.6% and 0.25% for the protein rich phase and 4.3% and 0.48% for the polysaccharide rich phase, with mass balances error lower than 10%.
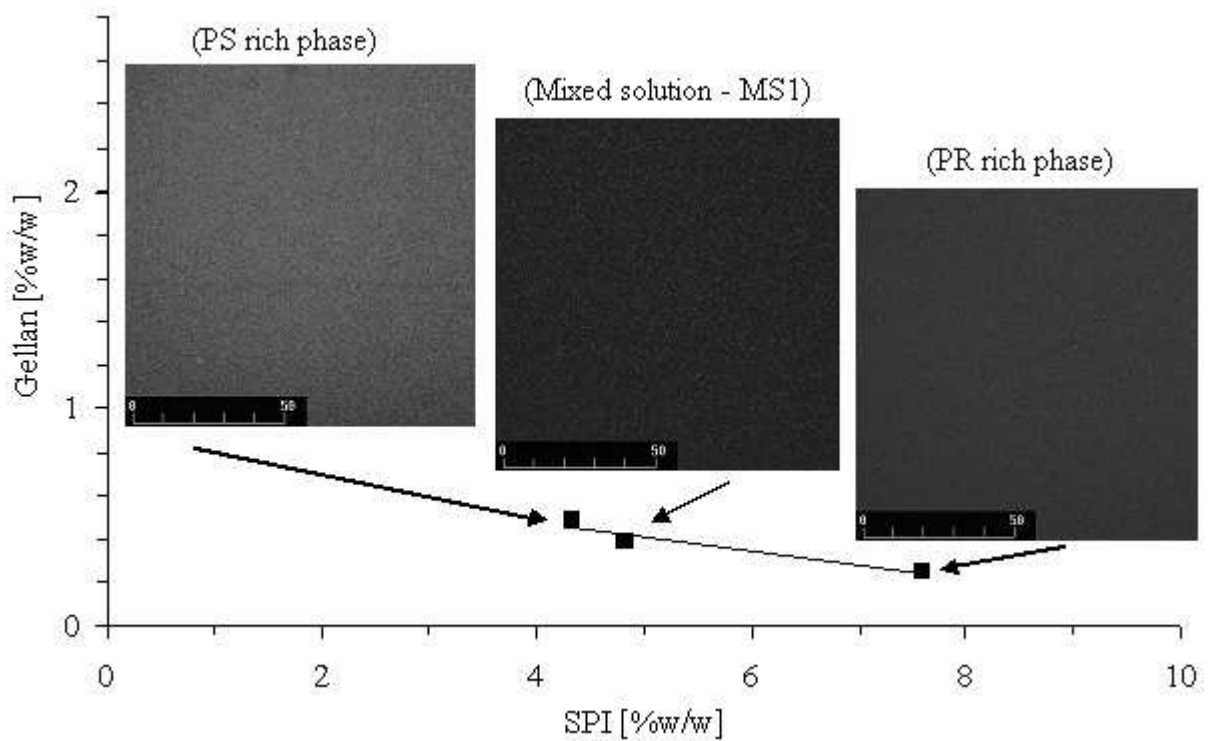
Figure 10. Confocal micrographs at 25 °C of the mixed solution, protein and polysaccharide rich phases of SG (SPI - Gellan) system. Squares are experimentally determined biopolymer concentration of MS, PR$_{rp}$ and PS$_{rp}$. The light regions in the micrographs indicate protein area, scale bar = 50μm.

In the micrograph of MS and PR$_{rp}$ the fluorescence was regularly distributed indicating that the SPI particles were homogenously distributed in all the samples. However, the PS$_{rp}$ micrograph was similar to the above ones, which could be due to some

_____

protein dissolved in the polysaccharide rich phase. It was not possible to determine the degree of phase separation from the micrographs of the rich phases, since it was not observed any inclusions and the polysaccharide molecule was not stained. The homogeneity of all micrographs could be attributed to the low interfacial tension between the coexisting phases. In addition those coexisting phases were unstable, which means that they could easily be remixed to form a homogeneous solution.

The mechanical spectra (Figure 11a) of SG systems indicated that G'' was greater than the corresponding G' over all frequency range for all samples. The protein rich phase exhibited the lowest G' and G'' values. The PS_{rp} and MS samples showed a semi-diluted solution behaviour as the G' and G'' cross-over point was estimated to be at a frequency near 10 s^{-1}.
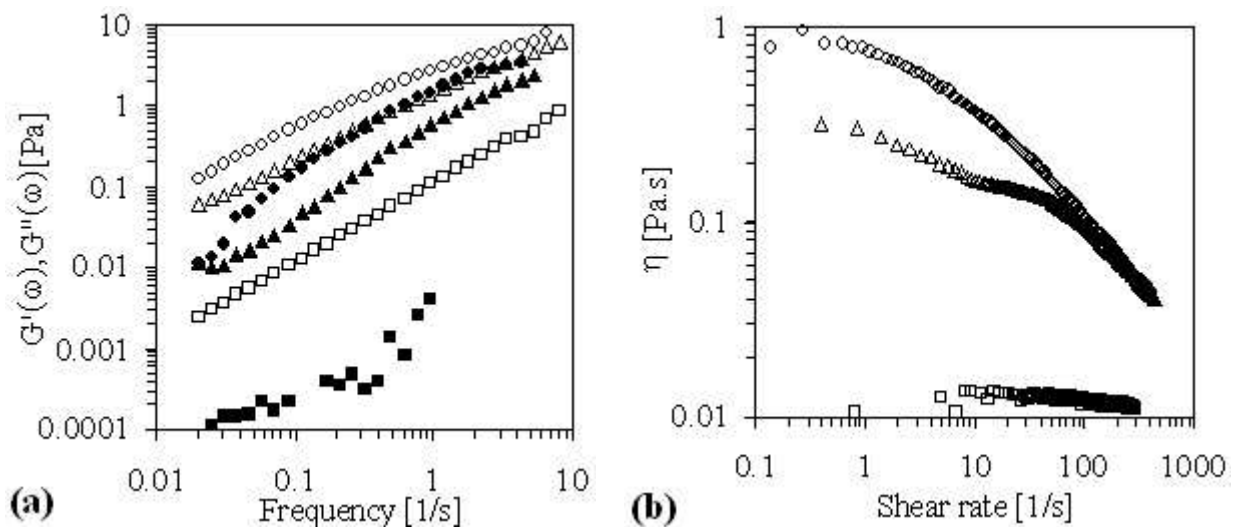

(a)   **(b)**

Figure 11. Frequency sweeps (a) and flow curves (b) for SG (SPI 4.8% - Gellan 0.4%) mixture (▲), protein (■) and polysaccharide (●) rich-phases after centrifugation at 60000g for 1h. Closed symbols correspond to G'(ω) and open symbols correspond to G''(ω) or η.

The flow curves of the SG system are shown in Figure 11b. The polysaccharide rich phase exhibited shear thinning behaviour with a first Newtonian plateau at viscosity of 0.8 Pa.s until a shear rate close to 1 s⁻¹. The slippage phenomenon was observed for the mixed solution, making not possible to determine the first Newtonian plateau. The viscosity values of this flow curve were significantly lower than that of the polysaccharide rich phase up to 50 s⁻¹, but the curves fell on a single curve from this value. The protein rich phase exhibited Newtonian flow behaviour with a viscosity of 0.01 Pa.s.

3.2.4. Na-caseinate - gellan mixture

Figure 12 shows the tie-line and the corresponding micrographs of the CG system. The tie-line data were obtained by measuring the protein and polysaccharide concentrations of the mixed solution (C_{PR} = 5.0 %, C_{PS} = 0.37 %), protein rich phase (C_{PR} = 5.2 %, C_{PS} = 0.18 %) and polysaccharide rich phase (C_{PR} = 3.0 %, C_{PS} = 1.6 %). The mass balances for the protein showed an error of 6%, while the polysaccharide exhibited an error of 20 %. These values confirm the above discussion about the difficulties associated with the phase collection for such system.

The CLSM micrograph of the mixed solution exhibited regularly distributed fluorescence indicating that the proteins and polysaccharide were completely homogenized (Figure 12). The micrograph of the protein rich phase was similar to the one of the mixed solution, and it was not possible to optically determine the degree of phase separation. The micrograph of the polysaccharide rich phase exhibited a black background with spherical and ellipsoidal white aggregates of proteins with diameters up to 10 µm. The shape of those inclusions could be attributed to the high interfacial tension between the gelified polysaccharide phase and the liquid protein one. In addition, when dealing with a gelling

_____

polysaccharide, the structure of the inclusions is mainly determined by the gelling process rate.
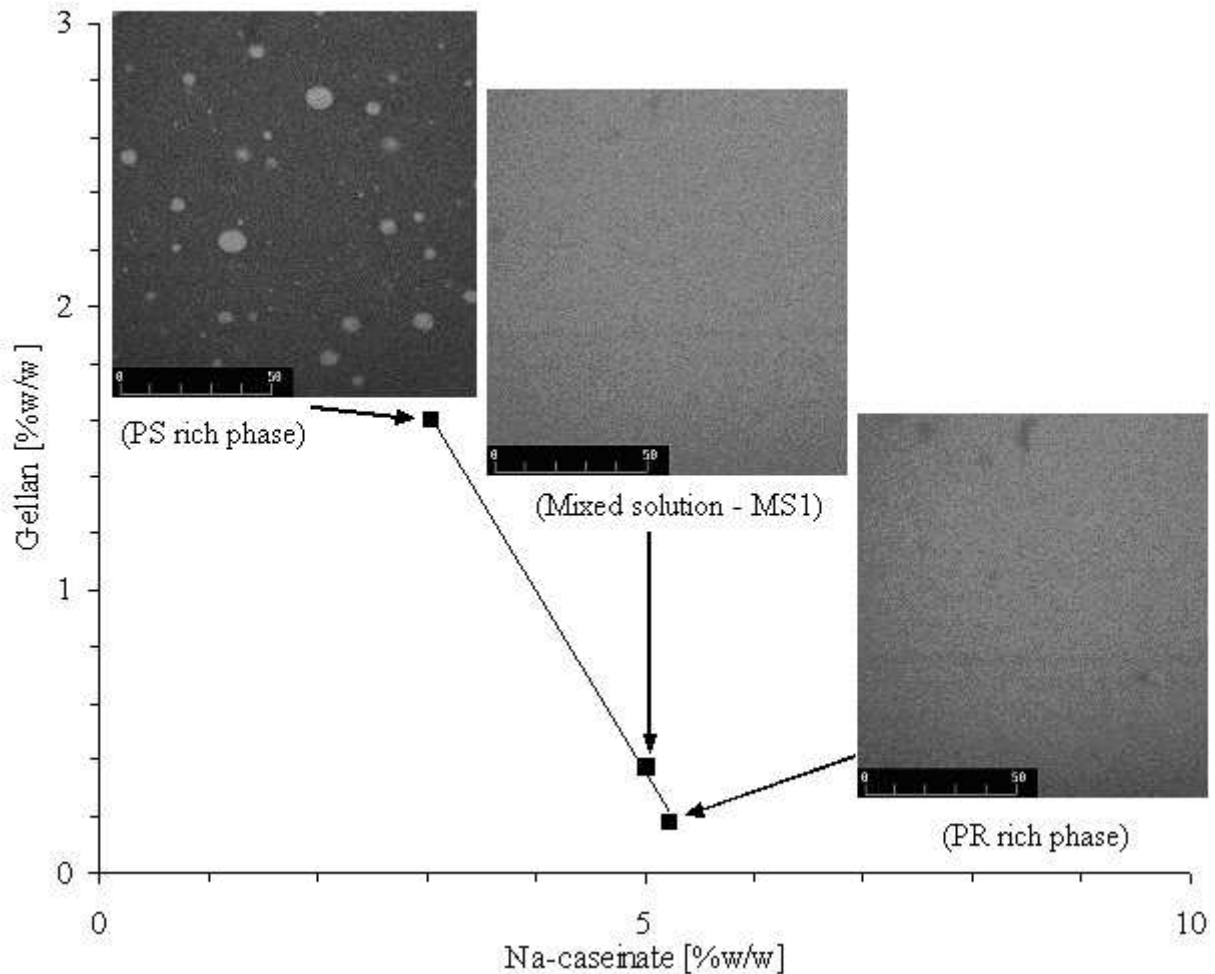
Figure 12. Confocal micrographs at 25 $^{\circ}$C of the mixed solution, protein and polysaccharide rich phases of CG (Na-caseinte - Gellan) system. Squares are experimentally determined biopolymer concentration of MS, PR_{rp} and PS_{rp}. The light regions in the micrographs indicate protein area, scale bar = 50μm.

Figure 13a shows the mechanical spectra of the CG system, which exhibited three different types of rheological behaviour as described by Steffe (1996). The mixed solution presented properties of a concentrated solution with an estimated cross-over point between storage (G') and loss modulus G" at around 3 s^{-1}. The liquid protein rich phase showed

properties of a diluted solution, since G' values were lower than G" over the entire frequency range. The G' values of the PS_{rp} was greater than G'' indicating the gel-like behaviour.
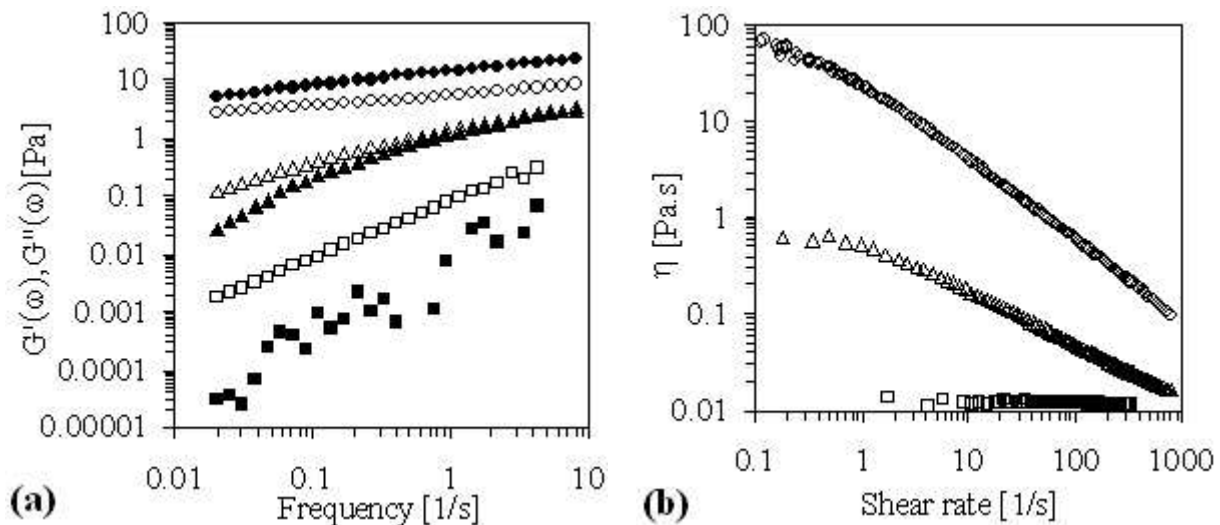
Figure 13. Frequency sweeps (a) and flow curves (b) for CG (Na-caseinate 5% – gellan 0.4%) mixture (▲), protein (■) and polysaccharide (●) rich-phases after centrifugation at 60000g for 1h. Closed symbols correspond to G'(ω) and open symbols correspond to G"(ω) or η.

The flow curves of the CG system (Figure 13b) confirmed the different characteristics of MS, PR_{rp} and PS_{rp}. The PS_{rp} system showed shear thinning character from the very low shear rate. The mixed solution could also be characterized as shear thinning fluid but with a first Newtonian plateau up to 0.5 s^{-1} and a Newtonian viscosity of 0.6 Pa.s. At high shear rates (>100 s^{-1}) it could be observed a viscosity tendency to attain the second Newtonian plateau. The protein rich phase was Newtonian, being the viscosity value equal to 0.012 s^{-1}.

3.2.5. Na-caseinate – Na-alginate mixture

197

The measured biopolymer concentrations of the CA system (Figure 14) were $C_{PR} = 2.9\%$ and $C_{PS} = 2.3\%$ in the mixed solution, $C_{PR} = 14.7\%$ and $C_{PS} = 0.4\%$ in the protein rich phase and $C_{PR} = 0.3\%$ and $C_{PS} = 2.7\%$ in the polysaccharide rich phase, with mass balances error lower than 5%. The tie-line presented in Figure 14 is in quantitative agreement with previous results available in the literature (Simeone et al., 2004, Antonov et al., 2004). However, the work done by Capron et al. (2001) showed a greater protein concentration in PS_{rp} than the present work. Studies about phase separation of CA mixture are done with different centrifugation conditions, varying from 15000 x g / 3 h (Capron et al., 2001) up to 100000 x g / 15 h (Simeone et al., 2004). In the present work, it was used the mild condition of 60000 x g / 1h, as that used by Antonov et al. (2004). Thus, the differences found in the phase composition could be attributed to incomplete phase separation, since a centrifugation at 15000 x g / 3 h is equivalent of 60000 g / 30 min that is half of the time used in the present work. This is supported by the fact that Simeone et al. (2004) observed an incomplete phase separation for a high viscous CA mixture even at 100000 x g / 15h.

The micrograph of the mixed solution (Figure 14) showed spherical protein aggregates of different sizes with diameters up to 20 μm. The protein in the PR_{rp} micrograph was regularly distributed without black areas. In the polysaccharide rich phase no aggregated protein could be noticed as the micrograph showed a continuous black colour without any white region. These micrographs indicated that complete phase separation was reached during the process of centrifugation. High interfacial forces were assumed to cause the spherical shape of the protein aggregates in the mixed solution, since

the obtained tie-line was localized far from the critical point (Capron et al., 2001, Antonov et al., 2004).
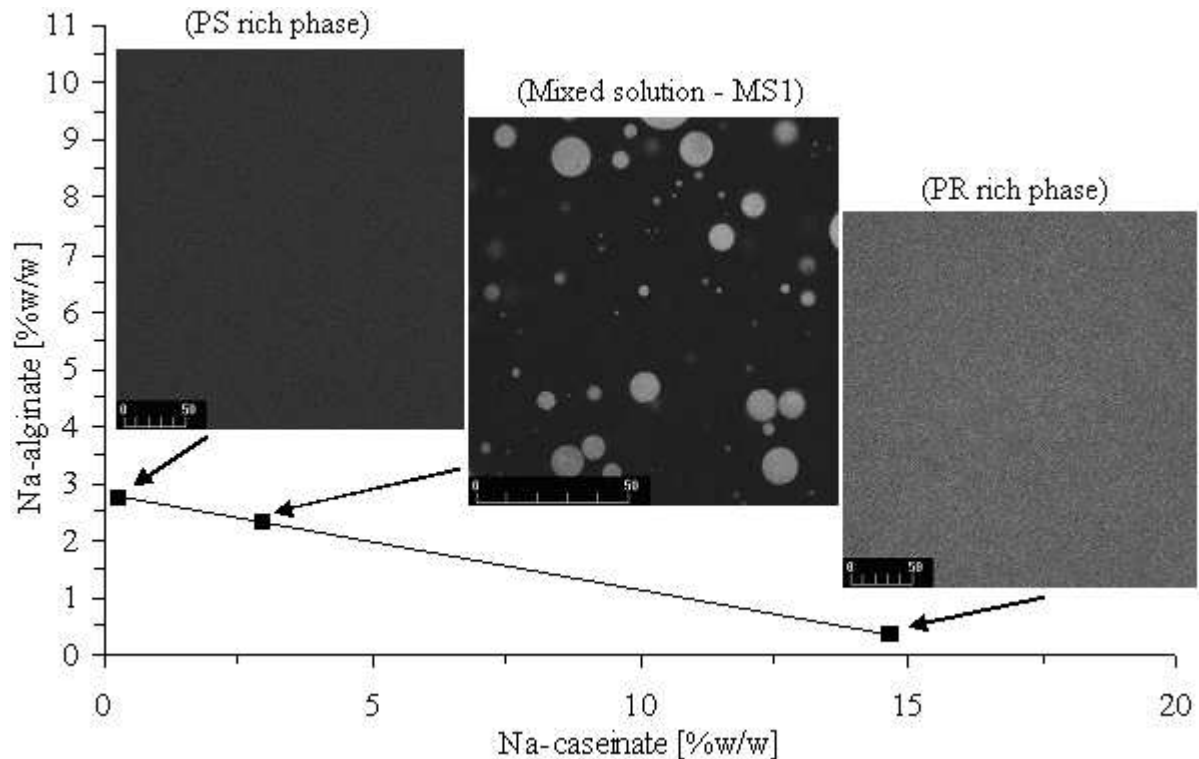
Figure 14. Confocal micrographs at 25°C of the mixed solution, protein and polysaccharide rich phases of CA (Na-caseinte – Na-alginate) system. Squares are experimentally determined biopolymer concentration of MS, PR_{rp} and PS_{rp}. The light regions in the micrographs indicate protein area, scale bar = 50μm.

The mixed solution, the protein rich phase and the polysaccharide rich phase of the CA system were liquid and the storage moduli were smaller than the loss moduli (Figure 15). The mixed solution and the polysaccharide rich-phase exhibited diluted solution behaviour with similar G"(ω) values. The storage modulus of the mixed solution formed a slight "shoulder" exhibiting increased G' values in the frequency range of 0.05-0.26 s^{-1}. Capron et al. (2001) and Simeone et. al. (2002) also observed this kind of shoulder for CA

mixtures. In both cases the Palierne equation (Palierne, 1990) was well fitted to the data. This phenomenon indicated the existence of dispersed particles in a continuous phase and confirmed the observations done for MS micrograph (Figure 14). The protein rich phase exhibited the greatest G' and G'' values of the CA system, with a estimated cross-over point close to 10 s^{-1}, indicating the properties of a semi-diluted solution.

The flow curves for all the samples of the CA system (Figure 15b) exhibited a Newtonian plateau at low shear rates, shear thinning behaviour at higher deformations and no slippage was noticed. The flow curve of the mixed solution ($\eta_0 = 2$ Pa.s) was closed to that of the polysaccharide rich phase ($\eta_0 = 1$ Pa.s) and both Newtonian plateau ended at a shear rate of about 10 s^{-1}. The protein rich phase ($\eta_0 = 19$ Pa.s) exhibited constant viscosity values until a shear rate of 1 s^{-1}, being all viscosities values about 10-fold greater than those obtained for MS.
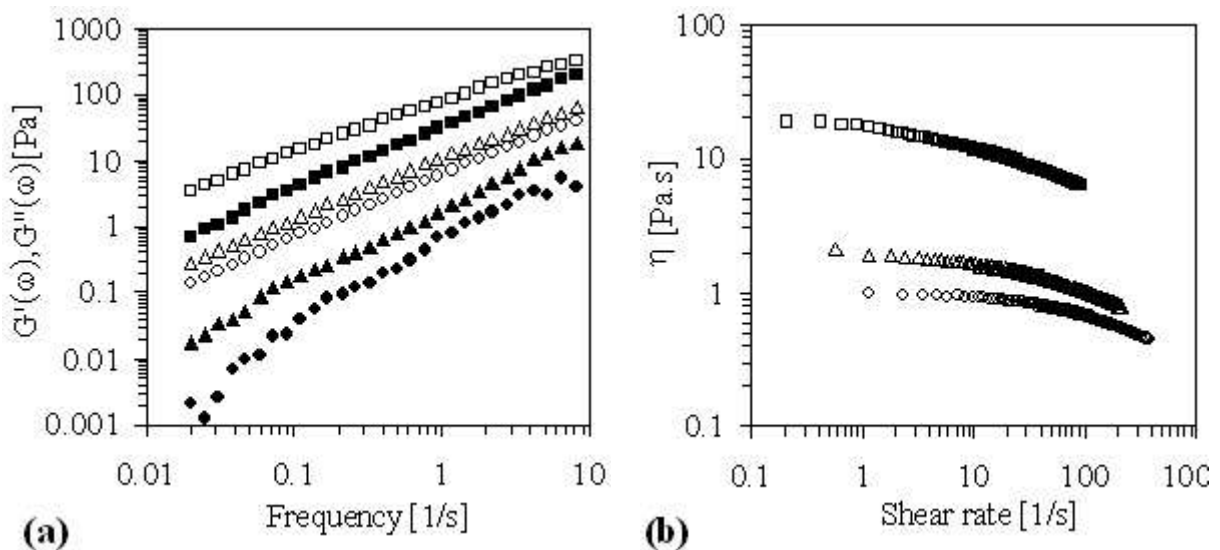
Figure 15. Frequency sweeps (a) and flow curves (b) for CA (Na-caseinate 2.9 % – Na-alginate 2.3 %) mixture (▲), protein (■) and polysaccharide (●) rich-phases after centrifugation at 60000g for 1h. Closed symbols correspond to G'(ω) and open symbols correspond to G''(ω) or η.

3.2.6. Na-caseinate – carrageenan mixture

Figure 16 shows the experimental values of biopolymer concentrations in the mixed solution (C_{PR} = 2.9%, C_{PS} = 2.0%), protein rich phase (C_{PR} = 8.4%, C_{PS} = 0.8%) and polysaccharide rich phase (C_{PR} = 0.3%, C_{PS} = 2.5%) together with their corresponding micrographs, with mass balances error lower than 5%.

Figure 16. Confocal micrographs at 25°C of the mixed solution, protein and polysaccharide rich phases of CC (Na-caseinate – κ-carrageenan) system. Squares are experimentally determined biopolymer concentrations of MS, PR_{rp} and PS_{rp}. The light regions in the micrographs indicate protein area, scale bar = 50μm.

The micrograph of the protein rich phase showed a background with regularly distributed fluorescence indicating prevalent protein presence. Round and irregular shaped regions devoid of protein, with a wide range of size up to 35 μm, indicated inclusions of polysaccharide. The micrograph of the polysaccharide rich phase exhibited sprinkled aggregates of protein smaller than 1.5 μm. A phase inversion was noticed between the pr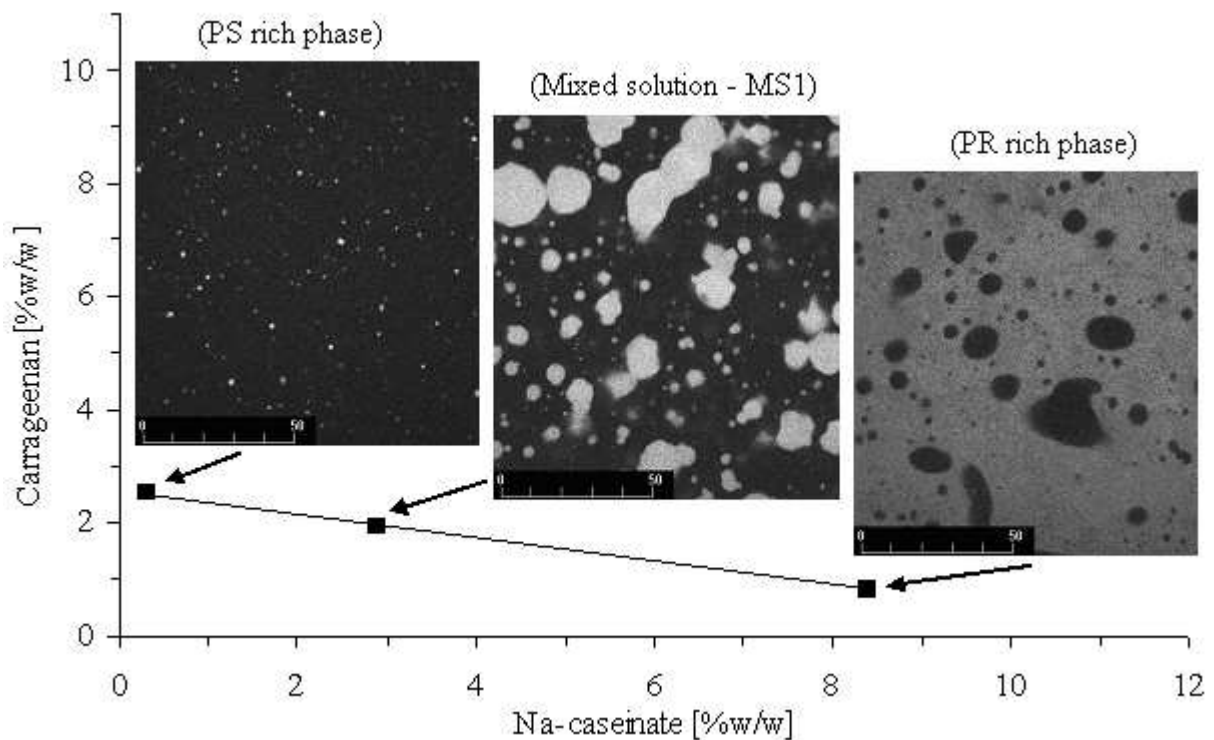otein rich phase and the polysaccharide rich phase. In a phase diagram if one moves along the tie-line, the composition of the two phases stay the same but their relative volumes change according to the relative length of the tie-line to the binodal (Norton and Frith, 2001). The mixed solution exhibited irregular shaped protein aggregates in a continuous polysaccharide rich phase, being the highest inclusion size up to 35 μm. This sample looked like an emulsion during the coalescence step as can be seen some regions with elongated structures made of attached droplets, which was interpreted as the initial step of the phase inversion.

The mechanical spectra of the CC system are shown in Figure 17. The protein rich phase behaved like a gel, being G' greater than G'' over the entire frequency range (Figure 17a). This result agrees with the observed CLSM micrographs (Figure 16) since the round shape of the polysaccharide inclusions could be attributed to the high interfacial tension between a liquid and a gel. The polysaccharide rich phase showed a semi-diluted solution behaviour with estimated cross-over points between G' and G'' near to the highest frequency evaluated, 10 s^{-1} (Figure 17b). The mixed solution exhibited a "shoulder" in the storage modulus curve at the low frequency region (Capron et al., 2001; Simeone et al., 2002, Palierne, 1990). In addition, a second overlapping "shoulder" could be observed increasing the frequency. From the MS micrograph (Figure 16) it can be supposed that the

second "shoulder" is somehow associated to the coalescence process of the dispersed phase.

At high shear rate region MS, PR$_{rp}$ and PS$_{rp}$ samples exhibited similar viscosity, whereas at low shear rate their flow behaviours were quite different (Figure 18). The viscosity value of PR$_{rp}$ was 44 Pa.s at low shear rate and decreased sharply as the shear rate was increased, which is typical of a shear-thinning behaviour. The MS showed similar zero shear viscosity but a shorter Newtonian plateau than PS$_{rp}$. However, the similar behaviour of MS and PS$_{rp}$ at large deformation was not observed in small deformation experiments (Figure 17). This suggests that the characteristics, such as shape and size, of the dispersed phase can not be quantified by large deformation rheological properties.
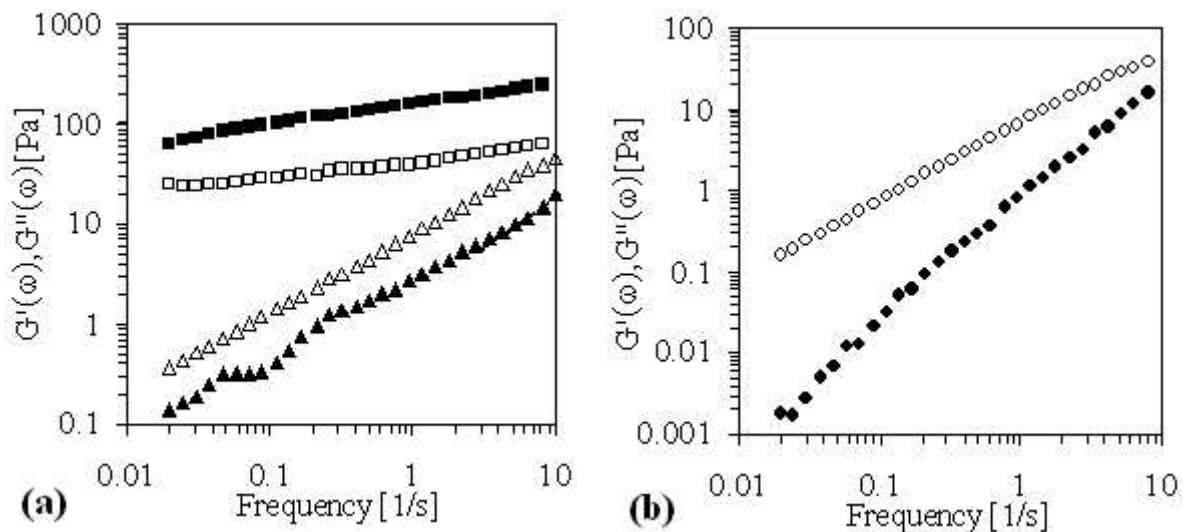
Figure 17. Frequency sweeps for CC (Na-caseinate – carrageenan). A) Mixture (▲) and the protein rich phase (■), B) polysaccharide rich phase (●). Closed symbols correspond to G'(ω) and open symbols correspond to G"(ω).
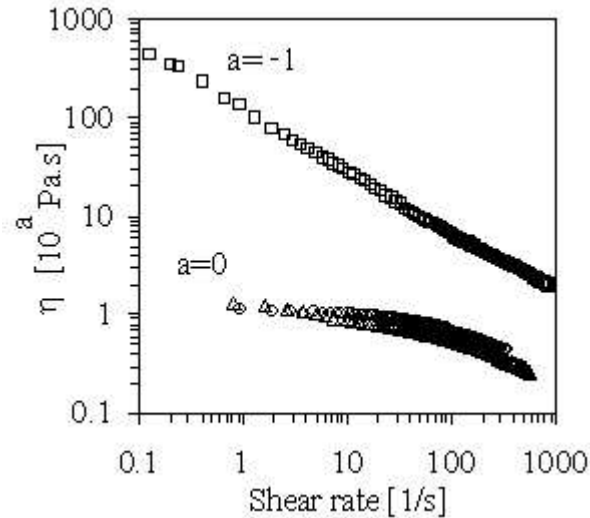
Figure 18. Flow curves for CC (Na-caseinate – carrageenan) mixture (Δ), protein (□) and polysaccharide (○) rich-phases after centrifugation at 60000g for 1h.

3.3. Comparison of the characteristics of MS, PR_{rp} and PS_{rp} systems

The tie-lines of the studied systems are shown in Figure 19. The systems containing SPI exhibited tie-lines with greater slope than the systems containing Na-caseinate independent on the investigated polysaccharide. The tie-line slope gives information about the hidrophilicity of the used biopolymers and the solvent quality. A decrease of the tie-line declination indicates an increase of both the polysaccharide hydrophilicity and the protein hidrophobicity. Thus, the results shown in Figure 19 indicated that SPI was more hydrophobic than Na-caseinate. Grinberg and Tolstoguzov (1997) observed that the soybean globulin was more hydrophobic than casein from the phase diagram asymmetry. The higher hydrophobicity of SPI enhanced the association of the protein molecules during the centrifugation of systems containing Na-alginate and κ-carrageenan, which resulted in the gelation of the PR_{rp}.
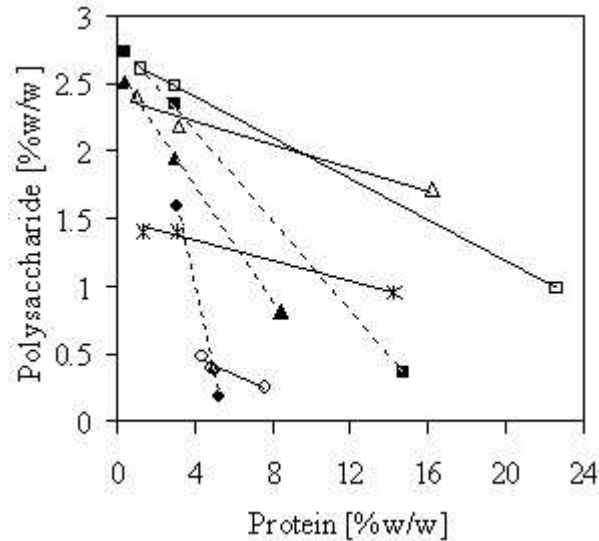
Figure 22. Phase composition for different protein-polysaccharide mixtures. CG (●), CA (■), CC (▲), SG (O), SA₂ (□), SC₂ (△),SC₁ (✳). Continuous line is the tie-line for SPI systems, dashed line is the tie-line for Na-caseinate systems.

The density difference for all kind of studied systems was calculated (Table 6) in order to have more information on the properties of phase behaviour. The density values were calculated from the mixing rule (Equation 7) and the density relations as a function of concentration for each biopolymer (Chapter 3 – 1ˢᵗ part).

$$\rho_{rp} = \rho_{PR} \cdot \phi + \rho_{PS} \cdot (1 - \phi) \tag{7}$$

where ρ (g/L) is the density ϕ is the protein mass fraction in the coexisting phase. The subscripts PR, PS, rp correspond, respectively, to protein, polysaccharide and rich phase.

The tie-line slope (Figure 19) was inversely proportional to the density differences ($\Delta\rho$) of the coexisting phases (Table 6) for MS of CA, CC, SA₂ and SC₂. Antonov et al. (2004) investigated the relation between $\Delta\rho$ and the interfacial tension for different tie-lines of CA systems. These authors observed a non-linear (power) dependency of interfacial tension on $\Delta\rho$ with a power equal to 3.1. Therefore, the magnitude order of the interfacial tension was estimated using a power of 3 predicted by the mean-field theory (Rowlinson

and Widon, 1984) and such values are shown in Table 6. The calculated Δρ as well as the estimated order of the interfacial tension for CA system were in agreement with other works (Simeone et al., 2004, Antonov et al., 2004, Capron et al., 2001, Guido et al., 2002), such that this method was extended to the other systems studied here.

The systems containing gellan exhibited very low Δρ (up to 8 g/L) indicating an extremely low interfacial tension of the order 10^{-10} and 10^{-8} N/m. These interfacial tension orders usually are found for systems located on the phase diagram closed to the critical point (Antonov et al., 2004). Such results explain the difficulties associated to the withdrawing of the phases and the homogeneous microstructure observed for PR_{rp} and MS of CG and for PR_{rp}, PS_{rp} and MS of SG. The systems containing κ-carrageenan and alginate showed higher interfacial tension than gellan samples with values orders up to 10^{-5} N/m. The meaning of these data could be better understood by analyzing the density difference values. Comparing Δρ values of those systems it was noticed three distinct groups, being Δρ of CC equal to 12.7 g/L, around 35 g/L for CA and SC, while the Δρ of SA_2 was 56.9 g/L. From all these systems, CA was the only one that formed two liquid rich-phases. In spite of that, the rich phases of CA exhibited a high Δρ value comparable to the values of SC, which formed a visual strong gel protein rich phase and a liquid polysaccharide rich phase explaining its high interfacial tension. These particular properties of the CA systems made the phase separation and withdrawing less difficult, which probably led to a great number of works to use such system as a model.

Table 6. Density difference and magnitude order of interfacial tension of coexisting phases of different protein-polysaccharide mixtures

System	Density difference (g/L)	Order of int. tension (N/m)
SG	1.7	10^{-10}
CG	7.4	10^{-8}
CC	12.7	10^{-7}
CA	31.9	10^{-6}
SC_1	36.2	10^{-6}
SC_2	36.8	10^{-6}
SA_2	56.9	10^{-5}

In the present study, the SC_1 system showed a complete phase separation as revealed from the absence of protein inclusions in the PS_{rp} micrograph (result not shown). However, the phase separation was not complete for SC_2 system, which could be partially attributed to the highest apparent viscosity of MS. Few works in the literature showed that the mixture viscosity affects the degree of phase separation (Clark, 2000, Simeone *et al.,* 2004, Cavallieri, 2003). Thus, the time and/or velocity of centrifugation should be adapted considering the mixture viscosity, in order to obtain a complete phase separation. Moreover, the centrifugation conditions shown in the literature are completely different for the same system (Section 3.2.5), indicating that there is not unanimity on that task.

Figure 20 shows the storage modulus (G') at 0.1 Hz, the zero shear viscosity for PR_{rp} of CA, SA_2, SC_2 and CC as well as the maximum area of each single inclusion (A_i) observed in micrographs. The G' and A_i values increased according to the following order of the systems $CA<SA_2<SC_2<CC$. The storage modulus reflects the elasticity of the sample and the higher values found for SA_2, SC_2 and CC were related to the formation of a protein network. When comparing the gelling systems, the differences of G' values could be

ascribed to the amount of polysaccharide present in the inclusions as observed by A_i values.

Thus, the storage modulus value of PR_{rp} can be used as an indicator of the degree of phase

contamination. Figure 20 shows that η_0 and G' values of the SA_2-PR_{rp} were similar to those

obtained for the SC_2-PR_{rp}. However, the area of the inclusions increased for SC_2 and the

polysaccharide mass fraction was 2.5 fold greater indicating that the repulsive forces in this

situation were smaller than for SA_2.
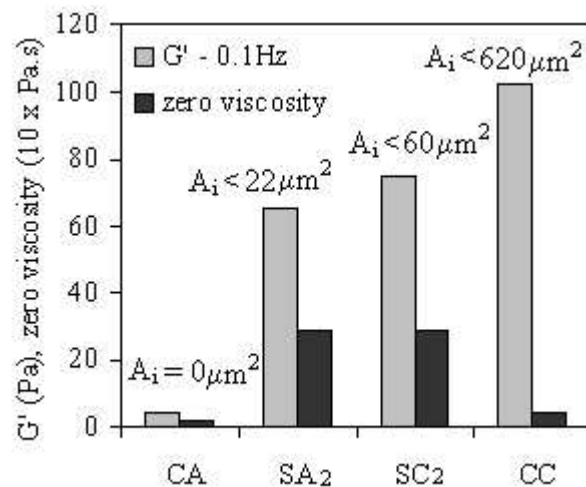
Figure 20. Rheological and morphological properties for the PR_{rp} of different systems.

The alginate was easily separated from Na-caseinate resulting in two liquid phases

exhibiting low G' at 0.1 Hz and any inclusions ($A_i = 0$ μm^2). This was in accordance with

the high non-gelling character of Na-caseinate in a pure system. In contrast, the PR_{rp} of CC

was a gel even with a lower protein concentration than the one found for CA-PR_{rp} (Figure

19). This fact indicated that the carrageenan contributed to the formation of the protein gel

(Figure 17) by protein-polysaccharide and polysaccharide-polysaccharide interactions

(Spagnuolo et al., 2005). The zero shear viscosity of PR_{rp} of CC was quite the same to the

one found for CA. This indicates that the protein network of CC-PR_{rp} was the most elastic

but exhibited a great capacity of rearrange due to the low viscosity. Those results suggested

that κ-carrageenan was more compatible with both soy protein and Na-caseinate than Na-alginate.

4. Conclusion

The results showed that SPI was more hydrophobic than the Na-caseinate, which induced the gelation of the protein rich phase of systems containing Na-alginate and κ-carrageenan. However, SPI-gellan sytems did not resut in gelified rich-phases, suggesting that gellan could be used as a thickner agent in soy products. In the presence of Na-alginate the SPI showed lower amount of polysaccharide inclusions as compared to the mixture of SPI with κ-carrageenan. κ-Carrageenan contributed to the formation of a gelified protein rich-phase by interaction with Na-caseinate. In the other hand, this polysaccharide was easily separated from Na-caseinate. The results indicated that κ-carrageenan was more compatible with SPI and Na-caseinate than Na-alginate.

The confocal micrographs revealed different degree of separation for a fixed centrifugation condition (60000 g during 1 h). Thus, the type of biopolymer and its concentration affected the degree of phase separation, which was attributed to the delaying effect of the viscosity on the separation process. Therefore, the time and/or velocity of centrifugation should be adapted considering the mixture viscosity in order to obtain a complete phase separation. The rheological behaviour of the systems varied from a diluted solution to a gel. An increase of system elasticity was observed for systems that showed round shape inclusions, which is typical of water-in-water emulsions.

5. Acknowledgements

6. References

Antonov, Y. A., van Puyvelde, P., Moldenaers, P. (2004). Interfacial tension of aqueous biopolymer mixtures close to the critical point. *International Journal of Biological Macromolecules*, 34, 29-35.

AOAC. Dairy Products. In: *Official Method of Analysis of AOAC International*, 16ᵗʰ edition, v.2, 1996.

Capron, I., Costeux, S., Djabourov, M. (2001). Water in water emulsions: phase separation and rheology of biopolymer solutions. *Rheologica Acta,* 40, 441-456.

Cavallieri, A. L. F. *Efeito do pH e da desnaturação térmica nas propriedades reológicas de proteínas do soro e na sua compatibilidade com xantana.* Dissertação de mestrado, Universidade Estadual de Campinas, 2003.

Clark, A. H. (2000). Direct analysis of experimental tie line data (two polymer – one solvent systems) using Flory-Huggins theory. *Carbohydrate Polymer,* 42, 337-351.

Dubois, M., Gilles, K.A., Hamilton, J. K., Rebers, P.A., Smith, F. (1956). Colorimetric method for determination of sugars and related substances. *Analytical Chemistry*, 28, 350–356.

Grinberg, V.Y., Tolstoguzov, V.B. (1997). Thermodynamic incompatibility of proteins and polysaccharides in solutions. *Food Hydrocolloids*, 11, 145-158.

Guido, S., Simeone, M., Alfani, A. (2002). Interfacial tension of aqueous mixtures of Na-caseinate and Na-alginate by drop deformation in shear flow. *Carbohydrate Polymers*, 48, 143–152.

Hemar, Y., Hall, C.E., Munro, P.A., Singh, H. (2002). Small and large deformation rheology and microstructure of κ-carrageenan gels containing commercial milk protein products. *International Dairy Journal*, 12, 371-381.

Ikeda, S., Nitta, Y., Temsiripong, T., Pongsawatmanit, R., Nishinari, K. (2004). Atomic force microscopy studies on cation-induced network formation of gellan. *Food Hydrocolloids*, 18, 727-735.

Norton, I. T., Frith, W. J. (2001). Microstructure design in mixed biopolymer composites, *Food Hydrocolloids,* 15, 543-553.

Pal, R. (2000). Slippage during the flow of emulsions in rheometers. *Colloids and Surfaces,* 162, 55-66.

Palierne, J. F. (1990). Linear rheology of viscoelastic emulsions with interfacial tension. *Rheologica. Acta,* 29, 204-214.

Petruccelli, S., Añón, M. C. (1995). Thermal aggregation of soy protein isolates. *Journal of Agricultural and Food Chemistry*, 43, 3035-3041.

Polyakov, V. I., Grinberg, V. Y., Tolstoguzov, V. B. (1980). Application of phase-volume ratio method for determining the phase diagram of water-casein-soybean globulins system. *Polymer Bulletin*, 2, 757-760.

Rowlinson, J.S., Widon, B. *Molecular theory of capillarity.* Oxford, UK: Clarendon press, 1984.

Simeone, M., Alfani, A., Guido, S. (2004). Phase diagram, rheology and interfacial tension of aqueous mixtures of Na-caseinate and Na-alginate. *Food Hydrocolloids*, 80, 463-470.

Simeone, M., Molè, F., Guido, S. (2002). Measurement of average drop size of aqueous mixtures of Na-alginate and Na-caseinate by linear oscillatory tests. *Food Hydrocolloids*, 16, 449-459.

Spagnuolo, P.A., Dalgleish, D.G., Goff, H.D., Morris, E.R. (2005). Kappa-carrageenan interactions in systems containing casein micelles and polysaccharide stabilizers. *Food Hydrocolloids*, 19, 371-377.

Steffe, J.F. *Rheological Methods in Food process Engineering*. Freeman Press, East Lansing, p. 1-93, 1996.

Tolstoguzov, V. B. (1995). Some physical-chemical aspects of protein processing foods. Multicomponent gels. *Food Hydrocolloids,* 9, 317-332.

Tolstoguzov, V. B. (2003). Some thermodynamic considerations in food formulation. *Food Hydrocolloids*, 17, 1-23.

Van Vliet, T., Martin, A. H., Bos, M. A. (2002). Gelation and interfacial behaviour of vegetable proteins. *Current Opinion in Colloid and Interface Science*, 7, 462-468.

Zeman, L., Patterson, D. (1972). Effect of the Solvent on Polymer Incompatibility in Solution. *Macromolecules*, 5, 513–516.

CHAPTER 5. Protein-polysaccharide interactions in aqueous systems at pH 7.0.

2nd PART: Morphology of protein-polysaccharides mixtures at rest and under shear.

(in collaboration with LMVT-ETHZ-Switzerland)

Abstract

Rheo-SALS and CLSM experiments were performed to characterize different mixtures of proteins and polysaccharides at rest and under shear. The results indicated that Na-caseinate – Na-alginate mixture showed a greater capacity to form water-in-water emulsions than Na-caseinate - carrageenan system. In addition, the system with SPI and Na-alginate also formed emulsions but with a gelified protein dispersed phase. The interfacial tension of systems containing gellan was very low resulting in homogeneous mixtures and no scattered light was observed by SALS.

Keywords: proteins, polysaccharides, rheo-SALS, CLSM, rheology.

1. Introduction

Aqueous mixtures of proteins and polysaccharides are commonly found in food products. However, these two kinds of biopolymers are usually incompatible showing segregative phase separation at pH 7.0. Sometimes microscopically phase separation can arise with interesting morphology, which can vary from elongated to droplet-like structures. In that kind of systems, each phase is highly enriched with one of the two biopolymers. When droplet-like morphology is formed the system can be regarded as emulsion of the water-in-water type (Tolstoguzov, 1986). The presence of biphasic morphology is essential for the mixture be able to mimic the properties of fat in food products (Capron et al., 2001). In addition, some studies have been carried out on the gelation of the dispersed phase (Wolf et al., 2000; Lundell et al., 2004) in order to produce new attractive textures.

The rheological behaviour of aqueous biopolymer mixtures is quite different from that of a pure biopolymer solution due to the hydrodynamic influence of the dispersed

phase (Simeone et al., 2002). The interfacial tension is considered as the most important property to maintain an emulsion-type structure (Van Puyvelde et al., 2002). However, an interesting feature of these systems is the extremely low interfacial tension that is around 0.1-100 µN/m. This fact adds a greater complexity when dealing with such systems.

Nowadays, big effort has been paid to elucidate the interfacial tension of biphasic systems as well as their behaviour under shear. For that purpose the technique of drop shape analysis (Guido et al., 2002) or rheo-optical methods (Mewis et al. 1998 and Van Puyvelde et al., 1998) based on small angle light scattering (SALS) patterns have been used. The most studied systems in the last years have been sodium alginate - sodium caseinate (Capron et al., 2001; Guido et al., 2002; Antonov et al., 2004), κ-carrageenan – gellan (Wolf et al., 2000), gelatin – dextran (Ding et al., 2002; Scholten et al., 2002), gelatin – arabic gum (Scholten et al., 2004) and gelatin – maltodextrin (Lundell et al., 2004). However, the morphology of some important aqueous mixtures for the food industry has not been studied yet, such as mixtures containing xanthan, galactomannans and soy proteins.

The objectives of this work were 1) to characterize morphologically at rest and under shear different mixtures of proteins and polysaccharides prepared after phase separation in order to discuss the formation of water-in-water emulsions, 2) to demonstrate that complementary techniques like CLSM and rheo-SALS should be used together to get complete information about the morphology of these systems. The morphology at rest was observed by confocal microscopy. Such measurements were supplemented with qualitative observations of SALS patterns under shear. The polysaccharides investigated were xanthan,

locust bean gum, gellan, κ-carrageenan and sodium alginate, while sodium caseinate and soy protein isolate (SPI) were used as protein source.

2. Material and methods

2.1. Material

The proteins used to prepare the model systems were casein (Sigma Chemical Co., USA) and soy protein isolate (SPI) obtained from defatted soy flour (Bunge Alimentos S.A., Brazil). The polysaccharides used were sodium (Na)-alginate, κ-carrageenan and gellan, all of them obtained from CP Kelco (USA). Table 1 shows the chemical characterization of each biopolymer. The moisture and ash contents were determined using the gravimetric method, in which the initial and final samples were weighed. The ash was obtained by heating the powder at 550°C until it becomes a carbon-free sample (AOAC, 1996). For moisture analysis the powder was dried in a vacuum-oven at 60 ^{o}C until the sample weight reached a constant value. The protein content was carried out using the Kjeldahl method (AOAC, 1996).

Table 1. Characterization of the biopolymers used to prepare the model systems.

Biopolymer	Moisture [%] (wet basis)	Protein [N% x 6.25] (wet basis)	Ash [%] (wet basis)
Casein	6.51 ± 0.10	89.64 ± 1.55	0.84 ± 0.08
SPI	6.44 ± 0.07	91.25 ± 0.45	3.45 ± 0.04
Na-alginate	5.75 ± 0.21	0.44 ± 0.01	21.52 ± 0.23
κ-carrageenan	7.84 ± 0.07	0.44 ± 0.03	15.29 ± 0.16
Gellan	6.42 ± 0.12	0.47 ± 0.02	9.85 ± 0.02

The soy proteins isolation procedure followed the method described by Petruccelli and Añón (1995). Defatted soy flour was dispersed in distilled water (1:10 w/w) and the pH

was adjusted to 8.0 with 2N NaOH. The dispersion was gently stirred for 2h at room temperature and then centrifuged at 10,000 x *g* for 30 min at 4ºC in a Sorvall RC5 Plus centrifuge (GSA-rotor, Dupont, UK). The supernatant was adjusted to pH 4.5 with 2N HCl and centrifuged at 5,000 x *g* (Sorvall GSA-rotor) for 15 min at 4ºC. The precipitate was then suspended in water and the pH adjusted to 8.0 with 2N NaOH, followed by freeze-drying of the suspension.

2.2. Preparation of biopolymers stock solutions

The Na-caseinate solution was prepared by dispersing casein powder in milli-Q water using magnetic stirring for 2 h at a maximum temperature of 50 ^{o}C. The pH was constantly adjusted to 7.0 with 10M NaOH. The soy protein isolate (SPI) solution (milli-Q water) was prepared at room temperature by magnetic stirring until the complete powder hydration and the pH was adjusted to 7.0 with 1M HCl. The polysaccharide solutions were prepared by first dispersing the powders in milli-Q water at room temperature by magnetic stirring and after heating in a water bath with a fixed temperature and time (Table 2). The prepared solutions were immediately cooled down to room temperature in an ice bath, and none of them gelified after this process. The insoluble particles of proteins and Na-alginate solutions were separated by centrifugation in a Sigma centrifuge 3K30 (rotor no 33310 – Sigma Laborzentrifugen GmbH, Germany) at 60,000 x *g* for 60 minutes at 25°C (Antonov et al., 2004). The κ-carrageenan and gellan solutions did not show any insoluble particles. The pH of all solutions was adjusted to 7.0. The concentrations of proteins, seadweeds polysaccharides and gellan solutions were 8%, 4% and 1% (w/w), respectively.

Table 2. Temperature and time used to prepare the polysaccharide solutions

Polysaccharide	Temperature (°C)	Time (min)

Gellan (Ikeda et al., 2004)	90	60
κ-carrageenan (Hemar et al., 2002)	90	60
Na-Alginate (Capron et al., 2001)	70	30

2.3. Preparation of biopolymers mixtures

Figure 1 shows the procedure to prepare the protein-polysaccharide mixtures (MS2) that were morphologically characterized. A initial biopolymer mixture (MS1) was obtained by mixing the purified solutions of protein and polysaccharide during 1 h at room temperature by magnetic stirring. These solutions were poured into polycarbonate tubes of 25 mL that were centrifuged in a Sigma centrifuge 3K30 (rotor no 33310 – Sigma Laborzentrifugen GmbH, Germany) at 60,000 x *g* for 1 h at 25°C (Antonov et al., 2004). The phases were then carefully withdrawn. An aliquote of 0.1 g of the protein-rich phase (PR$_{rp}$) and of 9.9 g of the polysaccharide-rich phase (PS$_{rp}$) were mixed to obtain a second mixture (MS2), which was analysed by confocal microscopy and rheo-SALS.

Table 3 shows the composition (protein and polysaccharide concentrations) of the initial mixture (MS1) and the protein and polysaccharide rich-phases obtained after phase separation for different protein-polysaccharide systems. The composition of the studied MS2 mixtures was determined based on PS$_{rp}$ and PR$_{rp}$ composition. The system containing sodium alginate – sodium caseinate was taken as a reference because of the extensive studies already done with that system.
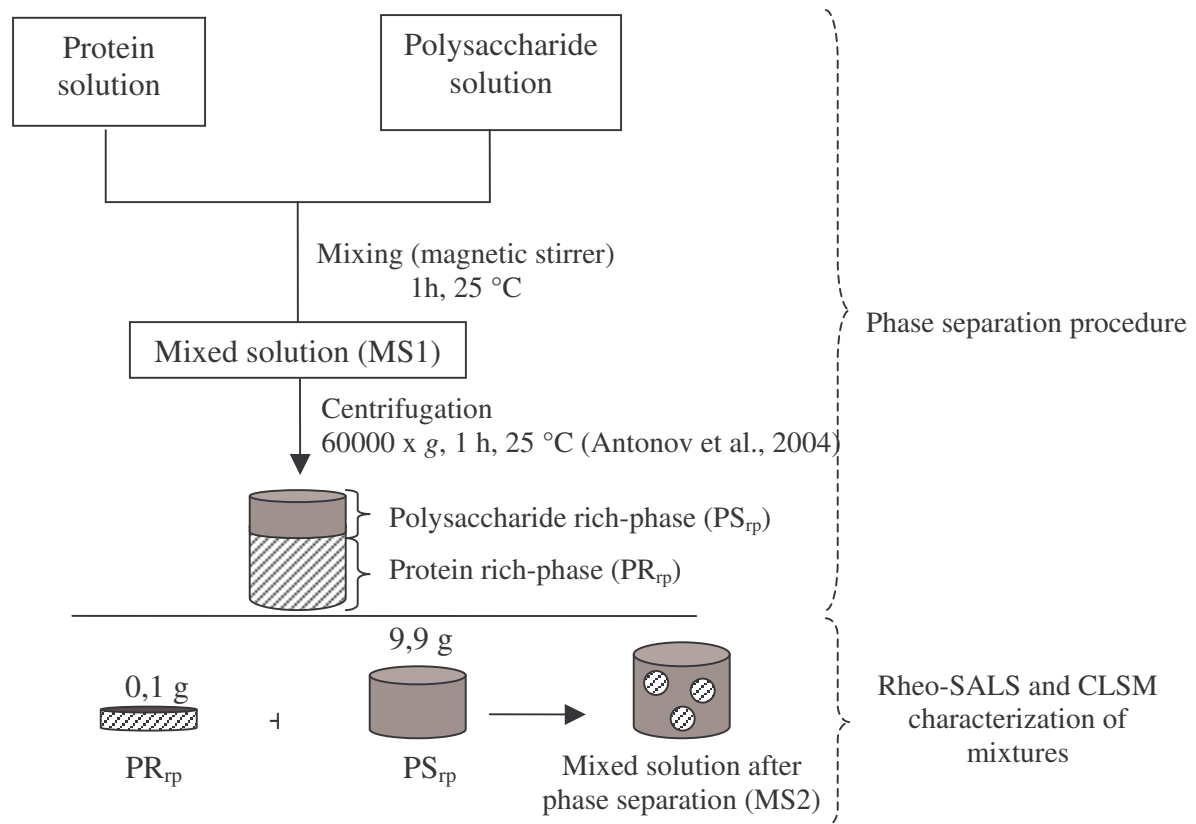
Figure 1. Procedure to prepare the protein-polysaccharide mixtures.

Table 3. Protein (C_{PR}) and polysaccharide (C_{PS}) concentrations of MS1, PR_{rp} and PS_{rp} used to prepare the mixture MS2.

Protein/polysaccharide mixture (nomenclature)	Initial mixture (MS1)	Protein rich-phase	Polysaccharide rich-phase
Na-caseinate / Na-Alginate (CA)	C_{PR} = 2.9%, C_{PS} = 2.3%	C_{PR} = 14.7%, C_{PS} = 0.4%	C_{PR} = 0.3%, C_{PS} = 2.7%
Na-caseinate / Carrageenan (CC)	C_{PR} = 2.9%, C_{PS} = 2.0%	C_{PR} = 8.4%, C_{PS} = 0.8%	C_{PR} = 0.3%, C_{PS} = 2.5%
Na-caseinate / Gellan (CG)	C_{PR} = 5.0%, C_{PS} = 0.4%	C_{PR} = 5.2%, C_{PS} = 0.2%	C_{PR} = 3.0%, C_{PS} = 1.6%
SPI / Na-Alginate (SA)	C_{PR} = 3.0%, C_{PS} = 2.5%	C_{PR} = 22.5%, C_{PS} = 1.0%	C_{PR} = 1.2%, C_{PS} = 2.6%
SPI / Carrageenan (SC)	C_{PR} = 3.1%, C_{PS} = 2.2%	C_{PR} = 16.2%, C_{PS} = 1.7%	C_{PR} = 1.0%, C_{PS} = 2.4%
SPI / Gellan (SG)	C_{PR} = 4.8%, C_{PS} = 0.4%	C_{PR} = 7.6%, C_{PS} = 0.3%	C_{PR} = 4.3%, C_{PS} = 0.5%

*The values of protein and polysaccharide concentration were determined, respectively, by Kjeldhal (AOAC, 1996) and Phenol-sulphuric acid methods (Dubois, 1956).

2.4. Rheo-Small Angle Light Scattering (rheo-SALS)

Light scattering measurements under shear were performed using a home built SALS set up designed for the stress controlled Rheometrics® DSR rheometer (USA). Creep tests in the stress range of 0.1-1000 Pa were performed during 30 s. The steady state laser scattering profile and apparent viscosity were obtained. Apparent viscosity versus shear rate data were ploted and the Cross model (Equation 1) was used to fit those data.

$$\frac{\eta - \eta_{\infty}}{\eta_0 - \eta_{\infty}} = \frac{1}{1 + k\dot{\gamma}} \qquad (1)$$

where η is the apparent viscosity and the subscripts 0 and ∞, respectively, indicate the zero shear viscosity and the infinite Newtonian viscosity. The shear rate is referred as $\dot{\gamma}$, k is a parameter with the dimensions of time and n is a fitting parameter that gives information about the degree of pseudoplasticity at $\eta \ll \eta_0$ and $\eta \gg \eta_{\infty}$.

The schematic of the set up and the top view of a typical scattering profile are shown in Figure 2. A 5 mW He-Ne laser (Melles Griot) provided a monochromatic light of wavelength 632.8 nm. Using three prisms the laser beam was deflected and sent through the sample placed between transparent quartz parallel plates (gap = 0.5 mm). The light propagated through the velocity gradient direction thus probing the structure in the plane of flow and vorticity (Figure 2). The scattered light at small angles was intercepted on a screen under the sample that consists of a semi-transparent plastic. The scattering images were captured using a Sony CCD camera (DFW-V 500, Japan), which was mounted under the screen. Regarding the camera position, it was necessary to add a main beam stop in the plastic screen, such that the camera could record only the scattered light.
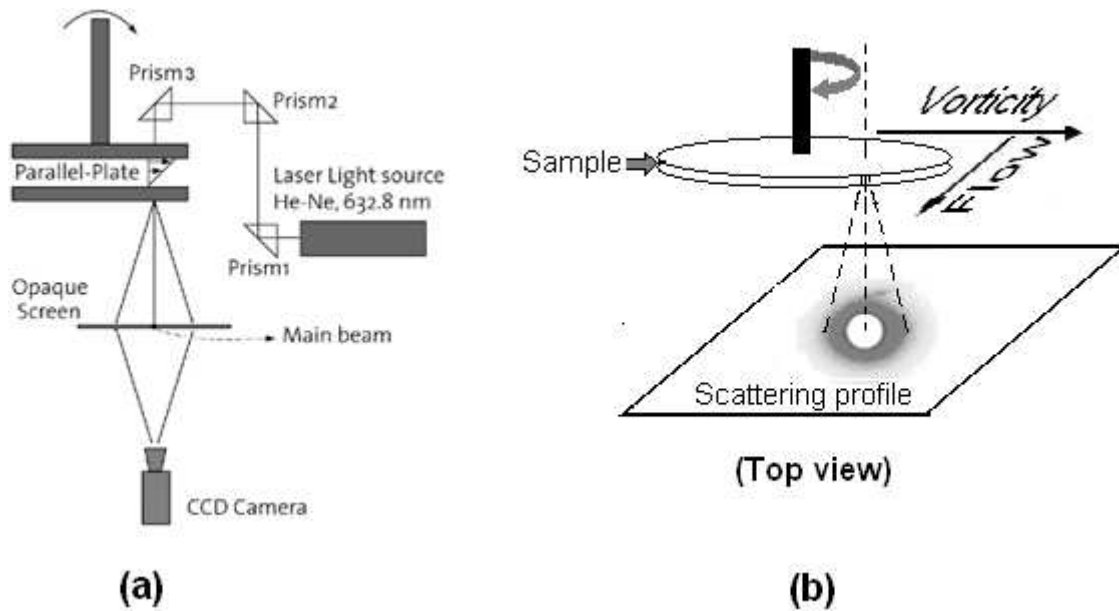
Figure 2. Schematic of rheo-small angle light scattering constructed for the stress controlled Rheometrics® DSR rheometer (a) and the top view of a typical scattering profile (b).

2.5. Confocal laser scanning microscope (CLSM)

The protein-polysaccharide mixtures (MS2) (Table 3) were observed under confocal laser scanning microscope (CSLM). Rhodamine B was added and mixed carefully with about 1 mL of sample. Such a fluorescent dye was used in order to stain the protein. The samples were placed in indentations of microscope slides, covered with a glass cover slip and sealed with nail polish to prevent evaporation. A dual-channel laser confocal system (MRC 1024 UV, Biorad, USA) mounted on an Axiovert 100 Zeiss inverted microscope and equipped with Ar-Kr lasers was used for the trials. The Ar-Kr lasers emitted polarized light with a wavelength of 568 nm exciting the Rhodamine-labeled proteins. Images were taken using a 100x oil immersion objective. To obtain a representative structure 15 micrographs of each sample were taken.

3. Results and discussion

Some authors mentioned the existence of a water-in-water emulsion at biopolymer concentrations near the binodal curve. This emulsion could be obtained by mixing two complete separated phases in a PR_{rp}/PS_{rp} ratio of 1/99 or vice-versa. In the present work, this ratio was kept to form the MS2 systems (Figure 1), although the equilibrium of the phases was not reached for all systems (Chapter 5 - 1st part). Table 4 shows the visual characterization of the protein and polysaccharide rich-phases. Almost all systems showed one of the phases gelified, except for CA and SG where two liquid phases were observed. Thus, when preparing the liquid MS2 samples the systems were stirred until any visible gel particle could be observed by eye.

Table 4. Visual characterization of protein and polysaccharide rich-phases.

Mixture	Protein rich-phase	Polysaccharide rich-phase
CA	Opaque-liquid	Transparent-yellowish-liquid
CC	Opaque-white-gel	Transparent-liquid
CG	Transparent-liquid	Translucent-gel
SA	Opaque-yellowish-gel	Transparent-yellowish-liquid
SC	Opaque-yellowish-gel	Transparent-liquid
SG	Translucent-yellowish-liquid	Transparent-yellowish-liquid

Figure 3 shows the confocal micrograph at rest (Figure 3a) for CA-MS2 as well the variation of the apparent viscosity and SALS patterns as a function of different shear rates (Figure 3b). The CA-MS2 mixture at rest showed spherical protein aggregates (white regions in the micrograph) with diameters up to 5 µm indicating a microstructure typical of water-in-water emulsion (Capron et al., 2001). The SALS pattern was isotropic at rest and low shear rates for CA system, but it showed a strong anisotropy perpendicular to the flow

direction increasing shear rate, which reflects the deformation of the droplets. At higher shear rates, the anisotropy gradually relaxes (440 s^{-1}) and finally, an isotropic pattern was again obtained (6300 s^{-1}). It has been demonstrated (Van Puyvelde et al., 2003) that while the droplets are continuously stretched, their cross-section becomes smaller and consequently the interfacial stress increases. As a result, interfacial instabilities will start to develop and will eventually disintegrate the droplets. During this process, the anisotropy of the structure decreases, as seen in Figure 3. Thus, this evolution from anisotropy, relaxation and steady-state elliptic pattern could be explained on the basis of deformation, breakup, and coalescence of the dispersed droplets. Hence, under these conditions, the biopolymer emulsion behaves according to the theoretical relations for conventional emulsions and similar to synthetic blends (Van Puyvelde et al., 2003).

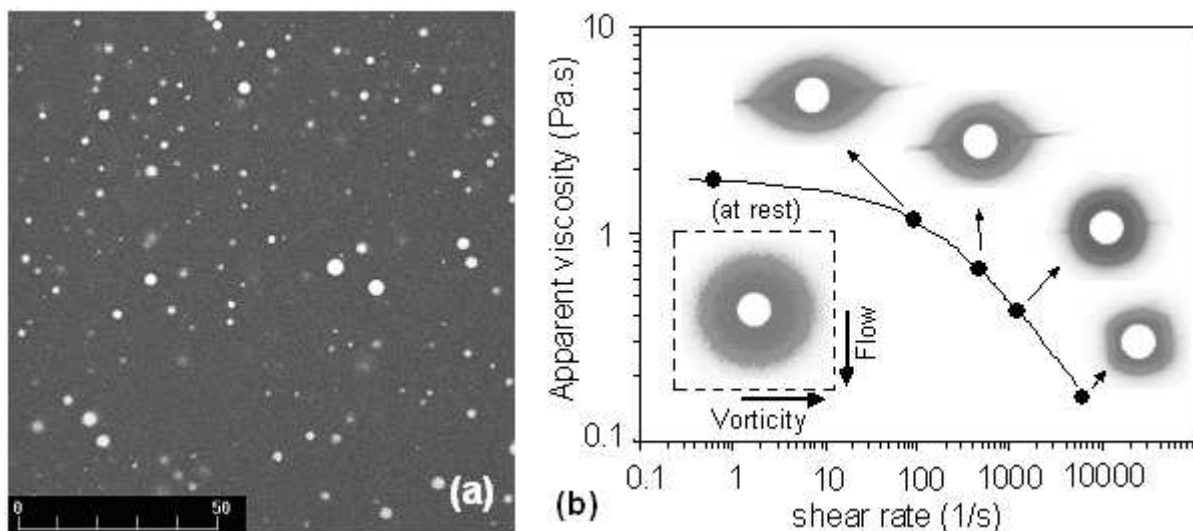Figure 3. Rheological and optical characterization of the MS2 system (1% PR$_{rp}$ + 99% PS$_{rp}$) containing 0.44% Na-caseinate and 2.68% Na-alginate. A) Confocal microstructure; B) Apparent viscosity and 2D-SALS pattern as a function of the shear rate, the line represent the fit of Cross equation to the data. The light regions in the CLSM micrograph (a) indicate protein area, scale bar = 50μm.

The MS2 of the SA$_2$ (Figures 4a, 4b) system, was formed from a visual hard gel of the protein rich phase and a liquid polysaccharide rich phase (Table 4). The CLSM results (Figure 4a) exhibited square-edged irregular protein aggregates measuring up to 8 µm in highest size. The shapes of the aggregates suggest that the dispersion was a gel.
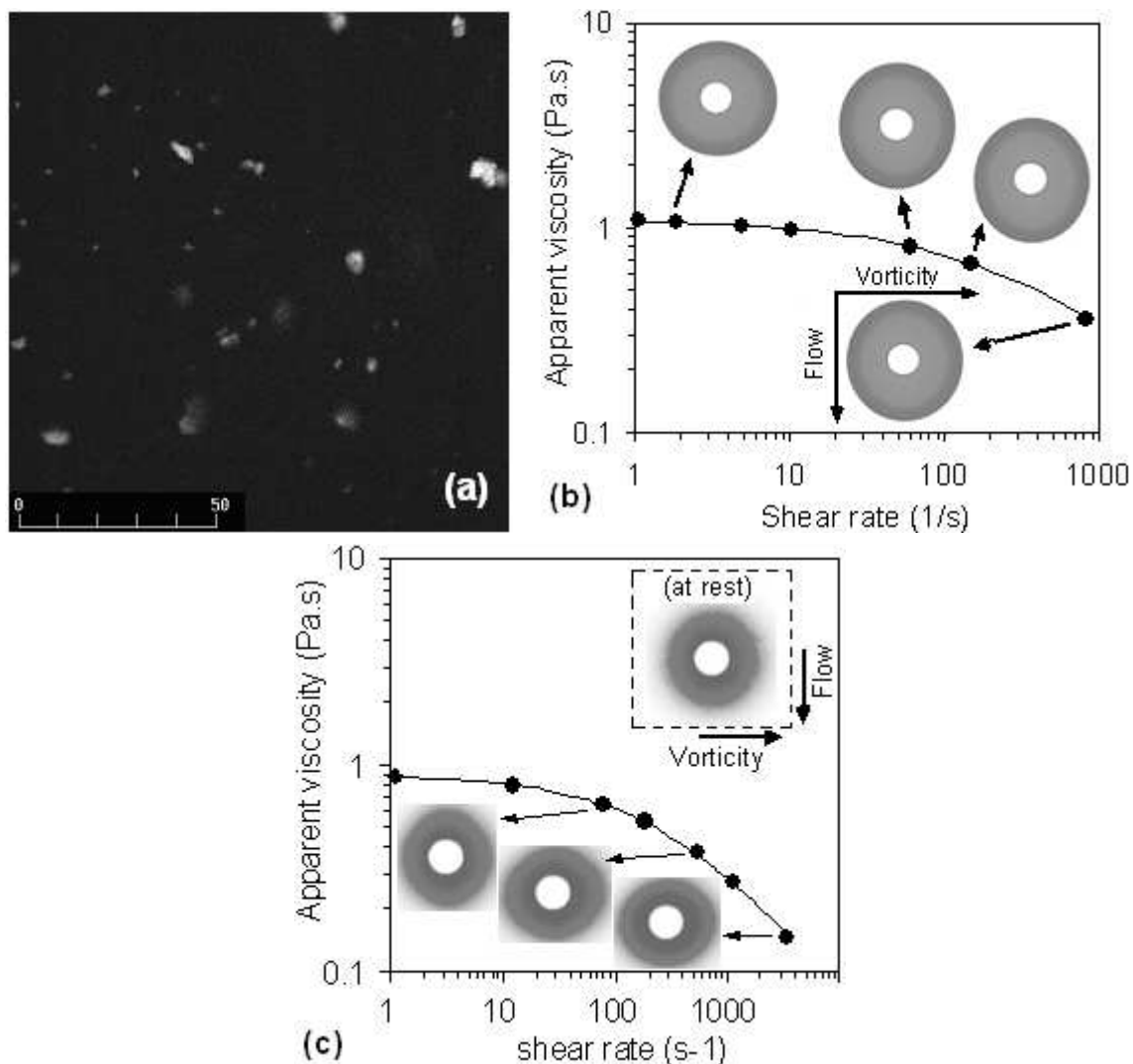
Figure 4. CLSM microstructural (a) and rheo-optical (b, c) characterization of the MS2 system (1% PR$_{rp}$ + 99% PS$_{rp}$) containing 1.4% SPI and 2.6% Na-alginate (a, b) and of SA$_2$-PSrp system with 1.2% protein plus 2.6% polysaccharide (c). The light regions in the CLSM micrograph (a) indicate protein area, scale bar = 50µm. The lines in rheological graphs (b, c) represent the fit of Cross equation to the data.

This system behaved as a shear-thinning fluid (Figure 4b). From the inserts Figure4, it can be observed that the light was scattered in high angles in a great intensity. In addition,

the scattering profile was isotropic at low shear rates showing that the dispersed gels were homogeneously distributed in the continuous phase. In contrast to CA system, it was not observed an anisotropic evolution perpendicular to the flow direction. Instead, a slight anisotropy in the flow direction was checked in the beginning of the non-Newtonian region.

As discussed in chapter 5 – 1st part the phase separation of SA was not complete. The CLSM microstructure of its PS$_{rp}$ looked like a water-in-water emulsion, with droplets dispersed in a continuous phase (Figure 3). Hence, the SALS pattern under shear of this system (PS$_{rp}$-SA containing 1.2% protein and 2.6% polysaccharide) was evaluated in order to compare the properties of two emulsions containing one protein (SPI or Na-caseinate) and Na-alginate. In addition, the amount of Na-alginate in both systems was quite the same (2.6-2.7%). The SALS pattern of PS$_{rp}$-SA (Figure 4c) was isotropic at rest, as expected from the homogeneous distributed dispersed phase. Once more, it was observed an anisotropic structure in the flow direction at the beginning of the non-Newtonian region. Only at high shear rates (3500 s^{-1}) a slight deformation perpendicular to the flow direction was developed, even though the CLSM micrographs showed a water-in-water emulsion. These results corroborate with the above suggestion that the dispersed protein droplets were indeed gels, such that it was difficult to deform the droplets under shear.

The SC system showed a shear-thinning behaviour and the shape of the inclusions varied from droplet-like to irregular square-edged. Those inclusions measured up to 6 μm in highest size. The anisotropic SALS pattern (Figure 5b) perpendicular to the flow direction was developed only at very high shear rates, 4000s^{-1}. In addition, it was observed a slight anisotropy shape in the flow direction at the beginning of the non-newtonian region (data not shown), as previously mentioned for SA system. The micrograph of the CC

system exhibited small inclusions of protein with sizes up to 3 μm (Figure 6a). Figure 6b

shows that this system behaved as shear-thinning fluid and showed an isotropic SALS

pattern at low and very high shear rates. However, for intermediate shear rates it was not

observed a similar pattern of CA, as expected due to the formation of an emulsion at rest.

Instead, an anisotropic pattern in the flow direction was observed in the shear thinning

region.

Figure 5. Rheological and optical characterization of the MS2 system (1% PR$_{rp}$ + 99% PS$_{rp}$) containing 1.2% SPI and 2.4% κ-carrageenan. A) Confocal microstructure; B) Apparent viscosity and 2D-SALS pattern as a function of the shear rate, the line represent the fit of Cross equation to the data. The light regions in the CLSM micrograph (a) indicate protein area, scale bar = 50μm.
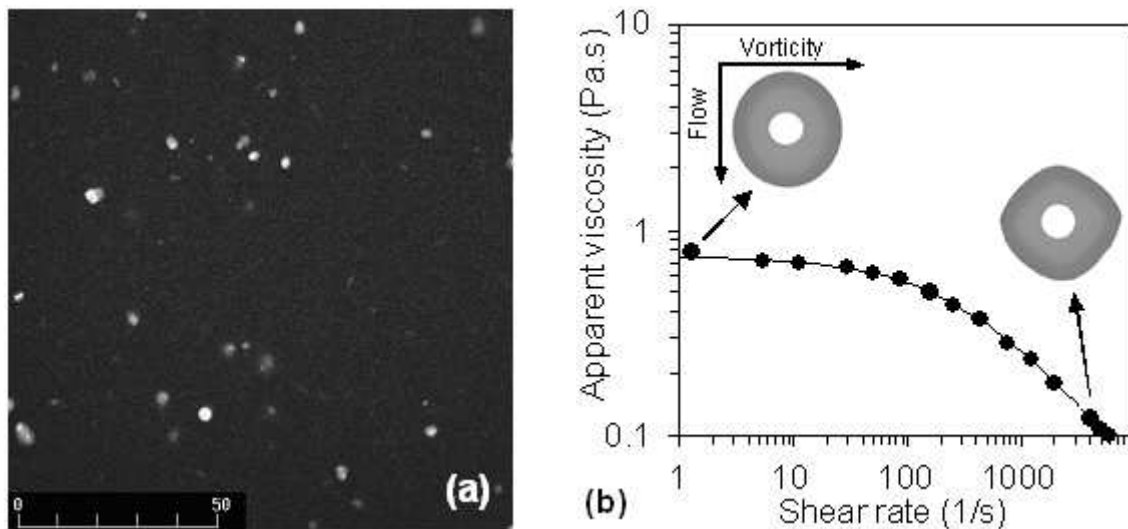

Figure 6. Rheological and optical characterization of the MS2 system (1% PR$_{rp}$ + 99% PS$_{rp}$) containing 0.4% Na-caseinate and 2.5% κ-carrageenan. A) Confocal microstructure; B) Apparent

viscosity and 2D-SALS pattern as a function of the shear rate, the line represents the fit of Cross equation to the data. The light regions in the CLSM micrograph (a) indicate protein area, scale bar = 50µm.
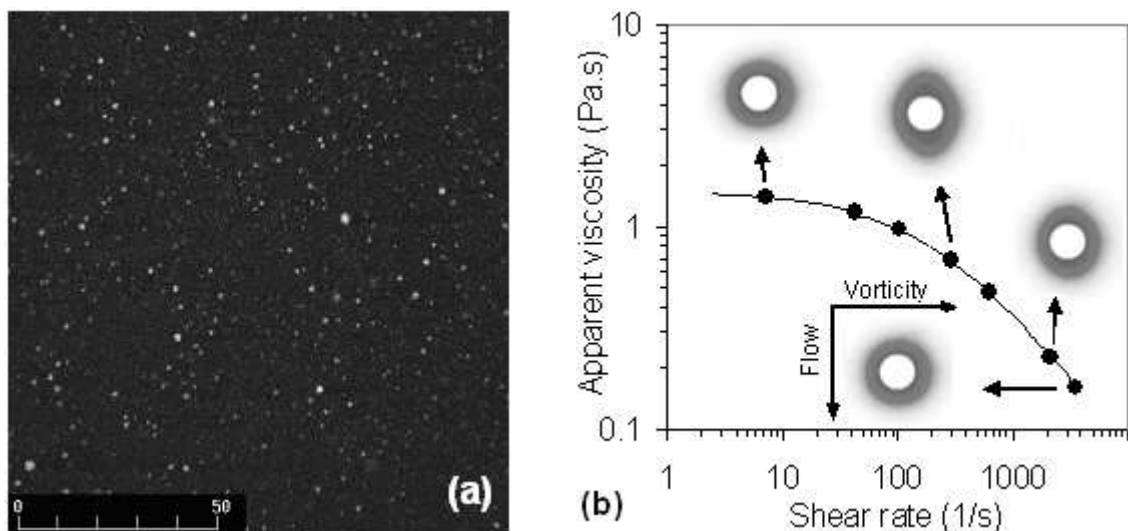
In contrast to the other examined systems, the CG sample formed a gelified PS_{rp} and a liquid PR_{rp}. The confocal microstructure (Figure 7a) of MS2-CG system showed big and round protein inclusions with diameters up to 30 µm. However, it was not possible to perform the rheo-SALS experiments of such system due to its fragile characteristic with a great release of water during shearing. Thus, a system containing 1% PS_{rp} and 99% PR_{rp} (in the other end of the tie-line) was investigated, since some works reported the formation of an emulsion with a protein continuous phase (Antonov et al., 2004, Schorsch et al., 1999). The CLSM microstructure of such system is shown in Figure 7b and it was not observed the formation of an emulsion. Instead, the proteins were homogeneously distributed, which resulted in absence of scattered light in rheo-optics experiments (Figure 7c) over the entire shear rate range. This indicates that the sample was homogenized on the length scales probed by light scattering. The same trend was observed for MS2-SG system (Figure 7d). Those behaviours could be explained by the low interfacial forces acting in such systems (Chapter 5 – 1st part). This indicates that soy proteins can not be gelled using gellan, in contrast to what happened with Na-alginate and κ-carrageenan. Hence, gellan would be used as a good thickener for soy products.
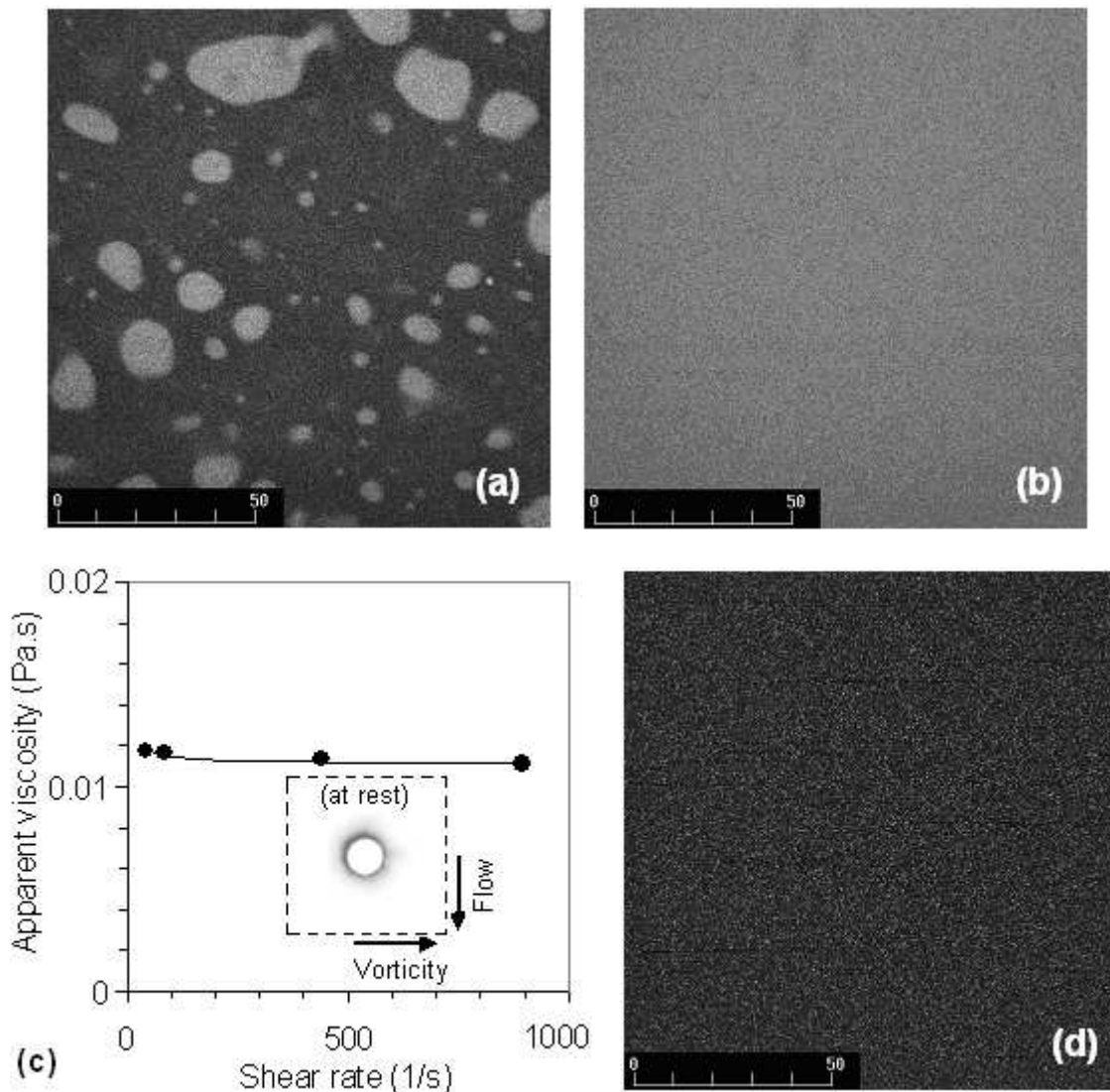
Figure 7. CLSM microstructural (a, b, d) and rheo-optical (c) characterization of systems containing gellan. A) MS2 (1% PR_{rp} + 99% PS_{rp}) system containing 3% Na-caseinate – gellan 1.6%; B, C) MS2 modified (1% PS_{rp} + 99% PR_{rp}) system containing 5.2% Na-caseinate – gellan 0.2%; D) MS2 (1% PR_{rp} + 99% PS_{rp}) system containing 4.3% SPI – gellan 0.5%. The light regions in the CLSM micrographs (a, b, d) indicate protein area, scale bar = 50µm. The line in rheological graph (c) represents the fit of Cross equation to the data.

The above results revealed that systems containing SPI and Na-alginate or κ-carrgeenan resulted in gelified dispersed phase, since they could only be deformed at very high shear rates. However, the CLSM micrograph of PS_{rp}-SA showed droplet-like inclusions as observed for CA system. These indicate that CLSM and rheo-SALS techniques should be used complementary to each other to completely explain the

229

morphology of protein-polysaccharide systems. In addition, the systems with a gelified dispersed phase (SA, SC and CC) showed an unexpected anisotropy in the flow direction at the beginning of the non-Newtonian region. The increase of the anisotropic pattern follows the order: MS2-SA < PS$_{rp}$-SA < MS2-CC; suggesting that the amount of droplets in the system is related with the development of such anisotropic behaviour. It is also interesting to note that mixtures containing SPI - Na-alginate and SPI - κ-carrageenan (Figures 4 and 5) scattered the light in higher angles as compared to the systems containing Na-caseinate (Figures 3 and 6).

The mixing of the protein- and the polysaccharide-rich phase in a ratio of 1/99 formed a mixture lying on the tie-lines near to the polysaccharide rich phase. Comparing the MS2 micrographs of CA and CC with the corresponding micrographs of the polysaccharide rich phases (Chapter 5 – 1ˢᵗ part) an increase of the protein volume fraction was observed for MS2. The microstructure of PS$_{rp}$ of CA (Chapter 5 – 1ˢᵗ part) did not have any droplets, while MS2-CA showed a great amount of relatively big droplets. In the other hand, the morphology of PS$_{rp}$-CC (Chapter 5 – 1ˢᵗ part) showed small droplets inclusions, while MS2-CC had a similar microstructure but the droplets have slightly higher diameter (Figure 6). Those results indicated that the CA system showed a greater capacity to form emulsions than CC system. It is interesting to note that SG system would never form emulsion as well as the CG systems with protein continuous phase. These suggest that the PS$_{rp}$/PR$_{rp}$ ratio of 1/99 or vice-versa can not be used as a general criterion for emulsion formation.

The differences in the dispersed phase, gel or liquid-like, droplet or square shape as well the capacity of a system to form emulsions did not changed significantly the relaxation

time (k) or the flow behaviour index (n) of the system. The latter parameters were obtained by fitting the Cross model (R^2>0.999) to the data and a value between 0.01-0.03 s was found for k, while n was ~0.7 for all systems. These results indicate that the rheological behaviour under large deformations did not give information about the emulsions structure, as occurred by analyzing the small deformation behaviour (Capron et al., 2001, Palierne, 1990).

4. Conclusion

The MS2 systems could be divided into three groups, namely, 1) water-in-water emulsions; 2) gelified dispersed phase in a continuous liquid phase or vice-versa; 3) homogenous protein-polysaccharide solution. Regarding the type 1 systems, the Na-caseinate – Na-alginate mixture showed a greater capacity to form emulsions than Na-caseinate - carrageenan system, although both systems could be used in dairy products as fat replacers. Among the systems with gelified dispersed phase, the PS_{rp}-SA could also be considered a water-in-water emulsion. However, the typical emulsion SALS pattern was observed only for CA sample. The delays in the anisotropic development in the perpendicular flow direction as well as the appearance of an anisotropic pattern in the flow direction were attributed to the presence of a gelified dispersed phase. Therefore, the CLSM and SALS techniques should be used complementary to each other to completely explain the morphology of protein-polysaccharide systems.

5. Acknowledgements

6. References

Antonov, Y. A., van Puyvelde, P., Moldenaers, P. (2004). Interfacial tension of aqueous biopolymer mixtures close to the critical point. *International Journal of Biological Macromolecules*, 34, 29-35.

AOAC. Dairy Products. In: *Official Method of Analysis of AOAC International*, 16th edition, v.2, 1996.

Capron, I., Costeux, S., Djabourov, M. (2001). Water in water emulsions: phase separation and rheology of biopolymer solutions. *Rheologica Acta,* 40, 441-456.

Ding, P., Wolf, B., Frith, W.J., Clark, A.H., Norton, I.T., Pacek, A.W. (2002). Interfacial tension in phase-separated gelatin/dextran aqueous mixtures. *Journal of Colloid and Interface Science*, 253, 367–376.

Dubois, M., Gilles, K.A., Hamilton, J. K., Rebers, P.A., Smith, F. (1956). Colorimetric method for determination of sugars and related substances. *Analytical Chemistry*, 28, 350–356.

Guido, S., Simeone, M., Alfani, A. (2002). Interfacial tension of aqueous mixtures of Na-caseinate and Na-alginate by drop deformation in shear flow. *Carbohydrate Polymers*, 48, 143–152.

Hemar, Y., Hall, C.E., Munro, P.A., Singh, H. (2002). Small and large deformation rheology and microstructure of κ-carrageenan gels containing commercial milk protein products. *International Dairy Journal*, 12, 371-381.

Ikeda, S., Nitta, Y., Temsiripong, T., Pongsawatmanit, R., Nishinari, K. (2004). Atomic force microscopy studies on cation-induced network formation of gellan. *Food Hydrocolloids*, 18, 727-735.

Lundell, C., Walkenström, P., Lorén, N., Hermansson, A.M. (2004). Influence of elongational flow on phase separated inclusions within gelling biopolymer drops. *Food Hydrocolloids*, 18, 805-815.

Mewis, J., Yang, H., Van Puyvelde, P., Moldenaers, P., Walker, L.M. (1998). Small angle light scattering study of droplet breakup in emulsions and polymer blends. *Chemical Engineering Science*, 53, 2231-2239.

Palierne, J. F. (1990). Linear rheology of viscoelastic emulsions with interfacial tension. *Rheologica. Acta,* 29, 204-214.

Petruccelli, S., Añón, M. C. (1995). Thermal aggregation of soy protein isolates. *Journal of Agricultural and Food Chemistry*, 43, 3035-3041.

Scholten, E., Tuinier, R., Tromp, R.H., Lekkerkerker, H.N.W. (2002). Interfacial tension of a decomposed biopolymer mixture. *Langmuir*, 18, 2234-2238.

Scholten, E., Visser, J.E., Sagis, L.M.C., Van der Linden, E. (2004). Ultralow interfacial tensions in an aqueous phase-separated gelatin/dextran and gelatin/gum arabic system: A comparison. *Langmuir*, 20, 2292-2297.

Schorsch, C., Jones, M.G., Norton, I.T. (1999). Thermodynamic incompatibility and microstructure of milk protein/locust bean gum/sucrose systems. *Food Hydrocolloids*, 13, 89-99.

Simeone, M., Molè, F., Guido, S. (2002). Measurement of average drop size of aqueous mixtures of Na-alginate and Na-caseinate by linear oscillatory tests. *Food Hydrocolloids*, 16, 449-459.

Tolstoguzov, V.B. Functional properties of protein-polysaccharide mixtures. *Functional properties of food macromolecules*. Eds. J.R. Mitchell & D.A. Ledward. London: Elsevier, p. 385-415, 1986.

Van Puyvelde, P., Antonov, Y.A., Moldenaers, P. (2002). Rheo-optical measurement of the interfacial tension of aqueous biopolymers mixtures. *Food Hydrocolloids,* 16, 395-402.

Van Puyvelde, P., Antonov, Y.A., Moldenaers, P. (2003). Morphology evolution of aqueous biopolymer emulsions during a weak shear flow. *Food Hydrololloids*, 17, 327-332.

Van Puyvelde, P., Yang, H., Mewis, J., Moldenaers, P. (1998). Rheo-optical probing of relaxational phenomena in immiscible polymer blends. *Journal of Colloid and Interface Science*. 200, 86-94.

Wolf, B., Scirocco, R., Frith, W.J., Norton, I.T. (2000). Shear induced anisotropic microstructure in phase separated biopolymer mixtures. *Food Hydrocolloids*, 14, 217-225.

CAPÍTULO 6. Conclusões gerais

As interações complexas entre proteínas e polissacarídeos são resultado das propriedades físicas de cada biopolímero puro em solução. No presente estudo observou-se que dentro do intervalo de concentrações estudado (1-12%), que é o comumente utilizado em produtos alimentícios, soluções de proteína seguem um comportamento Newtoniano, enquanto que os polissacarídeos apresentam comportamento Newtoniano à baixa concentração e pseudoplástico com o aumento desta. Os valores de viscosidade aparente e densidade das soluções puras foram função do tipo de biopolímero (polissacarídeo ou proteína) e da fonte de obtenção dos polissacarídeos. O aumento da viscosidade aparente e redução da densidade seguiu a seguinte ordem para uma dada concentração e taxa de deformação: 1) proteínas, 2) polissacarídeos de origem microbiana (xantana e gelana), 3) polissacarídeo extraído de plantas (jataí ou LBG) e 4) polissacarídeos obtidos a partir de algas (Na-alginato e κ-carragena). Os maiores valores de densidade foram explicados por uma maior capacidade de estruturação dos polissacarídeos obtidos de algas e plantas em solução, nas concentrações estudadas, o que resultou em maior retenção de solvente em um menor volume.

No estudo do comportamento reológico de soluções de xantana tratadas térmicamente e adicionadas de sacarose, foram observadas três transições da solução, dependentes da temperatura e concentração do sistema. Estas foram associadas às regiões com anisotropia e/ou isotropia e à mudança da conformação molecular de um estado ordenado (hélice) para um desordenado. O aumento da temperatura de tratamento térmico e a adição de sacarose reduziram a elasticidade da solução de xantana, sendo que a adição de sacarose afetou as propriedades reológicas apenas de soluções anisotrópicas ou bifásicas (mistas). Assim, foi sugerido que soluções contendo sacarose são menos interconectadas do

que soluções puras de xantana provavelmente devido aos efeitos cosmotrópicos deste co-soluto. Quando KCl foi adicionado às soluções deste polissacarídeo, observou-se um aumento da elasticidade do sistema. Assim, as propriedades físicas das soluções puras de biopolímeros pareceram ser altamente dependentes da presença de um co-soluto e do processamento térmico, sendo relacionadas à conformação molecular apresentada em solução, como formação de duplas hélices, de ultra-agregados e desordenamento molecular.

De forma geral, os três tipos de interações entre proteínas e polissacarídeos, miscibilidade, incompatibilidade ou coacervação complexa, foram observados nos géis e em soluções mistas considerando os biopolímeros estudados. As misturas contendo LBG e uma proteína foram miscíveis, visto que não separaram de fases após centrifugação a 60000 x g durante 1h, o que caracteriza uma grande compatibilidade deste polissacarídeo com ambas proteínas avaliadas. O comportamento de misturas com goma xantana foi dependente do tipo de proteína adicionada, sendo observada miscibilidade na presença de Na-caseinato e de incompatibilidade em concentrações de SPI maiores do que 5%. As demais soluções mistas apresentaram incompatibilidade entre a proteína e o polissacarídeo nas condições de temperatura, força iônica, pH e concentração de ingredientes estudadas.

As soluções aquosas incompatíveis foram caracterizadas por rheo-SALS ("rheo-small angle light scattering") e CLSM (microscopia confocal de varredura laser) a fim de entender o papel de diferentes biopolímeros sobre o comportamento das fases e sobre a formação de emulsão tipo água-água sendo observado que estas duas técnicas devem ser utilizadas conjuntamente a fim de obter-se uma completa descrição morfológica de tais sistemas. A alta hidrofobicidade das proteínas da soja intensificou as associações entre as moléculas de proteína durante a centrifugação resultando na gelificação da fase protéica em misturas com κ-carragena e Na-alginato. No entanto, isto não foi observado para sistemas

contendo gelana ou xantana, sendo que as fases ricas em cada biopolímero eram facilmente remisturadas provavelmente devido a uma baixa tensão interfacial do sistema. Assim, estes dois polissacarídeos seriam mais indicados para serem utilizados em produtos líquidos à base de soja, enquanto a κ-carragena e o Na-alginato seriam interessantes em produtos onde a agregação protéica fosse desejada ou não interferisse na aceitabilidade do produto. Comparando-se os dois polissacarídeos de origem de algas, observou-se que a κ-carragena apresentou maior compatibilidade com o Na-caseinato e com SPI do que o Na-alginato. É interessante notar que a carragena já vem sendo utilizada acertadamente pela a indústria de alimentos em sorvetes a base de soja, e em uma grande variedade de produtos lácteos, apesar do seu uso ter sido ditado pela experiência prática da carragena em produtos lácteos.

No entanto, os resultados mostraram que misturas de Na-caseinato e Na-alginato apresentaram melhor capacidade de formar emulsões do tipo água-água quando comparada com todos os sistemas estudados, o que é interessante industrialmente pela possibilidade de substituição das gotas de gordura por gotas de soluções de biopolímeros (fase dispersa). O sistema SPI - Na-alginato e Na-caseinato – κ-carragena também formaram emulsões, mas com a fase dispersa de proteína gelificada. Este último resultado é bastante interessante do ponto de vista de desenvolvimento de novos produtos com texturas diferentes. Em especial, poderia ser aplicado na fabricação de chocolates com teor de gordura reduzido, visto que a fase dispersa de Na-caseinato apresentou a particularidade de ser um gel à temperatura ambiente e liquefazer-se com um pequeno aumento da temperatura, o que ocorreria durante a degustação do produto.

Nos sistemas gelificados não foi observada a formação de géis ácidos incompatíveis. Estudos prévios mostraram que sistemas-modelo contendo Na-caseinato e

xantana apresentaram coacervação complexa, mesmo quando adicionados de um co-soluto, como a sacarose. Assim, a xantana não pareceu ser um polissacarídeo muito indicado na formulação de iogurtes. No entanto, géis formados por xantana e SPI apresentaram uma única fase e não foi observada sinerese, o que classifica estes géis como miscíveis sendo estes biopolímeros compatíveis em pH ácido. Mesmo a adição de um sal, KCl, não alterou este comportamento, apesar de ter influenciado todas as propriedades dos géis mistos devido aos efeitos de salting-in e salting-out da proteína. O uso de microscopia confocal, no último tipo de sistema, permitiu classificar os géis mistos sem sal como de estrutura organizada enquanto que os géis com sal apresentaram uma estrutura particulada aleatória. Os géis térmicos de SPI-xantana foram estabilizados por interações não-covalentes (hidrofóbicas e ponte de H) e pontes S-S, enquanto que géis adicionados de KCl foram também estabilizados por interações eletrostáticas.

A adição de xantana enfraqueceu os géis térmicos de SPI, provavelmente devido a ligação deste polissacarídeo com a sub-unidade β-7S da SPI. Por outro lado, a adição de xantana aumentou a tensão e a deformação de ruptura em géis de SPI acidificados lentamente pela ação do GDL. De uma forma geral, em géis formados com GDL, a redução da tensão e deformação de ruptura foi obtida pela diminuição da concentração de proteína em géis puros de SPI e Na-caseinato ou pelo aumento do conteúdo de proteína em géis contendo xantana. Neste último caso, foi verificada a formação de uma estrutura esponjosa com o aumento do conteúdo de proteína. Além disto, a adição de xantana resultou em grande aumento da capacidade de retenção de água de géis de SPI independente do processo de formação da rede protéica, por tratamento térmico e por ação de GDL. Assim, o uso de xantana em produtos à base de soja seria indicado por exemplo para aumentar a

retenção de água em GDL-tofu, o que é de grande valia econômica para os produtores deste queijo. Outra interessante aplicação desta goma seria para a manutenção da rede protéica em produtos aerados contendo mais de 6% de proteína. No entanto, a xantana não melhora as propriedades de produtos com alta quantidade de sal (em torno de 2%).

A taxa de acidificação (variação na quantidade de GDL) não afetou as propriedades reológicas em cisalhamento de géis puros de Na-caseinato, mas teve um efeito significativo sobre as propriedades em compressão. A acidificação lenta promoveu uma rede protéica mais interconectada e, portanto, mais forte. A velocidade de acidificação também afetou as propriedades reológicas de géis de SPI e SPI-xantana, sendo obtidos géis mais duros e elásticos quando a acidificação foi mais lenta devido à baixa temperatura do processo. Por fim, um novo modelo baseado na equação de BST foi proposto para predizer um maior número de propriedades mecânicas dos géis biopoliméricos, tendo sido observado um bom ajuste dos dados e uma ótima predição das propriedades de géis de SPI acidificados com GDL.

APENDICE: Preliminary studies on the phase separation of biopolymers mixtures.

1. Importance of the phase separation procedure.

The existence of a water-in-water emulsion at biopolymer concentrations near the binodal curve is reported and it can be obtained by mixing two complete separated phases in a PR_{rp}-PS_{rp} ratio of 1/99 or vice-versa (Capron et al., 2001; Guido et al., 2002; Antonov et al., 2004). However, preliminary studies showed that the thermodynamic equilibrium between the phases as well as the procedure to withdraw the rich-phases are not always a simple task. Thus, two protein-polysaccharide mixtures with similar compositions but prepared according to two different procedures were evaluated under rheo-optics experiments (Figure 1) in order to evaluate the effect of phase separation step on the optical properties of the systems. For that purpose, the Na-caseinate – Na-alginate system was chosen, since this is the most studied water-in-water emulsion system in the literature (Capron et al., 2001; Guido et al., 2002; Antonov et al., 2004).
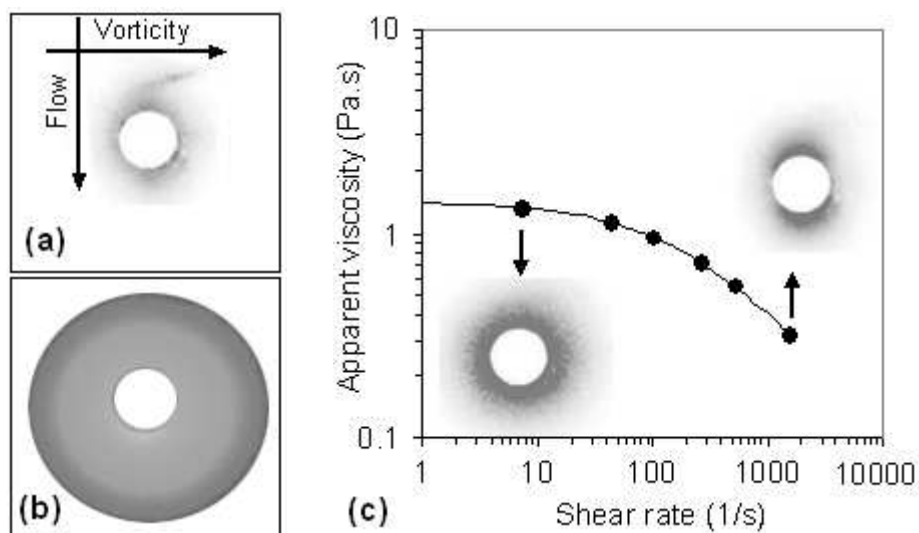

Figure 1. Typical 2D-SALS patterns for systems containing Na-alginate. A) Pure 2.8% Na-alginate solution at rest; B) 0.13% Na-caseinate – Na-alginate 2.8% system mixed without the phase separation step independent of shear rate; C) Polysaccharide rich-phase (0.3% protein + 2.7% polysaccharide) of CA system as a function of shear rate.

Figure 1a shows the SALS pattern at rest for a pure Na-alginate solution and it was not observed any scattered light in the flow-vorticity plane, which is typical of a homogeneous system. Similar pattern was observed for the optical properties of the polysaccharide rich phase obtained after phase separation of Na-caseinate – Na-alginate sample (Figure 1c). The low intensity scattering of the light observed at very low angles was in accordance with the CLSM micrograph at rest, in which was not observed any protein at the highest (100x) magnification (Chapter 5 – 1st part). At higher shear rates it was not observed light scattering any more, characterizing that the system was completely mixed at least on the length scales probed by light scattering. The chemical characterization of PS$_{rp}$ indicated the following composition: 0.3% of protein and 2.7% of polysaccharide, revealing that even 0.3% of protein did not contributed to scatter the light. However, a system with similar composition but mixed without the phase separation step shows a high intensity scattering profile at large angles independent of the shear rate/shear stress applied (Figure 1b). This indicates the formation of very small dispersed phase (small droplets scatter at high angles) that was not elongated under shear as observed typically for water-in-water emulsions (Chapter 5- 2nd part and Antonov et al., 2004). The above results showed that (1) systems with similar composition (and also extended to the same composition) but prepared in different manners (with or without phase separation) did not have the same optical and consequently rheological behaviour at rest and under shear; (2) a previous phase separation process before the preparation of biopolymer mixture is necessary to form water-in-water emulsions.

2. Visual characterization of different protein-polysaccharide mixtures after centrifugation.

Different biopolymer1-biopolymer2 systems were centrifuged at 60000 x *g* during 1h (Antonov et al., 2004) and the compatibility/incompatibility (checked by the macroscopic phase separation) of the systems are shown in Table 1. All combinations of one protein and one polysaccharide (considering the biopolymers studied in the present Ph.D. thesis) were studied as well as protein1-protein2 and LBG - Na-alginate, since the latter polysaccharides are the two most hydrophobic ones (preliminary studies not shown). The concentration of each ingredient was chosen taking in consideration the following factors: 1) the incompatible region for Na-caseinate – Na-alginate systems reported in literature; 2) a high total biopolymer content to ensure that the sample would be in the incompatible region of the phase diagram; 3) a zero shear viscosity of the mixture lower than 1 Pa.s (value similar to the pure polysaccharide solution shown in Chapter 3) was used to avoid the influence of the viscosity on a complete phase separation (Clark, 2000, Cavallieri, 2003).

The systems protein-LBG or Na-caseinte - xanthan revealed to be compatible with a single phase after centrifugation. The same trend was found for the protein-protein and polysaccharide-polysaccharide mixtures studied, even when an unfolded SPI (denaturation at 80 $^{\circ}$C during 30 min) was present.

Table 1. Visual characterization of protein-polysaccharide MS1 systems after centrifugation.

Mixture (biopolymer 1 – biopolymer 2)	Biopolymer 1 Concentration (%)	Biopolymer 2 Concentration (%)	Visual appearance
Na-caseinate - Na-alginate	3.0	2.0	2-phases
Na-caseinate - Na-alginate	3.0	2.5	2-phases
Na-caseinate - Na-alginate	7.5	1.0	2-phases
Na-caseinate - κ-carrageenan	3.0	2.5	2-phases
Na-caseinate - Gellan	5.6	0.4	2-phases
SPI - Na-alginate	3.0	2.0	2-phases
Denaturated SPI – Na-alginate*	2.5	2.0	2-phases
SPI - κ-carrageenan	3.0	2.5	2-phases
SPI – Xanthan	7.0	0.05	2-phases
SPI – Gellan	4.8	0.4	2-phases
Denaturated SPI – Gellan*	3.5	0.3	2-phases
Na-caseinate – Xanthan	5.0	0.1	1-phase
Na-caseinate – LBG	7.5	0.8	1-phase
Denaturated SPI – LBG*	4.5	0.2	1-phase
Na-caseinate – Denaturated SPI*	10.3	1.5	1-phase
Na-caseinate – SPI	2.9	9.6	1-phase
Na-caseinate – SPI	7.3	6.0	1-phase
Na-caseinate – SPI	11.7	2.4	1-phase
LBG – Na-alginate	0.3	3.2	1-phase
LBG – Na-alginate	0.8	2.0	1-phase
LBG – Na-alginate	1.3	0.8	1-phase

*Denaturation at 80 ^{o}C during 30 min

Among the incompatible systems, it was very difficult to withdraw the rich phases of SPI-xanthan systems, since the polysaccharide rich-phase looked-like a cloudy making difficult to determine the interface. Thus, the incompatibility of SPI-xanthan was also

checked for a greater number of samples with different concentrations and without centrifugation (at rest). Figure 2 shows a phase diagram for SPI-xanthan mixtures obtained according to the guided by eye method at rest after 2 days of the mixture preparation at 25 ^{o}C. Systems with more than 5% of protein were incompatible even in the presence of a very low polysaccharide concentration (0.02% w/w). However, it was observed the same difficulties to withdraw the rich-phases, such that SPI-xanthan mixture was not selected for further phase behaviour studies.
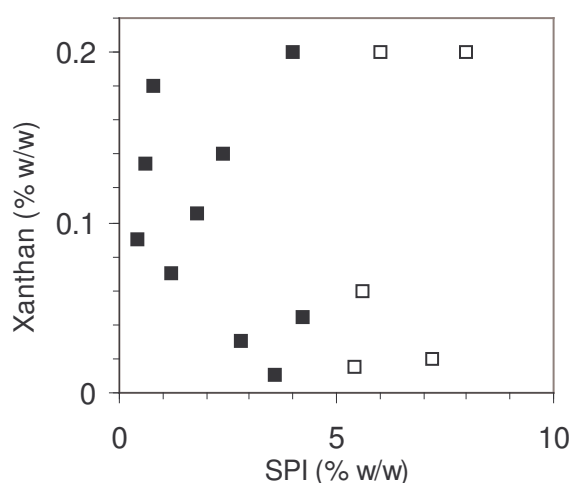

Figure 2. Compatible, one-phase, (■) and incompatible, two-phases (□) regions of SPI-xanthan mixtures, pH 7.0.

From the above results, the systems studied in Chapter 5 were selected, taking in consideration the systems that were incompatible. When possible, the protein or polysaccharide concentrations were kept the same in order to compare the effect of different biopolymers on phase behaviour. The concentration of gellan (Chapter 5) was much lower than the others polysaccharides concentrations, since gellan gelified at concentrations greater than 1%.

3. References

Antonov, Y. A., van Puyvelde, P., Moldenaers, P. (2004). Interfacial tension of aqueous biopolymer mixtures close to the critical point. *International Journal of Biological Macromolecules*, 34, 29-35.

Capron, I., Costeux, S., Djabourov, M. (2001). Water in water emulsions: phase separation and rheology of biopolymer solutions. *Rheologica Acta,* 40, 441-456.

Cavallieri, A. L. F. *Efeito do pH e da desnaturação térmica nas propriedades reológicas de proteínas do soro e na sua compatibilidade com xantana.* Dissertação de mestrado, Universidade Estadual de Campinas, 2003.

Clark, A. H. (2000). Direct analysis of experimental tie line data (two polymer – one solvent systems) using Flory-Huggins theory. *Carbohydrate Polymer,* 42, 337-351.

Guido, S., Simeone, M., Alfani, A. (2002). Interfacial tension of aqueous mixtures of Na-caseinate and Na-alginate by drop deformation in shear flow. *Carbohydrate Polymers*, 48, 143–152.

ANEXO: Lista de trabalhos sobre biopolímeros apresentados em congressos ou publicados em revistas no período do doutorado (2002-2006).

Artigos submetidos à revista:

1* **BRAGA, A. L. M.,** AZEVEDO, A., MARQUES, M. J., MENOSSI, M., CUNHA, R. L.
Interactions between soy protein isolate and xanthan in heat-induced gels: the effect of salt addition. Food Hydrocolloids. Aceito 12/2005.

2* **BRAGA, A. L. M.,** MENOSSI, M., CUNHA, R. L.
The effect of the glucono-δ-lactone/caseinate ratio on sodium caseinate gelation. International Dairy Journal. Oxford, England, 16, 389-398, 2006.

3 **BRAGA, A. L. M.,** CUNHA, R. L.
The effect of sucrose on unfrozen water and syneresis of acidified sodium caseinate-xanthan gels. International Journal of Biological Macromolecules. Oxford, England, 36, 33-38, 2005.

4 **BRAGA, A. L. M.,** CUNHA, R. L.
The effects of xanthan conformation and sucrose concentration on the rheological properties of acidified sodium caseinate-xanthan gels. Food Hydrocolloids. Oxford, England, 18, 977-986, 2004.

Artigos a serem submetidos à revista:

1[*] **BRAGA, A. L. M.,** CUNHA, R. L.
Rheological behaviour and microstructure of xanthan solutions: annealing temperature and sucrose effects. Previsão de submissão: fevereiro/2006.

2* **BRAGA, A. L. M.,** PERRECHIL, F. A., CUNHA, R. L.
Small- and large-strain rheological properties of GDL-induced soy protein isolate gels: effect of gelation temperature and xanthan addition. Previsão de submissão: março/2006.

3* **BRAGA, A. L. M.,** LOBMAIER, R.A., HERLE, V., CUNHA, R. L., FISCHER, P., WINDHAB, E.J.
Morphology of protein and polysaccharides mixtures at rest and under shear. Previsão de submissão: fevereiro/2006.

4* **BRAGA, A.L.M.,** LOBMAIER, R.A., FISCHER, P., WINDHAB, E.J., CUNHA, R. L.
Rheological and phase-separation behaviours of protein-polysaccharide mixtures at pH 7.0. Previsão de submissão: abril/2006.

5 **BRAGA, A. L. M.,** CUNHA, R. L.
Gelation process of Na-caseinate/xanthan/sucrose systems: Winter-Chambon criterion. Previsão de submissão: maio/2006.

---

[*] Trabalhos referentes à tese de doutorado

Artigos apresentados em congressos:

1[*] **BRAGA, A. L. M.,** LOBMAIER, R.A., HERLE, V., CUNHA, R. L., FISCHER, P., WINDHAB, E.J.
Morphology of protein and polysaccharides mixtures at rest and under shear. In: Proceedings of 4th International Symposium on Food Rheology and Structure, 2006, Zürich, Suíça. In press.

2 PERRECHIL, F. A., **BRAGA, A. L. M.,** CUNHA, R. L.
Influence of heat-treatment on acidified soy protein-LBG gels. In: Programa y libro de resúmenes del V Congreso Iberoamericano de Ingeníeria de Alimentos, 2005. Puerto Vallarta, v.1, p.xi-57.

3 **BRAGA, A. L. M.,** CUNHA, R. L.
Mechanical Properties of heat-induced gels of soy protein isolate and locust bean gum. In: XIX Congresso Brasileiro de Ciência e Tecnologia de Alimentos, 2004, Recife, Brasil. In press.

4* **BRAGA, A. L. M.,** CUNHA, R. L.
The effect of annealing temperature and sucrose addition on rheological behaviour of xanthan solutions In: Proceedings of 9th International Congress on Engineering and Food, 2004, Montpellier, França, v.1, 281 - 286

5 MOTTA, E. M. P., **BRAGA, A. L. M.,** SANTOS-ZAGO, L. F., NETTO, F. M.
The effect of ageing of soy protein isolates on the properties of the gel In: Proceedings of 9th International Congress on Engineering and Food, 2004, Montpellier, França, v.1, 416-421.

6 PERRECHIL, F. A., **BRAGA, A. L. M.,** CUNHA, R. L.
Mechanical properties of acidified sodium caseinate - LBG gels In: Proceedings 9th International Congress on Engineering and Food, 2004, Montpellier, França, v.1, 440-445.

7 **BRAGA, A. L. M.,** CUNHA, R. L.
Rheological characterization of gelation process in acidified food systems: the Winter-Chambon criterion In: Proceedings of 3rd International Symposium on Food Rheology and Structure, 2003, Zürich, Suíça, v.1. p.563 – 564.

8 **BRAGA, A. L. M.,** JAROSZEWSKI, A. R., CUNHA, R. L.
Stress relaxation and mechanical properties of caseinate-annealed xanthan-sucrose gels acidified with glucono-delta-lactone. In: Proceedings of 3rd International Symposium on Food Rheology and Structure, 2003, Zurich, Suíça, v.1. p.503 – 504.

9 JAROSZEWSKI, A. R., **BRAGA, A. L. M.,** CUNHA, R. L.
Effect of locust bean gum (LBG) and NaCl/KCl on the gelation process of acidified casein In: Proceedings of 3rd International Symposium on Food Rheology and Structure, 2003, Zurich, Suíça, v.1. p.565 – 566.

10 **BRAGA, A. L. M.,** CUNHA, R. L.
Ligações da água em géis ácidos de caseína-xantana-sacarose In: Anais do XVIII Congresso Brasileiro de Ciência e Tecnologia de Alimentos, Porto Alegre: Marca

---

Visual Criações Gráficas, 2002, p.2821 – 2824.

11 TAKEUCHI, K. P., **BRAGA, A. L. M.,** CUNHA, R. L.
Comportamento Reológico de soluções de caseinato de sódio acidificadas com glucona-d-lactona a 4ºC e 10ºC In: Anais do XVIII Congresso Brasileiro de Ciência e Tecnologia de Alimentos, 2002, Porto Alegre: Marca Visual Criações Gráficas, 2002, p.2825 – 2828.

Resumos apresentados em congressos:

1[*] **BRAGA, A. L. M.,** FISCHER, P., WINDHAB, E.J., CUNHA, R. L.
Curvas de escoamento de soluções aquosas de proteínas e polissacarídeos. In: cd-room of 6 Simpósio Latino Americano de Ciência de Alimentos, 2005, Campinas, Brasil.

2 **BRAGA, A. L. M.,** POLLARD, M., FISCHER, P., WINDHAB, E.J., CUNHA, R. L.
Gelation process of protein-polysaccharide systems: A discussion about the gel point criteria. Annual Meeting of the Swiss Rheology Group. Abstract Booklet, p.16. 2004, Lausanne, Suíça.

3[*] **BRAGA, A. L. M.,** MENOSSI, M., CUNHA, R. L.
Influência da taxa de acidificação na formação de géis de caseinato de sódio In: cd-room of V Simpósio Latino Americano de Ciência de Alimentos, 2003, Campinas, Brasil.

4[*] AZEVEDO, A., **BRAGA, A. L. M.,** CUNHA, R. L.
Caracterização reológica de soluções de xantana adicionadas de KCl. In: cd-room of V Simpósio Latino Americano de Ciência de Alimentos, 2003, Campinas, Brasil.

5[*] AZEVEDO, A., **BRAGA, A. L. M.,** CUNHA, R. L.
Interactions between soy protein isolate and xanthan in gels containing KCl. In: Programa y libro de resúmenes del IV Congreso Iberoamericano de Ingeniería de Alimentos, 2003. v.1. p.166 – 166.

---

[*] Trabalhos referentes à tese de doutorado